

TREATMENT OF CHLOROPHENOLS IN INDUSTRIAL EFFLUENTS USING ADVANCED OXIDATION PROCESSES (AOPs)

**A Thesis Submitted
In Partial Fulfilment of the Requirements for the Degree of**

DOCTOR OF PHILOSOPHY

by

**SHIVANI YADAV
(2K19/PHDEN/06)**

Under the joint supervision of

**Prof. A. K. HARITASH
Delhi Technological University,
Delhi**

**Dr. SUNIL KUMAR
Solaris Chemtech Industries Pvt. Ltd.,
Gujarat, India**



DEPARTMENT OF ENVIRONMENTAL ENGINEERING

DELHI TECHNOLOGICAL UNIVERSITY

(Formerly Delhi College of Engineering)

Shahbad Daultpur, Main Bawana Road, Delhi-110042. India

December, 2024

TREATMENT OF CHLOROPHENOLS IN INDUSTRIAL EFFLUENTS USING ADVANCED OXIDATION PROCESSES (AOPs)

**A Thesis Submitted
In Partial Fulfilment of the Requirements for the Degree of**

DOCTOR OF PHILOSOPHY

by

**SHIVANI YADAV
(2K19/PHDEN/06)**

Under the joint supervision of

**Prof. A. K. HARITASH
Delhi Technological University,
Delhi**

**Dr. SUNIL KUMAR
Solaris Chemtech Industries Pvt. Ltd.,
Gujarat, India**



DEPARTMENT OF ENVIRONMENTAL ENGINEERING

DELHI TECHNOLOGICAL UNIVERSITY

(Formerly Delhi College of Engineering)

Shahbad Daultpur, Main Bawana Road, Delhi-110042. India

December, 2024

ACKNOWLEDGMENT

Completing this Ph.D thesis has been a challenging yet transformative experience, and I owe gratitude to numerous individuals and institutions without whom this would not have been possible.

First and foremost, I express my sincere gratitude to my supervisors, Prof. Anil Kumar Haritash and Dr. Sunil Kumar for their invaluable guidance, unwavering support, and scholarly insight throughout every stage of this research. Their mentorship has been instrumental in shaping my academic growth and refining the quality of this research. Their constructive feedback, scholarly expertise, encouragement and insightful critiques have greatly enhanced the rigour and depth of this work. I am true to the cooperation and support of Lab technician Mrs. Navita, Mr. Sahil, Mr. Keshav in the Department of Environmental Engineering for fostering an intellectually stimulating environment conducive to research and learning. I am indebted to the departmental office staff Mr. Jaiveer and Mr. Ajit Pandey for their administrative support and assistance.

I extend my heartfelt thanks to my fellow lab mate and friend Mr. Harsh Pipil who has provided camaraderie, inspiration, and valuable insights throughout this journey. I am fortunate to have worked alongside you and your friendship and collaboration have made this endeavour both enjoyable and enriching. I would also like to express my sincere thanks to Dr. Saurav Ambastha, and Dr. Akansha Gupta for their help and motivation during this journey.

I owe a deep debt of gratitude to my parents Mr. Ved Prakash and Mrs. Aman Yadav, my uncle Mr. Kamal and my aunt Mrs. Sushma, for their unconditional love, support, and faith in me to pursue my goals. Not to forget those who made the challenging moments more bearable and sustaining, my cousins-cum-siblings, my niece and nephew for their unwavering love, encouragement, and understanding during this demanding period.

Finally, I would like to dedicate this thesis to both my paternal and maternal grandfathers Mr. Rohtash Singh and Mr. Kartar Singh. Your teachings have been a continuous source of encouragement and inspiration, and this work is a testament to your impact on my life.

I offer my sincerest appreciation to all those mentioned above and the countless others who have contributed to this in various ways. This thesis stands as an outcome to your collective support and encouragement.

Shivani Yadav



DELHI TECHNOLOGICAL UNIVERSITY

(Formerly Delhi College of Engineering)

Shahbad Daultapur, Main Bawana Road, Delhi-110042

CANDIDATE'S DECLARATION

I, Shivani Yadav, Roll No.: 2K19/PHDEN/06 student of Ph.D. (Environmental Engineering), hereby declare that the work which is being presented in the thesis entitled "Treatment of Chlorophenols in Industrial Effluents using Advanced Oxidation Processes (AOPs)" in partial fulfilment of the requirement for the award of Degree of Doctorate of Philosophy, submitted in the Department of Environmental Engineering, Delhi Technological University is an authentic record of my own work carried out during the period from August, 2019 to August, 2024 under the joint supervision of Prof. Anil Kumar Haritash (Delhi Technological University), and Dr. Sunil Kumar (Solaris Chemtech Industries, Gujarat, India).

The matter presented in the thesis has not been submitted by me for the award of any degree of this or any other Institute.

Place: Delhi

(SHIVANI YADAV)

Date:



DELHI TECHNOLOGICAL UNIVERSITY

(Formerly Delhi College of Engineering)

Shahbad Daultapur, Main Bawana Road, Delhi-110042

CERTIFICATE BY THE SUPERVISORS

Certified that **Shivani Yadav** (2K19/PHDEN/06) has carried out her search work presented in this thesis entitled **“Treatment of Chlorophenols in Industrial Effluents using Advanced Oxidation Processes (AOPs)”** for the award of **Doctor of Philosophy** from Delhi Technological University, Delhi, under our supervision. The thesis embodies results of original work, and studies are carried out by the student herself and the contents of the thesis do not form the basis for the award of any other degree to the candidate or to anybody else from this or any other University/Institution.

Prof. Anil Kumar Haritash
Head of Department
Department of Environmental
Engineering, Delhi Technological
University,
Delhi, India

Date:

Dr. Sunil Kumar
General Manager
Research & Development Centre
Solaris Chemtech Industries Pvt Ltd,
Bhuj, Gujarat
India

Date:

ABSTRACT

Chlorophenols are the ubiquitous compounds representing one of the most abundant families of toxic pollutants emerging from various industrial manufacturing units. The toxicity of these chloroderivatives is proportional to the number and position of chlorine atoms on the benzene ring. In the aquatic environment, these pollutants accumulate in the tissues of living organisms, primarily in fishes, inducing mortality at an early embryonic stage. Contemplating the behaviour of such xenobiotics and their prevalence in different environmental components, it is crucial to remove/degrade the chlorophenol from contaminated environment. Advanced Oxidation Processes (AOPs) are effective in degrading such organics with enhanced rate and efficiency. Different processes such as sonication, photocatalysis, and Fenton's treatment are discussed for the degradation of chlorophenols (CPs). Furthermore, a statistical approach, Response Surface Methodology was employed to validate the optimum conditions of regulating parameters of different processes for maximum contaminant removal. The degradation of 4-CP using photocatalysis under optimised conditions (Nano-TiO₂= 0.1g/l; H₂O₂=10.0mM; pH= 5.0) resulted in complete (~98%) removal in 3.5 hours whereas, in the case of Photo-Fenton's process, at optimised condition (pH= 3.0; Fe²⁺= 0.7mM; H₂O₂= 7.0mM), 100% removal was achieved in 6 minutes. ANOVA results displayed high regression and fitting values between experimentally observed data against RSM-predicted values. The removal efficiency of different integrated processes employed towards the degradation of 4-CP reported the Fenton's and Fenton-integrated processes as more efficient ones towards effective removal of 4-CP. In the case of 2,4-DCP, Complete degradation of 2,4-DCP was reported using AOPs- Photocatalysis (in 210 min) and Photo-Fenton (in 5 min) treatment. Under optimised conditions, with a photocatalyst dose of 0.2 g/L, oxidant concentration of 10.0 mM and pH 5.0, complete removal of 2,4-dichlorophenol (2,4-DCP) was observed in 210 minutes in photocatalytic treatment. In the case of the photo-Fenton process, at an H₂O₂ dose of 5.0 mM and Fe²⁺ concentration of 0.5 mM, the organic pollutant was eliminated within 5 minutes of reaction time under acidic conditions (pH 3.0). The RSM model reported the perfect fit of experimental data with the predicted response. For the obtained optimised conditions, sonication

and solar energy-driven processes were incorporated to study enhanced mineralisation. The solar-assisted Fenton process was found to be the most efficient with the maximum degree of mineralisation (90%) of 2,4-DCP; and cost-effective (\$0.01/litre for 100 mg/L 2,4-DCP) treatment among different hybrid oxidation processes. Photocatalytic degradation of 2,4,6-Trichlorophenol using nano-TiO₂ exhibited higher potential towards the removal with nearly complete degradation within 3.5 h, as compared to analytical grade TiO₂. Under the optimal dose of 250 mg/L of nano-TiO₂, around 97% removal was observed. No effect of addition of oxidant was observed in case of removal of 2,4,6-TCP. In case of Photo-Fenton's process, under optimized conditions (at pH= 3.0, Fe²⁺= 0.5 mM, and H₂O₂= 10.0 mM), complete degradation of TCP was attained in 6 minutes with 50% mineralisation. However, Solar-Fenton reported complete removal and nearly complete mineralisation (98%) of 2,4,6-TCP within 4 minutes. Degradation of Mixed-CPs under optimised conditions obtained for individual chlorophenols was further investigated. In photocatalysis degradation, rapid and complete removal of mixed-CPs was reported at pH 6.0, TiO₂ dose of 0.25g/L, and H₂O₂ concentration of 10.0mM within 270 minutes. In the case of Photo-Fenton's process, complete removal was observed in 12 minutes at pH 3.0, Fe(II) 0.5mM, and H₂O₂ 10.0mM. Different integrated-AOPs employed towards removal of CPs at optimised conditions reported that Solar-derived processes exhibiting enhanced degradation rates. The work thus provides insight into harnessing the naturally available solar energy, reducing the overall treatment cost, and opting for a sustainable treatment method towards degradation of organics. Toxicity analysis of treated effluent using *Eichhornia crassipes* resulted in the death of the plant inferring the presence of such intermediary by-products which hamper the growth and metabolic activities of the plants. Toxicity analysis study suggested the invasive macrophyte is intolerant to oxidative stress conditions even when cultured in treated effluent thus suggesting the need for further treatment of the AOP-treated wastewater.

Table of Content

Title	Page No.
Acknowledgment	i
Candidate's declaration	ii
Certificate	iii
Abstract	iv
Table of Content	vi
List of Figures	xi
List of Tables	xv
List of Abbreviations	xviii
CHAPTER 1: INTRODUCTION	1-4
1.1 Background	1
1.2 Requirement of treatment of CPs	2
1.3 Treatment methods	3
1.4 Objectives of the present study	4
CHAPTER 2: REVIEW OF LITERATURE	5-81
2.1 Introduction	5
2.2 Sources	6
2.2.1 Natural formation (synthesis) of CPs	8
2.3 Fate of Chlorophenols in the environment	8
2.3.1 Properties of Chlorophenols	10
2.4 Ecotoxicity of CP	12
2.4.1 Effect of PCP on soil	12
2.4.2 Effect of PCP on aquatic biota	14
2.4.3 Effect on human beings	18

2.5	Treatment of chlorophenols	21
2.5.1	Natural attenuation of chlorophenols	21
2.5.2	Oxidation and Evaporation	23
2.5.3	Sorption	23
2.5.3.1	Adsorption	24
2.5.4	Membrane Technology	26
2.5.5	Microbial degradation of Chlorophenol	26
2.6	Treatment of CPs by Advanced Oxidation Processes	37
2.6.1	Physical AOPs	40
2.6.2	Photocatalysis	48
2.6.2.1	Solar energy driven heterostructure photocatalysis	52
2.6.3	Fenton's Process	54
2.6.4	Electrochemical AOPs	60
2.6.5	Ozonolysis	62
2.6.6	Sustainability Evaluation	64
2.7	Phytoremediation of PCP	68
2.7.1	Phenolic compound uptake and translocation	70
2.8	Integrated Management of Chlorophenols	73
2.8.1	Management options for PCP	75
2.9	Ecorestoration	79
CHAPTER 3:	MATERIALS AND METHODS	82-104
3.1	Chemicals	82
3.2	Analytical methods and Instrumentation	82

3.3	Experimental Setup of UV induced AOPs	87
3.4	Experimental Setup of Photocatalysis Process	87
3.5	Sonication assisted Photocatalysis Process	90
3.6	Solar-Catalysis	90
3.7	Sono-Solar-Catalysis	92
3.8	Photo-Fenton	92
3.9	Sono-Photo-Fenton	94
3.10	Fenton's Process	94
3.11	Sono-Fenton	95
3.12	Solar-Fenton	96
3.13	Sono-Solar Fenton	97
3.14	Design of Experiment	97
3.14.1	Conventional Approach-One Factor at Time (OFAT)	97
3.14.2	Statistical Approach: Response Surface Methodology (RSM)	98
3.15	Toxicity Analysis	100
CHAPTER 4:	RESULTS AND DISCUSSION	105-209
4.1	Photocatalytic degradation of 4-Chlorophenol	105
4.2	Photo-Fenton's degradation of 4-Chlorophenol	112
4.3	Adequacy of Model (ANOVA) for Degradation of 4-CP	117
4.4	Optimization of Process and Effect of Operating Parameters	123
4.4.1	Influence of Photocatalytic Factors	124
4.4.2	Influence of Photo-Fenton's Factors	128
4.5	Synergic-approach induce Integrated-Oxidation	132

4.5.1	Photocatalysis-integrated Processes	135
4.5.2	Fenton's-integrated Processes	136
4.6	Economic Efficiency of different AOPs for degradation of 4-CP	137
4.7	Photocatalytic degradation of 2,4-Dichlorophenol	140
4.8	Photo-Fenton's degradation of 2,4-Dichlorophenol	148
4.9	RSM Modelling and Adequacy of Model (ANOVA) for Degradation of 2,4-DCP	154
4.10	Process Optimization and Effect of Variables	160
4.10.1	Effect of Photocatalytic Variables	161
4.10.2	Effect of Photo-Fenton Variables	162
4.11	Synergistic Effect of Integrated Oxidation Systems	165
4.11.1	Sonication Coupled AOPs	168
4.11.2	Solar driven AOPs	169
4.12	Economic Analysis of Different AOPs for degradation of 2,4-DCP	170
4.13	Photocatalytic degradation of 2,4,6-Trichlorophenol	174
4.13.1	Mineralization of TCP	177
4.14	Photo-Fenton's degradation of 2,4,6-Trichlorophenol	178
4.15	Optimization of TCP-degradation	182
4.16	Regression model and Analysis of Variance	185
4.17	Integrated Treatment Processes for enhanced degradation of 2,4,6-TCP	187
4.17.1	Solar-Induced Photocatalysis	187
4.17.2	Fenton's-integrated Process	189
4.18	Economic Analysis of different AOPs for degradation of 2,4,6-TCP	193
4.19	Photocatalytic degradation of Mixed-Chlorophenols	196

4.20	Photo-Fenton's degradation of Mixed-Chlorophenols	197
4.21	Integrated Processes towards degradation of Mi-CPs	198
4.21.1	Ultrasound assisted Photocatalysis process	201
4.21.2	Solar-induce AOPs	201
4.22	Economic analysis of different AOPs for degradation of Mi-CPs	202
4.23	Combination of AOPs with biological treatment for enhanced mineralization of residual chlorophenols and assessment of toxicity of treated effluent	204
4.23.1	Toxicity Assessment using <i>Eichhornia crassipes</i>	205
4.24	Significance of the study	207
4.24.1	Environmental impact	207
4.24.2	Social impact	209
CHAPTER 5:	CONCLUSION AND RECOMMENDATION	210-212
5.1	Conclusion	210
5.2	Recommendation	211
5.3	Future Scope	212
	REFERENCES	213-263
	List of Publications	264-265
	Circular Vitae	266-269

List of Figures

Figure No.	Figure Caption	Page No.
2.1	Fate of Chlorophenols	9
2.2	Aerobic and anaerobic microbial degradation mechanism of PCP	36
2.3	Classification of AOPs	38
2.4	Generalised mechanism of AOPs for PCP degradation sharing similar intermediates at some stages	39
2.5	Global-warming potential for different AOPs	68
3.1 (a)	Experimental setup of UV-driven processes	88
3.1 (b)	Schematic diagram of experimental setup	88
3.2	Experimental Setup of Solar-Catalysis	91
3.3	Experimental Setup of Solar-Fenton	96
3.4	Experimental design for Toxicity assessment	101
4.1	Effect of different catalyst dose on removal efficiency of 4-CP using Photocatalysis	107
4.2	Effect of different pH on removal efficiency of 4-CP using Photocatalysis Process	109
4.3	Effect of different oxidant concentration on removal efficiency of 4-CP using Photocatalysis Process	111
4.4	Effect of different Fe ²⁺ concentration on removal efficiency of 4-CP using Photo-Fenton Process	113
4.5	Effect of different pH on removal efficiency of 4-CP using Photo-Fenton Process	115
4.6	Effect of different H ₂ O ₂ concentration on removal efficiency of 4-CP using Photo-Fenton Process	117
4.7 (a)	Normal Plot of residuals for 4-CP in Photocatalysis	119
4.7 (b)	Predicted vs Observed Photocatalytic Response for 4-CP	119

4.8 (a)	Normal Plot of residuals of 4-CP in Photo-Fenton's Process	120
4.8 (b)	Predicted vs Observed Photo-Fenton's response for 4-CP	120
4.9 (a)	Optimisation plot of regulating parameters for 4-CP in Photocatalysis	123
4.9 (b)	Optimisation plot of regulating parameters for 4-CP in Photo-Fenton's process	123
4.10	Contour plots and surface overlaid contour graphs showing effect of process regulating parameters in Photocatalysis for 4-CP	127
4.11	Contour plots and surface overlaid contour graphs showing effect of process regulating parameters in Photo-Fenton's treatment for 4-CP	131
4.12	Comparison of different AOPs towards maximum removal of 4-CP	132
4.13	Removal efficiency of 2,4-DCP at different catalyst dose in Photocatalysis Process	142
4.14	Removal efficiency of 2,4-DCP at different pH in Photocatalysis Process	145
4.15	Removal efficiency of 2,4-DCP at different oxidant concentration in Photocatalysis Process	147
4.16	Optimization of Fe ²⁺ concentration for 2,4-DCP in Photo-Fenton Process	150
4.17	Optimization of pH for 2,4-DCP in Photo-Fenton Process	151
4.18	Optimization of Oxidant concentration for 2,4-DCP in Photo-Fenton Process	153
4.19 (a)	Normal Plot of residuals for 2,4-DCP in Photocatalysis	156
4.19 (b)	Predicted vs Observed Photocatalytic Response for 4-CP	156
4.20 (a)	Normal Plot of residuals of 2,4-DCP in Photo-Fenton's Process	157

4.20 (b)	Predicted vs Observed Photo-Fenton's response for 2,4-DCP	157
4.21 (a)	Optimisation plot of regulating parameters for 2,4-DCP in Photocatalysis	160
4.21 (b)	Optimisation plot of regulating parameters for 2,4-DCP in Photo-Fenton's process	160
4.22	Two-dimensional contour plots showing effect of regulating parameters towards 2,4-DCP degradation in photocatalysis process	163
4.23	Two-dimensional contour plots showing effect of regulating parameters towards 2,4-DCP degradation in Photo-Fenton's process	164
4.24	Comparison of different AOPs towards maximum removal of 2,4-DCP	165
4.25	UV365 induced degradation of 2,4,6-TCP using Commercial-TiO ₂ and Nano-TiO ₂	174
4.26	Removal efficiency of 2,4,6-TCP (Ci-100 mg/L) at varying Catalyst dose	176
4.27	Chromatogram of 2,4,6-TCP before and after degradation depicting intermediate formation	178
4.28	Response Surface Plot of interactive effects of regulating parameters in Photo-Fenton's degradation of 2,4,6-TCP	184
4.29	Optimization of regulating parameters for degradation of 2,4,6-TCP by Photo-Fenton (UV365) treatment	183
4.30	Normal Plot of Observed degradation (%) of 2,4,6-TCP against the Predicted value	185
4.31	Comparison of different ultrasound and light (UV and solar) integrated AOPs for degradation of 2,4,6-TCP	187
4.32	Removal efficiency of 2,4,6-TCP under solar and UV light as a function of time	188
4.33	Removal efficiency of 2,4,6-TCP under Solar and UV light as a function of accumulated energy	188

4.34	The HPLC spectra of 2,4,6-TCP (100 mg/L untreated), Photo-Fenton (UV365) and Solar-Fenton treated TCP-containing wastewater confirming mineralisation	190
4.35	Effect of process conditioning parameters for Photocatalytic degradation of Mi-CPs	196
4.36	Photo-Fenton degradation of Mi-CPs	197
4.37	Removal efficiency and mineralisation percent of different AOPs for degradation of Mi-CPs	198
4.38	Physical appearance of plant before and after 7 days	206
4.39	United Nation's Sustainable Development Goals aligning with the current study	208

List of Table

Table No.	Title	Page No.
2.1	Properties of Chlorophenols	11
2.2	Microbial Degradation of Chlorophenols	32
2.3	Heterogeneous Fenton process for the degradation of chlorophenols	57
2.4	SWOT Analysis of Different Effluent Treatment Methods	66
2.5	Plant species used to remove phenolic compounds	69
2.6	Environment-friendly chemical choice in wet textile processing	77
3.1	Operating conditions of Photocatalytic degradation of Chlorophenols	89
3.2	Operating conditions for Sonication assisted Photocatalysis of Chlorophenols	90
3.3	Operating conditions for Solar driven Catalytic degradation of Chlorophenols	91
3.4	Operating conditions for Sonication assisted Solarcatalysis of Chlorophenols	92
3.5	Operating conditions for Photo-Fenton's degradation of Chlorophenols	93
3.6	Operating conditions for Sono-Photo-Fenton's Treatment of Chlorophenols	94
3.7	Operating conditions for Fenton's treatment of Chlorophenols	95
3.8	Operating conditions for Sono-Fenton's degradation of Chlorophenols	95

3.9	Operating conditions for Solar driven Fenton's Treatment of Chlorophenols	96
3.10	Operating conditions for Solar driven Sono-Fenton's degradation of Chlorophenols	97
3.11	Design of Experiment using RSM for different process	99
4.1	Box Behnken design for three independent variables, predicted and observed responses for Photocatalytic degradation of 4-CP	105
4.2	Box Behnken design for three independent variables, predicted and observed responses for Photo-Fenton's degradation of 4-CP	112
4.3	Analysis of Variance (ANOVA) for percentage degradation of 4-CP by Photocatalysis (UV365) and Photo-Fenton's treatment	121
4.4	Comparison of Different processes for maximum time taken for degradation of 4-CP	133
4.5	Economic analysis of the operating cost of different AOPs used for degradation of 4-CP	138
4.6	Box Behnken design for three independent variables, predicted and observed responses for Photocatalytic degradation of 2,4-DCP	141
4.7	Box Behnken design for three independent variables, predicted and observed responses for Photo-Fenton's degradation of 2,4-DCP	148
4.8	Analysis of Variance (ANOVA) for percentage degradation of 2,4-DCP by Photocatalysis (UV365) and Photo-Fenton's treatment	158
4.9	Comparison of different processes for maximum time taken for degradation of 2,4-DCP	166
4.10	Economic analysis of the operating cost of different AOPs used for degradation of 2,4-DCP	172

4.11	Box Behnken design for three independent variables, predicted and observed responses for Photo-Fenton's degradation of 2,4,6-TCP	179
4.12	Analysis of Variance (ANOVA) for percentage degradation of 2,4,6-TCP by Photo-Fenton treatment	186
4.13	Comparison of different processes for maximum time taken for degradation of 2,4,6-TCP	191
4.14	Economic analysis of the operating cost of different AOPs used for degradation of 2,4-DCP	194
4.15	Comparison of different processes for maximum time taken for degradation of Mi-CPs	199
4.16	Economic analysis of the operating cost of different AOPs used for degradation of Mi-CPs	203
4.17	Physiological response of water hyacinth	205

List of Abbreviations

2,4-DCP	2,4-Dichlorophenol
2,4-DNP	2,4-Dinitrophenol
2,4,6-TCP	2,4,6-Trichlorophenol
2-CP	2-Chlorophenol
4-CP	4-Chlorophenol
ANOVA	Analysis Of Variance
AOPs	Advanced Oxidation Processes
AOX	Adsorbable Organic Halides
ATP	Adenosine Triphosphate
BBD	Box Behnken Design
BDD	Boron-Doped Diamond
BET	Brunauer-Emmett-Teller
BOD	Biochemical Oxygen Demand
BPA	Bisphenol A
CBZ	Carbamazepine
CC	Chlorocatechol
CDH	Central Drug House
CHMs	Chlorinated Anisyl Metabolites
CNFs	Carbon Nanofibers
CPK	Carica-Papaya-Model-Kaolinite
CPs	Chlorophenols
CTAB	Cetyl Trimethyl Ammonium Bromide
DCP	Dichlorophenol
Diol	Deiodinase
EDCs	Endocrine-Disrupting Chemicals

ER	Estrogen Receptor
FSP	Fenugreek Seed Peroxidase
GWP	Global Warming Potential
HOBT	1-Hydroxy Benzotriazole
HPLC	High-Performance Liquid Chromatography
HQ	Hydroquinone
HRP	Horseradish Peroxidases
IARC	International Agency For Research On Cancer
IC	Inorganic Carbon
IL	Interleukin
LCA	Life Cycle Assessment
MCP	Monochlorophenol
Mi-CPs	Mixed-Chlorophenols
MNP	Magnetic Nanoparticles
MWNT	Multi-Walled Carbon Nanotubes
NAD ⁺	Nicotinamide Adenine Dinucleotide
NC	Nanocarbon
NMNO	N-Methyl-N-Oxide
NPC	Nano-TiO ₂ Photocatalyst
NTP	TiO ₂ -Nano Particles
OFAT	One Factor At Time
PAP	Para-Aminophenol
<i>p</i> -CBA	Para-Chlorobenzoic
PCK	Pine-Cone-Modified
PCP	Pentachlorophenol
POPs	Persistent Organic Pollutants
PPO	Polyphenol Oxidases

pzc	Point Of Zero Charge
ROS	Reactive Oxygen Species
RSM	Response Surface Methodology
SDG	Sustainable Development Goal
SOM	Soil Organic Matter
SR	Sulfate Radicals
SS	Suspended Solids
SWNT	Single-Walled Carbon Nanotubes
SWOT	Strengths, Weakness, Opportunities, And Threats
TC	Total Carbon
TCA	The Citric Acid
TCHQ	Tetrachlorohydroquinone
TCMP	2,3,5,6-Tetrachloro-4-Methoxyphenol
TCP	Trichlorophenol
TDI	Total Dissolved Iron
TeCP	Tetrachlorophenol
THR _s	Thyroid Hormone Receptors
TOC	Total Organic Carbon
TSCF	Transpiration Stream Concentration Factor
TTP	Travancore Titanium Products
TTR	Transthyretin
US	Ultrasound
USEPA	Us Environmental Protecting Agency
VTG	Vitellogenin
ZVI	Zero Valent Iron

CHAPTER 1

INTRODUCTION

"Waterways have taken the brunt of economic development". However, it is no less important to internalise environmental costs in the midst of global climate change. The state of the environment can be indirectly inferred from the technologies being used in industries. The industries depend on freshwater and consume a significant share as process water, resulting in added pressure over the freshwater resources. However, the discharge of partially treated wastewater and the unintended release of harmful chemical compounds into the surroundings, disrupts the structure and functioning of natural ecosystems. An alternative to tackle the growing water crisis and reduce the pressure over freshwater resources is to recycle and reuse treated wastewater. Thus, the critical challenge today is the treatment and utilization of wastewater. Currently, between 80% and 90% of the wastewater worldwide is discharged into the environment without treatment (UNESCOUN-Water, 2020).

1.1 Background

Various industrial manufacturing processes and units generate effluent containing different toxic organic compounds, resins, acids, chlorinated hydrocarbons, phenols, dioxins, and furans etc. These potentially toxic compounds are termed as adsorbable organic halides (AOX). Chlorophenols (CPs) such as monochlorophenols (MCP), dichlorophenols (DCP), trichlorophenols (TCP), tetrachlorophenols (TeCP), and Pentachlorophenols (PCP) constitute a significant component of AOX (Singh and Garg, 2019) originating from industries. These are discharged directly into the natural environment through various industries such as pharmaceutical, petrochemical, plastic, iron, steel, textile, paper, paints, polymer intermediates, flame retardants, wood preservatives etc (Eslami et al., 2018). Some CPs are precursors to agricultural products like pesticides, herbicides, fungicides, molluscicides, acaricides, bactericides, and mould inhibitors (Yang and Lee, 2008). CPs are resistant to biodegradation and persist in the natural environment for a long period of up to 28 years (Jensen, 1996). They are classified as kind of priority

pollutants by United States Environmental Protecting Agency (USEPA) by virtue of their estrogenic, mutagenic and carcinogenic effects. Because of their persistent nature and low biodegradability even at trace levels, the U.S. Agency for Toxic Substance and Disease Registry has listed them on priority list of hazardous substances (Agency for Toxic Substances and Disease Registry, 1999; EPA, 1999). Investigations across the globe on environmental monitoring has confirmed the presence of CPs in the atmosphere, surface and groundwater ecosystems, soil and bottom sediments, thus posing threat to humans and other associated organisms in the food-chain (Sinkkonen and Paasivirta, 2000). The lipophilic property of CPs allows them to pass through the cell membrane and bioaccumulate in the living organisms. PCP being environmentally persistent and bioaccumulative, possesses lethal toxicity, affecting aquatic fauna. It causes liver damage, induces respiratory stress mixed-function oxygenase activity, affects the sexual maturation and reproduction as well. It has been reported to disrupt the organism's energy metabolism, inhibiting the synthesis of adenosine triphosphate (ATP), and affecting the fecundity of certain invertebrates (Cao et al., 2019). It has been listed as a probable 2B carcinogen category by International Agency for Research on Cancer (IARC) (IARC, 2004). Although PCP is restricted in most of the countries, it has been continuously detected in the lakes and rivers, with concentration exceeding the maximum acceptable limit of surface waters (1µg/L).

1.2 Requirement of treatment of CPs

Physical, chemical and biological treatment process failed to achieve complete degradation when employed for eliminating CPs from industrial effluent. The techniques like coagulation-flocculation, adsorption, foam floatation, membrane filtration, etc., result in phase transfer of pollutants, resulting in generation of toxic sludge and issues associated with final disposal. Improper storage and handling of sludge containing CPs may result in reintroduction of the contaminants in the environment. These techniques cannot remove organic contaminants efficiently because of high chemical stability and low biodegradability of CPs (Karimi et al., 2010). Chemical oxidation tends to become more and more resistant as the reaction proceeds and becomes energy intensive

towards degradation. This leads to increase in treatment time and decreased rate of degradation. Due to increase in the complexity of the chemical structure, it becomes difficult for the microbial community to degrade it and it appears to become resistant towards biodegradation. In spite of the fact that microbial degradation has been continuously employed, it still requires to explore the metabolic capacity of microbes towards degradation of CPs within the indigenous microbial consortia in various ecosystems.

1.3 Treatment methods

The treatment of chlorophenols is necessary as they are lipophilic and persistent in nature; they tend to accumulate in river sediments and are bioaccumulative in aquatic organisms. With the high sustainability waves, increasing water shortages, and environmental restrictions, there is a need to switch to alternative wastewater treatment solutions that can help minimize the water footprint. To fill the gap between treatability attained from conventional biological and physico-chemical treatment, the application of the Advanced Oxidation Processes (AOPs) technique has made a gateway towards degradation of such xenobiotic compounds (Dewil et al., 2017). As an environmental-friendly technique, its application neither causes the transformation of pollutants from one phase to another (in case of chemical precipitation and adsorption) nor produces an enormous amount of hazardous sludge. The process is based on the principle of *in-situ* generation of oxidation radicals, a highly potent chemical oxidant that reacts with the contaminant and lowers down the toxic level of contaminants in water permissible limit. AOPs are nowadays widely focused because of the rapid degradation efficiency towards xenobiotic compounds including CPs. AOPs consist of different treatment methods like catalysis, photocatalysis, Fenton's process, Photo-Fenton's treatment, sonication, ozonation, etc. The developments in AOPs have gained the scientific world's attention by emerging as a promising and advantageous methodology for reducing pollutants. Over the globe, researchers have evaluated the efficiency of AOPs in effluent generated from various industrial sectors like the textile industry, tanneries, pulp and paper industry, distilleries, fertilizer producing industry, pharmaceutical wastewater, pesticides etc. Hence

there is a fundamental requirement of attention for a sustainable, environment-friendly, and techno-economic solution to treat the effluent generated having toxic recalcitrants.

Since sustainability is the need of the hour, every sector worldwide concentrates on removing environmentally dangerous aspects from their supply chain. The industrial sector has been pressurized to switch from conventional effluent treatment techniques to more refined and efficient ones to meet the current environmental standards. A goal of the effluent decontamination employing AOP procedures is to reduce the chemical contaminants and the toxicity to such an extent that the cleaned effluent may be reintroduced into receiving streams or, at least, into a conventional system. Hence the proposed research study is a step towards degradation and treatment of toxicant chlorophenols using AOPs as the conventional techniques fail to treat due to their high resistivity towards degradation. Therefore, it can be the field of AOPs being lying at the interface of science and engineering can greatly enhance the advancement in the area of environmental applications and can contribute towards successfully tackling the problems. Considering all the facts mentioned above, the following objectives have been proposed for the present study:

1.4 Objectives of the present study

Considering the shortcoming of the conventional treatment methods, the following objectives were set forth for the present study:

- (i) Determination of efficiency of different AOPs (Photocatalysis, Fenton's process, and Sonication) towards treatment of Chlorophenols individually as well as in combination.
- (ii) Optimization of parameters regulating the efficiency of different AOPs with the help of Response Surface Methodology (RSM) and validation of results.
- (iii) Combination of AOPs with biological treatment for enhanced mineralization of residual chlorophenols and assessment of toxicity of treated effluent.

CHAPTER 2

REVIEW OF LITERATURE

2.1 Introduction

Emerging recalcitrant contaminants in effluent originating from industrial manufacturing units pose threats to human health and the eco-biota when discharged into the environment without treatment. With the rapid development of the global economy, these chemical compounds are essential in many industrial activities (Igbinsosa et al., 2013). Nevertheless, these persistent organic compounds have the potential to cause considerable environmental harm even when present in low content (Faludi et al., 2015). The continuous release of organic pollutants from industrial units is causing the deterioration of the quality of aquatic ecosystems. The widespread use of chlorinated organics in industrial and manufacturing processes has resulted in the introduction of toxicity in the aquatic environment. The bleaching unit in the textile industry and pulp and paper industry generates effluent loaded with chlorinated aromatic organics (Ahlborg et al., 1980). According to a report, the production of one ton of paper requires 100 kg of colour-imparting materials and around 2–5 kg of organochlorides to the bleaching section, resulting in the introduction of CPs in the wastewater generated (Nagarathnamma et al., 1999). The prevalence of CPs is continuously detected in various environmental matrices like water, soil, sediments, air, food commodities, and biological tissues, as well. Although the occurrence of these emerging pollutants is in trace amounts in the natural environment, usually in ng/l to µg/l, they are reportedly found in the concentration up to 190 mg/L in polluted surface and ground water (Olaniran and Igbinsosa 2011). Considering the harmful effect over the aquatic environment, emphasis is given on managing the water quality and subsequently removing the CPs from aquatic environment. Because of the chemical and structural stability, traditional methods cannot break the C–Cl bonds associated with aromatic structures; biological treatment is inefficient in treating these harmful organics when present in lower concentration, whereas high levels of CPs inhibit the growth of

microbial community (Czaplicka 2004). The metabolites generated from their partial degradation like chlorocatechols or chlorine substituted fission products suppress the development of halo aromatic-utilizing microorganisms (Annachhatre and Gheewala 1996).

2.2 Sources

The industrialisation, reliance over chemical complex nature of process, and limited efficiency of treatment processes have substantially contributed to CPs to a prodigious degree in ambient environment. The principal point sources of CPs in the environment are the industrial waste, and leaching of CPs from landfills, while the non-point sources are CPs -based pesticides, chlorination phase in wastewater treatment, wood distillation processes; sludge, storage tanks, etc. (Garba et al., 2019; Samanta et al., 2002; Zhang & Bennett, 2005). As soon as any pollutant or chemical substance enters the atmosphere, air currents transmit it to longer distances before the deposition. CPs are dispersed in the ambient air as vapour from the advent production-related activities and manufacturing of specific CPs, and combustion of municipal wastes, hazardous waste, organic matter, coal, or wood (El-Sayed et al., 2009). The release of CPs in the atmosphere is via volatilization because of the volatile nature of few CPs, however, TCP and TeCPs being slightly volatile, are primarily emitted in the smaller fraction in the vapour form only. TCPs have been identified in flue gas condensates in fly ash released from municipal incinerators. Additionally, DCPs, TCPs, and TeCPs are detected in fly debris emissions from oil and coal-fired power stations as well (Hamad et al 2010). A considerable amount of PCP is released into the atmosphere and in soil following the burning of wood pre-treated with PCP-based preservatives. The accidental spills, and biodegradation of pesticides and herbicides has also brought forth ample CPs as intermediary metabolites during their decomposition (Eslami et al., 2018; Garba et al., 2019). The transport of contaminants in soil is governed by factors like the organic content of the soil, porosity, solubility in water, the processes carried out by the biological system, etc. The other emission sources of CPs in soil have also been reported at the sites composting yard waste and municipal solid waste.

Since PCP is exercised as wood preservatives, it has prompted the soil biome's deterioration around the sawmills (Garba et al 2019; Olaniran and Igbinsosa, 2011). The problem of soil pollution by CPs is of significant concern for the areas where fungicides and plant-protecting agents are employed at large. As the CP-contaminated soil is washed and carried along as surface run-off from rainwater, along with the underlying unconsolidated materials, weathering of bedrock, and atmospheric deposition, CPs enter the aquatic ecosystem (Bhattacharya & Chakraborty, 2018), thus, deteriorating the marine and riverine environment. CPs have also been detected in effluent released from industrial manufacturing units like iron and steel, pharmaceuticals and organic chemicals, photographic pieces of equipment, electrical components, pulp & paper board mills (Eslami et al., 2018). The bleaching stage in the paper-making process uses chlorine compounds to increase the brightness of paper (Garba et al., 2019; Kringstad & Lindström, 1984) resulting in formation of CPs in the effluent. The direct sources of CPs into the marine ecosystem include discharge from sewage treatment plants, industrial processes, drinking water treatment etc. (Faizah, 1992). The strong biocidal property of PCP is exploited in the timber industry, where it is used as an anti-sapstain agent to prevent wood staining on freshly felled timber caused by fungal growth. It is also used as a treatment towards wood infected with fungal growth and to treat masonry infected with dry rot fungus. Accidental spills of PCP containing liquids, drainage from the wood treatment and storage sites can also cause local soil or water contamination. In the textile and leather industries, PCP-containing formulations deter fungal and bacterial attacks in manufactured goods. Administrative route of PCP in the environment occurs through accidental spillage, through the volatilization process during the drying stage of treated textiles which is more than the amount of PCP loss from treated woods, while a majority of the PCP is released through wastewater from textile batch treatments. The wastewater containing PCP either enters the sewage system or is directly received by waterbodies. Water undergoes a chlorination procedure as part of the drinking water treatment and is intended to disinfect the water. PCP form a consequence of reaction between added chlorine and phenols already present in the water. Therefore, PCP levels in treated water are observed to be higher than in untreated water at times

(Hamad et al., 2010). The chlorination of water has resulted in formation of some chlorophenolic by-products like DCP, TCP, TeCP (Czaplicka, 2004).

2.2.1 Natural formation (synthesis) of CPs

The reactivity of aqueous chlorine solutions to microorganisms has led to widespread use as a disinfectant for municipal water supplies and wastewaters. The reactivity insinuates the organic pollutants in aqueous medium to react and yield the chlorine-containing products (Smith et al., 1976). Though it is evident from the research that anthropogenic activity is responsible for the presence of halogenated compounds in the environment, recent explorations have validated that many organohalides are biologically synthesized (De Jong & Field, 1997) and degraded within the global halogen cycle. Milliken et al., (2004) revealed a novel biodegradation route for accumulation of CPs using a pure culture of *Desulfitobacterium* sp. strain PCE1 and mixed microbial communities from estuarine sediment. The microbial culture was subjected to degradation of 2,3,5,6-tetrachloro-4-methoxyphenol (TCMP) under inoculated under laboratory conditions. At some stage of the degradation of TCMP, the bacteria reductively dehydroxylated and dechlorinated it resulting in formation of TCP and TeCPs as major products. In a similar study, production of CPs was reported in incubated forest soil with Na³⁷Cl over a year. Chlorinated anisyl metabolites (CHMs) are synthesized by fungi in soils undergo demethylation and reductive dehalogenation by anaerobic microbial community thus producing DCP (Hoekstra et al., 1999) as well naturally.

2.3 Fate of Chlorophenols in the environment

Fate and transformation of any chemical compound's strictly hinges upon the dissociation components and the partition coefficient, piloted further based on the molecular complexity. The primary processes defining the fate and transport of CPs are sorption, volatilization, degradation, and leaching. CPs are subjected to a series of physical, chemical, and biological transformations. The significant factors

like pH of water, soil, and sediments regulate fate and transport as the compound's degree of ionization fosters surges in pH. The other physicochemical properties that define the doom of CPs in the environment are Henry's law constant, organic carbon sorption coefficient, volatilization rate, and photolysis (Guo et al., 2004). Since CPs are preferentially adsorbed on soil constituents, these processes are also influenced by environmental parameters like organic content and clay content of the soil, sediments, and water. Figure 2.1 shows the different sources of CPs and their fate in environment.

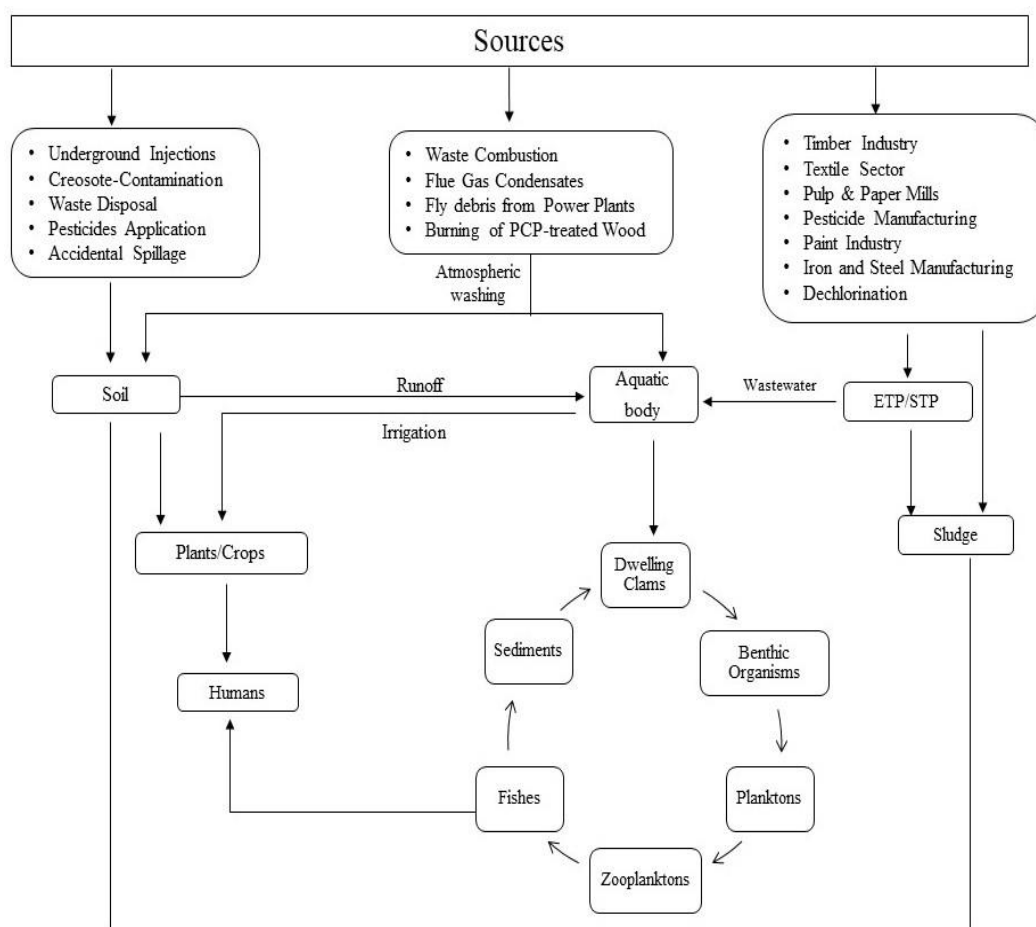


Fig. 2.1 Fate of Chlorophenols

CPs absorb the ultraviolet radiations; thus, solar degradation is possibly the principal degradation because of the overlap between their absorption spectra and the tropospheric solar spectrum. Photolysis and hydroxyl ($\cdot\text{OH}$) radical attacks are complementary processes for a few of the CPs such as 2-Chlorophenol (2-CP) and

4-Chlorophenol (4-CP), however increasing chlorination increased the photolytic degradation and decreased hydroxyl attack (Bunce & Nakai, 1989). Singlet oxygen formed by ultraviolet radiation along with hydroxyl radicals react with CPs in addition to the process of direct photolysis, resulting in CPs degradation near the water surface. As the chlorine's position on the ring strongly influences the transformation, the photolysis of MCPs in water results in dechlorination (Boule et al., 1982). Isomers of CPs undergo biodegradation in soils under the aerobic environment. The isomers are abundant by present plant metabolites that decompose sluggishly in soils compared to other soil organic matter (SOM). In soil dynamics models, parameters such as soil pH, organic carbon content, biomass, isomers of CPs, and concentration determine the rate and extent of biodegradation (Min et al., 2015). Generally, the complete mineralization to carbon dioxide (CO₂) is more generous in soils with slightly alkaline pH, low organic carbon, increased inoculum concentrations, and increased temperatures (Baker et al., 1980; Balfanz & Rehm, 1991; Adeola, 2018).

2.3.1 Properties of Chlorophenols

CPs are the chlorinated aromatic structure comprised of a benzene ring, OH group, and chlorine atoms. The major CPs, are illustrated based on their molecular configuration and physical and chemical properties, are presented in Table 2.1 All the CP compounds exist in the solid-state at room temperature, except 2-CP which occurs in a liquid state. The melting point of CPs ranges from 33°C to 191°C, and most of them are sparingly soluble in an aqueous solution (Ivanciuc et al., 2006). The acidity of CPs is proportionate to the number of chlorine that could be substituted, *i.e.*, with an increase in chlorine atoms' substitution, the acidity is correspondingly increased. The tendency of CPs to bioconcentrate and partition into sediments and lipids increases with chlorination (Chiou et al., 2005).

Table 2.1 Properties of Chlorophenols

Compound	Formula	Molecular weight	*Melting point (°C)	*Boiling point (°C)	#Density (g/cc)	#Henry's law constant (atm-m ³ /mol)	#Vapour pressure (mm Hg)	#Solubility in water (g/L)	*pKa	*Log K _{ow}	#Log K _{oc}
2-Chlorophenol	C ₆ H ₅ ClO	128.56	9.3	174.9	1.2634	6.8 × 10 ⁻⁶	0.99	28.5	8.3-8.6	2.12-2.17	1.25-3.7
4-Chlorophenol	C ₆ H ₅ ClO	128.56	43.2-43.7	220.0	1.2238	9.2 × 10 ⁻⁶	0.23	27.1	9.1-9.4	2.35-2.44	1.2-2.7
2,4-Dichlorophenol	C ₆ H ₄ Cl ₂ O	163.00	45.0	210.0	1.383	4.3 × 10 ⁻⁶	0.14	4.5	7.5-8.1	32.75-.30	2.42-3.98
2,4,5-Trichlorophenol	C ₆ H ₃ Cl ₃ O	197.45	67.0	Sublimes	1.678	5.1 × 10 ⁻⁶	0.05	0.948	7.00-7.7	3.72-4.10	2.55-3.98
2,4,6-Trichlorophenol	C ₆ H ₃ Cl ₃ O	197.45	69.0	246.0	1.901	5.7 × 10 ⁻⁶	0.03	0.434	6.0-7.42	3.60-4.05	1.94-3.34
2,3,4,5-Tetrachlorophenol	C ₆ H ₂ Cl ₄ O	231.89	116.0-117.0	Sublimes	1.67	1.3 × 10 ⁻⁶	0.0059	0.166	6.2-7.0	4.21-5.16	2.9-4.14
2,3,4,6-Tetrachlorophenol	C ₆ H ₂ Cl ₄ O	231.89	70.0	64.0	1.83	3.6 × 10 ⁻⁶	0.0059	0.183	5.3-6.6	4.10-4.81	3.2-4.21
2,3,5,6-tetrachlorophenol	C ₆ H ₂ Cl ₄ O	231.89	115.0	288.0	1.84	2.2 × 10 ⁻⁶	0.0059	0.1	5.2-5.5	3.88-4.92	3.88-4.90
Pentachlorophenol	C ₆ Cl ₅ OH	266.34	190.0	310.0	1.987	na	0.0002	0.01	4.74-4.9	5.01-5.86	5.01

Octanol–water partition coefficient (K_{ow}); organic-carbon partitioning coefficient (K_{oc}); dissociation constant (pKa); not available (na) (Source: #Olaniran and Igbinsosa, 2011; *Czaplicka, 2004)

The number of chlorine atoms outlines vapour pressure and water solubility, decreasing with an increase in chlorine atoms. In contrast, the boiling point of CPs increases with an increase in the chlorine atoms. The quantity of chlorine atoms also governs the degree of dissociation of CPs. It may be inferred that the stability/bio accumulation and toxicity of CPs is proportional to the number of chlorine atoms present in a compound.

2.4 Ecotoxicity of CP

Toxicity is the ability of the chemical substance to affect the biological systems adversely. It is generally related to the degree of exposure, chemical dose, exposure time and, the biological system properties (Priyadarshane et al., 2022). Certain phenols increase the number of neurotransmitters released during synaptic transmission, resulting in seizures. CPs toxicity is centred to the extent of chlorination and the orientation of the chlorine atoms in respect of the hydroxyl group. CPs with the chlorine atom substituted at position 2- are less toxic, whereas chlorine at the 3-, 4- and 5- positions in chlorophenolic compounds are relatively more toxic. This monotony may account for higher toxicity of 3,4,5-TCP compared to other CPs. 2,6-DCP is less harmful than 3,5-DCP because of the configuration of chlorine atoms substituted at the positions 2- and 6- which lessens the toxic properties of CPs (Saito et al., 1991; Salkinoja-Salonen et al., 1983). Considering the substantial toxicity of CPs and their prevalence in different environmental components, the effect has been reported on exposed organisms present in soil, water, vegetation, etc.

2.4.1 Effect of PCP on soil

Pollutants come in contact with soil primarily through the application, dispersion, or atmospheric deposition. PCP persists as a non-ionized form in the atmosphere, undergoes washout processes, and gets deposited over soil. In soil, it is generally adsorbed on the soil particles. The pollutant is expected to be found on the surface horizon because of its application as herbicide, biocides, and wood

preservatives (Faizah, 1992). The presence of such pollutants is directly associated with the biology of soil. PCP is expected to have a half-life of weeks to months depending upon the microbial population persisting in the soil. It reduces the microorganisms by destroying the membrane due to uncoupled oxidative phosphorylation and decreasing the enzymatic activities (Gałązka et al., 2018; Siczek et al., 2020). Rhizosphere soil, which is rich in plant exudates and mucilage, differs significantly from bulk soil in terms of microbial growth, abundance, diversity, and behavior and substantially affect plant productivity (Eisenhauer et al., 2017; Yang et al., 2017). In the faba bean rhizosphere investigated by Siczek et al., (2020), the most abundant bacterial phyla population, *Actinobacteria*, and *Proteobacteria*, were significantly reduced. The carbon utilization efficiency of certain indigenous microbes was also decreased because of contaminated soil. PCP significantly reduces dehydrogenase, respiration, protease, urease, and β -glucosidase activity (Siczek et al., 2020). The harmful effect of PCP has been noted for enzymes related to the nitrogen cycle, e.g., protease and urease. The effect of PCP on the metabolism and function of denitrifying bacteria (Zheng et al., 2014) revealed that the contact of PCP to *Paracoccus denitrificans* bacteria induced reduction of the critical enzyme activities connected to glycolysis process, thus obstructing the metabolism of glucose utilization and cell growth, subsequently disrupting the generation of electron donor (NADH) for denitrification via decreasing NAD^+ . PCP significantly inhibited the denitrification at higher concentration further disturbing the nitrogen cycle in soil (Chen et al., 2016). It also hamper, the functioning of intracellular enzymes within the living cells of microorganisms. The phenolic compound also affect the extracellular enzymatic activity, thus reducing the rate of litter or soil SOM decomposition (Bernhard-Reversat, 1998; Northup et al., 1998). The decomposition rate of litter is inversely proportional to the concentration of phenolic compounds (Min et al., 2015).

As a primary interface with other environmental compartments, soil plays a vital role in defining the fate of organic pollutants. PCP-contaminated soil poses a severe threat to plants. In ryegrass, the development of root exudates was impaired by PCP contamination. The roots produced less citric acid and more malic and

succinic acids (Urrutia et al., 2013). The laboratory studies revealed a decrease in root length, plant biomass (aerial and root), and germination. Studies with *Triticum aestivum* demonstrated a similar outcome when PCP concentration of 100 mg kg⁻¹ decreased plant growth (Dams et al., 2007). Adverse effects on the *Rhizobium leguminosarum* population in a concentration-dependent manner have also been reported (Chaudri et al., 1996; Fox et al., 2007). It blocked the mechanism of nitrogen fixation by legumes via inhibiting the luteolin-induced nod gene expression by 90%. During cell differentiation, the apical meristematic cell functioning is related to root growth inhibition, cell elongation, and enzyme activation (Silveira et al., 2017). Root proliferation suppression was observed in *Allium cepa* (onion) and *Vigna radiata* (mung bean), resulting in reduced root growth when grown in PCP contaminated soil (Ranjan et al., 2021). In *Lactuca sativa* too, PCP inhibited both root length and shoot length (Martí et al., 2007).

2.4.2 Effect of PCP on aquatic biota

During the treatment of crops, much of the PCP applied as pesticides reach the soil, either because it is used directly or because the rain washes the foliage of treated plants (crops or weeds). The ground, therefore, occupies a position in central, representing a storage reservoir for these compounds. The agricultural surface runoff carrying the contaminated soil, and direct discharge of CP-contaminated industrial wastewater, is received by flowing streams, further alarming the aquatic ecology. The majority of known environmental release of CPs occurs to surface water. They exist in adsorbed on sediments and suspended organic matter depending on the condition in aquatic environment conditions. Waterbody sediments typically contain much higher levels of PCP than the overlying waters. PCP may then be released from the sediment deposits into the overlying water (Faizah, 1992). Thus, sediments act as both a sink and a source of PCP to the water (DeLaune et al., 1983). Sediment-dwelling organisms, like clams, have shown PCP levels of up to 133 mg/kg (IPCS, 1987). The residual CPs present in the aquatic environment can quickly accumulate in the tissue of living organisms (Ge et al., 2017a). Low levels of dissolved oxygen, low pH, and high temperature can further

enhance the toxic effects of PCP (Ge et al., 2017b). In addition to fish, various PCP bioassays have been performed on marine species for toxicity research that includes amphibians, benthic and planktonic invertebrates (Barahona & Sánchez-Fortún, 1996; Lawrence & Poulter, 1998). Algae is the most sensitive aquatic organisms, as little as 1 µg/litre of PCP can cause significant inhibition of the most sensitive algal species. Most aquatic invertebrates (annelids, molluscs, crustacea) and vertebrates (fish) are affected by PCP concentrations below 1 mg/L resulting in acute toxicity. Cladocerans, in particular daphnids, are the group of organisms dominating the zooplankton and littoral microfauna. These planktonic crustaceans being cosmopolitan in nature, are illustrative of diverse ecologically significant filter-feeding zooplankton taxonomic groups (Willis et al., 1995). They feed primarily on bacteria, algae, and protozoans and serve as a substantial food source for fish and other aquatic vertebrates (Lawrence, 1981; Poirier et al., 1988). Toxicity test on three age classes of *Daphnia magna* using pure PCP and technical PCP by Stephenson et al., (1991) found that pure PCP was equally toxic to all age classes; however, susceptibility to technical PCP was decreased with maturation. Cyclically parthenogenetic zooplanktons like rotifers are essential tools for the assessment of toxicity in aquatic ecosystems. The effect of PCP on both the sexual and asexual reproduction modes on rotifer, *Brachionus calyciflorus* has been studied (Snell et al., 1995). As sexual reproduction in rotifers is more sensitive to environmental stresses than asexual reproduction (Lubzens et al., 1985; Snell, 1986; Snell & Boyer, 1988), PCP exposure inhibits the initial mode of female sexual reproduction. The accumulation of toxicants significantly decreases the egg development without affecting the asexual reproduction. Toxicity of 2,3,4,6-TeCPs and PCP in female *Brachionus calyciflorus* carrying eggs recorded mortality among most adult females several hours prior to the hatching of the egg. (Liber & Solomon, 1994). The effect over *Artemia salina* was tested for eight phenolic compounds, including PCP (Barahona & Sánchez-Fortún, 1996), and the most toxic compounds for the three age ranges of the species were 2,4-DNP and PCP. Studies report that *Artemia salina* species (48 and 168 hours mature) are more susceptible to PCP than rotifers such as *Brachionus calyciflorus* (Ferrando et al., 1992).

Accumulation of CPs in fishes (with accumulated levels between 100 to 200 mg/kg body weight) results in lethal toxicity to fish (Kishino & Kobayashi, 1995; Kobayashi et al., 1979). CPs tend to accumulate in salmon embryos and adult *Oryzias latipes* (Japanese medaka) (Holcombe et al., 1982; Kondo et al., 2005). The tendency of CPs to accumulate depends upon environmental factors like temperature, pH, CPs species, number of chlorine atoms present in CPs species, other pollutants like nanoparticles, etc (Hanson et al., 2007; Kan et al., 2015; Kishino & Kobayashi, 1995; Yen et al., 2002). The accumulation of CPs in fish increases in exposure- and time-dependent manner. PCP concentration in *Oncorhynchus mykiss* (rainbow trout) increases with increase in concentration of PCP and its exposure periods (Niimi & Cho, 1983). Goldfish (*Carassius auratus*) exposed to PCP medium reported higher accumulation of PCP in the gallbladder, whereas the accumulation rate is lower in blood, hepato-pancreas, gills, blood, digestive tract, muscles, and kidney (Kobayashi et al., 1979). In general, fish embryos at early developmental stages are more sensitive to CPs. Because of variation of metabolic rates in different developmental stages, the sensitivity to CPs among embryonic, larval, and adult fish is significantly different (Holcombe et al., 1982). CP also induce mortality at early embryonic stage by binding to mitochondrial proteins and suppressing the activity of mitochondrial ATPase (Janik & Wolf, 1992). The compound also inhibits the expression of oxidative phosphorylation-related genes in fish, thereby affecting ATP production (Xu et al., 2014). The free radicals produced by the electron transport chain in fishes are eliminated by antioxidants (Ott et al., 2007). Excess of free radicals is a consequence of alterations in antioxidant enzyme activity, resulting in oxidative stress, indicated by the generation of reactive oxygen species (ROS) (Fang et al., 2015). Goldfish expressed ROS production when exposed to 4-CP or 2,4,6-TCP (Ji et al., 2007; Luo et al., 2006, 2008). Increased ROS levels further cause damage to proteins, lipids, DNA and may induces apoptosis (Fang et al., 2015; Luo et al., 2005). The disrupted mitochondrial function is directly associated with PCP-induced apoptosis. CP induce apoptosis by uncoupling oxidative phosphorylation of the substrate from ATP synthesis in mitochondria, converting the energy released by the electron transport system into heat instead of ATP. (Fern et al., 2005).

However, PCP is reported to reduce ATP production by suppressing the enzymes involved in ATP synthesis in *G. rarus* (Fang et al., 2010). CPs also impede the inflammatory response by obstructing the expression and secretion of immune factors at protein and molecular levels. (Luo et al., 2005). Thyroid hormones play a vital role in many metabolic processes, growth, development, and reproduction in vertebrates (Brown et al., 2004). Thyroxine (T4) is a prohormone secreted by the thyroid and is converted to triiodo-L-thyronine (T3) by deiodinases in fish. The deiodinases in fish share similarity with mammalian deiodinases (Dio1, Dio2 and, Dio3). Dio1 and Dio2 function externally in peripheral organs such as gills and kidneys. Dio3 has inner ring deiodination activities and takes T4 or T3 as the substrate to produce reversed T3 (rT3) or T2. Exposure to CPs influences the synthesis, transport, and binding of thyroid hormones, catabolism, and clearance (Yu et al., 2014). Introduction of zebrafish embryos to an established PCP concentration (10 µg/L for 96 hours and 14 days) resulted in decreased levels of thyroxine (T4) and elevated triiodo-L-thyronine (T3) whole body material (Cheng et al., 2015; Guo & Zhou, 2013). CPs can also hamper the T4 compensation while facilitating hyperthyroidism triggered by the down-regulation of circulating T4 and up-regulation of T3. The compounds fundamentally alter the levels of plasma thyroid hormone and thwart the expression of iodothyronine deiodinase. CPs have double the affinity to serum transthyretin (TTR) as T4, thereby effectively inhibiting the mechanism of T3 binding to TTR. CPs may compete with thyroid hormone receptors (THRs) as well and disrupt the transcription of genes necessary for development, growth, and reproduction. As their chemical structure parallels that of estrogen, CPs also bind competitively to estrogen binding receptors, resulting in inhibition of estrogen sulfotransferases. Exposure to CPs incites alteration of gene expression (Cyp17, Cyp1a, Cyp19a, Cyp17, 3βhsd, 17βhsd) consistent with sex hormone synthesis and process pathway. They also change the mRNA levels of estrogen receptor (ER), influencing the expression of vitellogenin (VTG) mRNA and eventual VTG protein synthesis. The CPs-ERs complex thus formed is transferred into the VTG promoter, which initiates VTG transcription. The impact of VTG expression by CPs has been investigated in teleosts such as *D. rerio*, *O. latipes*, and *G. rarus* (Menuet et al., 2004; Yamaguchi

et al., 2005; Zhang et al., 2008). CPs have inherent potential as direct-acting ER-agonists as 2,4-DCP, and PCP dramatically increase the mRNA levels of ER β 1 and ER β 2 in male *G. rarus*. The compounds may serve as an antagonist for the androgen receptor. Heedlessly of the estrogenic, anti-estrogenic, or anti-androgenic effects on organisms, CPs are potential endocrine disruptors that interfere with ER-mediated processes (Li et al., 2010; B. Zhao et al., 2006). In general, however, after CPs disperse across aquatic living species, they typically interrupt the metabolism of free radicals, reaction to immune factors, apoptosis, and normal thyroid and gonad activity. The toxicity of CPs eventually causes multiple organs and endocrine systems to malfunction, leading to irregular growth and malformation and reduced reproductive rates. CPs also facilitate the expression of proliferative factors and induce carcinogenesis. The offsprings may inherit genetic mutations caused by CPs. Elevated levels of CPs could become a significant threat to fish and other populations in marine ecosystems and the biosphere (Ge et al., 2017a).

2.4.3 Effect on human beings

The main concern about CP contamination in the ecosystem is their propensity to contaminate aquatic ecosystems (ground and surface waters), posing a significant risk to humans and other animals associated with the aquatic eco-biota food chain. Due to its pervasive use in treatment goods such as textiles, leather, and paper products, and consuming PCP polluted water, the public can be susceptible to PCP. The toxicity of PCP is associated with decoupling oxidative phosphorylation, allowing protons to pass through cell membranes. The H⁺ ions and electrical potential gradient are dissipated, resulting in alterations in membrane functionality (Steiert et al., 1988).

Occupational Exposure

Farmers and agricultural workers in rural communities and the workers engaged in manufacturing industries are at risk for hematopoietic tumours (Greaves, 2004; Van Maele-Fabry et al., 2007). They often suffer from lung cancer,

heart disease, sarcoma, non-Hodgkin's lymphoma, asthma. Drinking CP-contaminated water (present as a by-product of water disinfectant with chlorinated oxidants) often leads to respiratory illness, gastrointestinal infections, and morbidity (Hooived et al., 1998). Residues of PCP have been reported in the human liver, testes, prostate gland, and adipose tissues. The increased concentration of PCP in the blood leads to increased interleukin-8 serum levels, dysfunction of T-lymphocyte, sometimes increasing the lymphocytic responses (Daniel et al., 2001, 1995).

DNA damage and Oxidative Stress

Exposure to chlorinated compounds causes the DNA strands to break (single or double) and oxidation of DNA bases. CPs and their derivatives induced oxidative DNA damage was studied using lesion-specific enzymes Endonuclease III (Endo III) and Formamidopyrimidine-DNA glycosylase (Fpg) (Andersson & Hellman, 2005; Collins et al., 1993; Michałowicz & Majsterek, 2010). The enzymes were responsible for monitoring the oxidized pyrimidines and purines at the DNA damage sites. DNA damaging effects were observed with samples treated with both the above-mentioned enzymes proving oxidation of both purines and pyrimidines by the CPs. PCP, when present in lower concentrations, is reported to induce chromosomal aberrations too. PCP-intermediate like tetrachlorohydroquinone (TCHQ) and other harmful intermediates result in the formation of tetrachlorosemiquinone radical, enhancing DNA damage and handicaps mechanism of DNA repair. DNA strand breakage in mammalian cells, the conjugation of glutathione and the decrease in the content of glutathione in the liver tissue is induced by TCHQ (Wang & Lin, 1995; Wang et al., 1997). Another PCP-metabolite, 4-chlorohydrocarbohydrate induces necrosis and have the ability of breaking DNA chains, resulting in severe toxicity of PCP. The tissue injuries catalysed by free radicals, play a fundamental role in human disease. 2,4-DCP increased the carbonyl content in human erythrocytes, interrelated with increased production of reactive oxygen species. CPs are potential source of formation of ROS, oxidizing lipids and protein as well (Bukowska et al., 2007; Bukowska et al.,

2008; Duchnowicz & Koter, 2003). It is reported to undergo oxidative dechlorination in the human liver forming TCHQ. The auto redox reaction between TCHQ and semiquinone radical results in production of superoxide radicals in the presence of oxygen.

Carcinogenicity

The most consistently observed relationship between cancer and CPs exposure is the non-Hodgkin's lymphoma (Garabedian et al., 1999) and soft tissue sarcoma (Hoppin et al., 1998). CPs are also responsible for cancers of lung, kidney, nasopharyngeal and sinonasal cancer and multiple myeloma (Mirabelli et al., 2000). Microsomal activation of cytochrome P450 hepatocytes is associated with cancer development in humans exposed to CPs (Tsai et al., 2001). The oxidation of xenobiotic results in their conversion to electrophilic forms which then interacts with the cell structures. PCP induces oxidative stress and proliferation of hepatocellular cells, thus, causing liver carcinogenesis, however a PCP-metabolite, TCHQ in liver enhances toxicity and carcinogenicity, and inducing oxidative damage to cellular DNA (Umemura et al., 1999). PCP inhibits the process of apoptosis in liver and bladder, promoting tumour formation (Sai et al., 2001; Wang et al., 2000b; Wang et al., 2001). Balanced hormonal environment governs the functioning and development of thyroid hormone. CPs affects the levels of the hormone disrupting the endocrine receptors or inducing abnormal gene expression. Because of the similarity in the structure of CPs and estradiol, the former binds competitively with estrogen-receptors α and β inducing interference of thyroid, eventually leading to the occurrence of thyroid cancer (Yang et al., 2021). When present in lower concentrations, CPs trigger cell proliferation, fostering the cancer-prone environment which further increases the rate of oxidative lesions and point mutations (Ge et al., 2017b). Dose-response relationship presented a positive correlation between thyroid cancer and 2,4-DCP; 2,4,6-TCP and PCP (Yang et al., 2021). The functioning of thyroid hormone is also adjourned to the immune state of the individual as well. Immune system plays a decisive role in inducing carcinogenesis (Upadhyay et al., 2018). PCP alters the lytic and binding functioning

of natural killer cells in humans, further hampering the tumor destroying function. It stimulates immune cells to produce Intraleukin, IL-6 thus inducing cancer and causing chronic inflammation (Martin et al., 2019; Massawe et al., 2017). CPs such as DCP reduces the mitochondrial membrane potential, alters the cell cycle while damage to DNA and leads to apoptosis of immune system cells (Lone et al., 2017). Throughout the years, studies on environmental contamination have focused on the fate of CPs in ecosystems. They along with their metabolites pose a health hazard to numerous organisms. It is both relevant and important to reduce the input of these xenobiotic chemicals into the environment and to study methods for their removal from contaminated sites. It'll further aid in developing management strategies to minimize their persistence in the environment.

2.5 Treatment of chlorophenols

Owing to their widespread and toxic effects on living species, the eradication of CPs has dragged more attention in recent years. So far, both abiotic and biotic methods have been investigated to remove CPs. Biotic degradation of CPs involves bacteria and fungi, while abiotic degradation incorporates multiple approaches like photolysis, adsorption, ion exchange, and chemical degradation. The degradation of CPs is very complex under natural conditions and cannot be quickly processed for the following reasons: first, the aromatic rings in CPs are relatively stable; second, the degradation of CPs is typically incomplete; third, the degradation mechanism is greatly influenced by the pH in water, soil, and sediment.

2.5.1 Natural attenuation of chlorophenols

CPs in the natural environment are degraded through photochemical reactions. They are physically transformed by evaporation or adsorption, accompanied by oxidation and hydrolysis. The photochemical processes comprise reactions like photo-dissociation, photo-substitution, photo-oxidation, and photo-reduction. CPs are wholly or partially decomposed by photochemical reactions caused via UV-Vis irradiation and biodegradation (Czaplicka, 2004). The CO₂,

H₂O, and Cl are the end products of the decomposition processes of CPs in the atmosphere. Various factors such as the wavelength of radiation, exposure time, state of reaction environment, and the maximum light absorption by the compound undergoing the process govern the photodegradation process. The process is also affected by occurrence form of CP-compound (non-dissociated or anionic phenolates), pH of environment, position of chlorine atom *w.r.t* hydroxyl group. Chlorine located at 4- and 6- position is photo-labile whereas non-photoreactive at 3rd and 5th position (Kochany and Boltan, 1991). The phenomenon of photodegradation predominates in the air and marine habitats. The mechanism and kinetics of the photo degradation of CPs in ambient air, conducted by Bunce & Nakai (1989) described co-occurrence of both the immediate photolysis and the hydroxyl radical attack. The photolytic degradation's efficiency of MCP, DCP and TCP is considerably lower than that of the radical reaction. DCP degradation when irradiated with 254 nm light formed chloroquinone and chlorocyclopentadiene acid isomers whereas in another study with DCP, hydroxybenzoquinone, 4-chloro-1,2-benzenediol, 1,2,4-BT, polymeric humic acid products were observed (Boule et al., 1982). Photodegradation of CPs in the water affects the direct photolysis of CP or CP's reaction among the oxygen singlet and the peroxy radicals produced by sunlight (Crosby & Wong, 1978; Kawaguchi, 1992; Nakagawa & Shimokawa, 2002; Ononye et al., 1986). Degradation process is rapid during summers as compared to winters (Kawaguchi 1992). For instance, half-time of MCP (2-CP) was season-dependant for a year. Half-life of 2,4-DCP has been reported 0.8h in summers while it was 3h during winters. In a proposed photodegradation pathway of a 2-CP, cleavage of C-Cl bond was followed by C-OH bond as a result of combined oxygen and hydroxyl radicals effect at ortho-position (Boule et al., 1982). According to the Diels- Alder reaction, the photodegradation of anionic forms results in pyrocatechol or cyclopentadienic acid dimers as product of non-dissociated molecules (Boule et al., 1982; Czaplicka, 2004). Hydrochloric acid emerged as by-product of the reaction. In another meta-positioned 3-CP, UV irradiation generated resorcinol as final product. Apart from photodegradation, light-induced other process such as photooxidation, photomineralization and

photocatalytic degradation of organic chloroderivatives in the aquatic environment have been studied across.

2.5.2 Oxidation and Evaporation

CPs consisting of higher chlorine atoms in a molecule are usually immune to the oxidation process under ambient temperature. The rate of oxidation is governed by temperature and the concentration of the compound present in the environment. It is further enhanced with the increase in temperature. CPs undergo auto-oxidation reaction and catalysis predominantly on surfaces comprised of clay and silica. Metal ions particularly catalyze the reactions (Czaplicka, 2004). The behaviour of CPs is also affected by the evaporation process under natural conditions. The evaporation rate is governed by water vapour pressure and solubility (Henry's law constant). Under laboratory conditions, evaporative processes significantly removed CPs from the water (Chiou et al., 1980; Piwoni et al., 1986). The process was observed by Drever (1997) during the rapid mixing of waters. The evaporation of CPs also takes place from shallow surface water when the temperature is above 20°C.

2.5.3 Sorption

The sorption of CPs is a function of their partition coefficients between water and solid phase sediments, or suspended particulates. The properties of CPs in the water, especially in bottom sediments and on the suspended matter, are favorable for their accumulation (Boyd, 1982; Peuravuori et al., 2002; Schellenberg et al., 1984). The mechanism is not solely reliant on their lipophilicity but is also strongly influenced by the presence of any other chemical compound, pH and number of chlorine atoms in the compound (Xie et al., 1986). CPs accumulate in sediments depending upon the nature and concentration of organic matter's (Czaplicka, 2004). CPs form covalent bond with organic matter thus influencing the release of bound PCP in sediments. The reaction between organic matter and CPs is either biologically or chemically catalysed. The increased amount of

dissolved humic matter affects the equilibrium partitioning of PCP between the solid sediment matter and dissolved humic matter (Paaso et al., 2002). The distribution of PCP in octanol-water and soil-water solutions is affected by solvents and sorbents. Non-equilibrium sorption study conducted revealed the transport of CPs in soil relies on extent of ionisation of solute ($\text{pH}-\text{pK}_a$), increased solubility due to co-solvent effect and production of ionic pairs as result of electrolyte effect (Brusseau and Rao, 1991). The transport movement velocity is influenced by equilibrium sorption coefficients, octanol-water partition coefficients; dissociated or non-dissociated form of compound, however, the ionised form is more susceptible to leaching as compared to the later (Drever, 1997). The CPs leach to groundwater from PCP-contaminated sandy soil or soil where biodegradation is slow. The sorption kinetics of PCP in the soil is affected by its concentration and other organic structures such as benzoic acid, lactic acid, and catechol (Divincenzo & Sparks, 1997).

2.5.3.1 Adsorption

Owing to the simplicity in design and applicability, kinetics, effectiveness, and universal nature, the adsorption of CPs is influenced by factors like temperature, pH, and forces involved. In case of endothermic process, increasing temperature increases the adsorption process by virtue of increasing the mobility of adsorbate, thus increasing the active sites for adsorption (Yagub et al., 2014). High temperature eliminates the influence of repulsive forces which act as barriers during the process (Olu-Owolabi et al., 2017). In addition, raising the temperature was observed to increase the surface activity and diffusion rate of CP molecules in both the external boundary layer and the internal pores of the adsorbent particle due to the decline in solution viscosity (Agarry et al., 2013). Uptake of phenolic compounds by adsorbents increases under acidic pH whereas in alkaline conditions, occurrence of hydroxyl group and dissociation of carboxyl groups decreases the efficiency of the process (Caqueret et al., 2008). Various adsorbents ranging from the most widely used activated carbon, agricultural wastes, nanomaterials, industrial by-products, inorganic materials, and biosorbents have been applied to

remove CPs from wastewater. Adsorption of 2,4-DCP, methylene blue, and tetracycline on polyamide (PI)-based carbon nanofibers (CNFs) was found ideal for their elimination. The reusability of PI-based CNFs showed that removing 2,4-DCP kept its efficiency high even after five consecutive cycles (Zhang et al., 2018a). Efficient removal of 2-chlorophenol, 2-chloroaniline, and methylene blue onto fuel oil fly ash has been reported (Andini et al., 2008). Composites of Carica-papaya-model-kaolinite (CPK) and pine-cone-modified (PCK) were prepared for removal of 2,4,6- TCP by the calcination of pure Kaolinite (KAC) (Olu-Owolabi et al., 2017). CPK and PCK were comparatively quicker to adsorb 2,4,6- TCP (30 minutes) and attain equilibrium than KAC (60 min). Modifications increased adsorption in PCK and CPK by 52% and 250%, respectively, and with temperature, the adsorption process increased. The performance of different carbon structures, including single-walled carbon nanotubes (SWNT), multi-walled carbon nanotubes (MWNT), nanocarbon (NC), carbon nanofibers (CNF), nanoporous graphene (G), and mesoporous carbon (CMK), have also been examined as sorbents for the removal of 4-chlorophenol from water (Madannejad et al., 2018). CMK reported the highest balance adsorption potential for various nanostructures and preserved nearly 90 percent of its initial adsorption capacity even after three regeneration-reuse cycles, owing to its surface characteristics. The aqueous phase adsorption mechanism of 2-chlorophenol used zeolite and cetyl trimethyl ammonium bromide (CTAB) as an adsorbent attributing to the strong binding between the cationic head groups of loose CTAB bilayers and polarizable aromatic moieties of the CP (Peng et al., 2017). Adsorption of TCP increased on increasing the temperature from 20 to 50°C over oil palm empty fruit bunch activated carbon. Enhanced adsorption of 2,4,6- TCP on montmorillonite has also been reported under acidic pH (2.0-5.0) whereas further increasing pH decreased the adsorption (Yang et al., 2017). Similar effect of pH has been observed with DCP and para-CPs on activated carbon adsorbent prepared from *Prosopis Africana* seed hulls (Garba and Rahim, 2016). Under alkaline conditions, CPs dissociate into chlorophenolate ions leading to intra as well as inter-electrostatic repulsion among chlorophenolate-chlorophenolate anions and chlorophenolate and negative surface charge of adsorbent. The negative surface charge of the adsorbent is attributed to their chemical characteristics *w.r.t*

acidic point of zero charges (pH_{pzc}). pH_{pzc} lesser than pH of the solution will cause the total negative charge on the surface (Garba and Rahim, 2016).

2.5.4 Membrane Technology

Membrane technology has become one of the prominent methods for the removal of CPs which includes micro filtration, nano-filtration and ultra-filtration. Membrane separation is considered one of the most efficient technologies for removal of CPs from wastewater because of low capital cost, easy to augment scale, and eco-friendly production with lesser emission of residual toxic compounds (Raza et al., 2019). Hidalgo et al., (2013) investigated the use of three different polyamide membranes (NF-97, NF-99 and RO98pHt) for nano-filtration for the removal of 4-MCP in which the pressure and initial concentration was varied. The rejection coefficient of the RO98pHt membrane was reported to be highest which leads to the lowest permeate flux. On the other hand, NF-99 membrane had the lowest rejection coefficient leading to the highest permeate flux. In another study by Musteret et al., (2017), in a laboratory scale set-up, author used AFC 40 membrane nano-filter. It was reported that the parameters which influence CP removal efficiency are pressure, cleaning conditions and different initial concentrations of CPs. For lower pressure and low concentration of CP, the removal efficiency was reported upto 85%. However, it was suggested that for removal of higher concentration of CP from wastewater, the nano-filtration technology can be coupled with other wastewater treatment methods such as AOPs and adsorption.

2.5.5 Microbial degradation of Chlorophenol

The two crucial pathways for reducing CPs from the water-soil system are biological transformation and degradation. (Czaplicka, 2004). Poly-CPs are more recalcitrant to bacterial degradation than MCPs because of the stability induced by more chlorine atoms at the phenolic rings (Arora & Bae, 2014). Various studies using different cultures and strains of bacteria under aerobic and anaerobic

conditions (Table 2.2) have been carried out. The best-described bacterium that degrades CP under anaerobic conditions is *Desulfomonile tiedjei*, a purely anaerobic Gram-negative sulfate-reducing bacterium, while the aerobic degradation of CPs by microorganisms requires enzymes such as oxygenases which incorporate atmospheric oxygen into their substrates (Olaniran & Igbinosa, 2011). Strains of *Norcadia*, *Pseudomonas*, *Bacillus*, and *Mycobacterium Coeliacum* have been used in aerobic degradation of (Fulthorpe & Allen, 1995; Uotila et al., 1992) 2,4,6-TCP, 2,4,5-TCP, 3-methyl-4-chlorophenol, and PCP (Ahel et al., 1994). Pure PCP-degrading cultures can be effective for bioaugmentation in the remediation of soils and water contaminated with PCP (Bielefeldt & Cort, 2005; Crawford et al., 2007). MCPs act as the carbon and energy source for bacteria *Pseudomonas knackmussii* B-13 (previously known as *Pseudomonas* sp. B-13), *Ralstonia pickettii* LD1 (previously known as *Pseudomonas pickettii* LD1), *Rhodococcus opacus* 1G, *Alcaligenes* sp. A7-2, *Alcaligenes xylosoxidans* JH1, *Arthrobacter ureafaciens* CPR706, *Arthrobacter chlorophenolicus* A6, and *Herbaspirillum chlorophenolicum* CPW301 (previously known as *Comamonas testosteroni* CPW301) (Arora and Bae, 2014). Degradation of MCP occurs via two pathways categorized on the basis of the first degradation product. In Chlorocatechols (CC) pathway, the first intermediate form is CC which further undergo either ortho- or meta- ring cleavage. Ortho cleavage results in formation of Chloromuconate, and dechlorination of chloromuconate produces cis/trans-dienelactone which further generates maleyacetate. In case of meta-cleavage of 4-CP, 4CC produces toxic intermediate 5-chloro-2-hydroxyruconic semialdehyde which proceeds with formation of 5-chloro-2-hydroxypent-2,4-dienoic acid. Complete degradation of 4-CP was observed in *Comamonas testosterone* via CC pathway. In the hydroquinone (HQ) pathway, hydroquinone is formed from dechlorination (Bae et al., 1996). HQ further produced 1,2,4-BT which results in formation of maleyacetate. The end-products of both pathways then enter the citric acid (TCA) cycle and are mineralized. Similar CC degradation pathway via ortho-cleavage was observed in 2,4-DCP with suspended and immobilized cells of *Bacillus insolitus* (Wang et al., 2000a). Another study on O-cresol grown cells of *Cupriavidus necator* JMP222 caused removal of the DCP via distal meta-cleavage (Koh et al., 1997). Bacterial

degradation of TCPs studied using *Cupriavidus necator* JMP134 for 2,4,6-TCP and *Burkholderia phenoliruptrix* AC1100 for 2,4,5-TCP removed the pollutant via HQ pathway (Matus et al., 2003; Coenye et al., 2004; Webb et al., 2010). *Sphingomonas chlorophenolicum* L-1 has been reported for degradation of PCPs (Ohtsubo et al., 1999). Hydroxylation of the compound at para-position catalysed by monooxygenase results in formation of TCHQ indicating the process via hydroquinone pathway. Sequential dehalogenation of TCHQ resulted in production of 2,6-dichlorohydroquinone. The process then leads to formation of chloromallyacetate which further degraded via TCA cycle. In another experiment with *Mycobacterium chlorophenolicum* and *M. fortuitum*, PCP hydroxylation was initiated via P-450 cytochrome resulting in formation of TeCHQ. It further underwent hydrolytic and reductive dehalogenation forming 1,2,4-BT. The TCA cycle later process the abovementioned compound to CO₂ and H₂O (Uotila et al., 1992).

Few CPs like 2,4-DCP, 2,6-DCP, and 2-CP can be degraded microbially under aerobic and anaerobic conditions, though the pace of biodegradation is relatively slower. Process via reductive dehalogenation under anaerobic degradation involves replacement of chlorine atoms by hydrogen atoms (Field & Sierra-Alvarez, 2008). Although the biodegradation of PCP is relatively quick under anaerobic conditions than under aerobic conditions, the dechlorination of PCP under anaerobic conditions produces a mixture of tetra-, tri- and di- CPs. Further degradation of these intermediates results in formation of CH₄ and CO₂, thus, leading to mineralisation. Under anaerobic conditions, phenol-dehalogenating culture removes chlorine from PCP producing phenol and under reducing conditions (via iron or sulphate) phenol-degrading culture further degrades phenol (Yang et al., 2009a). In anaerobic sediment slurry reactors, Becker et al., (1999) examined two biotransformation pathways for 2-CP. In one pathway, the degradation process proceeds with reductive dehalogenation of parent compound forming phenol followed by its carboxylation thus, forming 4-hydroxybenzoic acid and at the end dehydroxylation results in formation of benzoic acid. In the other pathway, the carboxylation MCP at para- position resulted in formation of 3-chloro-

4-hydroxybenzoic acid which further dehydroxylated to 3-chlorobenzoic acid. In another study (Boyd and Shelton, 1984), the mineralization of ^{14}C -radiolabeled 2,4-DCP was studied in acclimated sludge where it was mineralized *via* 4-CP \rightarrow phenol \rightarrow 4-hydroxybenzoic acid \rightarrow benzoic acid \rightarrow $\text{CH}_4 + \text{CO}_2$ pathway. Anaerobic degradation and reductive dechlorination of CPs is favoured under methanogenic, denitrifying and reducing environment (Arora and Bae, 2014). Mineralization of CP has also been reported using sulfate reducing consortia from estuarine sediment with MCP as the sole source of carbon and energy (Hagglom and Young, 1995). Complete mineralization of 4-CP was observed under sulfate reducing environment where sulfate, sulphite or thiosulfate acted as electron acceptors (Hagglom and Young, 1995). Methanogenic consortia reductively dechlorinate PCP and TeCP while transformation of TCP has been reported by sewage sludge derived methanogenic enriched culture (Nicholson et al., 1992). Degradation of MCP from activated sludge enriched cultures reports complete mineralization where nitrate acts as an electron acceptor. CP-mineralizing sulfate reducing consortia from estuarine sediment mineralized 4-CP into CO_2 and pure bacterial cultures of *Desulfitobacterium hafniense* PCP-1, *D. hafniense* DCB-2, *D. dehalogenans* IW/IU-DC1 and *D. chlororespirans dehalogenates* have dehalogenating property towards CPs under anaerobic conditions (Villemur, 2013; Christiansen and Ahring, 1996; Mohn and Kennedy, 1992; Utkin et al., 1994; Sanford et al., 1996). During the oxidation of electron donating chemicals, these strains utilize CPs as electron acceptors for growth through process known as halorespiration. Generally, the complete mineralization to carbon dioxide (CO_2) is more generous with soils of slightly alkaline pH, low organic carbon content, increased inoculum concentrations and higher temperatures (Adeola, 2018). The method of dechlorination is a significant pathway for the removal of a majority of CPs, however, the number of atoms in a compound's molecule affects the biodegradation process by slowing down the degradation rate as demonstrated in the dechlorination pathway of PCP in contaminated sediment by Masunaga et al., (1996). Another approach known as cell bioaugmentation which uses activated soil directly either as inoculant or carrier without extracting the degraders from the soil has been assessed for removing PCP-contaminated wood-mill site and treated-pole storage

site (Barbeau et al., 1997). Activated soil is the soil exposed to the target contaminant and comprises a developed degrader population capable of eliminating the contaminant (Gentry et al., 2010). Another significant ecological group of organisms, basidiomycetes are capable of degrading the lignocellulose debris like wood, straw, and litter. The extracellular, lignin-degrading enzymes secreted by the group are responsible for oxidative degradation of CPs too. Several white-rot fungi, including *Irpex lacteus*, *Phanerochaete sordida*, *Trametes versicolor*, *Lentinula edodes*, *Phellinus badius*, *P. chrysosporium*, *Bjerkandera adusta*, and *Inonotus dryophilus* have the potential of effectively metabolizing or bio-transforming PCP (De Jong and Field, 1997). The degradation pathway for removal of 2,4,6- TCP using *Phanerochaete chrysosporium* was proposed by Reddy et al., (1998) while the compound's transformation was examined in the presence of *Ralstonia eutropha* JMP143 by Louie et al., (2002). Similar oxidative dechlorination reactions have been reported for other CP compounds as well (Hirai et al., 2004; Reddy & Gold, 2000).

Role of enzymes in degradation of chlorophenols

Enzymes govern the metabolic processes specific to reaction. The conversion of energy sustained by specific reactions act as the ultimate source for microbial metabolism. Presence of molecular oxygen initiate the enzymatic action on the aromatic rings in aerobic degradation of CPs. During phenol metabolization, phenol hydroxylase hydroxylates the ring to form catechol which further causes ring cleavage by ortho/meta oxidation. Based on the difference in cleaving sites and cleaving direction, catechol dioxygenases is classified as intradiol (C12O) and extradiol (C23O). Microbial degradation of CPs mainly involves oxygenases and dioxygenases. In the ortho-pathway, enzyme catechol 1, 2-dioxygenase (C12O) causes opening of the aromatic ring whereas enzyme catechol 2, 3-dioxygenase (C23O) cleave the ring in the meta-pathway. Hydroxylation of PCP to TCHQ was catalysed by membrane bound cytochrome P-450 enzyme in *Mycobacterium chlorophenolicum* and *Mycobacterium fortuitum* CG-2 (formerly *Rhodococcus* strains) (Uotila et al., 1991; 1992) whereas PCP-4-monooxygenase (PcpA)

catalyzes the conversion of PCP to TeCHQ in *Sphingomonas chlorophenolicum* L-1 (Lange et al., 1996; Ohtsubo et al., 1999; Orser & Lange, 1994). Studies have reported the biodegradation of many xenobiotics via enzymes like peroxidases, tyrosinases and laccases as well. The potential advantage of enzymes include their ability to treat a wide range of recalcitrant compounds with high reaction rate over wide range of pollutant concentration, pH, and temperature. The heme-containing oxidoreductases-peroxidases are also distributed widely in microbes, animals, plants, and the enzymes can catalyse aromatic compounds and their derivatives too (Bilal et al., 2020). Horseradish Peroxidases (HRP) is one of the most extensively studied peroxidases. HRP-catalysed polymerization process effectively reduces the phenol halogenated derivatives, CPs. The 2,4-DCP removal mediated by HRP showed almost complete removal within time span of 3 h in presence of hydrogen peroxide. Addition of H₂O₂ to the reaction system not only enhances the process but also overcomes the problem of formation of toxic intermediates formed during reaction course (Wagner and Nicell, 2002). During degradation of DCP via HRP/H₂O₂, several products generated in the mixture because of high molecularity and polymerization gravitate to precipitate. The products thus could be easily separated via liquid phase reaction, making the whole process an explorative tool towards treatment of CP-contaminated wastewater (Laurenti et al., 2003). Addition of metal ions with enzymes increase the rate of reaction by activating the site residues causing activation of enzymes thus leading to increment in long-term stability of HRP. Almost complete removal was reported for MCP and DCP with activated HRP stabilized by Ni⁺². HRP was capable of efficiently catalysing the oxidation and removal of PCP in presence of H₂O₂. The other sources of peroxidases effective against phenolic compounds include extracts from artichoke (*Cynara scolymus* L.) which is a rich source of peroxidase isoenzymes and polyphenol oxidases (PPO). Minced horseradish roots serve as a potent alternative towards phenol transformation in manure with deodorization effect, as peroxidase polymerizes the phenolic odorants thus reducing malodor. Astonishing results have been obtained from peroxidase pools from hairy root extracts of sweet potato, kangaroo apple, and carrot towards removal of MCP and DCPs.

Table 2.2 Microbial Degradation of Chlorophenols

Chlorophenol (concentration)	Microbes Used	Experimental conditions	Remarks	Reference
2,4-DCP (10.0-800.0 mg/L)	<i>Bacillus insolitus</i>	Immobilization: Alginate support Exposure time = 21 days	Immobilized cells showed a higher removal than suspended ones for concentration of 10.0-200.0 mg/L	Wang et al., 2000
Mixture of 4-CP (40.0-1000.0 mg/L) Phenol (200-1000 mg/L)	<i>Pseudomonas putida</i> ATCC 49451	Suspended cells v/s immobilized cells 15 asymmetric polysulfone hollow fibre membranes	Immobilized cells reported complete transformation of substrate even at maximum conc. of 1000.0 mg/L phenol and 4-CP	Li and Loh, 2005
PCP	<i>Tinea versicolor</i>	Experiment was carried out at 25°C for 8 days which is supplemented with glucose and ammonium sulphate	Complete degradation of PCP took place	Pedroza et al., 2007
MCP (130.0 mg/L)	<i>Stenotrophomonas maltophilia</i> KB2	Co-metabolite: phenol (280.0 mg/L); Subsequent identical dosage of phenol and chlorophenols Temperature= 30 °C	Complete degradation of 4-CP in presence of co-metabolite.	Nowak et al., 2015
PCP (500.0 mg/L)	Immobilized <i>Bacillus cereus</i> RMLAU1	Carbon, Nitrogen sources Exposure time= 60 h pH = 6.5-8.0 Temperature = 25.0-40.0 °C	Dechlorination of PCP resulted in formation of di, tri, and tetrachlorophenols.	Hou et al., 2016

2,4,6-TCP (2000.0 mg/L)	<i>Polyporaceae</i> <i>Tigrinus</i>	Experiment was carried out at 29°C for 21 days for 2,4-DCP concentration of 2000.0 mg/L	Upto 100% degradation of 2,4-DCP with initial concentration of 2000.0 mg/L	Leontievsky et al., 2002
4-CP (15.0-40.0 mg/L)	<i>Pseudomonas putida</i> LY1	Shaker: 120 rpm Variation of pH (3.0-9.0) Temperature (5.0, 15.0, 25.0, 35.0 °C) 4-CP: 15.0 mg/L	At 25°C highest degradation of 4-CP was observed at pH 7.0-8.0 Chlorophenol served as the source of carbon while temperature influenced the degradation rate.	Wang et al., 2015
PCP	<i>Phanerochaete chrysosporium</i>	Experiment was carried out at 30°C for 8 days which is supplemented with glucose	Upto 93% degradation of PCP was observed in the laboratory conditions	Udayasoorian et al., 2007
2,4-DCP (25.0-100.0 mg/L)	<i>Bacillus endophyticus</i> strain CP1R	Cultivation: 50.0 mg/L 2,4-DCP and 1.0 g/l peptone pH= 7	Complete degradation at concentration of 25.0-50.0 mg/L; 75-80% degradation for concentration of 100.0-400.0 mg/L	Patel et al., 2016
Mixture of CPs	<i>Pseudomonas putida</i> SM1443	Glucose-fed granules & plasmid pJP4 carrying donor strain SBR Conditions: 3-4 h cycle time (50% vol. exch.) Exposure time = 420 days Temperature = 25.0 °C	Granules enhanced the rate of degradation with faster acclimation for CPs. Change in the dynamics of granule microbial community.	Quan et al., 2003
2,4-DCP	<i>Phanerochaete chrysosporium</i> BKMF-1767 (CCTCC AF96007)	Incubation: 3 days Temperature= 37.0 °C	Presence of H ₂ S donor NaHS significantly heighten the degradation process.	Lv et al., 2014

PCP	<i>Mucor plumbeus</i> <i>Bonord</i> (DSM 16513; Fungi)	PCP= 4.0 mg/L pH= 6.0 Temperature= 27.0 °C Exposure time= 72 h	PCP resulted in uncoupling of oxidative phosphorylation in mitochondria.	Carvalho et al., 2013
PCP (50.0-600.0 mg/L)	<i>Pseudomonas stutzeri</i> CL7	Bacteria inoculated from pulp and paper mill secondary sludge) pH= 7.5, 8.5 and 9.5 Temperature = 25.0-37.0 °C	PCP utilized as energy source even at high concentration. 100% degradation efficiency for 100.0 mg/L PCP was observed after 120 h.	Karn et al., 2010a
PCP (50.0-600.0 mg/L)	<i>Bacillus megaterium</i> CL3, <i>Bacillus pumilus</i> CL5 <i>Bacillus thuringensis</i> CL11	Bacteria inoculated from pulp and paper mill secondary sludge) pH = 7.5, 8.5 and 9.5 Temperature = 25.0-37.0 °C	Isolated bacteria utilized PCP as energy source and were able to grow. 100% degradation efficiency for 100.0 mg/L PCP was observed after 168 h.	Karn et al., 2010b
4-CP	<i>Comamonas testosterone</i>	Co-metabolite: glucose (10.0-250.0 mg/L) or phenol (40.0-240.0 mg/L) pH = 7.2 Temperature = 30.0 °C	Addition of co-metabolites enhanced the rate of complete transformation of substrate.	Tobajas et al., 2012
2-CP 2,4-DCP 2,4,6-TCP	<i>Coriolus versicolor</i>	Enzyme extract used at 25.0°C for 24 hours	Almost complete degradation of chlorophenols was observed	Kadhim et al., 1999
2-CP	<i>Funalia trogii</i>	Experiment carried out for 6 days for 2-CP initial concentration of 500.0 mg/L	Upto 85% degradation of chlorophenols	Bayramoglu et al., 2009

2,4-DCP	<i>Phanerochaete chrysosporium</i>	Experiment was carried out at 37°C for 30 days while 2,4-DCP was added 6th day to prevent growth inhibition	Only 50% of the degradation of chlorophenols of its initial concentration took place	Valli and Gold, 1991
2,4-DCP	<i>Tinea versicolor</i>	Reaction carried out at 26°C for 816 hours while 2,4-DCP concentration varied from 200.0 to 1200.0 mg/L	Upto 85% degradation of 2,4-DCP	Sedarati et al., 2003
2,4,6-TCP	<i>Polyporaceae tigrinus</i> <i>Coriolus versicolor</i>	Degradation studied on submerged and solid media at 29°C	Upto 70-90% degradation of 2,4,6-TCP was seen when studied on different media	Leontievsky et al., 2000
PCP	<i>Phanerochaete chrysosporium</i>	PCP degradation for 30 days at temperature range 37.0 to 39.0°C	Almost complete degradation of PCP took place	Mileski et al., 1988
PCP	<i>Phanerochaete chrysosporium</i> <i>Phanerochaete sordida</i>	PCP degradation in 15 days at 30°C	PCP degradation efficiency was found between 82-96%	Lamar et al., 1990

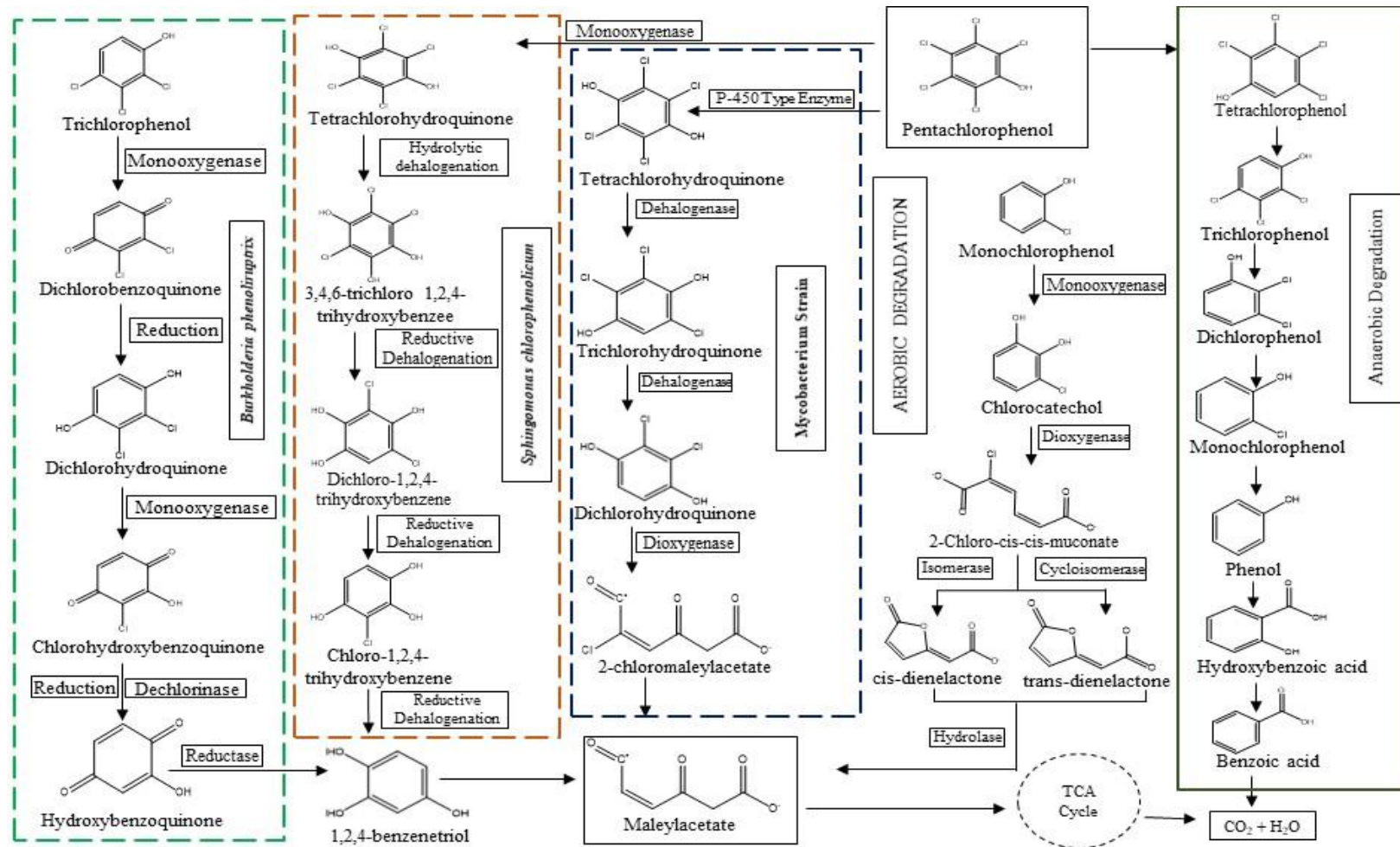


Fig. 2.2 Aerobic and anaerobic microbial degradation mechanism of PCP

Peroxidases from turnip and tomato hair roots have shown significant removal efficiency towards 2,4-DCP. Copper-containing Laccases are the glycoproteins localized in cell wall, catalysing the oxidation of phenolic substrate, and diphenols like hydroxyquinones and catechols are suitable substrates for majority of laccases. The oxidation of substrate results in formation of aryloxy-radical which on conversion forms to quinones. The immobilization of laccases from *Rhus vernicifera* on microporous polypropylene hollow fiber membrane showed catalytic activity and effectively degraded phenolic compounds present in industrial effluents (Georgieva et al., 2008). Figure 2.2 summarizes the aerobic and anaerobic degradation of CPs catalysed by enzymes produced microbially.

2.6 Treatment of CPs by Advanced Oxidation Processes

The lack of efficiency of conventional technologies is a justification for the need of other novel processes like AOPs which has gained the credit of “the 21st century’s effluent treatment process”. AOPs are efficient in removing contaminants as compared to conventional water treatment methods, making them suitable for treatment and reuse. They can grip multiple contaminants in water due to the remarkable reactivity of hydroxyl radicals. Being non-selective, it could virtually react with almost every aqueous pollutant without distinguishing. The technique exploits the strong reactive oxygen species generation ability in treating various classes of contaminants that include endocrine-disrupting chemicals (EDCs), persistent organic pollutants (POPs), total organic carbon (TOC), micropollutants and even the highly complex pharmaceutical waste containing antibiotics like Amoxicillin (Verma & Haritash, 2019). The integration of these processes has also shown tremendous potential towards the degradation of carcinogenic dyes like acid orange 7, AO7, Remazol Red, etc. (Pipil et al., 2022; Sharma et al., 2016). AOPs are the processes employed to make the treated effluent suitable for reuse. They act as a disinfectant by killing the microbes, causing a loss in the biological activity of pollutants, and remove false odour from drinking water without generating any toxicity (Sharma et al., 2018).

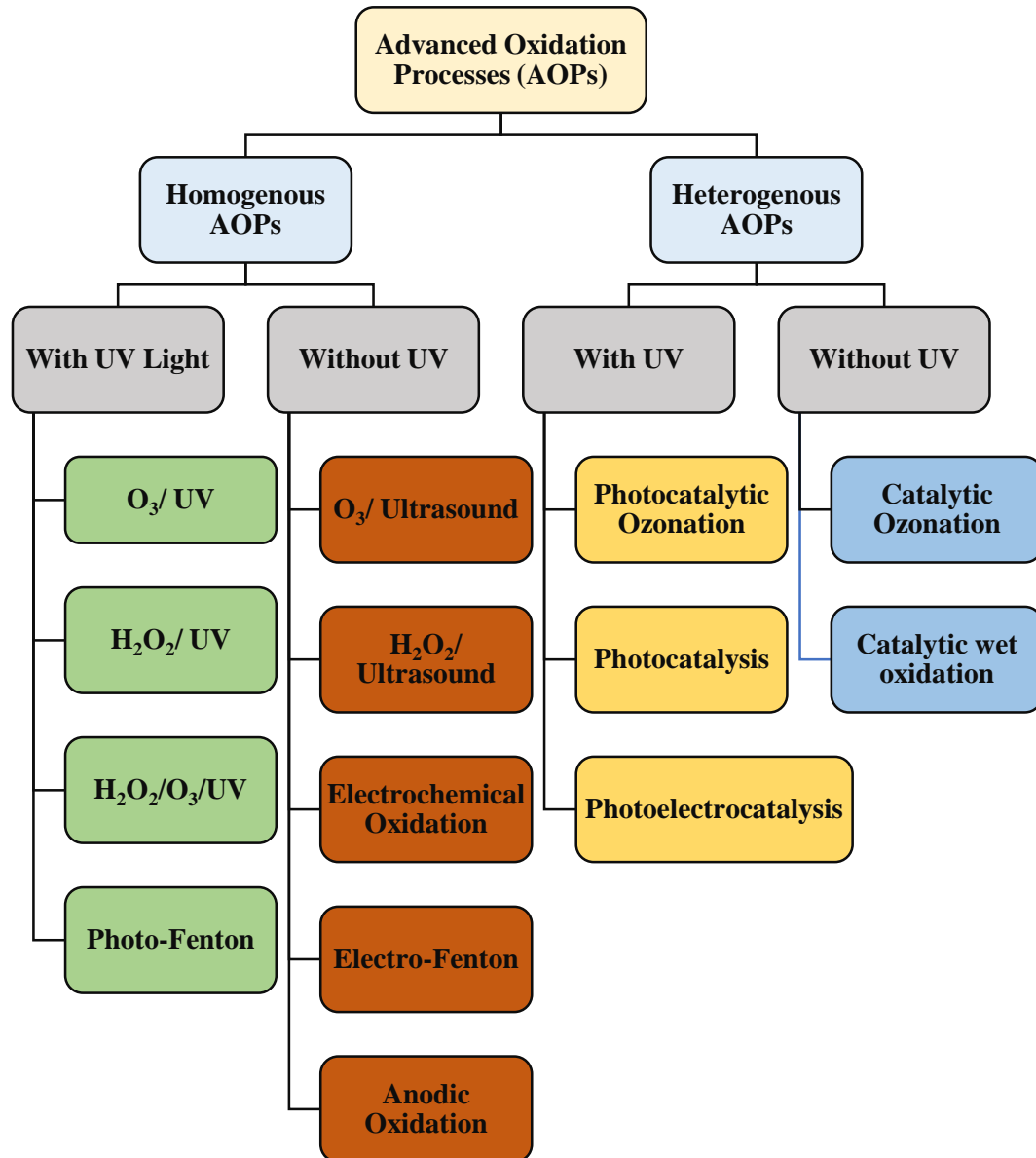


Fig. 2.3 Classification of AOPs

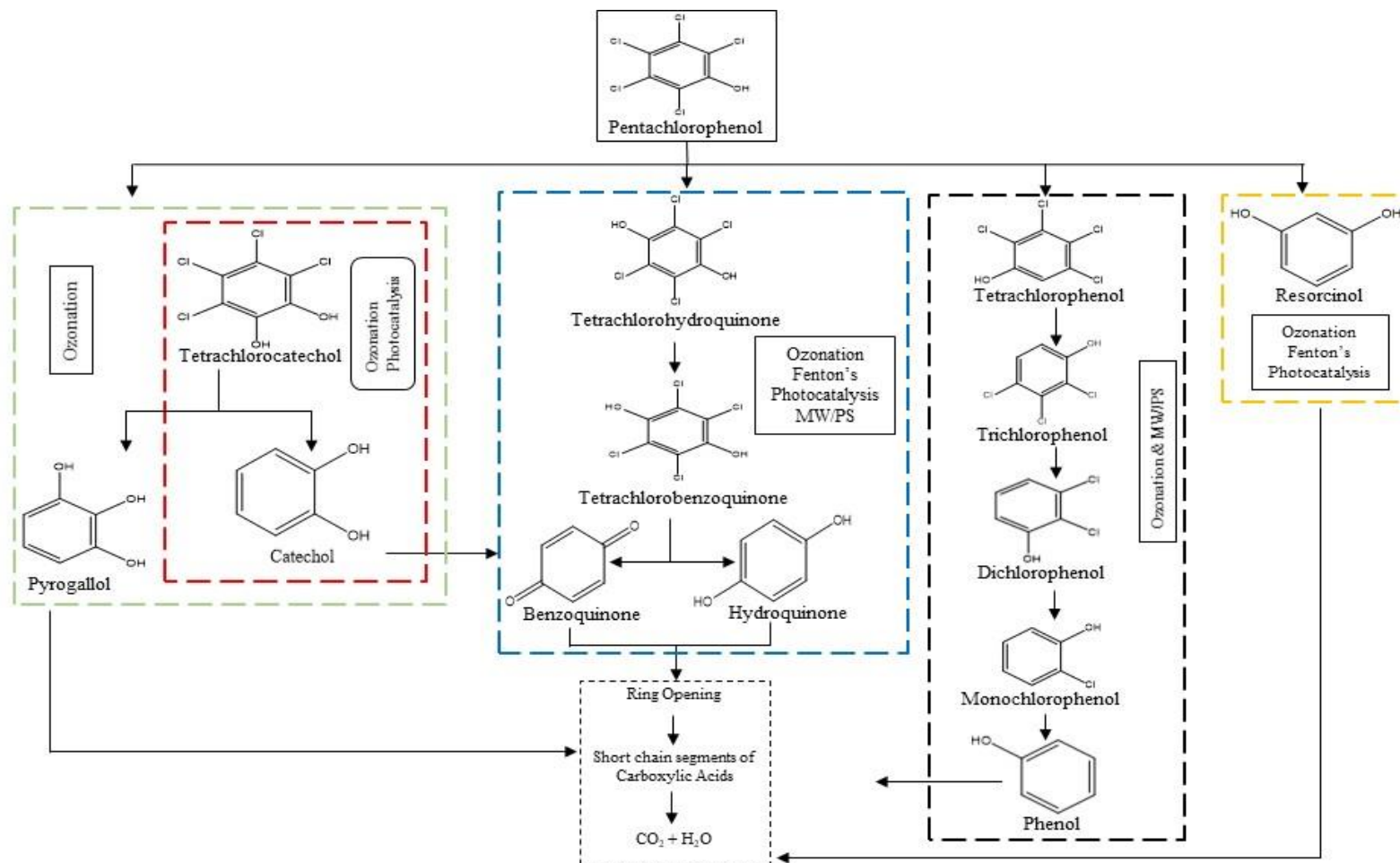


Fig. 2.4 Generalised mechanism of AOPs for PCP degradation sharing similar intermediates at some stages

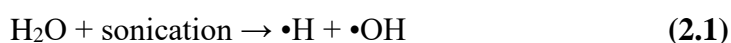
With the advantage of treating the effluent at a more accelerated pace and less generation of harmful intermediates, the method is beneficial towards reducing the toxicity levels and increasing the biodegradability of contaminants, hence bringing them under permissible limits or below which the conventional treatments fails to achieve. The contaminant materials are transformed into non-toxic and stable inorganic compounds such as water, carbon dioxide, and salts, i.e., they undergo mineralization. Hence, it is a step forward towards degradation and treatment of toxicants which the conventional techniques fail to treat because of their high resistivity towards degradation. A brief classification of different AOPs as depicted in Figure 2.3. AOPs are categorized on the basis of their ability to generate radicals like $\bullet\text{OH}$, $\text{HO}_2\bullet$, $\text{O}\bullet$, sulfate-based, etc. or whether the oxidation is to be carried in single phase or using heterogeneous catalyst under irradiation of UV or visible light. A generalised degradation mechanism of different AOPs sharing similar intermediates towards degradation of PCP has been illustrated in Figure 2.4

2.6.1 Physical AOPs

The application of high energy radiation in the microwave range (300 Mhz-300 GHz) has been investigated for oxidation of water contaminants. Microwaves increase the rate of reaction and induce selective heating of contaminants via internal vibration of the molecule. Microwaves can generate UV radiation through an electrodeless discharge lamp for MW/UV combination reactors. Microwaves have been used in combination with oxidants (H_2O_2) or catalysts (TiO_2) to aid in the degradation of organic pollutants. Unfortunately, most of the applied microwave energy is converted into heat. Another ionizing radiation from an electron beam source (0.01e-10 MeV) having accelerated electrons penetrate the surface water resulting in the generation of electronically excited ionic species and free radicals in the water is been utilized for water treatment. The energy of the incident electrons is directly proportional to the depth of penetration of the accelerated electrons.

Sonolysis

It is an eco-friendly process in which ultrasonic sound waves of frequency 20KHz to 10MHz result in formation of cavitation bubbles that carry out degradation of organic contaminants. Being a facile sludge free process with no additional production of secondary pollutants, the process is one of the most preferred treatment methods over Fenton's process, photolysis and Photo-Fenton. The generated cavitation bubbles collapse in their resonance size leading to the dissipation of stored energy, generating high temperature (>5000K) and pressure (>1000 bar) thus causing the explosions. Degradation begins at the bubble-liquid interface dominated by OH radicals while free radicals later migrate into the bulk liquid leading to secondary reactions inside it. The acoustic cavitation generates highly reactive radicals either by physically dissociating the water molecule (cavitation consisting of nucleation, growth and collapse of bubbles) (eq. 2.1) or indirectly via chemical where homolytic fragmentation of water and dioxygen molecules (eq. 2.2) occurs (Ghatak, 2014). Ultrasound waves are transmitted through aqueous solution in a sonochemical process. The highly oxidizing radicals along with hydrogen peroxide (formed when reactive hydrogen converts to hydroperoxyl radicals in the presence of oxygen atmosphere) causes destruction of organic contaminants through hydroxylation and oxidation.



The mineralization efficiency of the process can be enhanced by varying the significant parameters like concentration of the substrate, catalyst loading, pH, ultrasonic frequency and power. The sonolytic degradation of diclofenac, a pharmaceutical drug detected frequently in surface water and rivers, was studied at ultrasound frequency of 213 kHz and at varying ultrasound power (16-55 Mw mL⁻¹). Increase in the ultrasound power increased the degradation of diclofenac because

of the increased generation of hydroxyl radicals produced by cavitation bubbles (Madhavan et al., 2010). Sonochemical degradation of diclofenac also reported maximum degradation at ultrasound frequency of 617 kHz (Hartmann et al., 2008). The generation of hydrogen peroxide increased when the power increased from 50W to 150W as the number of collapsing bubbles also increased causing the degradation of diclofenac. Another contaminant, 2,4,6-TCP is continuously detected in effluent streams produced by paper and pulp mills because of the strong polarity. 2,4,6-TCP undergo oxidative sonolytic degradation by hydroxyl radicals generated during sonication. Despite having the ability of treating cloudy water and degradation of sparingly soluble and volatile organic pollutants via ROS generation, the process is highly energy intensive. Around 50% of the input energy is lost in thermal dissipation. Thus, its high energy consumption and limited degradation, directs the process to be integrated with AOPs like UV irradiation (sono-photolysis), oxidants like H₂O₂, O₃ (sono-ozonation), Photocatalysis (sono-photocatalysis), Photo-Fenton (sono-Fenton), etc.

Sonolysis coupled with Catalyst

In the sonication process, entire cavitation energy cannot be transformed into chemical and physical effects. Addition of various catalyst to the liquid provides appropriate environment and interface to the weak points for nucleation of cavitation bubbles to take place. Diclofenac degradation was carried out at different ultrasound frequencies (24, 216, 617 and 850 kHz) and with different catalysts (TiO₂, SiO₂, SnO₂ and titano-silicate) (Hartmann et al., 2008) and the micropores of the catalyst served as cavitation nuclei attributing to the higher rate of degradation in all cases though at frequency of 617 kHz. Degradation of methyl parathion with commercial anatase TiO₂, nano-sized anatase TiO₂ and rutile TiO₂ coupled with sonolysis showed more than 90% degradation within 2 hours of ultrasound irradiation. Intermediates like p-nitrophenol was observed in presence of nanometer-sized anatase TiO₂ and rutile TiO₂, thus, highlighting that coupling with other methods can help improve the degradation of organic contaminants substantially.

For example, sono-photocatalysis involves the use of ultraviolet radiation and ultrasonic waves in the presence of a semiconductor photocatalyst. The synergistic effect of ultrasonic/UV waves leads to a higher generation of reactive radicals leading to higher mineralization efficiency. Excitation of photocatalyst leads to the formation of the electron-hole pair. Photocatalyst enhances the bubble cavitation phenomenon causing increased migration of reactive species into the liquid bulk region. Thus, the intensification leads to a higher concentration of free radicals as a result of ultrasound in the peroxide species. The sono-photocatalysis pathway involves activation of the surface of photocatalyst, mass transfer of organic contaminants and breaking the aggregation. The sono-photocatalytic degradation of malachite green using homogenous and heterogeneous catalyst (photocatalyst loading TiO_2 and Fe^{2+} with H_2O_2) noticed quick and enhanced rate of degradation with intensification of the two processes. The synergistic integration of increased free radical formation and enhanced catalytic activity increased the efficiency of the process. Accelerated sono-photocatalytic degradation of organic pollutants has been reported under visible light coupled with ultrasound and different catalyst (ZnO , TiO_2 and Hombikat UV 100) (Kavitha and Palanisamy, 2011). Cavitation causes cleavage of H_2O_2 produced by coupling process, increased the generation of reactive radical species which further carry out the oxidation of the substrate and other intermediates. Higher production of OH radicals in the bubble-bulk interface enhances greater interaction with organic pollutant in the bulk-liquid medium. The sono-photocatalytic degradation with Fe-doped TiO_2 as catalyst reported more than 90% total organic removal (TOC) with 3 g/L of catalyst dose. Sonolysis coupled with solar-photocatalysis with TiO_2 catalyst in low concentration showed detrimental effect with enhanced cavitation activity for carrying out the degradation of Bisphenol A (BPA) (Torres et al., 2008). In addition, it was noted hydroxyl radicals are the key species that carry out degradation. The increased efficiency of the process could be attributed to- sonolytic cleavage of water causing enhanced generation of hydroxyl radical; enhanced mass transport of organics among catalyst surface and fluid phase due to shock wave propagation aided transport; excitation of catalyst because of ultrasound-induced luminescence having broad wavelength

range; ultrasound waves disintegrate the catalyst particles increasing the surface area thus mounting the catalytic activity; acoustic micro-steaming regenerates the active sites of the catalyst to be available for further reactions. Likewise, various other research studies have reported complete removal of contaminants using ultrasound technologies in presence of different chemical additives.

Sonolysis coupled with metal ions

The transient cavitation action of ultrasound coupled with Fenton process is found to increase the generation of hydroxyl radicals. M^{n+} (like Fe^{2+} or Fe^{3+}) initiates the decomposition of H_2O_2 in acidic environment generating the primary oxidizing species OH radical. Fenton process when coupled with ultrasound resulted in quicker and complete degradation of textile dye (Chakma and Moholkar, 2013). Synergistic effect of ultrasound coupled with Fenton's process (transition metals and oxidants) results in effective degradation. Complete degradation of carbofuran was reported by Maa and Sung (2010) when Fenton's process was combined with sonolysis.

Aquatic environment evidences the presence of various pharmaceuticals like hormones, anti-inflammatories, antibiotics, anesthetics in trace concentrations. Tetracycline, the second highest antibiotic in production used for treatment of infectious diseases in both animals and humans was effectively degraded by sonolysis at ultrasound frequency 20kHz coupled with Fe^{2+} and Co^{2+} metal ions (Liu et al., 2012). Enhanced and almost complete degradation of tetracycline was observed with sonolysis coupled with Fenton-like reagents, metal ions and oxidizing agents like H_2O_2 or $S_2O_8^{2-}$ (tetracycline concentration of 50 mg/L, H_2O_2 2.0mM, Fe^{2+} 0.2mM at pH 3.0). In another study, Fenton-like oxidation ($FeOOH-H_2O_2$) and sonolysis were used to carry out the degradation of para-chlorobenzoic acid (*p*-CBA) individually and in combination with each other under acidic condition (pH 3.0) (Neppolian et al., 2004). Degradation rate was higher when sonolysis was coupled with $FeOOH-H_2O_2$ compared to the respective processes alone. The acoustic cavitation causes regular and repetitive clearing and activation

of the surface of FeOOH-H₂O₂ thus increasing the interaction and movement of reactants and product in the solution phase and FeOOH surface. Intense micromixing from acoustic cavitation facilitates the effective utilization of reactive oxidation species in the reaction mixture.

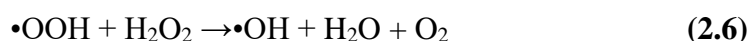
Sonication couples with ozonation

The generation of ROS occurs as a result of cavitation and thermolysis of ozone. Each O₃ molecule produces two •OH radicals and the transport of these radicals along with ozone leads to further in-situ generation of H₂O₂/HO•. Addition of peroxide and increase in pressure further improves the mineralization. The coupling of sonolysis with ozonation prevents the formation of toxic intermediates as also observed by Martins et al., (2006) while investigating the degradation of colorant pararosaniline using sono-ozonolysis. It was also noted that the mineralization products are more in coupling system as compared to the individual processes indicating the higher efficiency of coupled processes. The study on p-aminophenol (PAP) reported complete mineralisation within 30 minutes with sono-ozonolysis (He et al., 2007). The chemical synergism of ozone in combination with sonication efficiently carry out the degradation and mineralization of contaminants accredited to the enhanced decomposition of O₃ in the collapsing bubbles, thus, generating free radicals. Studies has proven the coupling of ozone and ultrasonic irradiation efficient in destruction of pollutants like phenol, nitrophenol, hydroquinone, benzoquinone, benzyl sulfonate, methyl orange, etc (Anandan et al., 2020).

Sonication coupled with H₂O₂

Dissociation of water molecule because of sonication results in formation of hydrogen peroxide which further dissociates into hydroxyl radicals triggering the formation of more of the different reactive oxidizing species efficiently carrying out the degradation of the organic contaminants (eq 2.5). Addition of hydrogen peroxide externally in the sonication system has advantage towards degradation of

harmful organics. Abundant presence of ROS in the reaction mixture produced from cleavage of water molecule and acoustic cavitation-induced dissociation of externally added H₂O₂ thus enhances the degradation process in the bulk-liquid interface. The sonication and H₂O₂ (added externally) process has been found to generate effluent of less toxicity as compared to conventionally treated wastewater stream containing phenol (Maleki et al., 2005).

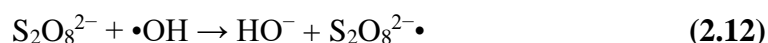
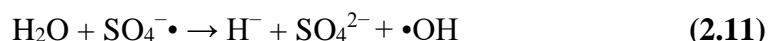
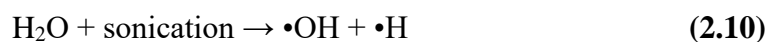
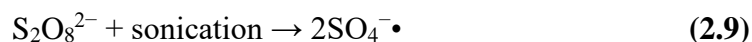


Several studies have proven the sonication/H₂O₂ system to degrade toxic organics with higher efficiency. Maleki et al., (2005) reported the US/H₂O₂ treated effluent 1.65 times less toxic compared to the wastewater stream from an industrial plant having phenol. The ultrasound/H₂O₂ system was found efficient in eliminating the associated toxicity with by-products formed during the degradation of phenol. The dosage of H₂O₂, however, is also a limiting factor in case of textile dyes. The optimum dosage is vital for efficient degradation/decolorisation of dyes. Concentration of H₂O₂ exceeding the optimized value results in a competitive reaction in which hydroperoxyl radicals are formed. These radicals are less reactive and don't participate actively in the degradation process hampering the reaction rate (Legrini et al., 1993). At higher pH, however, there is more production of hydroxyl radicals enhancing the degradation process. Studies have reported that the degradation system follows pseudo-first-order reaction kinetics with respect to oxidant dosage and pH (Legrini et al., 1993).

Sonication coupled with Persulfate

Typical AOP oxidizes the pollutants by $\bullet\text{OH}$ radicals, however, use of sulfate radicals-based oxidation (SR-AOPs) has gained attention in recent years. Sulfate radicals have higher mineralization rate as compared to OH radicals and are

more powerful oxidants. These radicals are activated from precursor molecules like persulfate (PS, $S_2O_8^{2-}$) and peroxymonosulphate (PMS, HSO_5^-). The high redox potential radicals non-selectively oxidise the harmful contaminants and could also be easily generated by sonolytic cleavage of persulfate anion.



The coupled system effectively carried out the degradation of carbamazepine (CBZ) in optimized conditions (Wang and Zhou, 2016). Coaction of coupled AOP system showed favourable results as compared to the processes performed individually. The degradation efficiency of Sonication/Persulfate binary system was 90% within 2 hours of duration as compared to mere degradation efficacy of 1.2% and 26% respectively with ultrasound and persulfate alone (Wang et al., 2016). The degradation of humic acid was investigated in presence of persulfate anion at ultrasound frequency of 40kHz, ultrasonic power of 200W and pH 3.0 (Wang et al., 2015). The system successfully oxidized 90% of the humic acid within time span of 2h. The collegial outcome of the system is by virtue of strong mechanical consequence in the homogeneous system strengthening the mass transfer in the solution and accelerated cleavage of persulfate from ultrasound irradiation-induced free-radical generation. Apart from this, electrolytic dissociation is also a potent approach to decompose persulfate anion and form oxidative radicals. The collective system of sonoelectrolytic mode in presence of persulfate was probed for degradation of aniline in wastewater (Chen and Huang, 2015). The enhanced mineralization resulted in formation of various by-products thus indicating the sono-electro-activated persulfate a compelling pathway towards mineralization of aromatic compounds.

Nevertheless, ultrasound has become a prominent process in wastewater treatment. It alone cannot be considered as a potent method as the cavitation energy cannot be effectively transformed to physical and chemical effects. Modernizing the existing treatment units with ultrasound could reduce the pretreatment time and cost, also reducing the addition of chemicals. The potential of sonochemistry can be incorporated as a green technology in remediation of environment.

2.6.2 Photocatalysis

In wastewater treatment, semiconductors have the potential to degrade recalcitrant like PCP either directly or via generating reactive oxidation species like free radicals. Photocatalysis makes use of semiconducting devices for degradation of contaminants. The semiconductor when irradiated with photons of energy higher than band gap energy results in formation of holes in the valence band while electrons in the conduction band. Holes oxidise the organic compounds into mineralization products whereas H_2O on reaction with holes generates $HO\bullet$. Electrons act as reducing agents, reacts with O_2 to form superoxide which further causes degradation of intermediates. CdS, ZnO, ZnS, TiO_2 , Fe_2O_3 are few of the semiconducting oxides used as photocatalyst. The efficiency of a photocatalyst highly depends on its crystal size associating its surface area and other structural properties that entails porosity, composition, distribution, energy band gap, particle size and surface hydroxyl density (Ahmed et al., 2011). Among the photocatalysts, TiO_2 is the commonly used as it can absorb UV light which forms only 4% fraction of the solar light, it is usually doped with semiconducting materials of narrow band gap and high conduction band. This extends the photoresponse of TiO_2 from UV to visible light region because vacancy of high concentration induces miniband generation below conduction band increasing the photocatalytic activity. The three forms of TiO_2 -crystalline, anatase and rutile have been extensively employed as photocatalyst. Titanium dioxide Degussa P25 other than PC 500, Hombikat UV100, and travancore titanium products (TTP) have been used for degradation of toxic dyes. In presence of Degussa P25, the degradation of dyes was maximum following

the order P25>UV100>PC500>TTP (Bahnemann et al., 2007). The photocatalytic degradation of methyl orange in presence of different photocatalyst showed P25 as the most efficient. The efficacy order of the catalyst reported P25>Pt-UV100>UV100>Mikro anatase>Prrios AV01. The higher photoactivity of P25 is attributed because of the slower rate of electron-hole pair recombination with specific BET surface area $50\text{m}^2/\text{g}$ and particle size 20nm. The crystalline composition of P25 having 75% anatase and 25% rutile, the latter absorbs photons because of the smaller bandgap generating electron-hole pair and electrons are thus transferred from conduction band of rutile to electron traps of anatase phase attributing to the higher photocatalytic activity of P25 by slowing the electron-hole recombination (Ahmed et al., 2011).

CPs falls under the large library of toxic organics recalcitrant to mineralization under natural conditions, and photodegradation of p-chlorophenol in presence of photoanode TiO_2 has reported complete degradation (Yang et al., 2009b). The degradation is initiated by hydroxyl radicals in presence of dissolved oxygen molecules results in formation of benzoquinone which further dissociates through opening of the benzene ring. Saturated and unsaturated dicarboxylic acids later are converted to harmless end products CO_2 and H_2O . The photocatalytic degradation of chlorophenol by Ag loaded nano TiO_2 photocatalyst has shown two different pathways of degradation. In one approach hydroxyl radicals attack at para position resulting in formation of hydroquinone which further oxidises to harmless products. In the other pathway, ortho-attack of hydroxyl group causes dechlorination which further results in simpler non-toxic molecules (Zhang et al., 2018b). A study on 4-chlorophenol with tetragonal BaTiO_3 revealed that the photodegradation reaction is triggered with chlorine removal via hydroxyl attack. The deformation of tetragonal BaTiO_3 generates piezoelectric potential which simultaneously degraded and dechlorinated the compound. The intermediate compounds formed are further oxidised to produce open-chain carboxylic acid finally mineralising to carbon dioxide and water (Lan et al., 2017). The degradation of MCP and 2-chlorophenol using trimetallic nanocomposites of lanthanum, cobalt and nickel metals supported by graphene oxide results in complete mineralisation

under visible light. The ortho, para mediated hydroxyl attack results in different intermediates which undergo further decomposition producing the carboxylic acids (Sharma et al., 2019). Photoelectrocatalytic removal of 2,4-DCP over WO_3 coupled and Mo doped BiVO_4 photoanode to Pd/Ni photocathode. Irradiation of light resulted in excitation of electrons from conduction band of WO_3 and transferred to photocathode causing reduction of photons forming nascent hydrogen ($\bullet\text{H}$). Sequential attack from $\bullet\text{H}$ forms phenol which is readily transferred to photoanode surface. The holes trigger its decomposition via $\bullet\text{OH}$ formed at photoanode surface because of adsorption of water. Consecutive $\bullet\text{OH}$ attack leads to formation of harmless byproducts. Since the dechlorination of MCP is $\bullet\text{H}$ induced (formed from proton adsorption), at low pH the proton availability affects the degradation rate (Li et al., 2019). The use of g- $\text{C}_3\text{N}_4/\text{TiO}_2$ for degradation of DCP under visible light irradiation has been reported. The hydroxyl radical-induced attack at para position resulted in formation of 2-chloro-4-hydroxyphenol. Further consecutive attack generates tetrahydroxybenzene. Cleavage of benzene rings produces subsequent aliphatic carboxylic acid compound which undergo decomposition and produce CO_2 and water (Zada et al., 2018). Excitation of band of semiconductor increases the electron density in conduction band. Molecular oxygen adsorbs the conduction band electrons and forms highly unstable degrading species. The super oxide anion radicals ($\bullet\text{O}_2^-$). The radical is less powerful as compared to $\bullet\text{OH}$ with redox potential of -0.33eV ; however, triggers the free radical reaction because of presence of unpaired electrons further forming the singlet oxygen species, $^1\text{O}_2$. The species, thus, formed is a powerful yet selective oxidizing species for many organic pollutants. They either directly degrade the pollutant or undergo a series of chemical reaction with water forming other reactive oxidizing species like hydrogen peroxide and hydroxyl free radicals. Photocatalytic degradation rate is strikingly higher in presence free adsorbed O_2 molecule. Super oxide radical anion ($\bullet\text{O}_2^-$)-induced degradation of 2,4-DCP in presence of g- C_3N_4 coupled active carbon fibre under visible light resulted in complete mineralisation of pollutant to simpler compounds (Chu et al., 2019). The photoactivity of g- C_3N_4 was significantly enhanced with phosphoric acid. The highly electronegative O atoms surrounding the P atom adsorb the molecular O_2 . The molecular O_2 then accepts the electron from conduction band

forming $\bullet\text{O}_2^-$ promoting separation of charging significantly hastening the degradation rate. Another super oxide radical anion ($\bullet\text{O}_2^-$)-induced degradation study investigated degradation of TCPs in the presence of g-C₃N₄ under visible light (Ji et al., 2013). Synergistic effect of hydroxyl radicals ($\bullet\text{OH}$), super oxide radical anion ($\bullet\text{O}_2^-$) and photogenerated holes enhance the degradation resulting in complete mineralisation. ($\bullet\text{O}_2^-$)-based degradation caused formation of TCP superoxide radical which further transforms to dichloro-4-hydroxyphenol eliminating chloride from para position. Cleavage of dichlorobenzoquinone results in ring opening further producing different aliphatic carboxylic acids. Consecutive attacks from degrading species form the end-products CO₂ and H₂O. An intermediate of meta-TeCP formed by chloride radical attachment is further decomposed to CO₂ and H₂O. Studies have shown that with increase of the chlorine atom count, the mechanism of degradation becomes complex increasing the number of intermediates. The variation among photocatalyst is because of the differences in Brunauer-Emmett-Teller (BET) surface, presence of any structural defect in the crystalline frame work or presence of any impurity or density of hydroxyl group on the surface of catalyst. These factors affect the lifespan and recombination rate of e-h pairs and adsorption behavior of pollutant or intermediate degradation. The initiation rate for photocatalysis and formation of electron-hole is strongly light intensity dependent. It determines the extent of absorption of light at a specific wavelength by the semiconductor catalyst. The mineralization of a contaminant is invariably influenced by the distribution of light intensity inside the reactor. The process has been demonstrated successfully for degradation of wastewater generated from textile industry, pharmaceuticals, pesticides, etc (Yadav et al., 2022; Verma and Haritash, 2019). TiO₂ assisted photocatalytic degradation of Remazol Red dye was studied and at optimized concentration of TiO₂ 1.0g/l, H₂O₂ dose 5.0mM and pH 7.0, complete degradation of dye was observed within 60 minutes of irradiation time (Pipil et al., 2021).

To avoid any impact of foreign element doping, self-doping is a highlight these days because of its ability to blend with the electronic structures. One such example is of Bi₂WO₆, a promising semiconductor because of its photostability,

chemically inert and environment friendly features. Self-doping of Bismuth increased the removal of sodium pentachlorophenate (Zhang et al., 2014). More generation of superoxide ions prompted the dechlorination process further resulting in cleavage of ring followed by mineralization of decomposable intermediates (Zhang et al., 2014). As electron-hole pair recombination inhibits the degradation process, molecular oxygen plays a key role of trapping the electrons thus producing $\bullet\text{O}_2^-$, leaving holes (major reacting species) to carry out oxidation of NaPCP. The degradation pathway followed the hole-induced oxidative dechlorination (major reaction) and $\bullet\text{O}_2^-$ - induced reductive dechlorination (minor reaction). This is followed by elimination of more of electron withdrawing groups, shifting the electron density from chlorine to oxygen and further destructing the conjugate π bonds resulting in formation of quinones. Consecutive reductive dechlorination causes ring-opening where further electrophilic attack of holes and $\text{OH}\bullet$ results in formation of small acids. These small acids are eventually mineralized into carbon dioxide and water.

2.6.2.1 Solar energy driven heterostructure photocatalysis

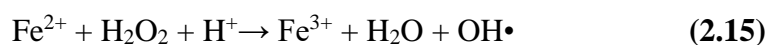
The magnitude of solar energy consumption is almost four times the total solar energy irradiating the surface of the earth (Balzani et al., 2019). Since no modification in solar spectrum can take place, however the solar energy could be exploited and harnessed to increase the efficiency of treatment systems. Considering the cumulative spectral distribution of solar light, the threshold of 885 nm (1.4eV) corresponds to maximum energy conversion efficiency (Balzani et al., 2014). Solar photochemistry plays a vital role in pollution remediation transforming the pollutants into non-toxic compounds. With the aim to improve the results on the degradation of contaminants from water. also, the combination of semiconductor particles has been developed, obtaining composites and hybrids materials, nanostructuring, forming heterojunctions (Kisch 2015). Such materials because of their excellent solar energy harnessing potential, narrow bandgaps, suitable band structure are prominent substances for photocatalytic treatment (Chava et al., 2022a). Irradiation of solar light over the semiconductor produces electron and

holes which further react with oxygen and hydroxyl ions to form hydroxyl radicals. Process of photocatalysis using semiconductors involves (a) formation of e-h pairs when irradiated with energy greater than or equals to bandgap energy of material, (b) formation of a depletion layer at the junction because of combination of some e-h pair as they migrate towards photocatalyst surface, (c) the unpaired/leftover electrons and holes are responsible for redox reactions on the surface. The synthesised heterojunctions result in photocatalytic water-splitting producing H_2 and degrading the organic contaminant (Kuriki et al., 2017). Synthesis of hybrid photo catalyst heterostructures such as CdS-In(OH)₃ reported more photoinduced charge transfer and increased surface area with enhanced degradation of tetracycline (Chava et al., 2022a). The fabricated photocatalyst CdS-In(OH)₃ followed Type-I path where both reduction and oxidation reactions took place in the single semiconductor. The process enhances the light harvesting and lessens the e-h recombination. For effective charge separation, Type-II heterostructure with S-scheme heterojunction makes use of two semiconductors in a staggered alignment resulting in opposite movement of charge carriers (Xu et al., 2020). In this type, electrons from one semiconductor migrate to another semiconductor on the basis of the redox potential gradient. Two different layers are formed at the junction, electron depletion layer and electron accumulation layer. This band bending and coulombic attraction results in accelerated flow of electrons between the valence band of one semiconductor to conduction band of adjacent semiconductor (Xu et al., 2020; Hu et al., 2020). Based on this, another photocatalyst CdS-In₂O₃ was fabricated which resulted in enhanced degradation (90%) of organic contaminant as compared to In(OH)₃ (72%) whereas CdS nanorods reported 50% removal of respective toxicant (Chava et al., 2020). In a similar study, plasmon-mediated metal/semiconductor heterostructure was investigated. Since metal sulfide like CdS has the ability to work under visible light, the fabrication of Bi quantum dots over CdS nanorods was conducted (Chava et al., 2022b). The electrons excited from conduction band of semiconductor transferred to the adjacent metal nanoparticles corresponding to their lower fermi energy level. Successive redox reaction is carried out by remains holes and electrons in semiconductor and metal component (Mascaretti et al., 2019). CdS/Bi reported almost complete photocatalytic

degradation within 60 minutes under visible light irradiation. The enhanced degradation rate is attributed to the charge separation between semiconductor and Bismuth (Chava et al., 2022b). Thus, fabrication of hetero-structured photocatalytic systems with a band structure alignment transition strategy for efficient green energy conversion is an emerging approach towards environmental remediation reactions.

2.6.3 Fenton's Process

Different AOPs operate under different reaction systems, but share the similar chemical feature of utilizing highly reactive oxidizing agent, hydroxyl radical having redox potential of 2.80 eV. Fenton's process has gained attention because of the rapid formation of hydroxyl radicals. The comprehensive research reported the process effective over a wide range of pollutants including chlorophenolic compounds, toxic dyes, pesticides, pharmaceuticals, surfactants, etc. The process consists of oxidation of ferrous ions (Fe^{2+}) to ferric ions (Fe^{3+}) reduction of ferric to ferrous, generating peroxy ($\text{HO}_2\cdot$) and hydroxyl radicals ($\text{OH}\cdot$).



Degradation with Fenton's process is rapid in the beginning while it slows down at later stage. During the Fenton's degradation of PCP, OH radicals cause rapid oxidation resulted in formation of short-chain organic acids like formic acid, oxalic acid, maleic acid, acetic acid. Ortho-para-attack of OH radicals on the aromatic ring results in formation of intermediates like quinones, benzoquinones, phenols, hydroquinones (HQ), chlorohydroquinones and chlorocatechols. Integration of UV light or visible light with Fenton's process increases the rate of reaction and efficiency of the system towards degradation of target contaminant. Photo-Fenton process has gained attention around the globe towards abatement of refractory contaminants. The process accelerates the generation of hydroxyl

radicals by rapid reduction of Fe^{3+} to Fe^{2+} . Direct photolysis of oxidant also yields hydroxyl radicals to further support degradation. Thus, synergistic catalytic effect more produces oxidising species.



Chlorinated aromatic compound 2-chlorophenol was subjected to degradation via photo-Fenton process and significant degradation was observed with 90% TOC removal within 30 minutes of reaction time (Perez-Moya et al., 2007). In a similar study, the feasibility of treatment of the MCP was investigated (Poulopoulos et al., 2008). Almost complete mineralization was observed within reaction time of 150 minutes. Presence of carboxylic acids like formic acid and acetic acid revealed that the process gradually proceeded with carbon dioxide as the end product. Cleavage of aromatic-Cl bond released inorganic chloride ions in the reaction solution indicating a decrease in toxicity as the hydroxylated intermediates are easily biodegradable (Poulopoulos et al., 2008). In another study, iron-pillared bentonite catalyzed photo-fenton was repeated for degradation of 4-chlorophenol (Del Campo et al., 2014). After 60 minutes of reaction time at optimized catalyst, oxidant and pH 3, around 95% removal of the pollutant was observed. The 2,4-DCP and 2,4,6- TCP when subjected to UV/Fe(II)/ H_2O_2 showed enhanced degradation within 10 minutes of time (Kuo et al., 1998). The use of sunlight as an alternative to UV-light has gained attention recently owing to energy efficiency. Compared to the conventional Fenton's process, solar assisted photo-Fenton process enhances the removal rate of TOC by 2.46 times to 90%, indicating it as an energy efficient environmentally friendly process (Zhang et al., 2019). Another study revealed that solar light accelerated the degradation of TCP when subjected to Photo-Fenton like method (Vinita et al., 2010).

The conventional Fenton process used homogeneous solution of iron catalyst. The heterogeneous Fenton process replaces it with solid catalyst. The efficiency of the system is enhanced because the catalytic reactions occur at active

sites on the surface of solid catalyst inhibiting the leaching of iron ions, broadening the pH range, reducing the production of sludge, reusability and stability of catalyst. The in-situ generation of H_2O_2 on the catalyst surface reduces the addition of excess H_2O_2 thus directly oxidizing the pollutant. H_2O_2 is an important parameter influencing the efficiency of degradation of organics. Natural and synthetic materials have been widely used as sources of iron for the treatment of chlorophenols. The most commonly used natural catalyst material are pyrite (FeS) and magnetite (Fe_3O_4). Other solid catalysts include ferrihydrite, hematite (Fe_2O_3), goethite (α - $FeOOH$), Zero-valent iron (ZVI, Fe^0), multimetallic iron particles etc. Table 2.3 represents the efficiency of different iron catalyst for degradation of chlorophenols (Kantar and Oral, 2021). Pertaining to the highly toxic nature of chlorophenols, the process can either be employed as a pretreatment step prior to biodegradation or post-treatment step. The intermediates produced from the process have much lower toxicity as compared to the parent compound. Pre-treatment of 2,4,6-TCP with nano Fe_3O_4/CeO_2 reduced the toxicity of the compound implying increased biodegradability (Xu and Wang, 2015). Improved biodegradation of 4-chlorophenol was observed with bacterial strain, *Bacillus-fusiformis* when pretreated with bentonite-supported bimetallic Fe/Pd nanoparticle (Kantar and Oral, 2021). Fenton-like Fe_3O_4 Magnetic Nanoparticles (MNPs) have also been successfully synthesized and used for degradation of 2,4-DCP (Wang, 2012). The radical collision of $OH\cdot$ on 2,4-DCP takes place at para position because of the steric effect resulting in formation of 2-chlorohydroquinone. Meanwhile, hydroxylated products like 4,6-dichlororesorcinol is formed because of the electrophilic attack of OH radical. Further dechlorination combined with oxidation degrade the chemical species to smaller molecular organic acids like formic acid and acetic acid.

Table 2.3 Heterogeneous Fenton process for the degradation of chlorophenols

Chlorophenol (concentration)	Catalyst	Experiment condition	Treatment efficiency	End-product	Reference
2-CP (50.0 mg/L)	ZVI	pH = 3.0 Catalyst = 0-44.0 mg/L	80%	chlorobenzoquinone	De la Plata et al., 2012
2-CP (50.0 mg/L)	Goethite	pH = 3.0 Catalyst = 0.5-2.0 g/l	99%	chlorobenzoquinone	De la Plata et al., 2010
2-CP (50.0 mg/L)	Goethite	pH = 3.0 Catalyst = 0.2-0.8g/l Ligand = 0.1-1.0mM H ₂ O ₂ = 0-3.9mM	100%	-	Lu et al., 2002
MCP; Poly-CP (100.0-500.0 mg/L)	Pyrite	pH = 3.0–5.0 H ₂ O ₂ = 0.3M Catalyst = 0.25–1.0 g/L	100%	Carboxylic acids	Li et al., 2015
2,4-DCP (20.0 mg/L)	Ni/Fe-Fe ₃ O ₄	pH = 3.0–10.0 Catalyst = 3.0g/l	92%	-	Xu et al., 2016
2,4-DCP (20.0-100.0 mg/L)	Fe-NPs (Fe ²⁺ , nFe ₃ O ₄ , nano ZVI)	pH = 3.0–7.0 Persulfate = 6.4–24.0 mg/L Catalyst = 1.0–2.0 g/l	98%	Maleic acid	Kantar and Oral, 2019
	Fe ₃ O ₄	pH = 2.0-5.0 H ₂ O ₂ = 0.6–30.0 mM Catalyst = 0.2–2.0 g/l	100%	Carboxylic acids	Xu and Wang, 2012

PCP (50.0 mg/L)	Magnetite	pH = 7.0 Catalyst = 2.0g/l H ₂ O ₂ Fe = 100.0 Ligand = 1.0 mM Temperature = 20.0 °C	100%	-	Xue et al., 2009
PCP (1.0 mg/L)	ZVI	pH = 3.0–7.0 Catalyst = 5.0 mg/L H ₂ O ₂ = 2.5 mg/L	90%	-	Santos-Juanes et al., 2019
4-CP (25.0-75.0 mg/L)	Mg/Fe-O ₂	pH = 2.0–5.0 Catalyst = 1.0–4.0 g/l	100%	-	Yang et al., 2019
4-CP (25.0 mg/L)	Au-Fe ₃ O ₄ magnetic nano composites	pH = 3.0-11.0 Catalyst = 0.05-0.1 g/l H ₂ O ₂ = 0.25–1.5 g/l Temperature = 20.0–40.0 °C	98%	Carboxylic acids	Liu et al., 2016
4-CP (25.0-100.0 mg/L)	Fe ₃ O ₄ -MnO ₂ core Shell nano composite	pH = 4.5–9.5 Catalyst = 0.1–1.0 g/l	100%	-	Liu et al., 2015
2,4,6-TCP (20.0-100.0 mg/L)	Fe ₃ O ₄ /CeO ₂	pH = 2.0–4.0 H ₂ O ₂ = 6.0–30.0 mM Catalyst = 0.5–2.5g/l	99%	Carboxylic acids	Xu and Wang, 2015
PCP (50.0 mg/L)	Fe ⁰ /CeO ₂	pH = 2.8-6.2 Catalyst = 1.0 g/l	100%	-	Xu et al., 2013

2,4,6-TCP (20.0 mg/L)	Pd/Fe	pH = 5.5 Catalyst = 5.0 g/l	94%	-	Zhou et al., 2010
PCP (10.0 mg/L)	Zerivalent Pd/Fe	Catalyst = 3.13, 6.25, 12.5 g /l Temperature = 5.0–45.0°C	98%	-	Shih et al., 2016
2,4-DCP 2,4,6-TCP (50.0 mg/L)	Yolk/shell Pd@Fe ₃ O ₄ @m etal organic framework	pH = 3.0–4.0 H ₂ O ₂ = 1.0–10.0 mM Catalyst = 0.5 g/l	100% (2,4-DCP) 75% (TCP)	-	Niu et al., 2018
2,4-DCP (200.0 mg/L) 2,4,6-TCP (100.0 mg/L)	Pd-Fe/ γ -Al ₂ O ₃	Catalyst = 2.0 g/l H ₂ O ₂ = 250.0 mg/L	100%	Carboxylic acids	Munoz et al., 2013
4-CP (100.0 mg/L)	Iron- glutamate- silicotungstate ternary complex (Fe ^{III} GluSiW)	pH = 3.0–8.0 H ₂ O ₂ = 10.0–20.0 mM Catalyst = 0.2–2.0 g/l	100%	-	Yin et al., 2015
	Iron- containing silicotungstate (Fe ^{III} AspSiW)	pH = 3.0–9.0 H ₂ O ₂ = 10.0–30.0 mM Catalyst = 0.1–1.0 g/l	100%	-	Chen et al., 2015

The generation of free sulfate-based radicals has also gained attention recently due to its high oxidation potential ($E_o = 2.5-3.1$). Activation of sulfate-based peroxygens like peroxymonosulfate (HSO_5^-), peroxydisulfate ($\text{S}_2\text{O}_8^{2-}$), persulfate, peroxysulfate etc. causes the production of Sulfate radical. Complete mineralization of PCP has been reported via microwave-activated persulfate (Qi et al., 2015). A plausible degradation pathway revealed the formation of different intermediate dechlorination species and hydroxylated products. As the electron cloud density is greater at para and ortho position as compared to meta, the generated sulfate radicals preferentially breaks the C-Cl bonds at these positions resulting in formation of dechlorination compounds (Ding et al., 2014). The degradation of PS from hydroxylated compounds results in production of quinone via hydrogen abstraction. In addition, the cleavage of C=C bond (s) via nucleophilic attack by sulfate radicals results in opening of the ring. The intermediates formed are further degraded into CO_2 and H_2O as the final degradation products. Similar fundamental mechanisms of electron transfer; hydrogen abstraction; replacement and addition reaction and pathway were observed under persulfate-ascorbic acid system and UV/sulfoxylate/phenol (USP) process where complete degradation of PCP was observed (Cao et al., 2019).

2.6.4 Electrochemical AOPs

The process is based on employing electric energy for degradation of the organic pollutants. The “green label” to the wastewater treatment is because it is chemical-free as the process requires electrons, and is operated at room temperature and atmospheric pressure. Earlier, the application was based on anodic oxidation accomplice either direct electrolysis of contaminants or oxidant-mediated chemical oxidation at the surface of anode. The process adverts increasing the mass transfer of oxidising radicals via turbulence and activating the oxidants at anode surface. An “oxidant cocktail” of oxidant species like ozone, peroxophosphates, peroxocarbonates, peroxosulphates, etc was observed though in a reaction cage and not on surface. The activation of is triggered by their interaction with other oxidants in bulk or either UV light or high frequency ultrasound irradiation. The electric

energy-based AOP like electro-Fenton and Photo-electro-Fenton, Sono-electro-photo-Fenton etc. oxidizes and destroys wide range of pollutants including the toxic agrochemicals and priority pesticides like endosulfan, PCP, hexachlorocyclohexanes, etc. (Govindan et al., 2014). Assertive operating parameters and conditions have been gauged and optimized in order to enhance the degradation efficiency of the system. The process has examined the use of electrodes such as platinum and graphite, carbon-based electrodes, metal oxide electrodes, and diamond coated electrodes. Boron-doped diamond (BDD) electrode used for removal of pesticides deltamethrin and endosulfan at pH 5.8-6.2, electrolyte concentration (NaCl, 1g/L), and current density of 60mA operated at room temperature reported more than 80% removal of COD in reaction time of 2 h (Errami et al., 2012). Another aspect of electrochemical process is efficient production of hydrogen peroxide from reduction of oxygen at cathode surface during electrolysis of wastewater. In order to enhance efficiency of the process, cathode plays a vital role in gas diffusion electrode approach. Coaction of cathodic production of hydrogen peroxide and anodic oxidation may result in 100% efficiency towards oxidation of organic impurities. Phenolic species and toxic dyes poses a serious challenge with an organic load sometimes increasing to level more than 10g/l of COD. Successful degradation of PCP has been achieved synergically via hydroxyl and sulfate radicals activated electrochemically from precursors peroxodisulfate, peroxomonosulfate and hydrogen peroxide (Govindan et al., 2014). The pollutant can also degrade electrochemically using TiO₂-modified zeolite-carbon composite electrodes. Persulfate activated radicals have proficiently resulted in degradation of hexachlorocyclohexane pesticide (Pimentel et al., 2008). Oxidative degradation and kinetics of mono and polychlorophenols have been investigated using electro-Fenton using carbon felt cathode (Oturán et al., 2009). Position and count of chlorine atom in the aromatic ring greatly influence oxidation of the compound. Mineralization rate significantly reduced with increased complexity of chlorophenolic structure following the order: 4-CP>2-CP>2,4-DCP>2,6-DCP>2,3,5-TCP>2,4,5-TCP>2,3,5,6-TeCP>PCP (Oturán et al., 2009). Simultaneous cleaving of aromatic structure and release of chlorine atoms from parent/intermediate structures decreases the toxicity of organochlorides in early

stages of the treatment. The process has emerged as a promising alternative for non-biodegradable wastewater. More of research is still awaiting to exploit the advantages of electrochemical process.

2.6.5 Ozonolysis

Ozone is a potent oxidant, selectively oxidizing inorganic and organic pollutants. It preferentially attacks the electron-rich functional groups like double bonds, amines, and aromatic rings (phenols). Being unsteady in water, the decomposition of ozone involves a complex series of atoms and single electron transport forming different ROS like OH^\cdot , HO_2^\cdot , HO_3^\cdot , O_2^- , $\cdot\text{OH}$, O_3^- , $\cdot\text{HO}_4$ thus enhancing efficiency of the system to degrade wide range of pollutants. The efficiency of ozonolysis predominantly depends on pH of the solution (Buffle et al., 2006). At alkaline pH condition (pH 8-9) ozone favors the generation of hydroxyl radicals increasing the degradation efficiency. Several studies have reported positive results of high pH on the efficiency of this process. The abundantly present hydroxide ions in system react with ozone and increase the yield of superoxide anion radicals which undergo a series of reactions producing hydroxyl radicals. Direct ozonation dominates in the environment when concentration of fast reacting species with molecular oxygen is high. Benitez et al., (2000) reported that the degradation rate enhanced with increasing the pH from 2.0 to 9.0 attributing to the enhanced hydroxyl radical generation and dissociation of phenols forming phenolate ions which have higher affinity to react with ozone. Ozonation reported to degrade harmful chlorophenolic compounds with great efficacy and enhanced degradation rate. Degradation of 2,4,5- TCP was carried out with ozone concentration of 1.5g/m^3 and pH 8 resulting in disappearance of all the phenolic pollutants within reaction time of 30 minutes. Incorporation of ozone with other AOPs enhances the degradation efficiency. Synergistic effect of sonocatalytic ozonation results in degradation of O_3 bubbles during sonolysis which leads to generation of more free radicals. The mineralization process of 2-chlorophenol enhances rapidly with ozonation integrated with photocatalysis (Oyama et al., 2011). With increase of catalyst dose (optimized at 1.0g/L), the dechlorination

occurs at enhanced rate. Complete degradation of 4-chlorophenol has been reported with TiO_2/O_3 within reaction time of 40 min (Oputu et al., 2015). Enhanced catalytic ozonation degradation of 2,4,6- TCP in presence of nano-ZnO catalyst at optimized dose and pH 7.5 was reported within reaction time of 30 minutes (Huang et al., 2005). The catalyst followed radical-induced mechanism initiating the production of hydroxyl radicals increasing the removal of pollutant. Ozonation and photocatalytic ozonation have proven effective for decomposition of 2,4-DCP (Aziz et al., 2018). The mineralization efficiency of the former was is, but complete TOC removal revealed enhanced mineralization with photocatalysis coupled ozonation. The 4-CP was subjected to degradation by different ozone-based processes- O_3/UV and $\text{O}_3/\text{H}_2\text{O}_2/\text{UV}$ (Peternel et al., 2012) and the oxidation of 4-chlorophenol by ozone resulted in formation of quinone which is subsequently degraded to compounds of lower molecular weight and aliphatic carboxylic acids like oxalic acid, formic acid etc. In the absence of scavengers in the reaction mixture, synergistic effect of $\text{O}_3/\text{OH}\cdot$ led to emergence of hydrogen peroxide. Reaction of ozone with dissociated HO_2^- resulted in generation of $\text{OH}\cdot$ radicals triggering a chain reaction which further produces olefins. Subsequent ozonation results in mineralization producing carbon dioxide and water. Complete degradation of the contaminant was observed with UV-induced ozonation process within reaction time of 1 h. Addition of oxidant H_2O_2 accelerates the ozone decomposition increasing the generation rate of hydroxyl radical. Degradation of another MCP via ozonation and O_3/UV system results in complete decomposition of the contaminant within 20 minutes of the reaction time (Ku et al., 2002). Presence of matrix pollutant, *t*-butanol promotes the degradation efficiency. The mineralization of intermediates results in formation of carbonate ions. The aforementioned processes were investigated during decomposition of 2,5-DCP (Alexander et al., 2016). Complete degradation by ozone was observed in 60 minutes while it took 40 minutes to achieve the same in presence of UV-light induced ozonation. The addition of oxidizing reagent H_2O_2 (516 mg/L) in the ozonation system was employed for degradation of 2,4,6-TCP in presence of humic acid as matrix pollutant (Graham et al., 2003). The ozone radical oxidation degraded 90% of the pollutant within 10 minutes of reaction time. Addition of H_2O_2

enhances the dechlorination while humic acid enhances degradation rate of TCP. Ozonolysis process has been employed for degradation of PCP where the direct nucleophilic attack by ozone initiated the degradation process takes place. Both ozone and secondary hydroxyl radicals simultaneously degrade the subsequent intermediates formed in the reaction matrix. The degradation of PCP via ozonation is either a direct reaction with O₃ or through secondary free radicals (OH•) from hydrolysis of O₃ or it could be via both (Hong and Zeng, 2002). Because of the presence of 5 electron-withdrawing group chlorine atoms, the electron density on the ring decreases thus paving the way for O₃ for the nucleophilic attack via addition-elimination mechanism which is a direct reaction with O₃ resulting in formation of tetrachloro-*p*-benzoquinone. Whereas, the degradation via free-radical pathway and result in formation of tetrachloro-*p*-hydroquinone, subsequent redox reactions involving free radicals and oxidation of intermediates resulted in formation of oxalic acids and simpler organic acids. The process has been reported fruitful when incorporated with conventional treatment methods. Aerobic biological system removed 70% TOC after pre-ozonation of 2,4-DCP (Contreras et al., 2003). Pre-ozonation also inhibits the formation of halophenols during chlorination in seawater (Ding et al., 2018). Ozonation significantly decreases the toxicity of parent pollutants generating less noxious intermediates and end-products with enhanced biodegradability. Ozone, thus, performs the dual function of an oxidant as well as disinfectant. The process is thus a promising approach towards degradation of recalcitrant xenobiotics. Regardless of the methodology, AOPs share a common mode of action: AOPs → Production of unselective radicals → Attack the organic pesticide → CO₂ + H₂O + inorganic ions

2.6.6 Sustainability Evaluation

Environmental performance of AOPs has demonstrated the energy demands and consumption of chemicals in short duration as the main problem. Thus, the challenges of AOPs are to use more environmentally friendly energy sources like solar energy, reducing more than 90% of the environmental impact. As wastewater is laden with impurities like chlorides and inorganic carbon as carbonates and

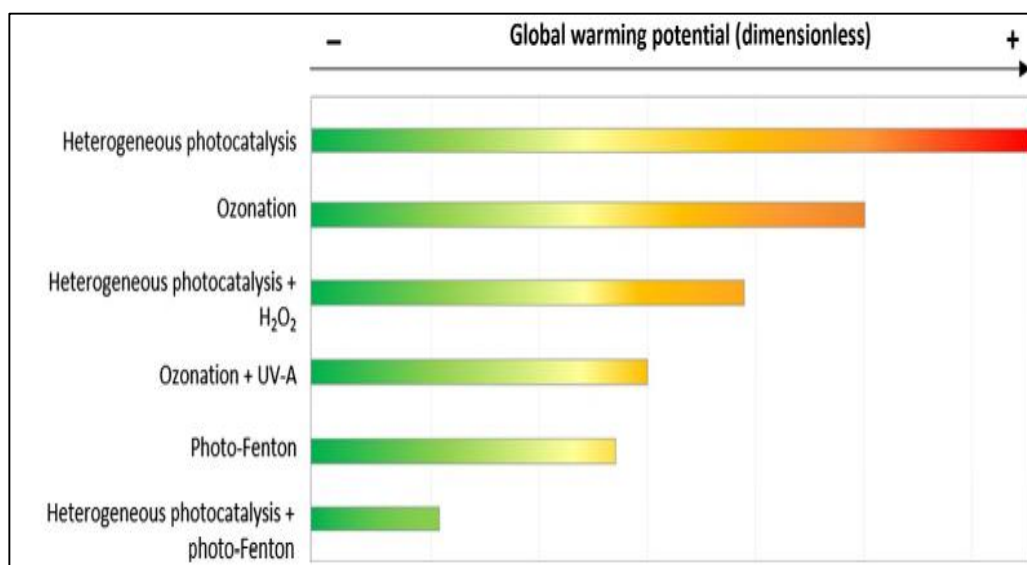
bicarbonates as well apart from the organic load, these species act as scavengers of hydroxyl radical generated via AOPs. The presence of these species hampers the performance of AOPs and removal efficiency of the target compound. Another significant factor is deactivation of catalyst. The inactivation of catalyst could be a consequence of surface blocking or deposits on the surface, leaching of the active compound, changes in the physical nature, reduction in the active sites. Since sustainability is a hot topic, the strengths, weakness, opportunities, and threats *i.e.*, SWOT analysis of AOPs and other processes has been illustrated in Table 2.4. The challenges associated with conventional wastewater treatment method is the concern over human health and environment, efficiency of resources, minimization of waste, and not the least but enhancing the circular economy approach. Nonconventional treatment methods, use of wetlands, biological filters, etc has been proposed in order to reduce the energy demands and cost. Application of LCA to AOPs reported that consumption of energy is associated with global-warming impact. There is a strong relationship between global warming potential (GWP) and energy consumption. AOPs are thus, more energy-intensive rather material-intensive processes (Munoz et al., 2005) (Figure 2.5.6). Photocatalysis is among one of the AOPs that represent a worse environmental scenario in terms of high energy demands. To minimize this, addition of H_2O_2 reduces the impact by 40% while also increasing the removal efficiency. Photocatalysis when coupled with photo-Fenton reduces the energy demands and simultaneously decreasing the global warming impact compared to the photo-Fenton (58% GWP reduction) and photocatalysis (86% GWP reduction). In case of Photo-Fenton, addition of chemicals like iron, H_2O_2 and energy demands are significant contributors towards environmental impact. In case of ozone-based AOPs, ozone results in high degree of mineralization, causing moderate to high environmental impact. Thus, switching to renewable energy resources could cut down the energy input by more than 90%. Further, using solar driven AOPs could help in easy implementation or popularisation of these technologies. For instance, in photo-Fenton and photocatalysis systems, electricity represents around 90% of the total impact, and in ozonation process 70%–80% of the impact results from the energy required to run the lamp.

Table 2.4 SWOT Analysis of Different Effluent Treatment Methods

S. No	Treatment methods	STRENGTH	WEAKNESS	OPPORTUNITY	THREAT
Advanced oxidation processes (AOPs)					
1.	Electrochemical Oxidation	Direct-Indirect Mechanism; No additional chemicals require.	Electricity consumption; Electrode material dependence and supporting electrolytes.	Simultaneous mineralization and disinfection.	Cost and life of electrode; Dependence on electrode manufacturing.
2.	Ozonation	Experience as oxidant and disinfectant.	pH dependant; Solubility of ozone and short life; Mass transfer limitation.	Catalytic ozonation; Combination with H ₂ O ₂ (peroxone).	Energy dependant for ozone generation.
3.	Sulfate-based radical	Selective nature; Longer life. High pH range.	Precursors require activation; Release of Sulfate ions.	New developments on nano-materials.	Dependence of commercial precursors.
4.	UV/H ₂ O ₂	Homogeneous phase; Simultaneous disinfection.	Cost of both material (H ₂ O ₂) and energy (UV Radiation).	Combination with ozone.	Light penetration and bubbles in effluents.
5.	Photo-Fenton	Radiation induces catalyst regeneration; Can operate under natural solar light.	pH restrictions; Sludge generation.	Combines with semiconductors; Organic ligands extends pH range and visible light use.	Light dependant; Cost of H ₂ O ₂ and energy (artificial radiation).
6.	Photocatalysis	Commercial TiO ₂ catalyst properties and price.	Catalyst limitations for visible light; Turbidity leads to low photon absorption efficiency.	New reactor design; New developments on nano-materials; Progresses on LEDs technology.	Catalyst reuse: in suspension requires separation or catalyst immobilization.

Continued...

Conventional treatment method:					
7.	Membrane technology	It can remove the dissolved impurities to produce cleaner water with lower turbidity.	Electricity is required to run the system with high installation and maintenance cost; Concentrated sludge is produced and its handling is an issue.	Cheaper membranes can be developed using different technologies.	Threat to price fluctuation; It requires pre-treatment of wastewater else, the membrane will clog faster.
8.	Coagulation and flocculation	Simplicity of method that can remove fine particles, virus, bacteria, and heavy metals.	Produces the sludge whose disposal and handling is a problem; It is sensitive to pH and produces greenhouse gases; Skilled supervision is required.	Use of different chemicals that enhance coagulation and flocculation efficiency at a cheaper rate.	Change in pH of wastewater affects formation floccs; Chemicals are prone to price change.
9.	Biological treatment	Low operational cost; Stable sludge is produced; Lesser quantity of sludge production.	It is a time taking process and a slow process; Temperature and pH dependent that can hamper the degradation rate.	Seeding of bacteria can improve the degradation rate; Development of new technologies such as ASP can improve rate of degradation of organic matter and its efficiency.	Lower degradation of organic matter in cold weather; Microbes could die in high toxicity, and high temperature wastewater discharge.



Source: Munoz et al., 2005

Fig. 2.5 Global-warming potential for different AOPs

2.7 Phytoremediation of PCP

Phytoremediation is a part of bioremediation that involves the biological entity, such as a plant or an organism, as a medium to remediate the polluted soil/water. It involves the use of promising plant species that can uptake the pollutants from water and sediments to degrade it. Compared to other physico-chemical treatment methods and techniques, phytoremediation is a safe, cheap, less disruptive, promising, environment-friendly, and a sustainable technique that changes the form of pollutant (Cunningham and Ow, 1996). Phytoremediation has been promisingly used to study the removal of nutrients (Nitrogen and Phosphorus) from wastewater using wetland plants such as *Phragmites australis*, *Canna lily*, and *Brachiaria mutica* (Haritash et al., 2015; Nandakumar et al., 2019; Pipil et al., 2021). Hence, it can be said that acts as the sink of pollutants. Remediation techniques using the plants are growing in demand because these do not require any energy source which makes it eco-friendly and sustainable in its approach; non-invasive, acceptable by common population too since it doesn't make use of the any harmful chemicals (Pilon-Smits, 2005).

Table 2.5 Plant species used to remove phenolic compounds

Plant species	Phenolic compound	Reference
<ul style="list-style-type: none"> • <i>Lemna gibba</i> • <i>Typha angustifolia</i> 	PCP	Werheni Ammeri et al., 2021; Werheni Ammeri et al., 2022
<ul style="list-style-type: none"> • <i>Salix interior</i> • <i>Trifolium pratense</i> 	PCP	Lachapelle et al., 2021
<ul style="list-style-type: none"> • <i>Salix purpurea,</i> • <i>Festuca arudinacea,</i> • <i>Medicago sativa</i> • <i>Brassica juncea</i> 	PCP	Yanitch et al., 2020
<ul style="list-style-type: none"> • <i>Nicotiana tabacum</i> 	Phenol 2,4-DCP	Paisio et al., 2021; Talano et al., 2010; Laurent et al., 2007
<ul style="list-style-type: none"> • <i>Brassica napus</i> 	2,4-DCP	Agostini et al., 2003
<ul style="list-style-type: none"> • <i>Eichhornia crassipes</i> 	Phenol	Singh et al., 2021
<ul style="list-style-type: none"> • <i>Hydrilla verticillata</i> 	Phenol	Chang et al., 2020
<ul style="list-style-type: none"> • <i>Lemna minuta</i> 	Phenol	Paisio et al., 2018
<ul style="list-style-type: none"> • <i>Datura stramonium</i> 	2,4-DCP	Ceylan et al., 2021

Plant species involved in phytoremediation use different mechanisms viz. phytoextraction, phytodegradation, phytovolatilization and rhizodegradation in order to convert the complex chemical compounds into the simpler forms (Gerhardt et al., 2009; Abhilash et al., 2009). Nowadays, genetic engineering is more focused on developing the genetically modified plant species that are more tolerant to toxic chemical shocks, higher pollutant removal efficiency, and higher degradation efficiency towards organic waste (Wenzel, 2009). The various plant species used in phytoremediation for removal of phenolic compounds from water and soil are given in Table 2.5.

2.7.1 Phenolic compound uptake and translocation

Plants, as their daily metabolic activity, absorbs the nutrients and contaminants from air, water and soil. The capacity of absorption by plant depends upon the biomass which also acts as the limiting factor for the removal of pollutants from water and soil. The uptake of the pollutants from contaminated matrix depends upon the characteristics of the pollutants, such as, its molecular mass, concentration, polarity; while it also depends upon the soil mineral content and its pH; the ambient temperature, sunshine hours, external stress to plant, etc. (Reid et al., 2000). Plants directly remove the pollutants either by sorption on its tissue, or by uptake and translocation, and metabolism of pollutants. Initially, the contaminants present in the water/soil come in contact with the roots and may sorb or bind with roots and its cell walls. The sorption of contaminant from the water to the roots has been reported in many studies (Haritash et al., 2017). Phenolic compounds are partially adsorbed over the surface of roots resulting in the removal of pollutants from water, however, this process of removal of phenolic compound from water shows poor removal efficiency which keeps on decreasing with time (Coniglio et al., 2008). Apart from root sorption, the absorption process performed by the plant is considered as an important process. It is carried out by roots and leaves, in which the roots, firstly, diffuses the pollutants over the surface abstracting them from surrounding, followed by slow accumulation of the pollutants over its surface (Korte et al., 2000). The pollutants will bind to the lipid bilayers due to

hydrophobicity to help in facilitating its transport. There is a parameter $\log K_{ow}$ that decides the pollutant uptake capacity by plant. The $\log K_{ow}$ for phenols, 4-CP, 2,4-DCP, and 2,4,6-TCP has the value 1.46, 2.85, 3.05, and 3.7, respectively (Pascal-Lorber et al., 2008; Weyens et al., 2009). The $\log K_{ow}$ value = 5.05 for PCP shows that it will be less absorbed by the plant roots, while phenols ($\log K_{ow} = 1.46$) are absorbed more by roots. The uptake and translocation of different organic pollutants differs among the different plant species, can be said that uptake efficiency varies among the plant species even if they belong to the same genus. The microbes present in phyllosphere can transform the organic pollutants. Rhizosphere microbes produce the metabolites and intermediate compounds through the transformation of contaminants, while, microbes present on leaves of plants can potentially contribute to phenolic attenuation (Sandhu et al., 2007).

Once the pollutants are absorbed by roots and leaves, they are translocated to different parts of the plant, and into their cells by transpiration, which is known to transport nutrients. Transpiration Stream Concentration Factor (TSCF) is used to estimate the uptake of pollutant by the plant, which may be defined as the ratio of the pollutant concentration in the transpiration stream of the plant to the concentration in water/ soil (Dietz and Schnoor, 2001a). TSCF varies between zero (no uptakes) to 1.0 which means uptake at the same concentration in transpiration as concentration present in water. TSCF for phenol and PCP indicates the value of 0.48 and 0.04 for the poplar trees (Dietz and Schnoor, 2001a). However, the translocation depends upon the rate of transpiration (litres per day), plant type, leaf area, soil moisture, temperature etc. make it obvious that the plants with higher transpiration rate, like poplar show more pollutant uptake as compared to other plant species used for same purpose of phytoremediation. Because of the inefficient excretory system in plants, the conjugates of xenobiotics are sequestered mainly in vacuoles or integrate in cell wall as bound residues. The potential mechanism involves microbial transformation by endophytes and rhizosphere microbes, sorption and uptake of pollutants and its metabolites by roots, extra and intracellular enzymes-catalysed transformations, transfer of compounds to leaves via xylem,

foliar uptake from air, probable transfer via phloem and bound residue formation. These mechanisms enhance the phytoremediation of phenolics from environment. The technique is a promising approach towards the remediation of persistent organic pollutants such as PCP. Plants are capable of the enzymatic transformation of PCP (phytotransformation); help alleviate PCP contamination via uptake from soil (phytoextraction) (Hechmi et al., 2014; Lin et al., 2008). Phytoremediation in symbiosis with microbes enhances the removal of xenobiotic compounds. Bacteria in association with plants can degrade catabolic diversity, accumulate, and transform the harmful organics via production of phytochelors, phytohormones, etc (Batty and Dolan 2013). PCP degradation significantly enhanced at sites with plants and the PCP-degrading, gram-negative bacterium *Sphingobium chlorophenolicum* compared to degradation of the plant alone (Dams et al., 2007). Numerous plant species such as ryegrass (*Lolium perenne*), radish (*Raphanus sativus*), willow (*Salix sp.*), poplar (*Populus sp.*), and sunflower (*Helianthus annuus*) are the promising entrants reported for phytoremediation of PCP (Ping , 2009). Plant-mediated dissipation of PCP under diverse cropping patterns in the presence of vegetation enhanced the degradation of PCP in the soil atmosphere using plant species alfalfa (*Medicago sativa*), ryegrass (*Lolium perenne*), White clover (*Trifolium repens*), and rapeseed (*Brassica napus*) (Hechmi et al., 2014). Aquatic macrophytes such as *Phragmites communis Trin*, *Theileria orientalis*, and *Scirpus validus Vahl* can treat PCP-contaminated sediments (Zhao et al., 2011). Plants modify the geochemical environment of rhizosphere by releasing various secondary metabolites, enhancing the microbial activity in the root zone, thereby increasing the biodegradation (rhizoremediation) (Dams et al., 2007; He et al., 2005). Plants species such as *Salvinia molesta*, *Helianthus annuus*, *Phragmites australis*, *Lemna minor*, *Pistia stratiotes*, *Phaseolus vulgaris*, *Arundo donax*, *Eichhornia crassipes*, *Trapa natans*, have been assessed for their ability to absorb and sequester toxic contaminants both from soil and water (Sweta et al., 2015; Tiwari et al., 2018). *Zea mays L.* species has the potential to enhance the remediation of soil with single PCP or Cd and coexistence with PCP-Cd (Hechmi et al., 2013). As the degradation gradient followed the order: near rhizosphere > root compartment > far-rhizosphere soil zones, it implies extreme proximity of

roots towards dissipation of PCP and *Zea mays L* significantly stimulated the activity of the microbial community in the region (He et al., 2005, 2007; Njoku et al., 2012). The growing interest in using trees (woody species) for phytoremediation has recently gained attention (Pulford & Watson, 2003). Trees such as willow exhibit phytoremediation qualities, such as quick growth, faster proliferation, deep rooting, ability to adapt to a wide variety of climatic conditions, and temporary tolerance to waterlogged environments (Jensen et al., 2009; Teodorescu et al., 2011).

2.8 Integrated Management of Chlorophenols

The pace of industrialization, the depletion of clean water supplies, and the huge fines levied by environmental regulations have made it possible to establish and introduce environmental processes and chemicals in the textile industry. (Toprak & Anis, 2017). Techniques such as the adoption of recovery to minimize environmental harm and energy consumption for environmental conservation, the use of ecologically friendly fabrics or other materials, the reduction of emissions, and the development of methods for subsequent pollution removal have become increasingly relevant. In the textile industry, about 2000 various chemicals are used, including dye, transfer agents, etc. (Shenai, 2001). Amending the principles of green chemistry ensures the "cleaner production" approach instead of the "end of pipe" (Sherburne, 2009). The ultimate aim in the atom economy is accomplished when all the reagents are consumed in the product with zero generation of by-product. While in practice this is often not possible, reaction schemes should be formulated in such a way that by-product \ll product

Industrial symbiosis could serve as a framework to combat pollution where surplus resources produced by an industrial process are retained instead of being thrown away or abandoned, then readdressed for use as a 'novel' input by one of the other companies for another process, providing mutual assistance or symbiosis (Fletcher, 2009).

The development of environmentally improved routes and the purpose of green chemicals are two facets of green chemistry assigned towards easing the impact of chemical processes on the environment (Ballivet-Tkatchenko et al., 2005). Textiles Industry has many working procedures that influence environmental health. Table 2.6 shows the environment-friendly chemicals which could serve as an alternative to the harmful chemicals used continuously in textile industries (Jeihanipour et al., 2010; Shenai, 2001). Several environmentally friendly fabrics, such as bamboo, hemp, ramie, mud silk, etc. have been developed that do not necessitate use of pesticides or chemicals. 'Organic linen' is manufactured from flax fibers without the application of harmful pesticides and fertilizers. A non-toxic, biodegradable, and completely recyclable organic hydrate solvent called N-methyl-n-oxide (NMNO) is used to regenerate cellulose to manufacture lyocell fibre (Perepelkin, 2007). The fibre is significantly more sustainable than oil-derived synthetic fibers and natural fibers such as cotton (need pesticides and fertilizers to grow). Land required for growing cotton is more than the eucalyptus trees, from which lyocell is made (Blackburn et al., 2005). Regenerating the cellulose can be significantly simplified by using ionic liquids that serve as the solvent and are almost entirely recycled. The bamboo fibers are very soft, taking dye to deeper shades than cotton, having natural anti-microbial properties, and are far more eco-friendly than cotton and other fibers (Hardin et al., 2009). Since the dyes are synthetically produced, the ortho-hydroxy group's effect on the dye's coloristic properties can be easily counterbalanced by choosing another appropriate substituent (Moozyckine & Davies, 2002). The dyeing of cationic cotton is more sustainable because it requires no salt, no alkali and can be dyed at relatively low temperatures with reactive dyes. The supercritical fluids can adopt properties midstream concerning gas and a liquid expanding to gratify its vessel like a gas but with a liquid density. Solvents like supercritical fluids used as a dyeing medium (called waterless dyeing) has received considerable attention. The most extensively used supercritical fluid is carbon dioxide (scCO₂), as it conglomerates a relatively mild critical point with non-flammability, non-toxicity, and is cost-benefit. It is among the best supercritical solvent for textile dyeing because of its green and safe character.

2.8.1 Management options for PCP

Incineration of waste

The PCP-treated wood disposed of in landfills, chances of leaching of PCP and micro-contaminants is a significant threat to the environment. Disposal of such type of hazardous waste preferably involves a high temperature-controlled combustion process. The combustion of PCP-treated wood at 910°C-1025°C detected no chemicals in the off-gas. At a temperature below 800°C, the incineration of PCP is not carried out properly, resulting in incomplete combustion (Pollutants, 2010). The advantage of high temperature is that it reduces the occurrence of dioxins and furans. The scrubbing process of the effluent gas minimizes the release of hydrogen gas.

Chemical Alternatives

An effective wood preservative must have the property of non-corrosive towards metals, must not itself harm the wood, must be toxic towards wood-destroying organisms. Copper azole (CBA), creosote, ammonical/alkaline copper quaternary (ACQ), sodium borates (SBX), copper and zinc naphthenates, copper arsenate (CCA), and copper HDO (CX-A), 3 yodo-2-propinyl-buthylcarbamate, propiconazole, and diclofuanide, are different chemicals analogous to PCP (Pollutants, 2010). However, these alternate chemicals possess certain disadvantages to their application field since no application is entirely dependent on PCP.

Material Substitution

Approach to material substitution, replacing existing materials with some more environmentally friendly materials, or reducing the weight and the thickness of the products, fabricating it in a mode that allows the product to be more efficiently recycled (Toprak & Anis, 2017). Most PCP is used to extend the useful life of wood,

principally utility poles, pilings, and crossties, a non-chemical alternative of replacing materials with concrete, steel, naturally resistant wood, etc., could be used—replacement of wood by these materials which don't leach and has more environmental benefits. Switching to decay-resistant wood like tropical hardwood or American chestnut wood can be potentially used without any treatment.

As peroxidase is well characterized for the removal of coloured aromatic compounds from wastewater, fenugreek (*Trigonella foenum-graecum*) (FSP) seed peroxidase has demonstrated its ability for decontamination of potentially harmful aromatic contaminants in the presence of various redox mediators (Husain et al., 2010). The effluent treated from FSP in the presence of redox mediator, 1-hydroxy benzotriazole (HOBT), produced insoluble aggregates, which can be easily eliminated via centrifugation. The oxidative polymerization and removal of bisphenol A, a highly toxic agent and endocrine disruptor, was further successfully activated by fly ash adsorbed peroxidase (Karim & Husain, 2010). The biosorption process is more efficient than conventional treatment for the retention of cations or organic compounds at trace amounts and highly energy efficient. Lignin, obtained as a by-product from the paper and pulp industries (50 million tonnes per year), is an affordable natural resource and the third fundamental component of plant biomass (16% to 33%) after cellulose and hemicellulose (Suteu et al., 2010). Frequent simulations conducted on reducing certain organic pollutant species with sorbents using lignin, modified lignin, and lingo-cellulosic materials suggest that lignin sorption is a step inward to the viewpoint approach. (Guo et al., 2008).

Table 2.6 Environment-friendly chemical choice in wet textile processing

Process	Chemical Used	Alternative
Sizing	Starch	Water-soluble PVA (polyvinyl alcohol)
Size preservatives	Pentachlorophenol	Sodium silico-fluoride
Desizing	Hydrochloric acid	Amylases
Scouring of cotton	Sodium hydroxide	Pectinases
Bleaching	Hypochlorite's	Hydrogen peroxide
Oxidation of vat & sulphur dyes	Potassium dichromate	Hydrogen peroxide, sodium perborate
Thickener	Kerosene	Water-based polyacrylate copolymers
Hydrotropic agent	Urea	Dicyanamide (partially)
Water Repellents	C8 fluorocarbons	C6 Fluorocarbons
Stabilizers	Phosphorous-based compounds	Nitrogenous stabilizer

Crease recovery chemicals	Formaldehyde-based resin	Polycarboxylic acid
Wetting agents and detergents	Alkyl phenol ethoxylates	Fatty alcohol phenol ethoxylates
Neutralization agent	Acetic acid	Formic acid
Peroxide killer	Sodium thiosulphate	Catalases
Mercerization	Sodium hydroxide	Liquid ammonia
Reducing agents	Sodium sulphide	Glucose, acetyl acetone, thiourea dioxide
Dyeing	Powder form of sulphur dyes	Pre-reduced dyes
Flame retardant	Bromated diphenyl ethers	Combination of inorganic salts and phosphonates
Shrink Proofing	Chlorination	Plasma treatment
Carriers in Polyester dyeing	Dichlorobenzene, trichlorobenzene	Butyl benzoate
Softening and water repelling	Silicones and monosilicons; alkyl phenol ethoxylates	Anionic/cationic softeners wax emulsion

2.9 Eco restoration

There has been an upsurge in sites contaminated with organic pollutants particularly in the developing nations. CP have large industrial applications which make it a widely used chemical for pesticides, wood preservatives, pharmaceuticals and dyes, etc. The application of pesticides to agricultural fields, fungicides applied to timber and paper for preservation, etc. are few applications that lead to its interaction with soil, aquatic and marine bodies. Soil and water, being the two rudiments of the ecosystem, are crucial for existence and development. These pollutants deteriorating soil and water quality have posed a severe threat to food safety, ecological balance, and agricultural sustainability. Thus, several eco-friendly measures are adopted to reclaim soil health using plants, microorganisms, organic amendments etc.

It is known that CPs are stable in inorganic soil which attribute to unfavourable conditions for microbes to degrade it (Valo and Salkinoja-Salonen, 1986). Cleanup of CP-contaminated soil via biological process is attributed due to the presence of certain degraders in the soil biota capable of mineralizing the compounds further justifying the natural origin of these toxicants somewhere in the ecological processes (Potgieter et al., 2009). Even if CP degrading microbes are present in the CP contaminated soil, the rate of degradation is very slow in natural environment which does not cope with soil contamination. Addition of pre-acclimatized microbial culture in contaminated soil increases the interaction with indigenous species thus enhance the natural self-purifying potential of soil (Lallai and Mura, 2004). The residual CPs in the soil are threat to contamination to groundwater through percolation (Valo et al., 1984), and hence the soil should be protected against leaching by using plastic sheets on ground surface during treatment of CP-contaminated soil. Usually, application of farmyard manure or compost is considered beneficial (Loick et al., 2012). Mixing of CP contaminated soil with bark and ash in different proportion provides a mixed culture for laboratory grown CP degrading bacteria that helps in degradation of CP (Valo et al., 1985). The CP contaminated soils are toxic to microbes and addition of bark can help in reducing its toxicity (Valo and Salkinoja-Salonen, 1986). Aerobic composting with bark chips and CP degraders has resulted substantial degradation

of CP residues. Similar effect of addition of bark chips and nutrients with compost has also been found beneficial (Barriuso et al., 1997). Increased content of organic matter after amendment of compost has the potential of increasing the microbial diversity and activity. In addition, if artificial environment is created for microbes by providing sufficient oxygen, maintaining suitable pH, temperature and moisture, the rate of CP degradation increases (Chen et al., 2015). In a study conducted by Valo & Salkinoja-Salonen et al., (1986) the removal of CP was of order 80% within a period of 4 months, but mixing and augmentation of large amount of organic additives to CP contaminated soil requires excavation of soil, its mixing and tilling, and its transport to another site (ex-situ) that makes it cost intensive. However, inspite of degradation of CP present in soil, bioremediation of CP contaminated soil is a cost-effective remediation procedure (Kästner, 2000). Amendment of organic and mineral soil is an essential step for reclamation of contaminated sites. Such amendments improve the remediation efficiency as various natural physical, chemical and biological processes in soil are enhanced (Sakshi et al., 2019). Organic amendments such as compost, manures, organic by-products while mineral amendments which include gypsum, volcanic ashes, foundry sand, coal combustion products, etc., are found efficient towards degradation of harmful toxicants (Fernández-Luqueño et al., 2017). Addition of sand increased the passage for oxygen and proton, improving the porosity of soil, enhancing the charge output and reducing the ohmic resistance. The amendment of sand increased the mineralisation of pollutants while retaining the soil functions (Sakshi et al., 2019). Treatment such as bioaugmentation, biostimulation, biofilters, bioreactors, bioventing, and phytoremediation are commonly applied methods to remediate the contaminated sites (Kumar et al., 2020). Bioremediation methods are ideal for organically polluted areas and have been the subject of a great deal of bioremediation studies (Cunningham et al., 1995). It can be achieved by adding bio-stimulating agents like nutrients, fertilizers and organic substrates, and bio-augmenting it through addition of CP degrading microbes (Antizar-Ladislao et al., 2004; Loick et al., 2012). Addition of bench scale compost on CP-contaminated soil resulted in 60% conversion to carbon dioxide (Laine and Jorgensen 1997). Application of compost not only improved the soil biota but also enhanced the potential contaminant degraders in the soil biome. The positive effect of composting process is reported to persist for more than 5 years in the long run (Hernández et al., 2015).

Landfarming is another bioremediation method where excavated contaminated soil is transported to landfarming site and is then outspread over a bed and periodically turned over for aeration. The microbial metabolic and oxidation processes cause degradation of pollutants (Sakshi et al., 2019; Riser-Roberts 1998).

The soil needs to be ecologically restored to its natural health after the concentration and toxicity of CP contaminated soil is reduced. It is always recommended to use the native plant species instead of exotic species. The native species have social, sacred and higher market value when compared with exotic species. They also have the potential to easily adapt to the local environment. However, sometimes exotic species may also be chosen for their quantity of timber, their properties, market value of their fruits, etc. Phytoremediation method includes a diverse collection of plant-based technologies that either use native and wild species or genetically engineered plants for remediating environments (Nandakumar et al., 2019; Pipil et al., 2021). While adopting tree species for ecorestoration, it is recommended to plant the trees in a specific layout, for instance, mixed species plantation established using two different tree species planted in alternate rows, mixed species plantation established using two species planted at random, mixed species plantation established using four species planted in rows, and mixed species plantation established using four species planted at random (Lamb, 1998). The degree of improvement through restoration of land has been found to be significant during mixed species tree plantation. Another ecological group, grasses represent an economically important plant family used in the food production industry as fuel and raw material, lawns and pasture, forage, sports, gardening, phytoremediation, and ecorestoration. The extensive root system, large biomass, and faster growth, occupying an excellent ground cover and monocots, makes them more advantageous in tolerating higher pollutants than dicots (Pandey & Singh, 2020). Although there are a number of studies on phytoremediation of metal contaminated soil, but, reports on ecorestoration of CP-contaminated soils are few. It is high time to explore the role of plants and associated rhizospheric microorganisms towards degradation of residual CPs in soil and improvement in soil health. In addition, the role of exogenously added nutrients and organic amendments should also be investigated to achieve even higher treatment rates under the set of optimized conditions.

CHAPTER 3

MATERIALS AND METHODS

3.1 Chemicals

To carry out the current study, the analytical grade 2,4,6-Trichlorophenol (purity 98%) was procured from Thermo Fisher Scientific (USA), whereas 2,4-Dichlorophenol (98% Purity), 4-Chlorophenol (98% Purity), $\text{FeSO}_4 \cdot 7\text{H}_2\text{O}$ as source of Fe (II), and Hydrogen peroxide H_2O_2 (30% w/v) which was used as an oxidant were purchased from Central Drug House (CDH), India. For pH adjustment, NaOH and H_2SO_4 were also obtained from Central Drug House (CDH), India. Sodium acetate, hydroxylammonium chloride, and 1,10-phenanthroline were purchased from SRL Chemicals, India. Degussa P25 Nano- TiO_2 (anatase to rutile ratio-80:20) used as photocatalyst was obtained from Evonik Industries, Germany. HPLC grade methanol was obtained from Merck & Co (India).

Preparation of Stock Solution

Synthetic stock solution of strength 100 mg/L for all the chlorophenolic compounds was prepared in Type 1 water. For MCP, 100 mg of Analytical grade 4-CP salt was mixed in 1000 ml Type 1 water. Similarly, 2,4-DCP and 2,4,6-TCP was prepared by mixing 100 mg each in 1000 ml. Mixed-Chlorophenol stock solution of strength 100 mg/L was prepared by mixing 4-CP, 2,4-DCP and 2,4,6-TCP in ratio 2:4:4.

3.2 Analytical methods and Instrumentation

UV-Vis Spectrophotometer

The degradation profile of CPs (2,4,6-TCP; 2,4-DCP and 4-CP) was continuously monitored using a double beam UV-vis spectrophotometer (Lab India make; UV 3092 model). An absorption spectrum in the wavelength range of 190

nm – 800 nm was plotted and the wavelength of maximum absorption (λ_{\max}) was obtained. For 2,4,6-TCP, 2,4-DCP, 4-CP, and mixed chlorophenols (Mi-CPs), the maximum adsorption wavelength was detected at 290 nm, 283 nm, 280 nm, and 280 nm, respectively. The calibration graph for all the chlorophenols were plotted in concentration range of 10-100 mg/L at 10 mg/L of intervals. For Mixed-chlorophenols (Mi-CPs), a mixture solution of MCP, DCP and TCP in ratio of 2:4:4 (strength 100 mg/L) was prepared. Calibration curve was plotted in the similar manner for individual chlorophenols. The removal efficiency was calculated using the following equation (eq 3.1):

$$\text{Efficiency (\%)} = \left[\frac{C_i - C_t}{C_i} \right] \times 100 \quad (3.1)$$

Where, C_i is the initial concentration of respective CPs (mg/L); C_t is the concentration of CPs at time 't' (mg/L)

High-Performance Liquid Chromatography (HPLC)

The residual reaction concentration of the model compound during the oxidation was ascertained using chromatographic analysis. The HPLC system (Shimadzu make LC-20AD) equipped with UV/Vis detector (SPD-20A) and C-18 column (Inertsil® ODS-3V, 5 μ m 4.6 \times 250 mm) was used for the detection of formation of intermediate chemical species. A standard curve of model chemical (TCP) was plotted at 10 mg/L intervals in the concentration range of 0.0–100.0 mg/L over the HPLC system. The mobile phase methanol and water (70:30 v/v) was used in binary mode at a flow rate of 1.5 ml/min for separation by HPLC, and the response was recorded at 290 nm in case of TCP.

Total Organic Carbon (TOC)

Mineralisation of TCP was confirmed using TOC Analyser to validate the observations over UV–Vis spectrophotometer and HPLC. Total organic carbon was analysed using Shimadzu make TOC analyzer (model TOC-LCPH) which conforms to APHA 5310 Total organic carbon (TOC). The instrument was

calibrated using standard solution of total carbon (TC) and inorganic carbon (IC). The TC standard solution of strength 1000 mg/L was prepared by adding 2.125 g of potassium hydrogen phthalate ($C_8H_5KO_4$) in 1000 ml Type-I water. Similarly, IC standard solution of strength 1000 mg/L was prepared by adding 3.497 g of sodium hydrogen carbonate ($NaHCO_3$) and 4.412 g of sodium carbonate (Na_2CO_3) in 1000 ml Type-I water. The instrument is calibrated for TC and IC with auto dilution, and TOC is calculated as a difference between TC and IC using the instrument. Pretreatment TOC of respective chlorophenols were measured before the commencement of degradation process and post treatment. TOC was measured to determine the degree of mineralization at the end of experiment. Mineralization percent was calculated using the following equation (eq 3.2):

$$\text{Mineralisation (\%)} = \left[\frac{TOC_i - TOC_f}{TOC_i} \right] \times 100 \quad (3.2)$$

Where, TOC_i is the TOC of CP before degradation begins; TOC_f is the TOC at the end of degradation.

Total Dissolved Iron

Residual iron was analysed through the Phenanthroline method (3500-Fe, APHA Method). All the reagents were prepared fresh in iron-free Type 1 water and stored in dark.

Reagents

1) Hydrochloric acid

Concentrated HCl having less than 0.00005 % iron concentration.

2) Hydroxylamine solution

10 g of hydroxylamine $NH_2OH.HCl$ was dissolve in 100 ml water.

3) Sodium acetate solution

200 g of sodium acetate $NaC_2H_3O_2.3H_2O$ was dissolve in 800 ml water.

4) Phenanthroline solution

100 mg of 1, 10-phenanthroline monohydrate $C_{12}H_8N_2 \cdot H_2O$ was dissolved in 100 ml of water by stirring and heated to 80°C. Do not boil. Heating is not required if 2 drops of conc. HCl is added to the water. Discard the solution if it becomes dark.

5) Preparation of standard iron solution

Standard iron solution of 100 mg/L was prepared by mixing 0.0496 g of $FeSO_4 \cdot 7H_2O$ was mixed in 100 ml of distilled water. Using the standard 100 mg/L solution, another standard of strength 10 mg/L was prepared by pipetting out 10 ml of this 100 mg/L iron standard solution and making up the volume to 100 ml. Standard 10 mg/L solution was then used to carry out series dilution was to get the standard solution from range 0.1 ppm to 1 ppm for preparation of a calibration curve.

Preparation of the Standard Curve

- 1) In a 50 ml volumetric flask, 5 ml of the standard solution was taken.
- 2) To the above standard solution, 1ml of hydroxylamine was added. The solution mix was shaken well.
- 3) 5 ml of sodium acetate solution was then added followed by a gentle shaking.
- 4) In the previous mixture solution, 5 ml phenanthroline solution was added and mixed it well. The solution obtained was having red or orange colour.
- 5) The remaining volume of the then solution was made 50 ml by Type 1 water.
- 6) The absorbance of the solution was taken after 10 minutes at 510 nm wavelength and 100 % transmittance.
- 7) The above procedure was followed for all the standards and standard concentration curve was obtained.

Analysis of Total Dissolved Iron (TDI)

- 1) In a 50 ml volumetric flask, 5 ml of the standard solution was taken.
- 2) To the above standard solution, 1 ml of hydroxylamine was added. The solution mix was shaken well.
- 3) 5 ml of sodium acetate solution was then added followed by a gentle shaking.

- 4) In the previous mixture solution, 5 ml phenanthroline solution was added and mixed well. The solution obtained a red or orange colour.
- 5) The remaining volume of the then solution was made 50 ml by Type 1 water.
- 6) The absorbance of the solution was taken after 10 minutes at 510 nm wavelength and 100 % transmittance.
- 7) The concentration of the total dissolved iron was obtained by multiplying the graph factor with the absorbance.

Analysis of Ferrous (Fe^{2+}) ions

- 1) In a 50 ml volumetric flask, 5 ml of the sample solution was taken.
- 2) To the sample solution, 5 ml of the sodium acetate solution was added and shaken.
- 3) To the above solution, 5 ml phenanthroline solution was added and mixed well. Red or orange colour was observed.
- 4) The volume of the above test solution was made upto 50 ml using Type 1 water.
- 5) The sample solution was made to rest for 10 minutes followed by taking the absorbance of the solution at 510 nm wavelength and 100 % transmittance.
- 6) The concentration of the ferrous was determined by multiplying the graph factor with the absorbance.

Analysis of Ferric (Fe^{3+}) ions

From the known concentration of TDI and ferrous (Fe^{2+}), concentration of ferric (Fe^{3+}) can be estimated. Ferric concentration is difference in concentration between TDI and ferrous (Fe^{2+}).

Determination of residual H_2O_2

Residual H_2O_2 was analysed in the sample after maximum degradation was achieved using iodometric titration method. In 10 ml of sample few drops of potassium iodide was added followed by addition of few drops of freshly prepared starch indicator. Development of blue colour was observed. The solution was then titrated against Sodium thiosulfate (0.125 N) until the solution becomes colourless

(end point). The titrant volume consumed was recorded and residual concentration of H₂O₂ was determined using the following formula:

$$N_1V_1=N_2V_2 \quad (3.3)$$

3.3 Experimental setup of UV induced AOPs

The UV-driven experiments were executed in a fabricated UV chamber integrated with eight UV tubes (Phillips 36 W each) of wavelength 365 nm having aerial arrangement, positioned parallel to each other as represented in Figure 3.1. The intensity of the source was determined by dividing the net power generated per unit area (W/m²) at a distance of 10 cm between the source of light and the surface of exposed solution (Verma and Haritash, 2019). The cumulative source intensity of UV-chamber as evaluated is 672 W/m². Synthetic stock solution of concentration 100 mg/L of MCP, DCP, TCP and Mi-CP each were prepared using Type-I Ultrapure water to study their respective removal profiles. The experiments were performed using 200 ml of the synthetic stock solution of respective CPs (100 mg/L). The reaction solution was subjected to continuous magnetic stirring at 200 rpm under continuous irradiation of UV light (λ -365 nm). A distance of 10.0 cm was maintained between UV source and sample for effective UV penetration.

3.4 Experimental setup of Photocatalysis process

The photocatalytic degradation process of chlorophenols was conducted by varying the dose of photocatalyst Degussa P25 Nano-TiO₂, H₂O₂ as oxidant, and pH (as mentioned in Table 3.1) to get the optimized conditions. Effect of presence and absence of oxidant on reaction degradation rate was also assessed in case of TCP.

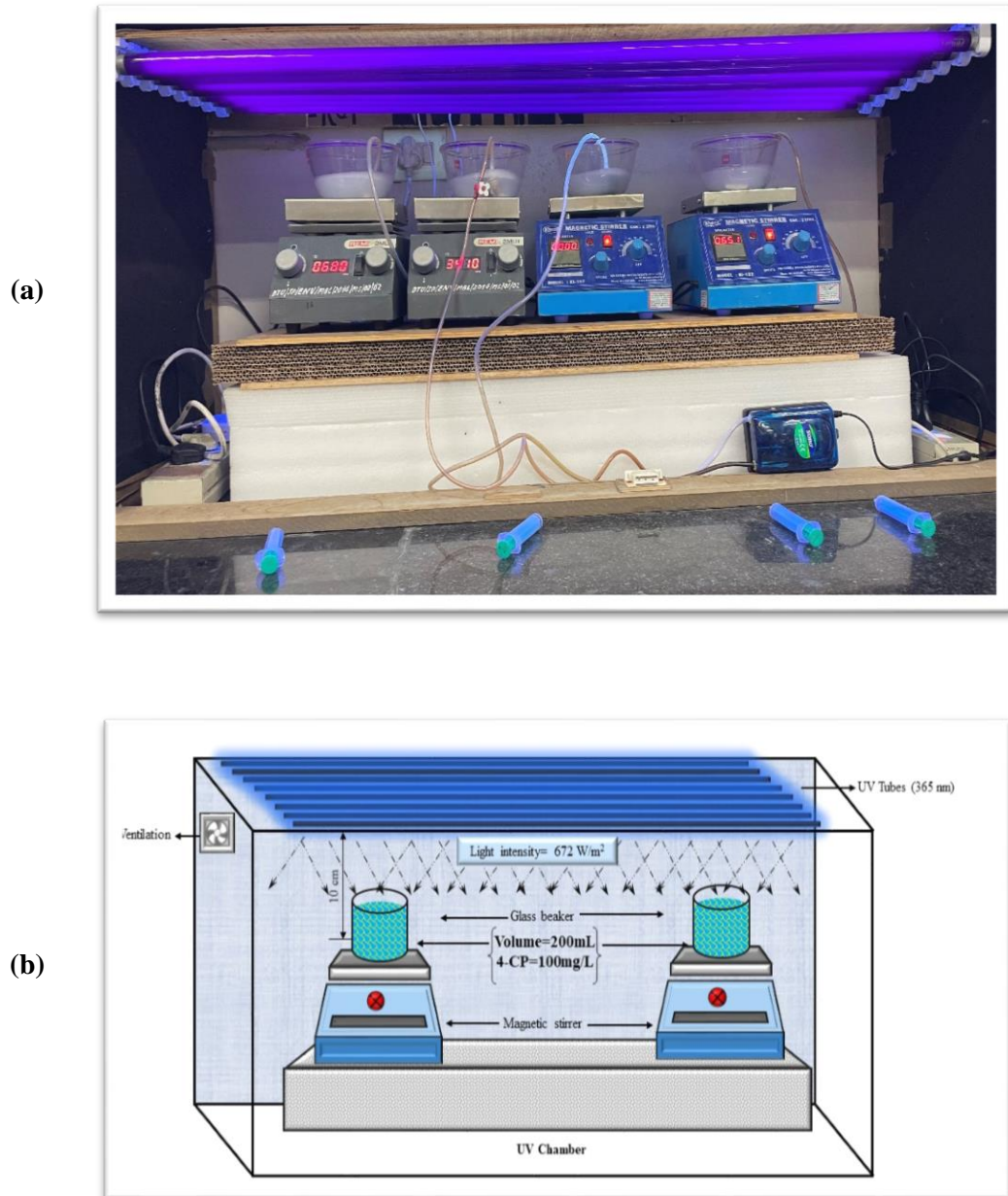


Fig. 3.1 (a) Experimental setup of UV-driven processes; (b) schematic diagram of experimental setup

Table 3.1 Experimental conditions of Photocatalytic degradation of Chlorophenols

Compound	Wavelength of maximum absorption (λ_{\max})	Source of Light	pH	Nano-TiO ₂ (g/L)	H ₂ O ₂ (mM)
4-CP	280 nm	UV ₃₆₅	3.0; 5.0[#] ; 7.0	0.05; 0.075; 0.1[#] ; 0.2; 0.3; 0.5	5.0; 10.0[#] ; 15.0
2,4-DCP	283 nm		4.0; 5.0[#] ; 6.0	0.1; 0.15; 0.2[#] ; 0.3; 0.5; 0.5; 0.6	5.0; 10.0[#] ; 15.0
2,4,6-TCP	290 nm		7.0	0.05; 0.1; 0.15; 0.25[#] ; 0.275; 0.3; 0.375; 0.5; 0.75	20.0; 50.0; 100.0
Mi-CP*	280 nm		4.0; 5.0; 6.0[#]	0.15; 0.2; 0.25[#]	10.0 [#]

*Mixed-Chlorophenol; [#]optimsed value at which maximal removal was observed

Comparative assessment was carried out for maximum removal efficiency of TCP using analytical grade commercially available Titanium Dioxide and Degussa P25 Nano-TiO₂ (anatase to rutile ratio-80:20). Prior to photocatalytic degradation, the solutions were kept under dark conditions to establish the adsorption/desorption equilibrium of CPs with photocatalyst. The aqueous suspension of respective CP and photocatalyst was then irradiated under UV light (λ -365nm) with constant magnetic stirring and air sparging. An aliquot of 5 ml was extracted for analysis using pre-rinsed syringe at regular intervals of 15 minutes and was then subjected to centrifugation at 5000 rpm for 5 minutes. The above procedure was repeated until residual concentration of respective chlorophenols got stabilised. Table 3.1 reflects the photocatalytic degradation conditions for respective CP compounds.

3.5 Sonication assisted Photocatalysis Process

The synergistic approach of Ultrasound with photocatalysis was studied towards degradation of chlorophenols. Sonication processes were performed using Ultrasonication bath of frequency 40kHz. Under the optimised conditions obtained for the photocatalysis process, sono-photocatalysis experiments were conducted by placing the ultrasonication bath having chlorophenol-containing synthetically prepared wastewater under UV light. The degradation profile of CPs was studied every 15 minutes until the process was stabilized. The following Table 3.2 describes the condition parameters of respective chlorophenol for sonolysis-induced photocatalytic degradation.

Table 3.2 Experimental conditions for Sonication assisted Photocatalysis of Chlorophenols

Compound	Wavelength of maximum absorption (λ_{max})	Light Source	Sonication Frequency (kHz)	pH	Nano-TiO ₂ (g/L)	H ₂ O ₂ (mM)
4-CP	280 nm	UV ₃₆₅	40	5.0	0.1	10.0
2,4-DCP	283 nm			5.0	0.2	
Mi-CP*	280 nm			6.0	0.25	

*Mixed-Chlorophenol

3.6 Solar-catalysis

Solar catalysis holds great potential for sustainable energy approach towards environmental remediation by utilizing the naturally available renewable source of light. The process was conducted under optimized conditions on a hot sunny day under natural conditions. Figure 3.2 depicts the experimental setup of Solar-Catalysis for degradation of chlorphenols. The following Table 3.3 describes the conditions at which solar-catalysis was operated for the degradation of different CPs.

Table 3.3 Experimental conditions for Solar driven catalytic degradation of Chlorophenols

Compound	Wavelength of maximum absorption (λ_{\max})	pH	Nano-TiO ₂ (g/L)	H ₂ O ₂ (mM)
4-CP	280 nm	5.0	0.1	10.0
2,4-DCP	283 nm	5.0	0.2	10.0
2,4,6-TCP	290 nm	7.0	0.25	-
Mi-CP*	280 nm	5.0	0.1	10.0

*Mixed-Chlorophenol



Fig. 3.2 Experimental setup of Solar-catalysis for degradation of CP

3.7 Sono-Solar-Catalysis

Sono-solar-catalysis involves a combination of three different processes, sonolysis, solar energy, and catalysis. The process involves utilizing both ultrasound waves and solar energy to drive catalytic reactions. Under the optimised conditions obtained for photocatalysis process, sono-photocatalysis experiments were conducted by placing the ultrasonication bath having CPs-containing synthetically prepared wastewater. The following table 3.4 represents the operating conditions of solar derived sonocatalytic degradation of CPs.

Table 3.4 Experimental conditions for Sonication assisted Solarcatalysis of Chlorophenols

Compound	Wavelength of maximum absorption (λ_{\max})	Source of Light	Sonication Frequency (kHz)	pH	Nano-TiO ₂ (g/L)	H ₂ O ₂ (mM)
4-CP	280 nm	Solar	40	5.0	0.1	10.0
2,4-DCP	283 nm			5.0	0.2	
Mi-CP*	280 nm			6.0	0.25	

*Mixed-Chlorophenol

3.8 Photo-Fenton

Experimentation work was performed based on Photo (UV365) Fenton, Sono-Photo-Fenton, Fenton, Solar-Fenton, Sono-Fenton, and Sono-Solar-Fenton. The optimization of key operating parameters like pH, oxidant dose, and iron concentration against degradation of CPs was studied. Synthetically prepared wastewater solution having strength 100 mg/L for 4-CP; 2,4-DCP; 2,4,6-TCP and Mi-CPs was prepared using Type-I water and was stored in dark. The Photo-

Fenton's treatment was performed by varying the concentration of Fe(II) and H₂O₂ at different pH according to the runs provided by Response Surface Methodology (RSM)-based Box–Behnken Design (BBD). The concentration of 2,4,6-TCP was kept constant (100 mg/L) and optimized conditions were noted. The research was carried out in a glass beaker with 200 ml of a synthetically prepared wastewater of CPs (100 mg/L). The reaction solution was subjected to continuous magnetic stirring at 200 RPM under continuous irradiation of UV light (λ -365 nm). The Photo-Fenton treatments were executed in a fabricated UV chamber integrated with eight UV tubes (Phillips 36 W each) of wavelength 365 nm having aerial arrangement, positioned parallel to each other. An aliquot of 5.0 ml was extracted using pre-rinsed syringe for analysis at regular intervals of 1 min. The above procedure was repeated until maximum/complete degradation was achieved or the residual concentration of CPs get stabilized. All the experiments were performed in triplicates to assure the reliability of analysis. The following Table 3.5 represents the operating parameters of Photo-Fenton's process towards degradation of different CPs.

Table 3.5 Experimental conditions for Photo-Fenton's degradation of Chlorophenols

Compound	Wavelength of maximum absorption (λ_{max})	Source of Light	pH	Fe ²⁺ (mM)	H ₂ O ₂ (mM)
4-CP	280 nm	UV ₃₆₅	1.0; 3.0[#] ; 5.0	0.3; 0.5; 0.7[#] ; 0.9	5.0; 7.0[#] ; 10.0
2,4-DCP	283 nm	UV ₃₆₅	1.0; 3.0[#] ; 5.0	0.3; 0.5[#] ; 0.7	3.0; 5.0[#] ; 7.0; 10.0
2,4,6-TCP	290 nm	UV ₃₆₅	1.0; 3.0[#] ; 5.0	0.1; 0.3; 0.5[#]	10.0[#] ; 35.0; 60.0
Mi-CP*	280 nm	UV ₃₆₅	3.0	0.5	10.0

*Mixed-Chlorophenols; [#]optimised value of respective parameter

3.9 Sono-Photo-Fenton

Integrating sonication with the Photo-Fenton reaction involves application of ultrasound waves to the reaction mixture containing CPs, iron (Fe^{2+}) and H_2O_2 , while simultaneously irradiating the mixture under UV light to enhance the degradation process. The process was performed under optimized conditions obtained for Photo-Fenton's process by keeping the ultrasonication bath containing the respective target compounds under the influence of UV light. Table 3.6 represents the optimized experimental conditions for which Sono-Photo-Fenton process was performed for different CPs.

Table 3.6 Experimental conditions for Sono-Photo-Fenton's Treatment of Chlorophenols

Compound	Wavelength of maximum absorption (λ_{max})	Source of Light	Sonication Frequency (kHz)	pH	Fe^{2+} (mM)	H_2O_2 (mM)
4-CP	280 nm	UV ₃₆₅	40	3.0	0.7	7.0
2,4-DCP	283 nm				0.5	5.0
2,4,6-TCP	290 nm				0.5	10.0

3.10 Fenton's Process

The process was carried out under the optimized conditions obtained for Photo-Fenton's process. The process entails the generation of highly reactive oxidative species, hydroxyl radicals ($\bullet\text{OH}$) through the reaction between Ferrous ions (Fe^{2+}) and H_2O_2 at pH 3.0 in the absence of UV light. Table 3.7 represents the working optimized experimental condition for Fenton's degradation of different CPs.

Table 3.7 Experimental conditions for Fenton's treatment of Chlorophenols

Compound	Wavelength of maximum absorption (λ_{\max})	pH	Fe ²⁺ (mM)	H ₂ O ₂ (mM)
4-CP	280 nm	3.0	0.7	7.0
2,4-DCP	283 nm		0.5	5.0
2,4,6-TCP	290 nm		0.5	10.0

3.11 Sono-Fenton

Sonication-induced Fenton's process is a hybrid process that combines ultrasound and Fenton's reaction. The process was performed under optimized conditions obtained for Photo-Fenton's process by keeping the ultrasonication bath (frequency 40KHz) containing the respective target compounds in absence of UV light. Table 3.8 represents the optimized experimental conditions at which Sono-Fenton process was conducted for degradation of different CPs.

Table 3.8 Experimental conditions for Sono-Fenton's degradation of Chlorophenols

Compound	Wavelength of maximum absorption (λ_{\max})	Sonication Frequency (kHz)	pH	Fe ²⁺ (mM)	H ₂ O ₂ (mM)
4-CP	280 nm	40	3.0	0.7	7.0
2,4-DCP	283 nm			0.5	5.0
2,4,6-TCP	290 nm			0.5	10.0

3.12 Solar-Fenton

Solar-Fenton's process harnesses solar energy to drive the oxidation of organic pollutants in synthetically prepared wastewater. Application of solar light is an approach to reduce the energy consumption, making the process more energy efficient and sustainable. Figure 3.3 shows the experimental setup of Solar-Fenton. The following Table 3.9 represents the optimized experimental conditions for degradation of different chlorophenolic compounds.



Fig. 3.3 Experimental setup of Solar-Fenton

Table 3.9 Experimental conditions for Solar driven Fenton's Treatment of Chlorophenols

Compound	Wavelength of maximum absorption (λ_{\max})	Source of Light	pH	Fe ²⁺ (mM)	H ₂ O ₂ (mM)
4-CP	280 nm	Solar	3.0	0.7	7.0
2,4-DCP	283 nm	Solar	3.0	0.5	5.0
2,4,6-TCP	290 nm	Solar	3.0	0.5	10.0
Mi-CPs*	280 nm	Solar	3.0	0.5	10.0

*Mi-CPs= Mixed Chlorophenols

3.13 Sono-Solar Fenton

The process involves the synergic approach for enhanced degradation efficiency because of integration of ultrasonic cavitation and Fenton's process under the influence of solar irradiation. The process was executed by keeping the ultrasonication bath containing the respective target compounds in sunlight. The process aimed to reduce energy consumption and operating costs by exploiting the renewable solar energy as a driving force for the degradation. The following Table 3.10 represents the operating parameters for different CPs at optimized conditions.

Table 3.10 Experimental conditions for Solar driven Sono-Fenton's degradation of Chlorophenols

Compound	Wavelength of maximum absorption (λ_{max})	Source of Light	Sonication Frequency (kHz)	pH	Fe ²⁺ (mM)	H ₂ O ₂ (mM)
4-CP	280 nm	Solar	40	3.0	0.7	7.0
2,4-DCP	283 nm	Solar			0.5	5.0
Mi-CPs*	280 nm	Solar			0.5	10.0

*Mi-CPs= Mixed Chlorophenols

3.14 Design of Experiment

3.14.1 Conventional Approach-One Factor at Time (OFAT)

One variable was studied at a time keeping other factors constant on the basis of experimental response. This approach ignored the interactive effects between the variables and also increases the number of experiments which is ultimately time consuming and added expenses for chemicals used in experiments (Bezerra, et al, 2008). This approach used only two observations at a time of the experiment to determine the response of various factors (Czitrom, 1999). In the present study, photocatalytic degradation of 2,4,6-TCP was observed by varying one factor at a time i.e. optimization of the catalyst dose (Nano-TiO₂) and keeping another variable constant. The degradation study for photocatalysis in presence of

H₂O₂ was also carried out by varying the H₂O₂ concentration keeping the catalyst dose and working pH constant

3.14.2 Statistical Approach: Response Surface Methodology (RSM)

RSM is a multivariate statistical tool widely used for designing of experiment and optimization of process parameters. Generally, RSM optimisation involves the identification of responses; screening the multivariates concerning the design of experiment; building an empirical response surface model; and applying various response optimisations through mathematical modelling (Kaur et al., 2021). RSM is an approach towards optimising the process conditioning parameters in order to increase the performance of such complex systems. Application of RSM overcomes the one factor at one time (OFAT) based conventional multifactor experiment approach by giving a limited and planned set of experiment runs. RSM is a multivariate statistical tool, helps in designing the experiment, determining the optimising conditions for desired response, building models and also assessing the significance of proposed model and parameters. The method quantifies the relationship between process controlling factors and obtained response. In the present study, RSM-Box Behnken Design (BBD) was selected as standard RSM for optimisation.

For a given target compound concentration, some preliminary experiments were conducted and a three level RSM based Box-Behnken Design for independent variables was formulated using MINITAB software, JSM Software and Sartorius Software. The effect of three independent variables, pH (X₁), catalyst dose (X₂) (Nano-TiO₂ in photocatalytic treatment and Fe(II) in Fenton's treatment), and oxidant dose (X₃) (H₂O₂) along with their interaction was studied and optimised for both the respective treatment processes in order to enhance the removal efficiency and minimize the imprecision of experiments (Table 3.11).

Table 3.11: Design of Experiment using RSM for different process

Compound	Process	Software	Type of Design	No. of Runs	No. of Variables	Response Variable (Y)	Independent Variables		
							pH (X ₁)	Catalyst dose (X ₂)	H ₂ O ₂ (X ₃)
4-CP	Photocatalysis	Sartorius MODDE [®] Pro	Box-Behnken	15	03	Degradation of 4-CP	3.0 to 7.0	Nano-TiO ₂ 0.05g/L to 0.15g/L	5.0 mM to 15.0 mM
	Fenton's		Box-Behnken	15	03		1.0 to 5.0	Fe(II) 0.5mM to 0.9mM	5.0mM to 9.0mM
2,4-DCP	Photocatalysis	MINITAB 16	Box-Behnken	15	03	Degradation of 2,4-DCP	4.0 to 6.0	Nano-TiO ₂ 0.1g/L to 0.3g/L	5.0mM to 15.0mM
	Fenton's		Box-Behnken	15	03		1.0 to 5.0	Fe(II) 0.3mM to 0.7mM	3.0mM to 7.0mM
2,4,6-TCP	Fenton's	JSM DOE 16.2.0	Box-Behnken	15	03	Degradation of 2,4,6-TCP	1.0 to 5.0	Fe(II) 0.1mM to 0.5mM	10.0mM to 60.0mM

A predictive model for degradation of three CPs (MCP, DCP, TCP) was obtained on the basis of second-order polynomial equation (eq 3.4), defining the mathematical relationship between corresponding parameters (X_1 , X_2 , and X_3) and efficiency of system (response Y).

$$Y = \beta_0 + \sum_{i=1}^n \beta_i X_i + \sum_{i=1}^n \beta_{ii} X_{ii}^2 + \sum_{i < j}^n \beta_{ij} X_i X_j \quad (3.4)$$

Where β_0 , β_i , β_{ii} , and β_{ij} represents the model coefficient, linear coefficient, quadratic coefficient and interaction parameters coefficient.

The predictive response was correlated with independent variables through a set of coefficients that includes intercept, linear terms, quadratic terms, and interactions. Regression analysis was carried out to fit the equation and the significance of regulating factors were investigated. The adequacy of the model was determined by analysis of variance (ANOVA) with predictability at 95% confidence limit and evaluating the regression coefficient R^2 .

3.15 Toxicity Analysis

Plant material

Water hyacinth of almost the similar size was collected from the pond in the university campus. The experimental design consists of three experimental cells: untreated wastewater, treated wastewater and control, as depicted in figure 3.4. Five to six plants were placed in 20 L of medium. The medium was placed inside HDPE buckets of volume 25 L each. The experiment was conducted for 7 days and the physiological response of plant samples was analyzed for pH, chlorophyll 'a', chlorophyll 'b' and carotenoids, ascorbic acid, and proline using standard procedure (Arnon, 1949; Sadasivam and Balasubramaniam, 1987; Bates et al., 1973) at the beginning of the experiment and at the end of 7 days.

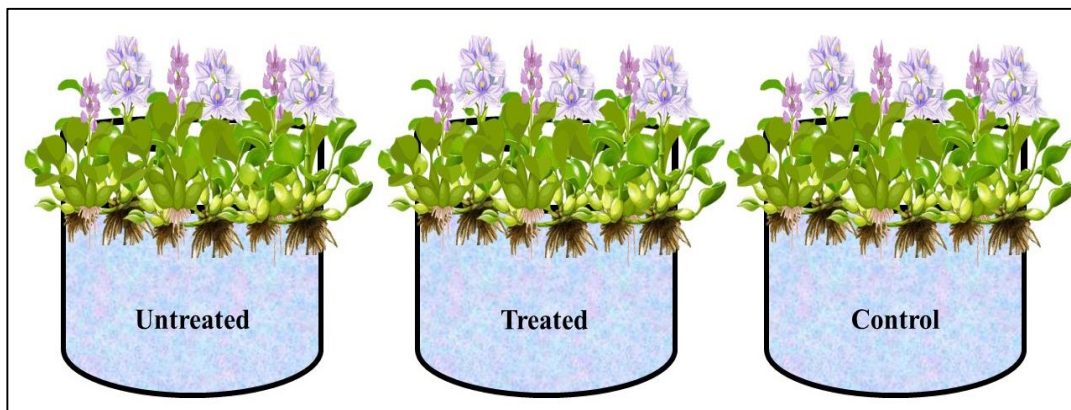


Fig. 3.4 Schematic diagram of experimental setup for toxicity assessment

Determination of pH of leaf extract

pH of leaf sap was determined by taking 5.0g of fresh leaves. The leaves were washed and homogenized in 25 ml distilled water and blended in mortar pestle. The blended mixture was subjected to centrifugation at 2500 RPM for 10 minutes and supernatant was extracted. The pH was determined using Bench-top multiparameter Labman India/LMPH10 consisting of potentiometer, a glass electrode, a reference electrode and a temperature compensating device. The pH values were recorded as per APHA 4500-H⁺ using electrometric method where the glass electrode measures the electromotive force (emf) produced in electrode system which varies linearly. The reference electrode is a half-cell having a constant electrode potential while the glass electrode is a sensor electrode consisting of bulb of glass of fixed concentration of HCl or a buffered chloride solution. The electrometric pH meter measures the activity of the hydrogen ions by potentiometric measurement using standard hydrogen electrode and reference electrode. The instrument was calibrated using the standard buffer solution of known pH of 4.0, 7.0 and 10.0 (Metrohm make) before measuring the pH of leaf sample. Following proper calibration, the electrode was thoroughly washed with distilled water and blot dried and later immersed in sample solution. pH of the leaf was noted once the readings were stabilised. The electrode was then taken out and washed and stored in storage solution when not in use.

Determination of Chlorophyll

Chlorophyll 'a', Chlorophyll 'b' and Carotenoids pigments were determined. 0.25 g of finely cut fresh leaves were grounded in mortar pestle using 10 ml to 15 ml of 80% acetone till the residue becomes colourless. The mixture solution was subjected to centrifugation at 5000 RPM for 10 minutes. The supernatant was collected and transferred to cuvette for analysis on the spectrophotometer. The optical density (O.D) for Chlorophyll 'a' was measured at 645 nm, for chlorophyll 'b' it was observed at 663 nm and 470 nm for carotenoids, respectively, against the solvent (acetone) blank. Chlorophyll 'a' was calculated using the following formula:

$$\text{Chlorophyll 'a' (mg/L)} = 12.70 \times O.D \ 663 - 02.69 \times O.D \ 645 \quad (3.5)$$

$$\text{Chlorophyll 'a' (mg/g)} = \frac{19.3 \times O.D \ 663 - 0.86 \times O.D \ 645 \times V}{1000 \times W} \quad (3.6)$$

Chlorophyll 'b' was calculated using the following formula:

$$\text{Chlorophyll 'b' (mg/L)} = 22.90 \times O.D \ 645 - 04.68 \times O.D \ 663 \quad (3.7)$$

$$\text{Chlorophyll 'b' (mg/g)} = \frac{19.3 \times O.D \ 645 - 3.6 \times O.D \ 663 \times V}{1000 \times W} \quad (3.8)$$

Carotenoid content was estimated using the following formula:

$$\text{Carotenoids (mg/g)} = \frac{100 \times O.D \ 470 - 3.27 \times \text{Chl a (mg/g)} - 104 \times \text{Chl b (mg/g)}}{227} \quad (3.9)$$

Where O.D is the optical density; V is the final volume of leaf extract; W is the dry weight of the leaf

Determining the Ascorbic acid content

Reagents

(1) Starch Indicator

5% starch indicator was prepared by mixing 5 g starch in 500 ml of distilled water.

(2) Iodine Solution

0.05M iodine solution was prepared by mixing 3.2 g iodine crystal in 2 g potassium iodide solution and making the volume 1000 ml.

(3) 0.05 M H₂SO₄

0.05 M of H₂SO₄ was made by diluting 28 ml of concentrated sulphuric acid to 1000 ml.

Extraction of Ascorbic acid content (AAC)

Fresh leaves weighing 10 g and 0.5 g oxalic acid were grounded in mortar pestle and 30 ml of 0.03 M H₂SO₄ followed by 20 ml of distilled water. The suspension was subjected to centrifugation at 5000 RPM for 10 minutes. The supernatant was collected and titrated against to the end point with 0.05M iodine solution using 5% starch indicator. Before the sample titration, blank determination was carried out followed by sample determination in triplicates.

Calculation

Ascorbic acid content was determined by using the following formula:

$$AAC (mg/L) = \frac{N \times V \times EW}{Volume\ of\ extract} \quad (3.10)$$

Where N is the normality of titrant; V is volume of titrant (ml); EW is the equivalent weight of Ascorbic acid.

Determining the Proline content

Reagents:

1. Sulphosalicylic acid

To make 3% sulphosalicylic acid, 3g of 5-sulfosalicylic acid (2-hydroxy-5-sulfobenzoic acid) was added in 80 mL distilled water and volume was made up to 100 mL.

2. Acidic Ninhydrin

1.25 g ninhydrin (1,2,3-indantrionemonohydrate) was mixed in 30 mL glacial acetic acid and 20 mL of 6 M orthophosphoric acid. The solution was uniformly dissolved by vortexing and gentle warming.

3. Orthophosphoric acid (85%)

20.5 ml of 85% orthophosphoric acid (Molarity 14.5 M) was added in 29.5 ml distilled water and volume was made up to 50 ml.

Analysis of Proline

Proline was determined using 0.5 g of fresh plant shoot, homogenized in 4 mL of 3.0% Sulphosalicylic acid. The homogenate was subjected to centrifugation at 3500 RPM for 10 min. The supernatant was collected and to 1 mL of the supernatant 2 mL of acid Ninhydrin reagent and 2.0 mL of glacial acetic acid were added in a test tube. The mixture was incubated in a water bath at 100 °C for 60 min and was then cooled in an ice bath. After cooling, 4 mL of toluene was added to the solution mixture and vortex. The chromophore containing toluene (upper layer) was transferred to a new test tube. The absorbance was recorded at 520 nm using a spectrophotometer against toluene as a blank. The concentration of proline was determined using the standard curve and expressed as mg/g.

CHAPTER 4

RESULTS AND DISCUSSIONS

4.1 Photocatalytic degradation of 4-Chlorophenol

Photocatalytic degradation of 4-CP using TiO₂-Nano particles (NTP) was effective towards the removal of the toxicant. The study examined the effect of the process governing factors such as the concentration of catalyst, the effect of pH, and the presence of oxidizing agent H₂O₂ corresponding to the RSM-BBD series of experimental runs and the results are described in Table 4.1. Under optimized conditions, NTP dose of 0.1g/L, pH= 5.0±0.2, and H₂O₂= 10.0mM, degradation of 4-CP was attained in 210 minutes of the reaction time.

Table 4.1 Box Behnken design for three independent variables, predicted and observed responses for Photocatalytic degradation of 4-CP

Run	pH	Nano-TiO ₂ (g/L)	H ₂ O ₂ (mM)	Removal Efficiency (%)	
				Observed	Predicted
1	3	0.15	10	47	51
2	3	0.1	15	43	39
3	3	0.05	10	26	29
4	3	0.1	5	42	39
5	5	0.1	10	99	98
6	5	0.1	10	99	98
7	5	0.1	10	99	98
8	5	0.05	5	32	32
9	5	0.15	5	30	29

10	5	0.15	15	20	20
11	5	0.05	15	17	18
12	7	0.15	10	47	44
13	7	0.1	15	40	43
14	7	0.1	5	61	65
15	7	0.05	10	70	66

Effect of Catalyst loading

The effect of varying concentrations of NTP was analysed as a function of time concerning photo-degradation of 4-CP (strength 100mg/L). Before the UV irradiation, the 4-CP and NTP suspension was kept in the dark for 30 minutes to establish the adsorption/desorption equilibrium. The experiments were performed for catalyst dose in the range from 0.05g/L to 0.5g/L at pH= 3.0 and H₂O₂= 10.0mM. It was observed that increasing the concentration of NTP from 0.05 g/L to 0.1 g/L resulted in enhanced degradation of 4-CP. Around ~99% removal of 4-CP was attained with an NTP dose of 0.1g/L in 210 minutes of reaction time as shown in Figure 4.1. The results are in strong agreement with another study where a similar dose of catalyst reported effective degradation of organic impurity (Thind et al., 2018). The Degussa NTP used in the present study comprises rutile and anatase phases in the ratio of 20:80. The rutile TiO₂ consists of a smaller band gap making it advantageous to produce electron-hole pair when irradiated with low energy photon (Pipil et al., 2024b; Bagbi et al., 2017). Since anatase TiO₂ demonstrates lesser chances of electron-hole pair recombination, it utilises the charge carriers generated by the rutile phase resulting in increased movement of these charge carriers from the inner to the surface of anatase TiO₂ (Pipil et al., 2024b). Thus, the synergistic outcome of both rutile and anatase phases of TiO₂ displays a vital role in photocatalytic oxidation. The electron donor species adsorbed on the catalyst surface is oxidized, while the electron acceptor species is

reduced by the photogenerated valence band holes and conduction band electrons. The photo-oxidation of 4-CP is carried out by hydroxyl and perhydroxyl radicals (Pipil et al., 2024a).

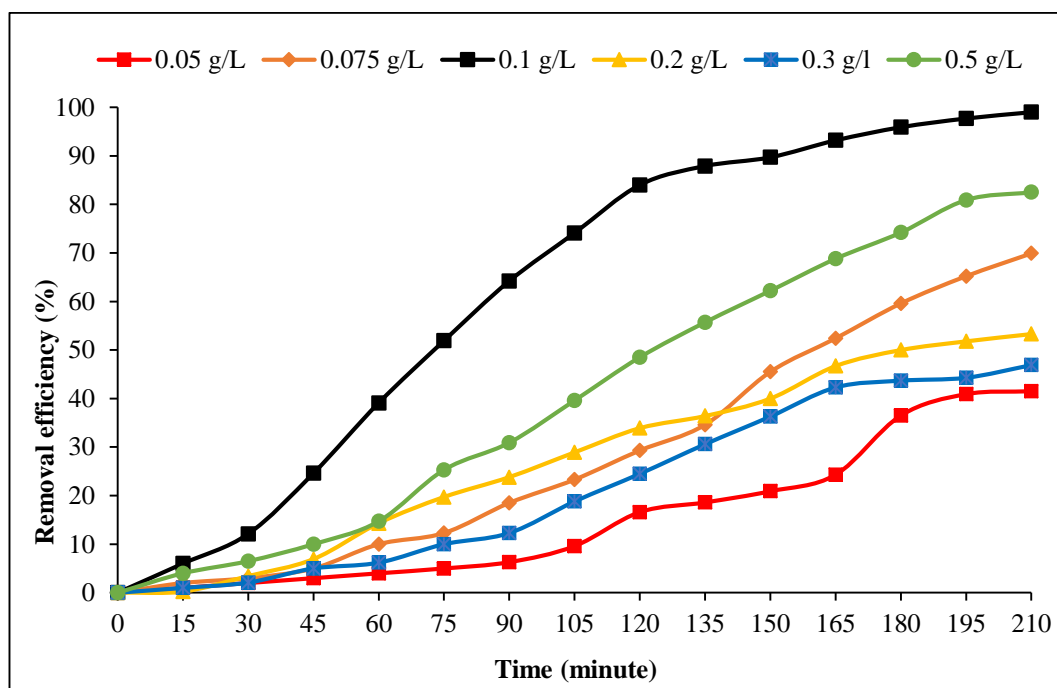


Fig. 4.1 Effect of different catalyst dose on removal efficiency of 4-CP using Photocatalysis



The adsorption process was hastened by the surge in NTP dosage since it also enhanced more active sites. The production of hydroxyl radicals is accelerated by the binding of electron-hole pair with water. However, a higher dose of NTP reported opacity in the solution suspension as it became turbid and cloudy. Following this, the effective penetration of UV light was prohibited while light scattering dominated, as reported the same in other studies as well (Pipil et al., 2022; Verma and Haritash 2020). The effect was observed in the current study as well where the removal rate of 4-CP was decreased on further increase in NTP dose from

0.2 g/L to 0.5 g/L. This decrease in the removal efficiency could also be rationalised because of the deactivation of the activated molecules on collision with the ground state catalyst. Several reports observed the degradation of different 4-CP at higher doses of catalyst in comparison to the present study. For instance, in a study, degradation of 2-CP, 3-CP and 4-CP of strength 25 mg/L using nanocomposites $\text{TiO}_2/\text{g-C}_3\text{N}_4$ was performed (Kobkeatthawin et al., 2022). The degradation of respective chlorophenols was of the order 50%, 87% and 64% with $\text{TiO}_2/\text{g-C}_3\text{N}_4$, 1g/L. In another study, photocatalytic degradation of 0.05mM nitrobenzene was treated using Copper-doped TiO_2 at 0.5g/L (50mg/100mL) dose (Akhtar et al., 2022). In the current study, the optimised NTP dose of 0.1 g/L was validated for maximum removal using response surface methodology to reduce its amount minimize the consumption, to ensure maximum removal efficiency and reduction of treatment cost. Successive experimentation was conducted using a 0.1g/L concentration of NTP.

Effect of pH

pH controls the surface charge characteristics of photocatalyst, which in turn controls the efficacy of the treatment system. The current study entails the effect of varying pH conditions- 3.0, 5.0, and 6.0 at an optimal NTP dose of 0.1g/L and H_2O_2 dose of 10.0mM. Figure 4.2 depicts the removal efficiency of 4-CP with respect to different pH. It was observed that under acidic conditions, at pH 3.0 and 5.0, almost complete removal (~98%) of the toxicant occurred. However, at pH 5.0, the rate of reaction and TOC mineralisation was also maximum. The degradation at pH 5.0 was attained in 210 minutes whereas at pH= 3.0, it took a little extra time (225 minutes) and 15 minutes more to degrade the same. The results are in strong agreement with other studies where photooxidation of harmful organic contaminants was found effective under similar pH conditions (Thind et al., 2018; Akhtar et al., 2022; Zulfiqar et al., 2019). pH medium of the working solution determines the ionization state of the photocatalyst surface to undergo either protonation or deprotonation (eqs. 4.4 and 4.5) where TiOH is the primary hydrated surface functionality of TiO_2 (Hofmann et al., 1995). The point of zero charge

(pzc) of TiO₂ is between 5.5 and 6.4, it carries a net positive charge, whereas the 4-CP compound has negative charges (pka= 9.41).

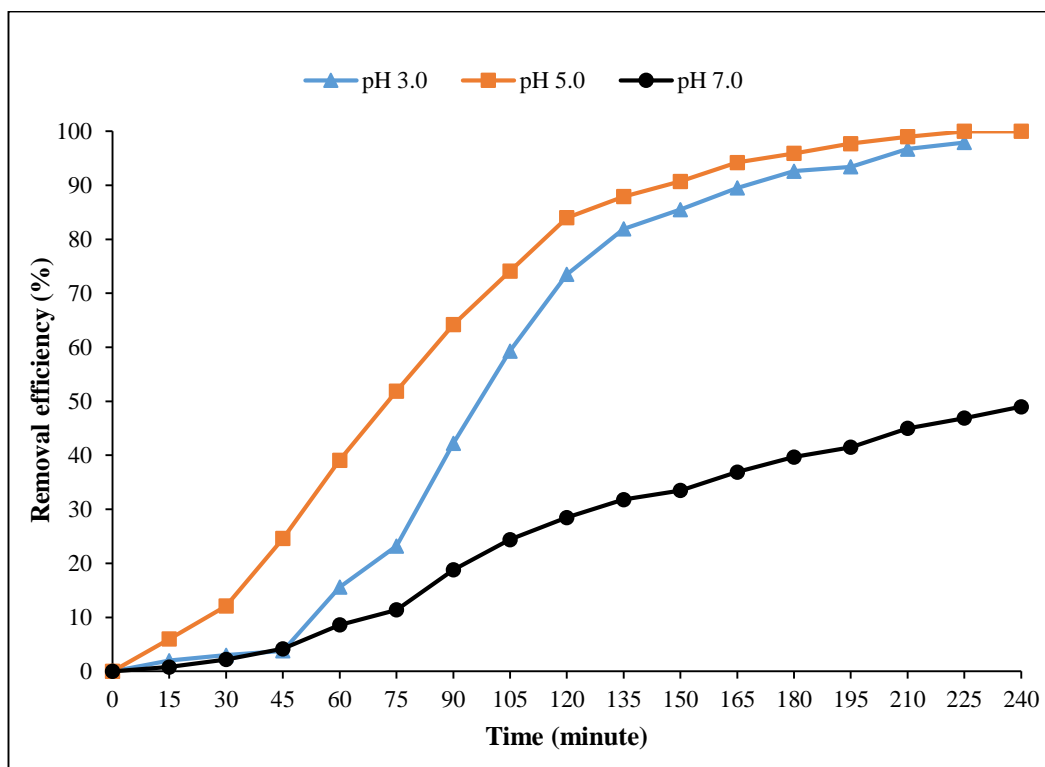


Fig. 4.2 Effect of different pH on removal efficiency of 4-CP using Photocatalysis process

Hence at pH 5.0 (< p*H*_{pzc}), the coulombic polar attraction between NTP and MCP escalates the adsorption of the organic pollutant/species over the photocatalyst surface, enhancing the photocatalytic degradation.

At pH < p*H*_{pzc}



However, at pH ≥ p*H*_{pzc}, TiO₂ carries a net negative charge (pH 6.0 > p*H*_{pzc}), hindering the adhesion of CP onto the catalyst surface.

At pH > p*H*_{pzc}



Since the isoelectric point of TiO₂ and pH of the solution (pH=6.0) is almost the same, minimal interaction between NTP and contaminant was observed because of the absence of any electrostatic force (Akhtar et al., 2022). Rather, the columbic repulsion leads to a lower rate of degradation and removal effectiveness because of the higher density of negatively charged NTP and chlorophenols. As a result, pH= 5.0 was chosen to be the optimal pH value for 4-CP breakdown.

Effect of oxidant concentration

The presence of H₂O₂ has a synergistic effect on enhancing the efficacy of the NTP/UV treatment system. It produces either two hydroxyl radicals or forms perhydroxyl radicals (Eqs. 4.6, 4.7, 4.8) (Pipil et al., 2022).



H₂O₂ acts as an effective electron acceptor of conduction band electrons thus inhibiting recombination of the charge carriers (Pipil et al., 2024a; Yadav et al., 2023a). Irradiation of UV light photolyzes H₂O₂ which generates hydroxyl radicals necessary for photo-mineralisation of organic pollutants (eq. 4.9).



The effect of H₂O₂ was analysed between 5.0mM to 15.0mM according to the RSM runs (Figure 4.3). It was observed that at 10.0mM of H₂O₂ dose, 98% of the MCP was degraded in 210 minutes of reaction duration whereas around 40-50% removal was observed in the case of 5.0mM and 15.0mM oxidant concentration. Similar findings have also reported enhanced removal of organic contaminants with the addition of H₂O₂ although at a higher oxidant concentration (Gong et al., 2015; Kayan et al., 2021). In the current study, at a higher concentration (15.0mM), only

40% of the 4-CP was treated in the same reaction duration. At elevated doses, H₂O₂ acts as a radical scavenger.

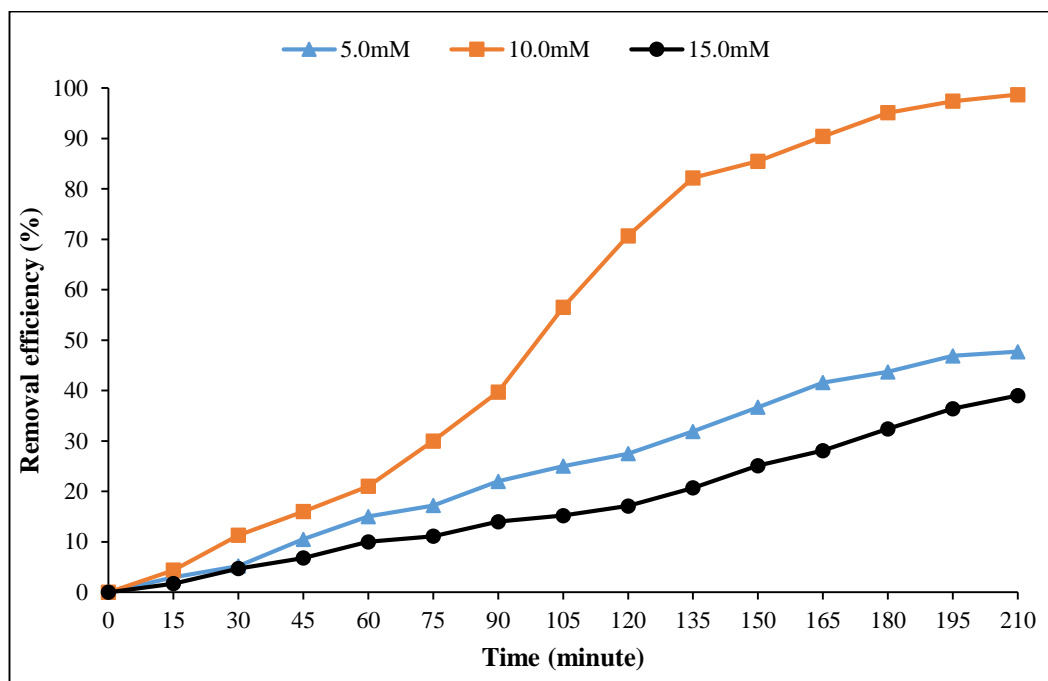
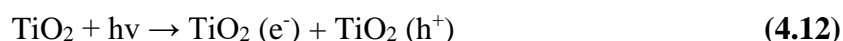


Fig. 4.3 Effect of different oxidant concentration on removal efficiency of 4-CP using Photocatalysis process

Excess of oxidant blocks the active sites for adsorption of water and production of hydroxyl radicals (Thind et al., 2018). Excess of H₂O₂ interacts with HO[•] to produce water, which hampers the breakdown of 4-CP (Eqs. 4.10 and 4.11).



Presence of abundant holes results in photo-oxidation of hydroxyl radicals aiding in slower treatment process (Eqs. 4.12 to 4.15).



4.2 Photo-Fenton's degradation of 4-Chlorophenol

The effect of different process parameters was inspected at variable concentrations referring to the experimental runs as recommended by RSM and the results are put together in Table 4.2. The solution promptly grew turbid following the addition of H₂O₂, imparting it a dark brown color. The colour of the mixture solution transformed from dark brown to pale yellow and colourless as the process progressed, indicating that the treatment completion. Under optimal dosages of pH= 3.0±0.2, Fe²⁺= 0.7mM and H₂O₂= 10.0mM, the residual concentration of 4-CP reached to non-detectable levels within 6 minutes of the reaction period.

Table 4.2 Box Behnken design for three independent variables, predicted and observed responses for Photo-Fenton's degradation of 4-CP

Run	pH	Fe ²⁺ (mM)	H ₂ O ₂ (mM)	Removal Efficiency (%)	
				Observed	Predicted
1	3	0.7	7	100	100
2	5	0.7	5	30	35
3	1	0.7	5	20	7
4	3	0.7	7	100	100
5	1	0.5	7	10	18
6	5	0.7	9	45	58
7	3	0.9	5	60	63
8	5	0.9	7	85	77
9	5	0.5	7	54	44
10	3	0.5	9	58	55
11	1	0.7	9	1	0
12	1	0.9	7	4	14
13	3	0.9	9	80	75
14	3	0.7	7	100	100
15	3	0.5	5	50	55

Effect of Fe²⁺ Dose

Ferrous ions (Fe²⁺) acts as the regulating factor in determining the kinetics of the reaction. To demonstrate the effect of iron, variable iron concentrations were reviewed between 0.3mM to 0.9mM towards degradation of 4-CP. Figure 4.4 corresponds to the effect of different Fe²⁺ concentrations towards the removal of organic contaminants.

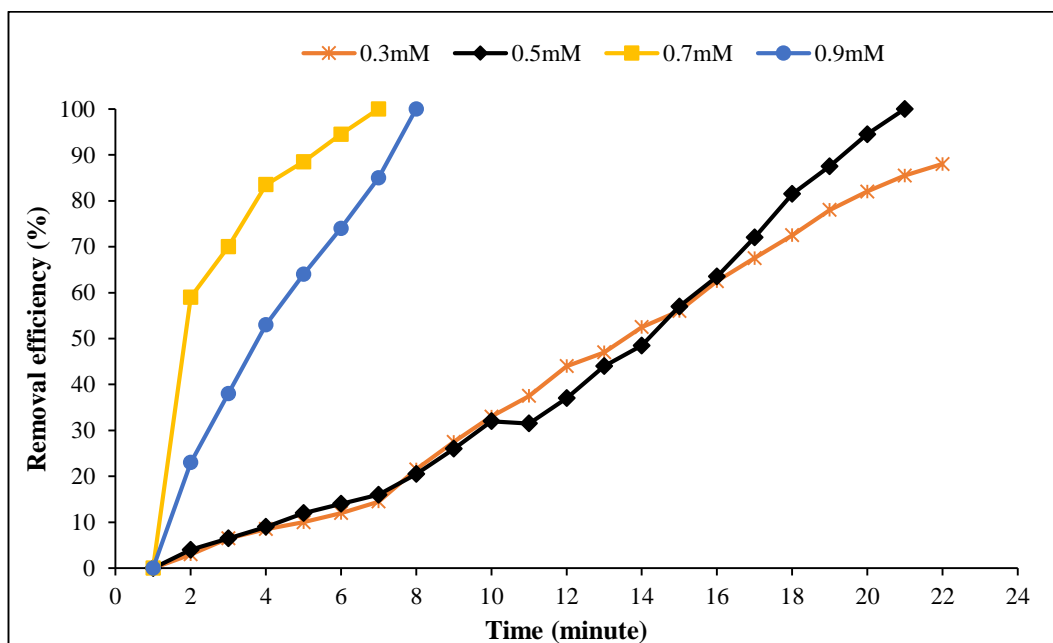
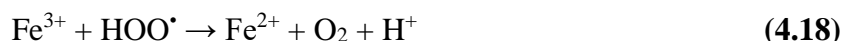
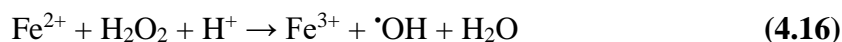


Fig. 4.4 Effect of different Fe²⁺ concentration on removal efficiency of 4-CP using Photo-Fenton process

It can be comprehended from the figure that, at a subordinate iron dose (0.3mM), nearly 80% removal was achieved in 22 minutes. Complete degradation of the organic pollutant was observed with an iron concentration of 0.5mM. However, the process was time-consuming and energy-intensive as it took 20 minutes to attain. This could be rationalised for the lesser hydroxyl radical availability which prolonged the oxidative duration and effective removal (Yadav et al., 2023a; 2023b). Complete elimination of 4-CP was accomplished with iron concentration 0.7mM within 5 minutes of the reaction time. The hydroxyl radicals attack the π bond in the benzene ring of the phenolic compound, prompting the

oxidation of chlorophenols (Kavitha and Palanivelu 2016). The redox recycling process of $\text{Fe}^{2+}/\text{Fe}^{3+}$ occurs in the bulk solution and further stimulates the formation of reactive oxidation species (eq. 4.16), at the same time certain ferrous ions are also surfaced through reactions (eq. 4.17) and (eq. 4.18) (Ye et al., 2019).



As the concentration of iron increased the removal process became increasingly time-consuming and failed to exhibit any discernible improvement in removal efficiency. It took two-fold the time to oxidise 4-CP at concentration 0.9 mM with no residual concentration of 4-CP detected after the tenth minute compared to what was accomplished at a concentration 0.7 mM. Inefficiency in the chemical breakdown of organic contaminant could be attributed to the ferrous ions' predominant hydroxyl radical scavenging action. Excess of Fe^{3+} cannot be complexed and is insoluble and unstable, which incites the formation of ferrous hydroxide, $[\text{Fe}(\text{OH})]^{2+}$ and it further undergoes hydrolysis and precipitates as $\text{Fe}(\text{OH})_3$ (eq. 4.19 and 4.20) (Yadav et al., 2023a; Verma and Haritash 2019):



The residual concentration of total dissolved iron (TDI) and Fe^{2+} as assessed at the end of the experiment reported complete consumption of ferrous ions, conversely 0.02mM of TDI remained in the solution.

Effect of pH

pH directs the iron speciation that further regulates the UV absorption, complexation and dissolution. The dissociation constant of CPs varies from 4.7 for PCP to 9.4 for MCP, implying to their ionization that occur under slight acidic

conditions. In the present research intends to examine the influence of different pH conditions from 1.0 pH to 5.0 pH (Figure 4.5). Under exceptionally high acidic conditions (at pH 1.0) mere pollutant oxidation was observed, however, the study witnessed absolute elimination of 4-CP at pH 3.0, attained within 7 minutes of the reaction period. Although a similar removal efficiency was observed at pH= 5.0 as well. However, the process took 2-3 minutes more as compared to removal at pH= 3.0. The difference was observed w.r.t. TOC mineralisation. Around 80% mineralisation was observed at pH 3.0 which is appreciably higher as compared to its near half under slightly alkaline conditions. Ferrous ions and peroxide display higher stability at pH 3.0 (Pipil et al., 2022; Yadav et al., 2022).

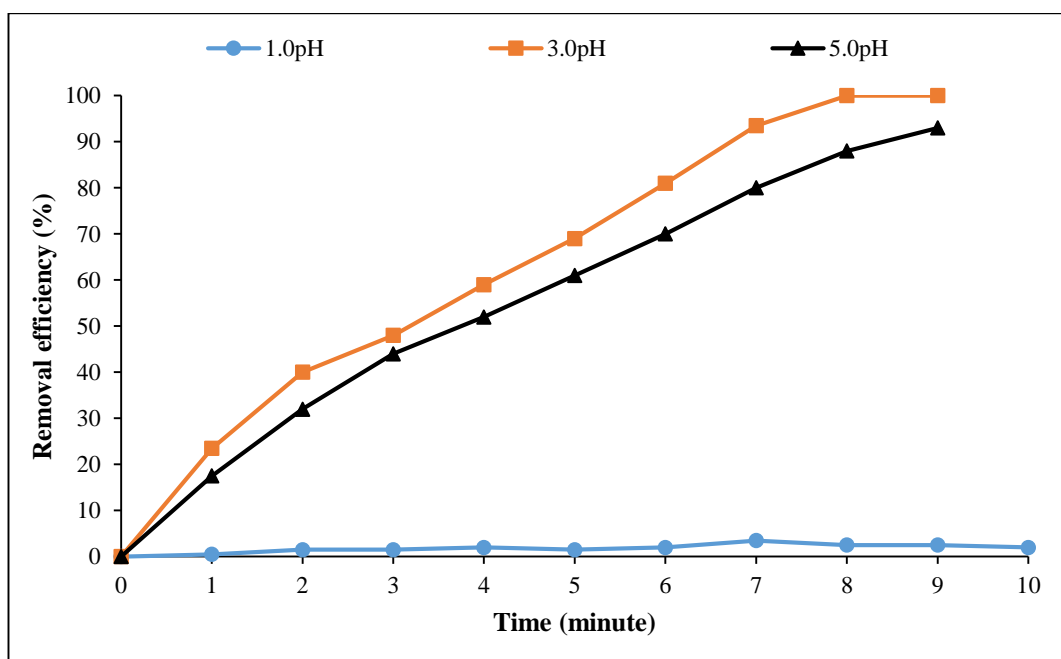


Fig. 4.5 Effect of different pH on removal efficiency of 4-CP using Photo-Fenton Process

The recorded observations are in strong agreement with other relevant studies where substantial removal of organic contaminant was observed under similar pH conditions (Yadav et al., 2023b; Yildiz et al., 2023; Minz et al., 2019). The oxidation power of the hydroxyl radicals at pH= 3.0 is enhanced leading to increased degradation of toxicant. The lessened removal effectiveness at pH 1.0 is pertinent to the scavenging action of H^+ , consuming hydroxyl radicals (eq. 4.21).

Furthermore, lesser solubility of ferrous ions results in the formation of complex ions species and peroxonium ions, H_3O_2^+ (eq. 4.22) as well perhaps because of increased peroxide stability and decreased reactivity of Fe(II) (Ghoneium et al., 2011).



The precipitate (ferric hydroxide complex) produced due to the unstable state of iron in alkaline environments prevents the generation of hydroxyl radicals by refraining from reacting with peroxide. Oxygen and water are generated as peroxide undergo self-decomposition in an alkaline solution. Moreover, under the following conditions, $2.0 < \text{pH} > 4.0$, the potential for hydroxyl radical decreases (Yadav et al., 2023a). A drop in pH was also observed in the range of 2.3-2.5 post-treatment, symptomatic of the feasibility of the formation of certain carboxylic acid species after degradation (Pipil et al., 2022; 2024b; Yadav et al., 2023b).

Effect of H_2O_2 concentration

The transparent reaction mixture having iron and 4-CP was turned into dark brown color with addition of H_2O_2 . As the reaction ensued, the dark colour washed out slowly and soon became colourless at the end. H_2O_2 was added in the concentration range 5.0mM to 10.0mM and iron dose of 0.5mM and pH= 3.0. Intermediary experimentation was also performed independent to the runs recommended by RSM to validate the findings of 4-CP degradation. At lower concentrations, only 50% removal efficiency was observed and the process was found to be time consuming as well. It took 30 minutes to reduce the pollutant concentration to half. Complete degradation was achieved with oxidant doses of 7.0mM and 10.0mM within 20 minutes of the reaction period (Figure 4.6). H_2O_2 acts as an e- acceptor, promoting the production of $\cdot\text{OH}$ radicals simultaneously prohibiting the electron-hole from recombining (Pipil et al., 2024a).



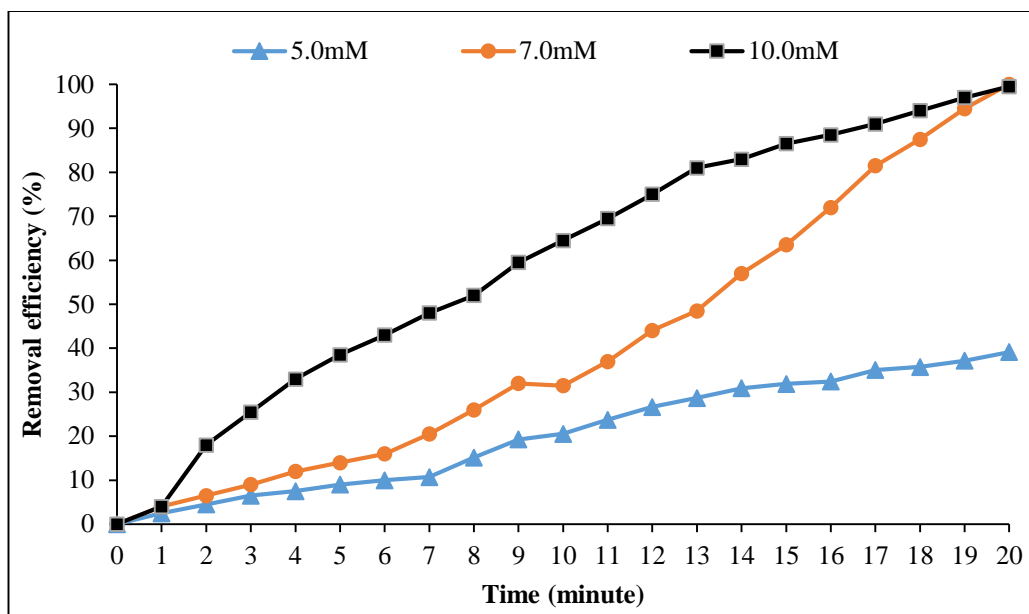


Fig. 4.6 Effect of different H₂O₂ concentration on removal efficiency of 4-CP using Photo-Fenton Process

The results are in strong agreement with another study which reported 90% degradation of 4-CP at 6.0mM oxidant concentration (Minz et al., 2019; Pipil et al., 2024a). A higher concentration of oxidant reported no significant improvement in the degradation rate. Hence, considering the operating cost of the treatment and utilization of chemicals, 7.0mM was considered as the optimised concentration of H₂O₂ for further experimentation as well.

4.3 Adequacy of Model (ANOVA) for degradation of 4-CP

The effect of independent variables of both the treatment methods towards the removal of 4-CP was examined. Table 4.1 and Table 4.2 lists the observed experimental results against the predicted response obtained through RSM towards effective removal for both treatment processes. Analysis of variance (ANOVA) determined the adeptness and significance of the proposed model and the results are presented in Table 4.3. The significance of the proposed model and the operating variable parameters is a function of their *p*-values (*p*-value < 0.05

signifies the model expression as significant). According to the ANOVA results, the quadratic models for both treatment processes are found significant ($p \leq 0.05$).

The modified quadratic regression equation (eq. 3.4) is expressed below in which Y1 represents the photocatalytic response and Y2 is the Photo-Fenton's response.

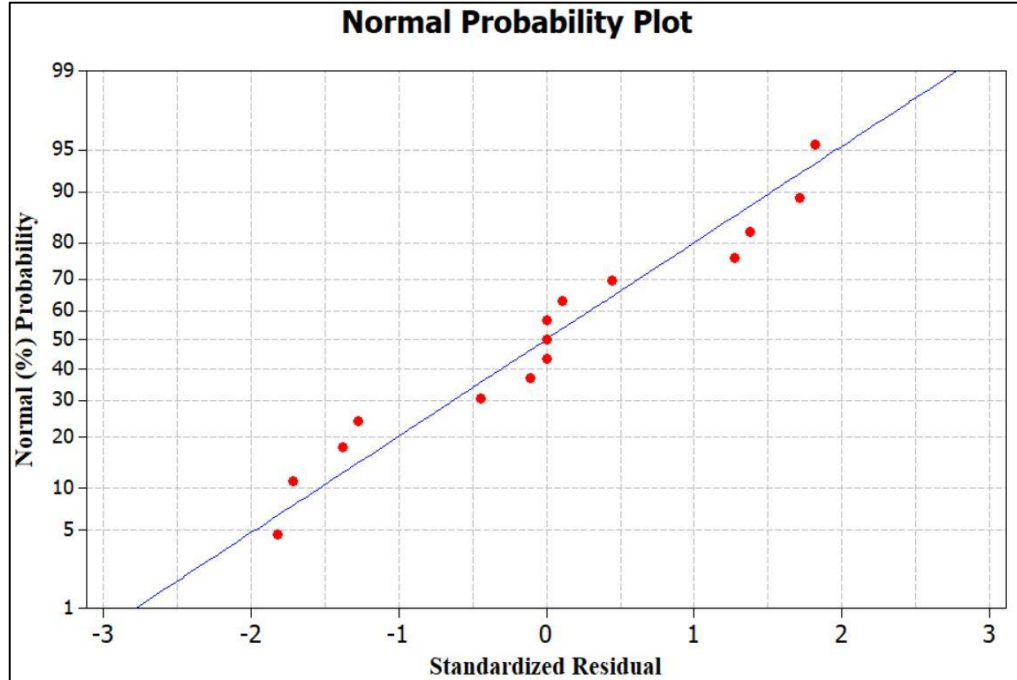
$$Y1 = -369.594 + 56.187X1 + 3.388X2 + 30.825X3 - 3.594X1^2 - 0.014X2^2 - 1.485X3^2 - 0.11X1X2 - 0.55X1X3 + 0.005X2X3 \quad (4.24)$$

$$Y2 = -416.781 + 54.938X1 + 329.375X2 + 81.312X3 - 12.469X1^2 - 296.875X2^2 - 6.531X3^2 + 23.125X1X2 + 2.125X1X3 + 7.500X2X3 \quad (4.25)$$

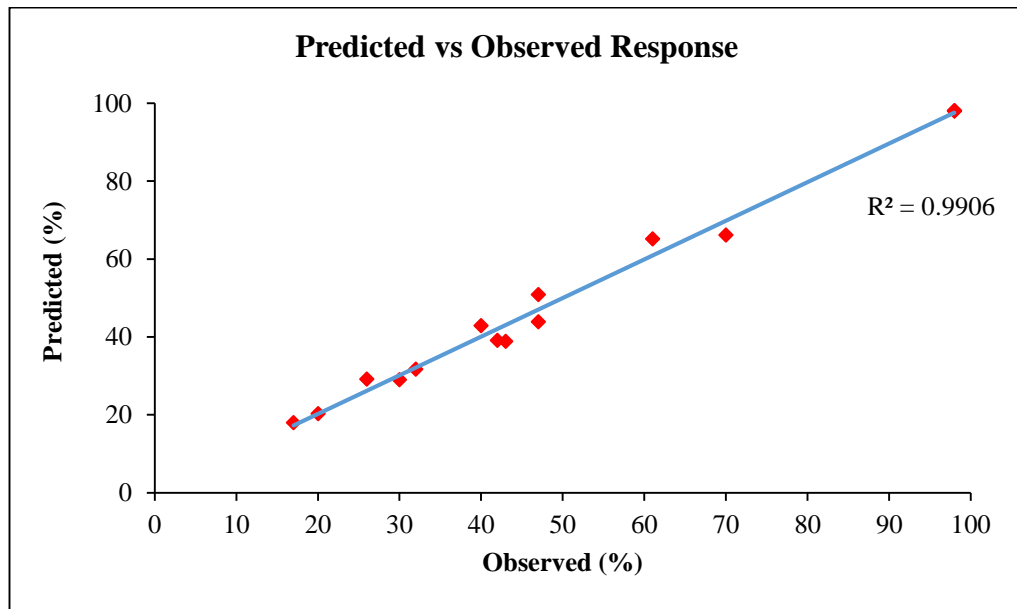
In the photocatalysis process, the comprehensive coefficients (linear, quadratic and interaction terms) were observed significant except for the individual interactive coefficient of NTP *H2O2 which was statistically non-significant. Similarly, in the case of Photo-Fenton's process, the overall coefficients for linear and quadratic terms were found significant, though, the individual linear and quadratic coefficients for Fe²⁺ were not significant. The overall as well as individual coefficients of interactions were also observed non-significant.

The normalcy of the results is potently supported by the coefficient of determination (R²). In the present study, for the Photocatalysis process, the observed R² value is 99.06% against the R² Adjusted value of 96.38%, whereas, in Photo-Fenton's treatment, the observed R² value noted is 95.53% against the Adjusted R² value of 87.49%. In both the aforementioned processes, the Predicted R² value lies in close proximity to actual R² values while the minimal difference between predicted R² and observed R² reflects the occurrence of non-significant components. Studies have documented that the value of R² closer to 1 ($R^2 \geq 0.8$) shows desired compliance among experimental response and projected response. The model adequacy was further assessed using some analytical plots like normal probability distribution and plots of predicted against observed values. Figure 4.8 and Figure 4.7 display the random distribution of residuals for photocatalytic and photo-Fenton's treatment process, respectively which is aligned linearly, thus ascertaining the reliability of the model. The plausible reasonability of the model

for each of the two treatment techniques is affirmed by the normal probability plot exhibiting the linear distribution.

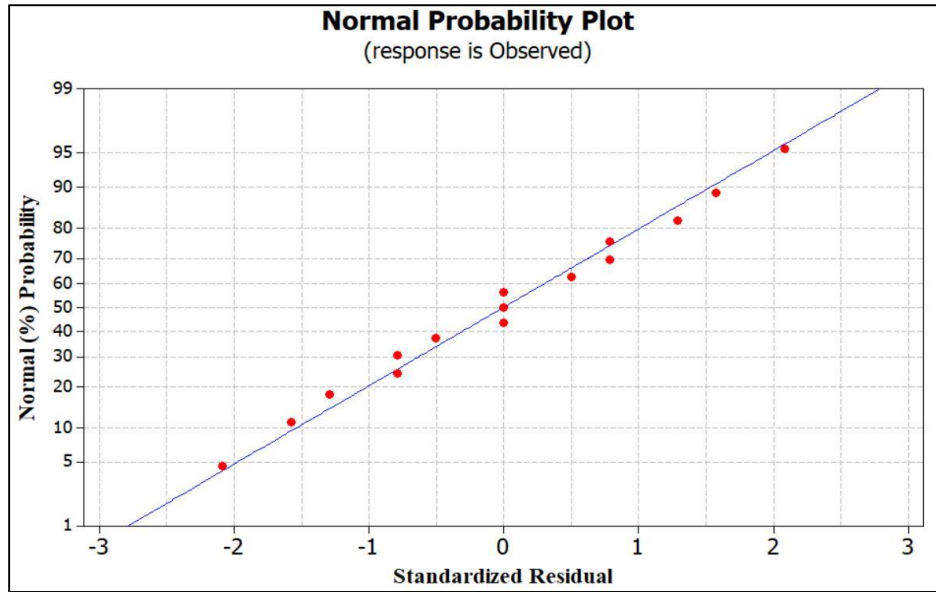


(a)

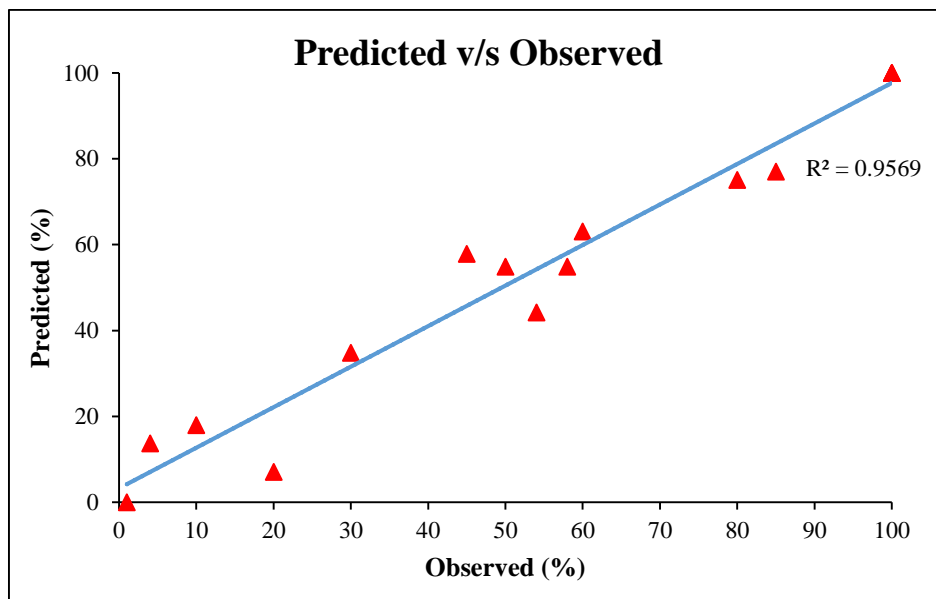


(b)

Fig. 4.7 (a) Normal Plot of residuals, and (b) Predicted vs Observed Photocatalytic response for 4-CP



(a)



(b)

Fig. 4.8 (a) Normal Plot of residuals, and (b) Predicted vs Observed Photo-Fenton's process response for 4-CP

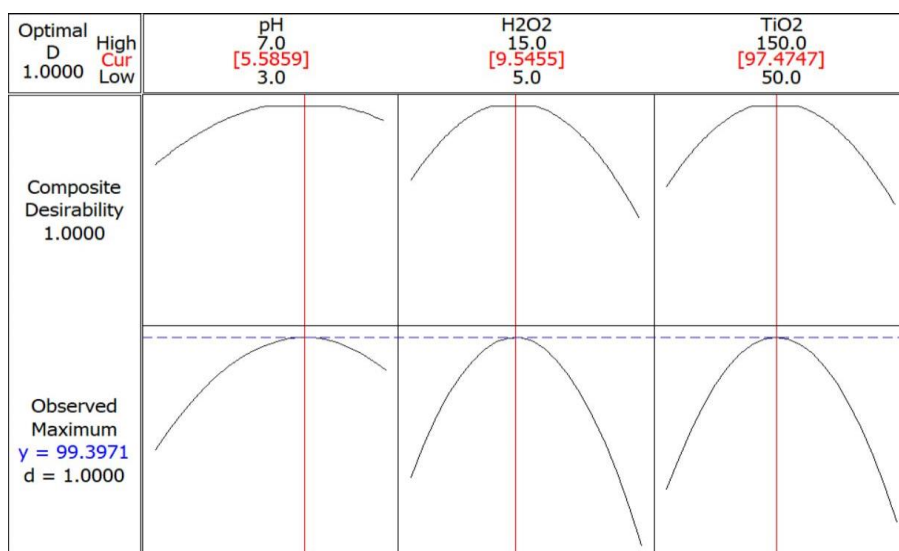
Table 4.3 Analysis of Variance (ANOVA) for percentage degradation of 4-CP by Photocatalysis (UV₃₆₅) and Photo-Fenton's treatment

Photocatalysis (a)							Photo-Fenton (b)						
Source	DF	Seq SS	Adj SS	Adj MS	F	P	Source	DF	Seq SS	Adj SS	Adj MS	F	P
Regression	9	10826.7	10826.7	1202.96	58.82	0	Regression	9	16335.5	16335.5	1815.05	11.87	0.007
Linear	3	703.2	6561.9	2187.31	106.96	0	Linear	3	4483.2	2583.4	861.12	5.63	0.046
pH	1	450	1419.6	1419.56	69.42	0	pH	1	4005.1	1389.6	1389.6	9.09	0.03
TiO₂	1	253.1	3383.4	3383.43	165.45	0	Fe	1	406.1	255	254.95	1.67	0.253
H₂O₂	1	0.1	4086.1	4086.11	199.81	0	H₂O₂	1	72	1553.8	1553.8	10.17	0.024
Square	3	9512.2	9512.2	3170.73	155.05	0	Square	3	11185	11185	3728.33	24.39	0.002
pH*pH	1	312.1	763	762.98	37.31	0.002	pH*pH	1	8303.4	9184.7	9184.67	60.09	0.001
TiO₂*TiO₂	1	4381.6	5089	5088.98	248.85	0	Fe*Fe	1	361.5	520.7	520.67	3.41	0.124

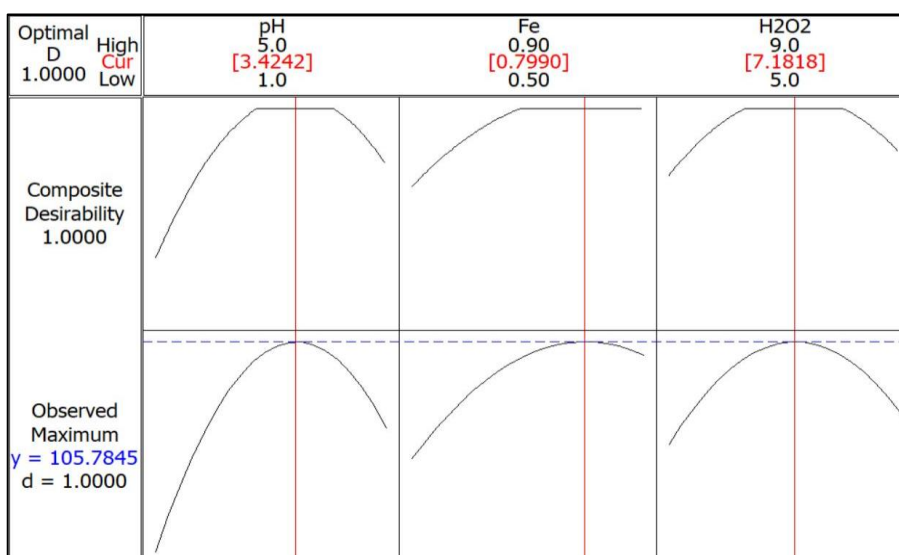
H₂O₂*H₂O₂	1	4818.5	4818.5	4818.52	235.62	0	H₂O₂*H₂O₂	1	2520.1	2520.1	2520.06	16.49	0.01
Interaction	3	611.3	611.3	203.75	9.96	0.015	Interaction	3	667.2	667.2	222.42	1.46	0.332
pH*TiO₂	1	121	121	121	5.92	0.059	pH*Fe	1	342.2	342.2	342.2	2.24	0.195
pH*H₂O₂	1	484	484	484	23.67	0.005	pH*H₂O₂	1	289	289	289	1.89	0.228
TiO₂*H₂O₂	1	6.2	6.2	6.25	0.31	0.604	Fe*H₂O₂	1	36	36	36	0.24	0.648
Residual Error	5	102.3	102.3	20.45	-	-	Residual Error	5	764.3	764.3	152.85	-	-
Lack-of-Fit	3	102.3	102.3	34.08	-	-	Lack-of-Fit	3	764.3	764.3	254.75	-	-
Pure Error	2	0	0	-	-	-	Pure Error	2	0	0	0	-	-
Total	14	10928.9	-	-	-	-	Total	14	17099.7	-	-	-	-
R.Sq	99.06%	-	-	-	-	-	R.Sq	95.53%	-	-	-	-	-
R-Sq Adj	96.38%	-	-	-	-	-	R-Sq Adj	87.49%	-	-	-	-	-

4.4 Optimization of process and effect of operating parameters

An interactive relationship for process operating variables was ascertained and the desirability function was employed. The desirability number was determined by taking into account the maximum removal proficiency for 4-CP. The predicted maximum efficacy in UV365-Photocatalysis was 98% for 4-CP with a composite desirability of 1.000 under optimal conditions.



(a)



(b)

Fig. 4.9 Optimisation plot of regulating parameters for 4-CP in (a) Photocatalysis, and (b) Photo-Fenton's process

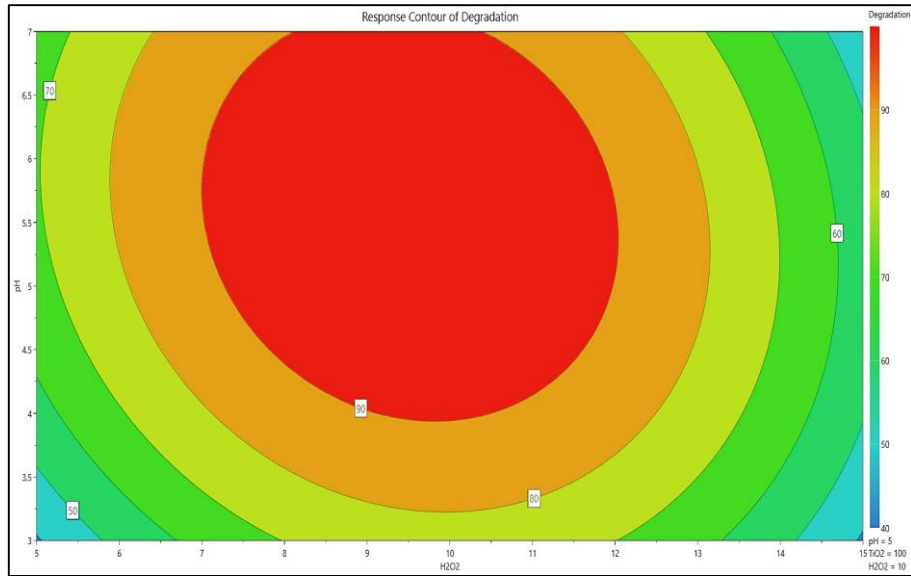
Correspondingly, in the Photo-Fenton's process, the model predicted 100% degradation of 4-CP having a desirability of 1.00 at optimum conditions. As reported, the photocatalytic process reported nearly complete degradation (~98%) while 100% degradation was observed in Photo-Fenton's process. Hence, the composite desirability for both processes was unity (Figures 4.9).

Moreover, the calculated and the predicted removal efficiency formulated by RSM closely bear a resemblance against each other thus validating the accurateness of the model as well as the proposed RSM-desirability function. Considering the second-order polynomial equation obtained for both the processes (eqs. 3.3a and 3.3b), contour plots and surface-contour overlay plots were generated as shown in Figure 4.10 and Figure 4.11, enlightening the effect of process regulating parameters of respective treatment methods, Photocatalysis and Photo-Fenton's towards degradation.

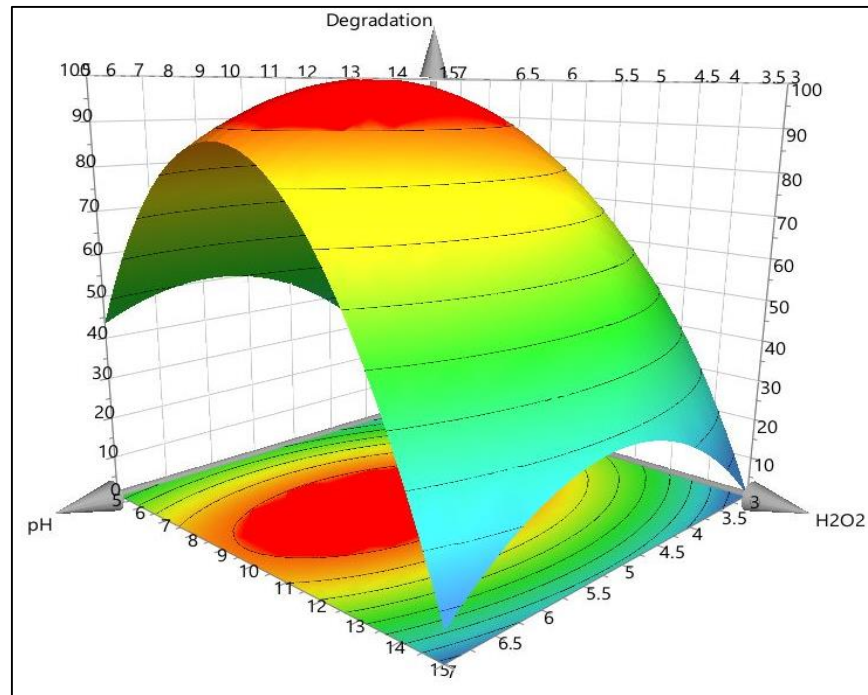
4.4.1 Influence of Photocatalytic factors

The interaction concerning the effect of concentration of H_2O_2 and pH is illustrated in Figure 4.10(a) and Figure 4.10(b). At a relatively low concentration of H_2O_2 , an increase in pH reported no substantial degradation. Conversely, the photo-oxidative proficiency increased with an increase in the concentration of H_2O_2 , and reached a maximum of 10.0mM. pH also exerts a significant impact on the process's efficacy. The removal rate of 4-CP increased at $pH = 5.0 \pm 0.2$. However, with a further rise in pH (in alkaline conditions), the efficiency of the process decreased. This is because, at higher pH levels, H_2O_2 undergoes self-decomposition, decreasing the formation of hydroxyl radicals, ultimately affecting the degradation rate. Relatedly, the photoactivity of NTP is also a function of pH as well (Figure 4.10(c) and Figure 4.10(d)). Notwithstanding the isoelectric point of TiO_2 (as reviewed earlier) as well as the pK_a value of chlorophenols, the photo-degradation of 4-CP was observed maximum at $pH < pH_{pzc}$ of TiO_2 . While the removal rate was lessened as $pH > pH_{pzc}$. At optimal dose, electron-hole pairs are

generated, which either react directly or with surface-bound water, yielding hydroxyl radicals effectively. It is worth emphasizing the significant interactive impact of H_2O_2 and NTP (Figure 4.10(e) and Figure 4.10(f)). Increasing doses of H_2O_2 and NTP reflected a proportionate effect on the oxidation rate of 4-CP and it ascended contemporarily.

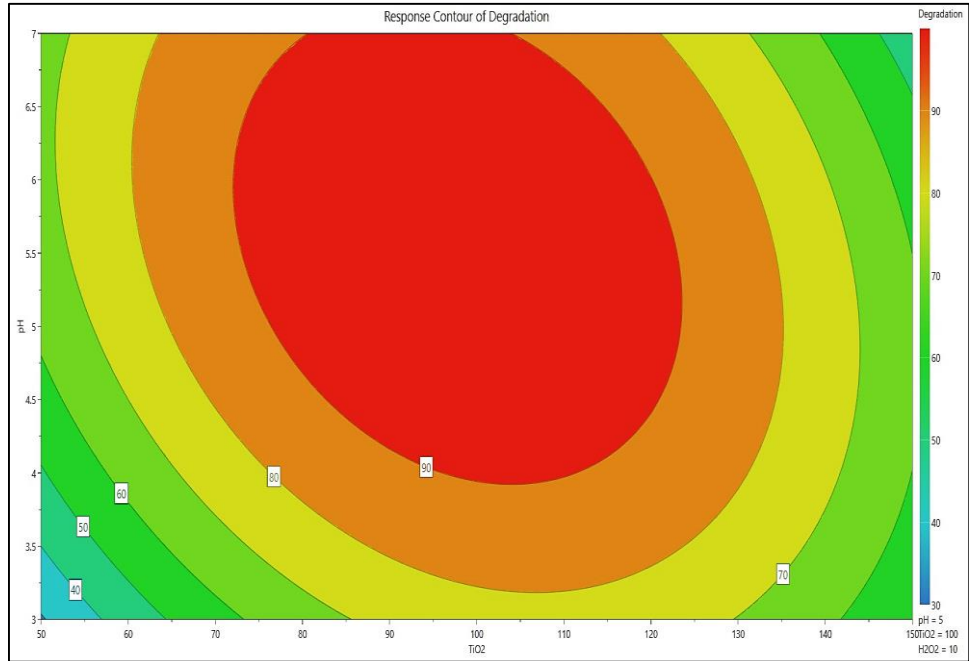


(a)

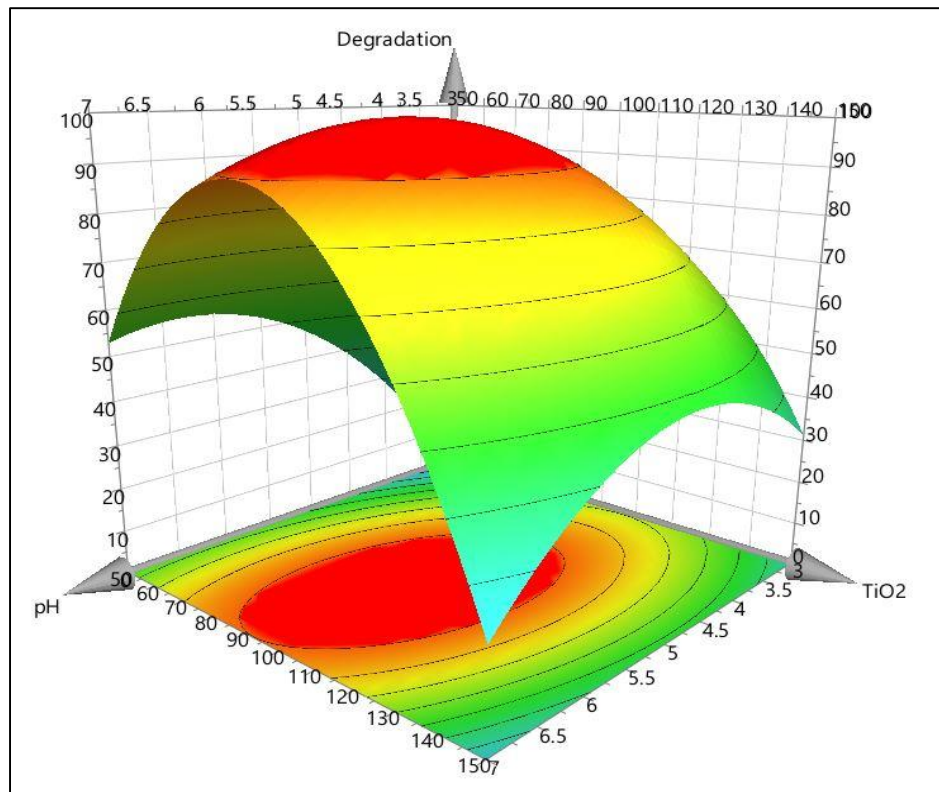


(b)

Interactive effect of pH against H_2O_2

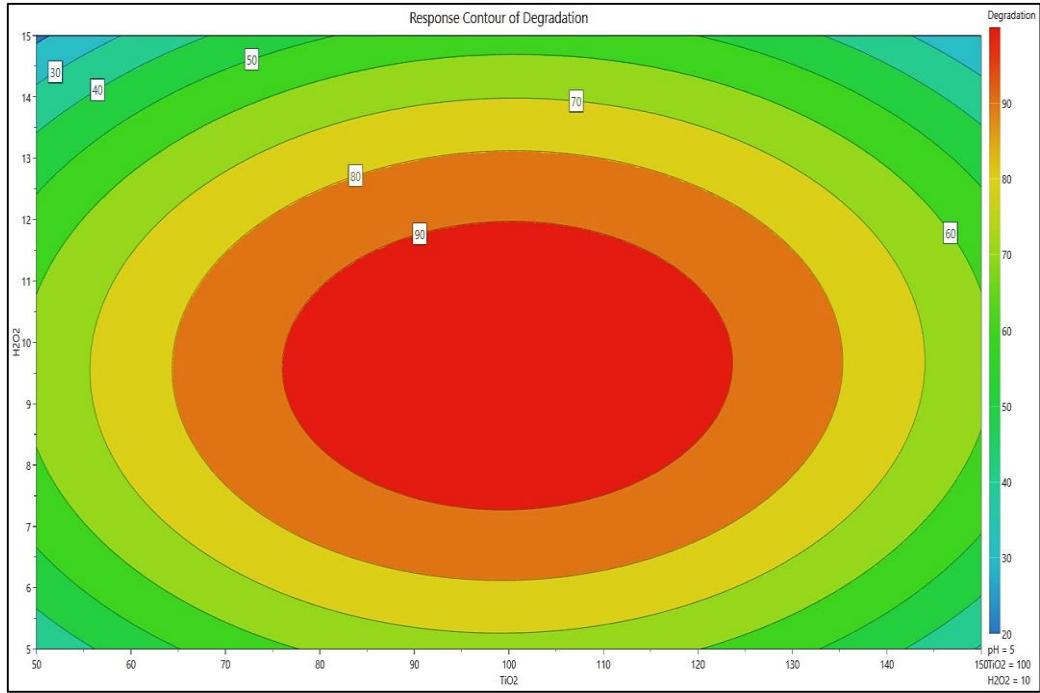


(c)

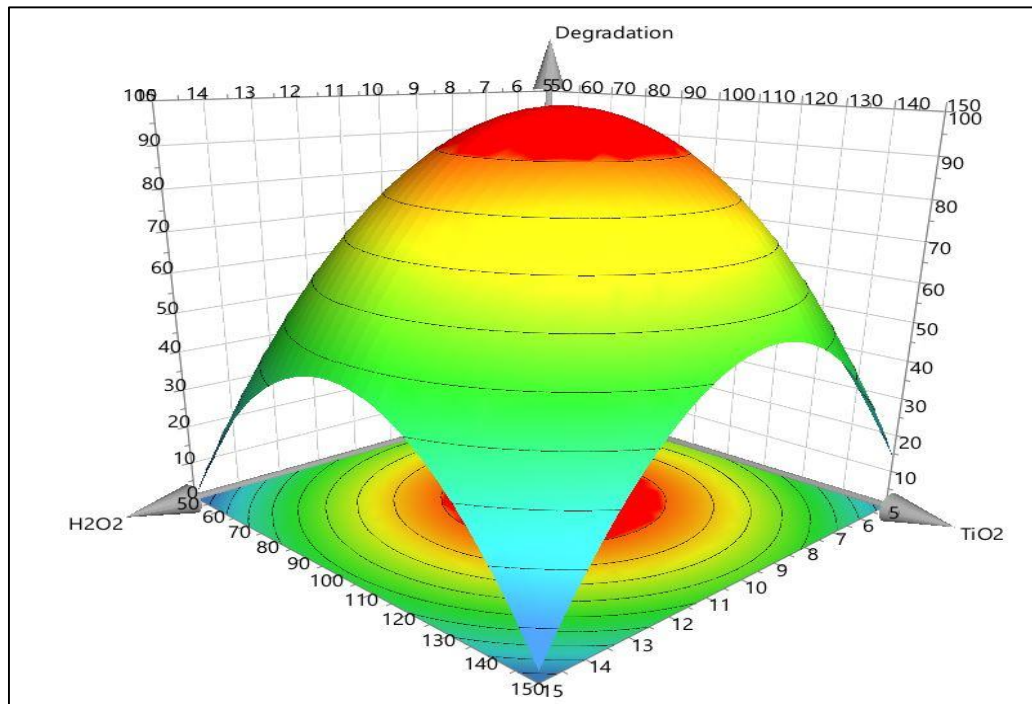


(d)

Interactive effect of pH and NTP



(e)



(f)

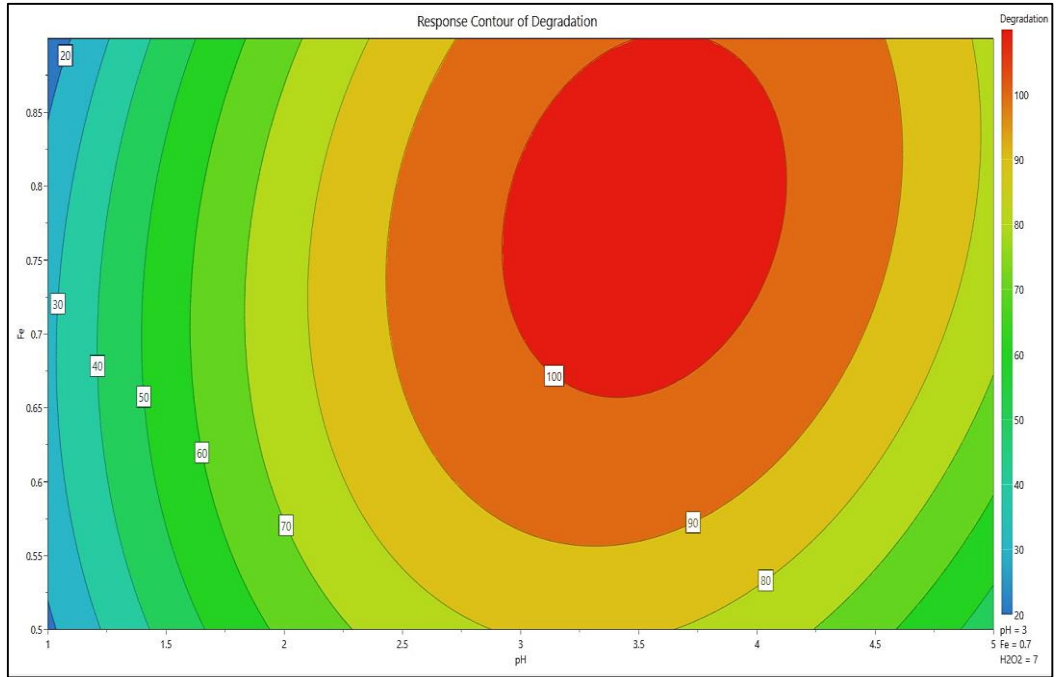
Interactive effect of H₂O₂ and NTP

Fig. 4.10 Contour plots and surface overlaid contour graphs showing effect of process regulating parameters in Photocatalysis for 4-CP

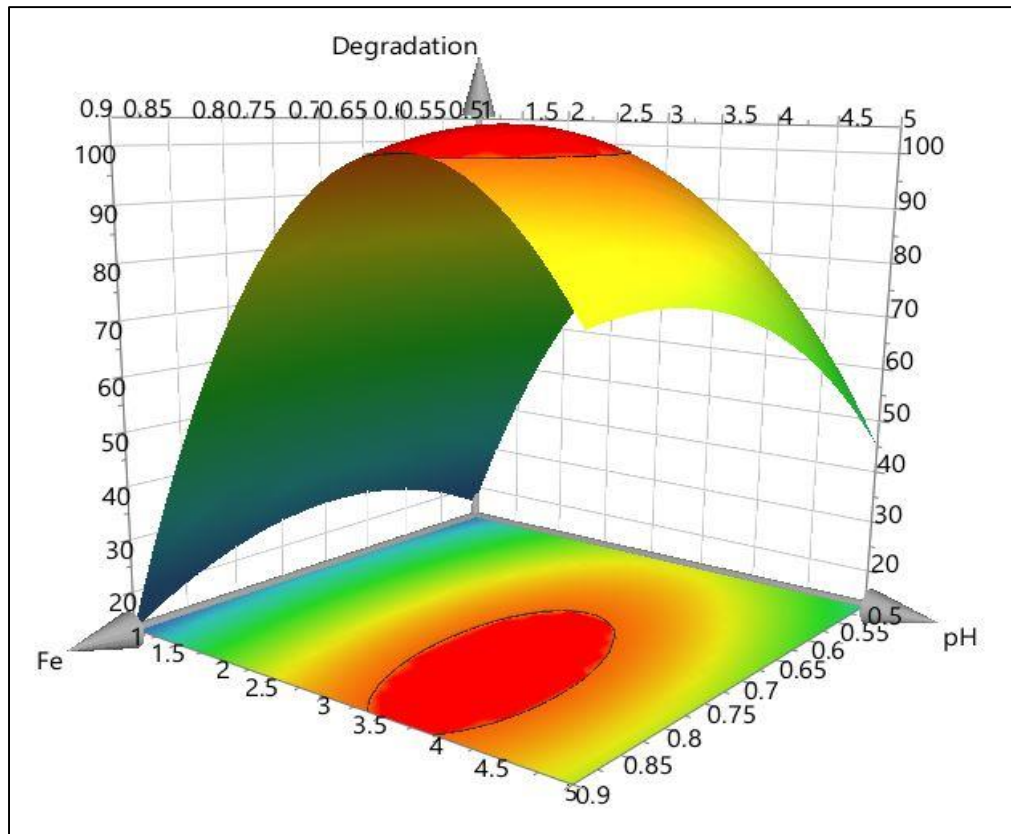
As the dose of NTP increased from 0.05g/L to 0.1g/L, maximal removal was attained and peaked at 0.1g/L corresponding to the increasing oxidant dose from 5.0mM to 10.0mM. Further addition reported no significant change, despite the degradation decreased. This is because the presence of an excessive catalyst increased the opacity of the solution which inhibited the effective penetration of UV Light.

4.4.2 Influence of Photo-Fenton's Factors

The Figure 4.11 demonstrates the interactive relationships between the operating factors governing the Photo-Fenton process. pH plays a crucial function in regulating the effectiveness of the Fenton process. Literature analyses have consistently implied that the treatment process attains maximum efficiency under acidic conditions. Concerning the effect of pH and iron concentration (Figure 4.11(a) and Figure 4.11(b)), it could be comprehended that increasing the pH values along with elevated iron dosage prominently enhanced the removal of chloro-derivative phenolic compound. Complete compound removal was observed at pH= 3.0±0.2 and 0.7mM iron concentration. Conversely, the removal rate decreased under alkaline conditions because of the relative formation of iron oxo-hydroxides and the ferric hydroxide precipitates. This demoted the availability of ferrous ions, consequently resulting in the lesser formation of hydroxyl radicals and a decrease in degradation. Excess or deficit concentration of H₂O₂ affects the degradation in a significant manner. As observed in Figure 4.11(c) and Figure 4.11(d), across the changing pH conditions, as the quantity of H₂O₂ increased, the degradation rate also enhanced and it peaked maximum at pH 3.0 and H₂O₂ concentration of 7.0mM. Subsequent additions of H₂O₂ reduced the effectiveness of the system as excess H₂O₂ confines the availability of hydroxyl radicals and triggers the deactivation of ferrous ions to ferric ions. Furthermore, at higher pH levels, H₂O₂ becomes unstable and experiences self-decomposition, further reducing the removal proficiency of the oxidation system. It is evident from Figure 4.11(e) and Figure 4.11(f) that the increase in the concentration of the oxidant as well as iron (Fe²⁺) enhanced the removal rate of 4-CP.

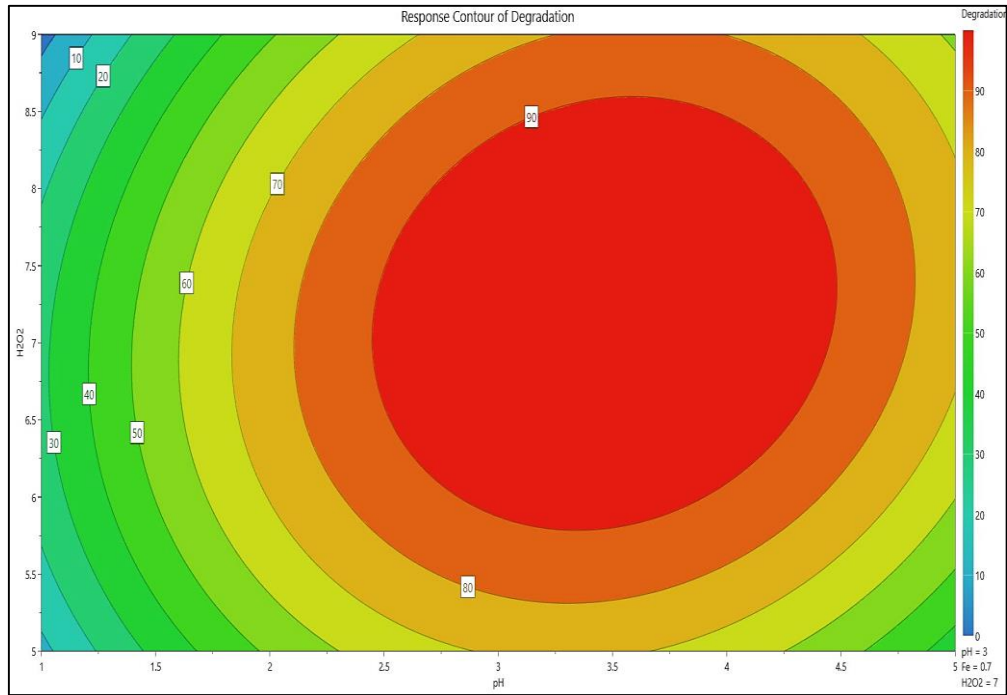


(a)

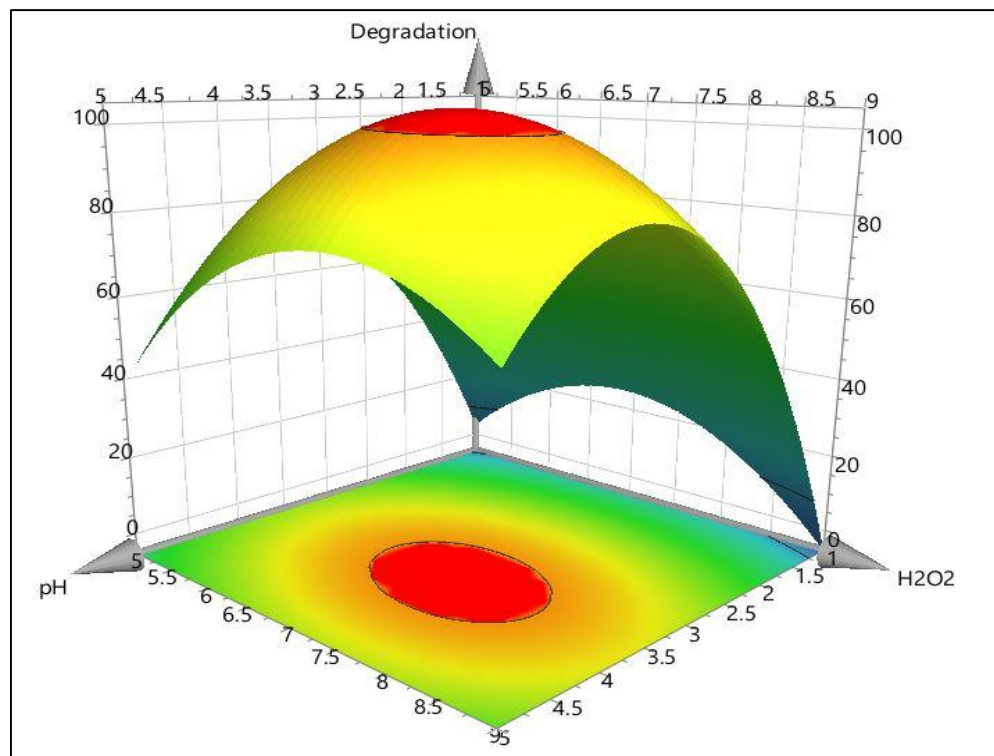


(b)

Interactive effect of Fe and pH

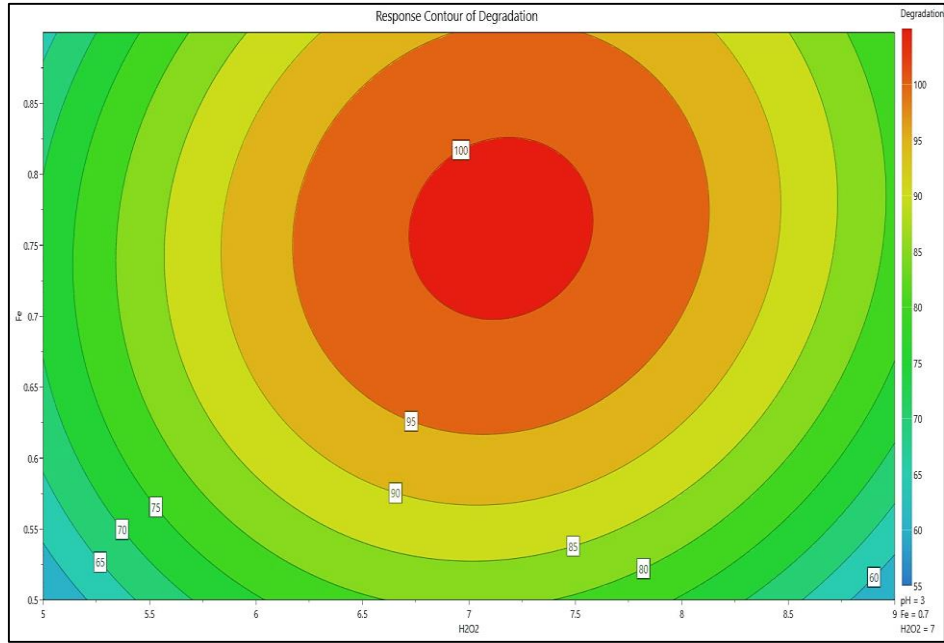


(c)

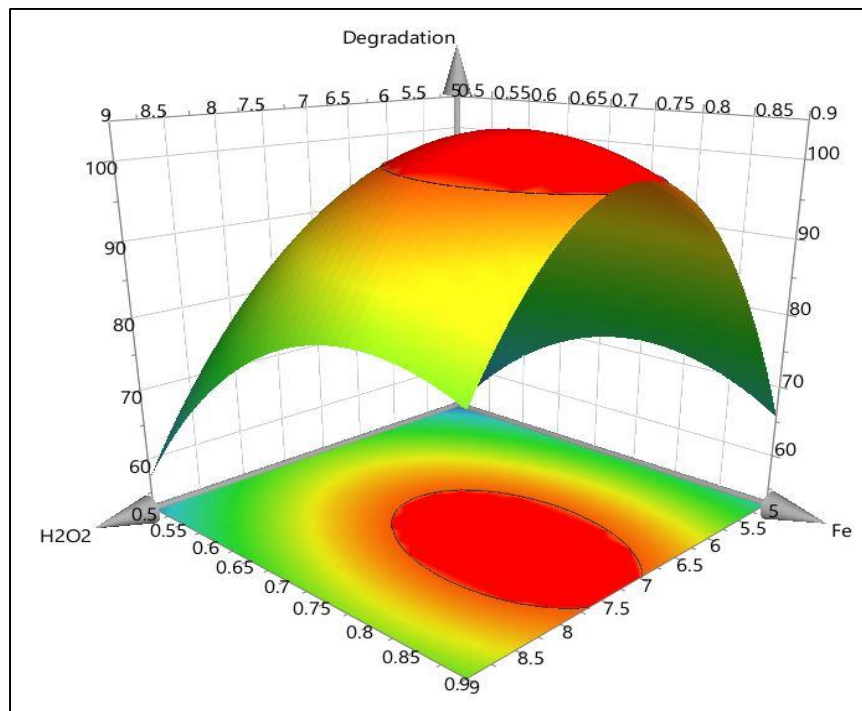


(d)

Interactive effect of H₂O₂ and pH



(e)



(f)

Interactive effect of Fe and H₂O₂

Fig. 4.11 Contour plots and surface overlaid contour graphs showing effect of process regulating parameters in Photo-Fenton's treatment for 4-CP

Markedly at 7.0 mM dose of H₂O₂ and 0.7 mM of iron, complete removal of organic contaminants was observed. Escalated production of the reactive oxidizing species, subsequently proliferated the treatment unit to bring the contaminant level non-detectable. However, additional increases in the dosage of these resulted in a reduction in the removal rate owing to the presence of excessive amounts of Fe²⁺ and H₂O₂, which induces the scavenging of hydroxyl radicals.

4.5 Synergic-approach induce Integrated-Oxidation

A comparative evaluation of various AOPs was investigated aimed towards the rapid degradation of the chlorine-derivative compound (Figure 4.12). The maximum removal efficiency of respective processes alongside their mineralisation efficacy is listed in Table 4.4. Based on the optimal conditions obtained for photocatalysis and Photo-Fenton's treatment, the above-mentioned processes were integrated with certain other AOPs and their synergistic effect was investigated on the degradation of refractory organics. The sonication-integrated experiments were performed at 40kHz frequency.

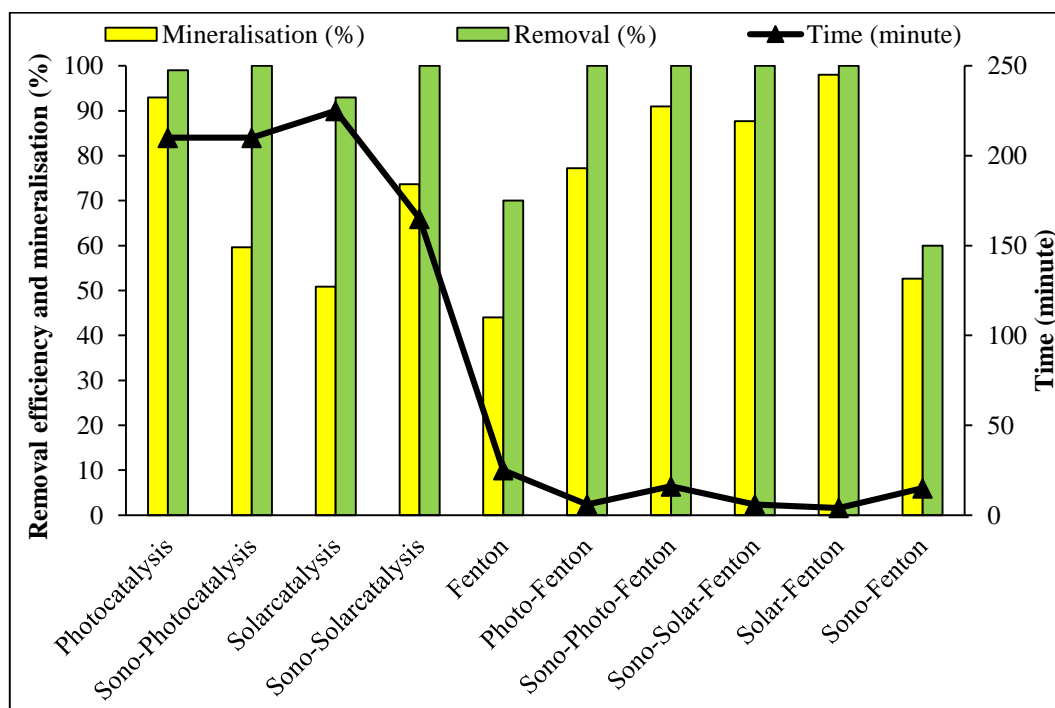


Fig. 4.12 Comparison of different AOPs towards maximum removal of 4-CP

Table 4.4. Comparison of different processes for maximum time taken for degradation of 4-CP

Processes	Conditions	Maximum degradation efficiency (%)	Time for complete/maximum degradation (minutes)	Mineralisation (%)
Photocatalysis	TiO ₂ : 0.1 g/L H ₂ O ₂ : 10.0mM pH: 5.0 Light Source: UV tubes (365nm) Intensity: 672W/m ²	99	210	93
Sono-Photocatalysis	TiO ₂ : 0.1 g/L H ₂ O ₂ : 10.0mM pH: 5.0 Light Source: UV tubes (365nm) Intensity: 672W/m ² Ultrasound: 40kHz	100	210	60
Solarcatalysis	TiO ₂ : 0.1 g/L H ₂ O ₂ : 10.0mM pH: 5.0 Light Source: Solar Intensity: 560 W/m ²	93	225	50
Sono-Solarcatalysis	TiO ₂ : 0.1 g/L H ₂ O ₂ : 10.0mM pH: 5.0 Light Source: Solar Intensity: 560 W/m ² Ultrasound: 40kHz	100	165	75

Photo-Fenton	Fe: 0.7mM H ₂ O ₂ : 7.0mM pH: 3.0 Light Source: UV tubes (365nm) Intensity: 672W/m ²	100	06	77
Solar-Sono-Fenton	Fe: 0.7mM H ₂ O ₂ : 7.0mM pH: 3.0 Light Source: Solar Intensity: 560 W/m ² Ultrasound Frequency: 40kHz	100	06	88
Sono-Photo-Fenton	Fe: 0.7mM H ₂ O ₂ : 7.0mM pH: 3.0 Light Source: UV tubes (365nm) Intensity: 672W/m ² Ultrasound Frequency: 40kHz	100	16	91
Sono-Fenton	Fe: 0.7mM H ₂ O ₂ : 7.0mM pH: 3.0 Ultrasound Frequency: 40kHz	60	15	55
Solar-Fenton	Fe: 0.7mM H ₂ O ₂ : 7.0mM pH: 3.0 Light Source: Solar Intensity: 560 W/m ²	100	04	98
Fenton	Fe: 0.7mM H ₂ O ₂ : 7.0mM pH: 3.0	70	25	44

4.5.1 Photocatalysis-integrated processes

The application of the ultrasonication process with photocatalysis towards the degradation of organic compounds was investigated. The synergistic effect of sonolysis coupled with photocatalysis was experimented with for faster degradation of chlorophenols. However, the ultrasound-aided UV₃₆₅/NTP/H₂O₂ system resulted in no drastic change in the removal rate of 4-chlorophenol. Both treatment systems UV₃₆₅/NTP/H₂O₂ and US/UV₃₆₅/NTP/H₂O₂ were able to degrade the contaminant in the same duration of 210 minutes, however the notable difference was observed in mineralisation per cent. The TOC mineralisation in the case of UV₃₆₅-Photocatalysis was higher (93%) as compared to sonication-integrated photocatalysis (60%). Since both the processes, UV₃₆₅-photocatalysis and sono-UV₃₆₅-photocatalysis are energy-intensive processes (Pipil et al., 2024a), solar light-induced treatment was explored to study the same. Degradation of 4-CP was carried out in sunlight on a hot sunny day when the temperature was nearly 43-47°C. Direct photolysis of the compound resulted in marginal or no degradation of it. However, the solar-catalysis process reported more than 90% removal of pollutants in 225 minutes. The average intensity of solar radiation received was 560 W/m². The process however resulted in only 50% mineralisation compared to photocatalysis. This could be reasoned because of the fractional proportion of UV in total solar terrestrial radiation resulting in lower energy and weak activation of NTP (Verma and Haritash 2020). In general, UV light makes up only 3-5% part of the solar spectrum, hence resulting in a slower rate of degradation (Pipil et al., 2022). The energy associated in the case of UV₃₆₅-Photocatalysis is higher and is sufficient enough to photo-activate NTP at a faster rate resulting in enhanced and rapid generation of hydroxyl radicals (Pipil et al., 2022; Ortiz et al., 2019). In photocatalysis, high intensity enhances electron excitation from the valence band to the conduction band of the photocatalyst and thus the rate of pollutant removal is also increased (Ortiz et al., 2019). The intensity of light is directly proportionate to the formation of OH• radicals which aids in the faster oxidation of 4-CP (Yadav et al., 2023a). In solar-driven sono-solarcatalysis, the degradation of the organic pollutant was very significant and it was not detected after 165 minutes. Although

the mineralisation observed was 75%, the process was less time-consuming and more energy efficient compared to UV₃₆₅-photocatalysis, sono-photocatalysis and solar-catalysis. Ultrasonic power in the sonolytic process generates expansion and compression cycles which form acoustic cavitation. These acoustic cavities oscillate in size, followed by cycles of expansion and compression. The collapse of the cavitation bubbles results in high atmosphere pressure and Kelvin temperature which ultimately aids in the degradation of contaminant (Van Aken et al., 2019). The sonolytic-induced acoustic cavities generate heat; enable the homogeneous mixing or mass transferral; stimulate effective interaction of reactive sites of photocatalyst with organic compound resulting in rapid degradation of contaminant (Anandan et al., 2020).

4.5.2 Fenton's-integrated processes

Based on the optimised conditions obtained in Photo-Fenton's process, synergistic studies involving the coupling of different AOPs with Fenton's process were conducted. Ultrasound and solar light assisted processes were employed with Fenton's process. The Fenton's process alone was inefficient in treating the synthetic wastewater containing monochlorophenol in a stipulated time of 30 minutes and only 70% removal efficiency was observed. The process was coupled with sonication to enhance the degradation process, however, failed to achieve the same. The process was stabilised after 15 minutes of the reaction time, degrading only 60% of the 4-CP. This is because of the inter-specific competition between Fenton's process and ultrasound towards the consumption of hydroxyl radicals generated by hydrogen peroxide. Similar phenomena have also been observed in other studies as well (Verma and Haritash 2020; Yadav et al., 2023b). It was eminent that under optimised conditions, Fenton's process was ineffective. Ultrasound-integrated UV₃₆₅-Photo-Fenton's treatment revealed complete degradation in 16 minutes with nearly complete mineralisation (>90%) as compared to Photo-Fenton (77%) alone. UV₃₆₅-driven Fenton's process was effective in the complete removal of pollutant in 06 minutes of duration because of the direct nucleophilic attack of the [•]OH radicals (Kavitha and Palanivelu 2016).

The UV₃₆₅-operated AOPs are considered energy-intensive processes. To switch to a sustainable and renewable approach, Solar energy-driven AOPs were investigated in the present study. Solar-driven Fenton's process has delivered encouraging results showcasing complete elimination of the recalcitrant in only 04 minutes with 98% reduction of TOC. The high-intensity solar light (average solar radiation intensity 560 W/m²) enhanced the degradation of monochlorophenol. The synergistic effect of ultrasound with solar light assisted Fenton's process was also experimented. The treatment system was found proficient with 100% removal efficacy and 88% mineralisation of 4-CP in 06 minutes of the reaction period.

4.6 Economic Efficiency of different AOPs for degradation of 4-CP

Based on the total energy consumed by the respective processes, the economic efficiency of the processes was calculated (Table 4.5). UV₃₆₅ Photocatalysis effectively degraded 4-CP in 3.5 hours with a photocatalyst dose of 0.1 g/L and 10.0mM oxidant concentration. The process was conducted in a UV light-equipped compartment comprising UV tubes (n=8) each of power rating 36W, making an aggregate of 288W. Combining the power rating of the magnetic stirrer (8.5W) and the air sparger (3.5W), the cumulative power consumed comes out to be 300W or 0.3kW. Considering the fractional amount of NTP was lost during analysis, centrifuging the sample, sample transfer etc, the residual part was recovered and dried in an oven at 105°C. The recovered fraction was determined using the formula as described:

$$TiO_2 \text{ Recovered} = \frac{w_2}{w_1} \times 100 \quad (4.26)$$

Where w_1 is the initial known weight of NTP; w_2 is the residual dried weight of NTP recovered post-treatment. In the present study, nearly ~85% of the photocatalyst was recovered.

Table 4.5 Economic analysis of the operating cost of different AOPs used for degradation of 4-CP

Treatment method	Energy (kWh)	Time for treatment (minute)	Rate of energy (per kWh) (INR)	Cost of electricity (INR)	Chemical consumed	Cost of chemical per litre (INR)	Cost of treatment in per litre (INR)	Cost of treatment in per litre (US\$)
Photo-Fenton (UV₃₆₅)	0.029	06	8.5	0.025	FeSO ₄ .7H ₂ O H ₂ O ₂ (30% w/v)	0.12 0.8	1.17	0.014
Photocatalysis (UV₃₆₅)	1.05	210	8.5	8.93	TiO ₂ (P25) H ₂ O ₂ (30% w/v)	4.54* 1.14	14.61	0.18
Fenton[#]	0.0034	25	8.5	0.029	FeSO ₄ .7H ₂ O H ₂ O ₂ (30% w/v)	0.12 0.8	0.94	0.011
Sono-Fenton[#]	0.03	15	8.5	0.25	FeSO ₄ .7H ₂ O H ₂ O ₂ (30% w/v)	0.12 0.8	1.17	0.014

Sono-Photo-Fenton (UV₃₆₅)	0.12	16	8.5	0.99	FeSO ₄ ·7H ₂ O H ₂ O ₂ (30% w/v)	0.12 0.8	1.90	0.023
Sono-Photocatalysis (UV₃₆₅)	1.37	210	8.5	11.65	TiO ₂ (P25) H ₂ O ₂ (30% w/v)	4.54* 1.14	17.33	0.21
Solar-Fenton	0.0006	04	8.5	0.0051	FeSO ₄ ·7H ₂ O H ₂ O ₂ (30% w/v)	0.12 0.8	0.92	0.011
Sono-Solar-Fenton	0.01	06	8.5	0.085	FeSO ₄ ·7H ₂ O H ₂ O ₂ (30% w/v)	0.12 0.8	1.0	0.012
Solar-catalysis	0.046	225	8.5	0.39	TiO ₂ (P25) H ₂ O ₂ (30% w/v)	4.54* 1.14	6.07	0.073
Sono-Solar-Catalysis	2.46	165	8.5	2.46	TiO ₂ (P25) H ₂ O ₂ (30% w/v)	4.54* 1.14	8.14	0.098

*15% loss is calculated; #Incomplete degradation;

The price of Degussa P25 NTP is INR 22,680/100g and since, only 15% of it was lost and not recovered, it cost INR 4.54/L for eliminating 100mg/L strength of synthetically prepared wastewater. Apart from this, the cost of hydrogen peroxide used as an oxidant was INR 1.14/L, thus constituting the overall operational cost of photocatalysis INR 14.61 or US\$ 0.18. The cost of electricity supplied to the industries in Delhi, India is INR 8.5 per unit kWh. The operational cost was increased in the case of Sono-UV₃₆₅ Photocatalysis (Sono-Photocatalysis) because of the increase in consumption of power. Solar-induced photocatalysis was more efficient as the energy consumed during the functioning of the process was negligible so was the treatment cost. In Photo-Fenton's treatment, the degradation was accomplished within a few minutes and since the cost of the catalyst, iron (used as a catalyst) was also lesser in comparison. Thus, the overall operating cost of the method was much less (INR 0.014) compared to photocatalysis. Sonication integrated Fenton's treatment cost was more because of the increased treatment time and added power of the sonication process. The operational cost was remarkable in solar-driven processes particularly, Solar-Fenton's and sono-solar-Fenton's processes. Therefore, harnessing solar energy is a more renewable and sustainable approach, reducing the reliance on other energy-intensive treatment processes.

4.7 Photocatalytic degradation of 2,4-Dichlorophenol

Photocatalytic oxidation of 2,4-DCP using P25 Nano-TiO₂ as a catalyst was found effective in removing the aforementioned organic pollutant. The study highlights the effect of process conditioning parameters like catalyst dose, effect of pH, and presence of oxidizing agent H₂O₂ for degradation of 2,4-DCP based on the RSM-BBD set of experiments suggested and the results are tabulated in Table 4.6. The optimised conditions, pH= 5.0±0.2, TiO₂ dose as 0.2g/L and H₂O₂= 10.0mM, 2,4-DCP was not detected after 210 minutes of the reaction time.

Table 4.6 Box Behnken design for three independent variables, predicted and observed responses for Photocatalytic degradation of 2,4-DCP

Run	pH	TiO ₂ dose (g/L)	H ₂ O ₂ (mM)	Removal Efficiency (%)	
				Observed	Predicted
1	4	0.3	10	60	63
2	6	0.1	10	35	34
3	5	0.2	10	98	98
4	5	0.2	10	98	98
5	6	0.2	15	40	41
6	4	0.2	5	60	59
7	6	0.2	5	40	42
8	6	0.3	10	65	66
9	5	0.3	15	90	89
10	5	0.1	5	75	76
11	5	0.2	10	98	98
12	4	0.2	15	70	68
13	4	0.1	10	80	79
14	5	0.3	5	60	58
15	5	0.1	15	50	53

Effect of Catalyst loading

The effect of different doses of photocatalyst Degussa P-25 Nano-TiO₂ was studied as a function of time towards the degradation of 2,4-DCP. The sample suspension of 100mg/L 2,4-DCP was subjected to UV irradiation after keeping the solution in the dark for 30 minutes. The experiment examined the effect of catalyst dose in the range of 0.1g/L to 0.6g/L at pH= 4.0 and oxidant dose of 10.0mM to ensure maximum removal efficiency and minimum consumption of catalyst. It can be observed from Figure 4.13, that the degradation rate increased with an increase

in the concentration of TiO_2 dose and peaked maximum at 0.2g/L while further increase in dose caused a decline in the degradation efficiency. At 0.2g/L of catalyst dose, almost complete (~98%) degradation was achieved in 255 minutes of reaction time. The greater efficiency could be rationalised in terms of the photocatalytic activity of TiO_2 that depends on three factors: (a) the capability of generation of electron-hole pair when illuminated with light less than 400nm wavelength; (b) inhibition of recombination of photo-generated charge pairs, and (c) efficiency of electron-hole pair to transfer charge to organic contaminants adsorbed on TiO_2 (Verma and Haritash, 2020; Pipil et al., 2022).

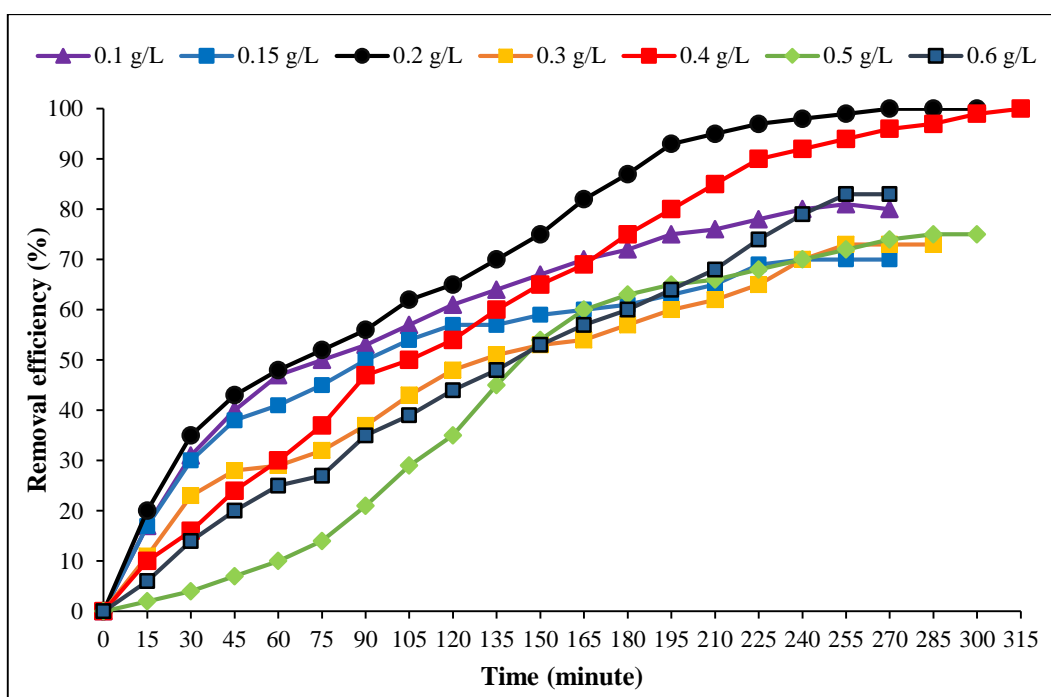
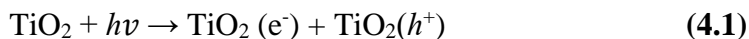


Fig. 4.13 Removal efficiency of 2,4-DCP at different catalyst dose in Photocatalysis process

The photo-generated valence band holes and conduction band electrons reduce the electron acceptor species and oxidise the electron donor species adsorbed on the catalyst surface. The hydroxyl and perhydroxyl radicals carry out the photo-oxidation of 2,4-DCP.



Increasing TiO₂ concentration increases the availability of active sites, thus escalating the adsorption process too. More binding of electron-hole pair with water accelerates the generation of the hydroxyl radicals. However, at a higher amount of TiO₂, the solution suspension becomes turbid and cloudy and the phenomena of light scattering dominate thus, reducing the UV penetration, which is also reported in other studies as well (Pipil et al., 2022; Yadav et al 2023a). Lesser illumination resulted in lesser production of ROS thus reducing the treatment efficiency of the system. Various studies have reported the degradation of 2,4-DCP using TiO₂ at higher concentrations in comparison to the present study. In one of the studies, a catalyst dose of 0.75g/L reported 90% degradation of 2,4-DCP solution (strength 125mg/L) in 6 hours while in another study only 50% degradation of 2,4-DCP (50mg/L) was achieved in 90 minutes (Bayarri et al., 2005; Kansal et al., 2012). Another study reported nearly 99.48% degradation of the phenolic compound with a TiO₂ concentration of 1.75g/L in 540 minutes of irradiation time (Zulfiqar et al., 2019). In the current study, the response surface methodology further validates the maximum removal efficiency with 0.2g/L of TiO₂ dose. Thus, optimisation of photocatalyst dose reduces its amount as well as treatment cost. Further experimentation was carried out using a 0.2g/L concentration of Nano-TiO₂.

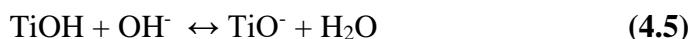
Effect of pH

The wastewater contains different organic compounds discharged at different pH, hence pH is a significant operating parameter regulating the efficiency of the treatment processes. pH determines the surface charge properties of photocatalyst which governs the behaviour of pollutants. In the present study, experiments were performed at different pH conditions- 4.0, 5.0, and 6.0 with optimised 0.2g/L of TiO₂ dose and oxidant concentration 10.0mM. Figure 4.14 illustrates the degradation of 2,4-DCP at different pH conditions in terms of

removal efficiency as a function of time. Almost complete removal (~98%) of 2,4-DCP was observed at pH= 4.0 and 5.0, however, at pH= 5.0, degradation was achieved in 210 minutes whereas, at pH= 4.0, the degradation process took 45 minutes more *i.e.* 255 minutes to degrade the same. Studies have also reported complete degradation of the chlorophenolic compound under similar pH conditions. One of the studies undertook the degradation of 2,4-DCP (~50 mg/L) and observed maximum removal efficiency at pH= 5.0 (Melián et al., 2013). Another research work revealed degradation of 2,4-DCP (~125 mg/L) maximum at pH= 5.5 (Bayarri et al 2005). The interaction and affinity between TiO₂ and 2,4-DCP is governed by pH. Variation in operating pH affects the surface charge or isoelectric point of Nano-TiO₂. The ionization state of the photocatalyst surface undergoes either protonation or deprotonation depending on the operating pH (eqs. 4.4 and 4.5) where TiOH is the primary hydrated surface functionality of TiO₂ (Hoffmann et al., 1995). Since the point of zero charge (p_{zc}) of TiO₂ is around 6.2, it carries a net positive charge (Wang, 2017), whereas the chloro-derivative phenol compounds have negative charges (p_{ka}= 7.98). Thus, at pH < p_{H_{pzc}}, the positive charge on the photocatalyst gradually exerts an electrostatic force of attraction towards the negatively charged chlorophenolic compound (eq. 4.4). Therefore, the polar attraction intensifies the adsorption of organics over the photocatalyst surface, facilitating photocatalytic degradation.



Consequently, at pH= 6.0, lesser degradation was observed because, in the case of pH ≥ p_{H_{pzc}}, TiO₂ carries a net negative charge (eq. 4.5), which hampers the adhesion of CP onto the catalyst surface.



The increased density of negatively charged catalysts and chlorophenols both exert coulombic repulsion, resulting in lesser adsorption of pollutant over the surface of TiO₂ (Chu et al., 2007). This results in a decreased rate of degradation

and lesser removal efficiency. Therefore, pH= 5.0 was considered as the optimum condition for degradation of 2,4-DCP in the present study. The results are also supported by a study carried out under similar operating pH (Zulfiqar et al., 2019). Although some research reports have also revealed pH= 4.0 appropriate towards organic decomposition (Kansal et al., 2012; Melián et al., 2013), one of the findings in the present study also showed the same. Nevertheless, the pace of reaction was faster in the case of pH= 5.0 and the TOC mineralisation as observed was also found maximum (70%) at pH= 5.0, whereas, it was 62% for pH= 4.0

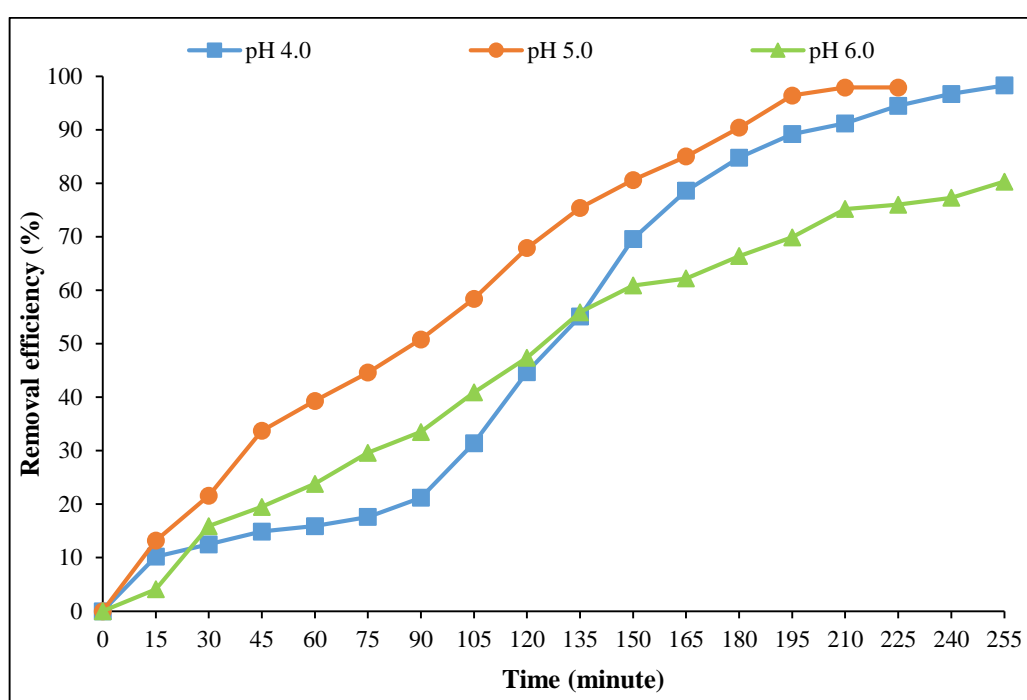


Fig. 4.14 Removal efficiency of 2,4-DCP at different pH in Photocatalysis process

Effect of oxidant concentration

The addition of oxidant enhances the degradation of organic contaminants. The effect of hydrogen peroxide was studied in the range of 5.0mM to 15.0mM based on run orders suggested by the RSM Software. It can be noted from Figure 4.15 that at a lesser concentration of H_2O_2 (0.5mM), the degradation efficiency was achieved around 70% attributing to lesser availability or generation of hydroxyl

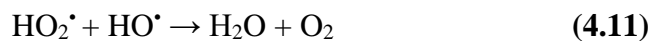
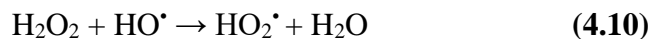
radicals. However, at 10.0mM of H₂O₂ dose, 98% of the degradation efficiency was attained in 270 minutes of reaction duration. Under the optimized conditions of Nano-TiO₂ (0.2g/L), the degradation with 10.0mM of H₂O₂ was faster, resulting in the complete elimination of the 2,4-DCP within 210 minutes. It can be rationalised as H₂O₂ is a more efficient electron acceptor than oxygen and generates hydroxyl radicals by reacting with conduction band electrons and inhibiting the electron-hole pair recombination. UV irradiation photolyzes H₂O₂ which generates hydroxyl radicals necessary for photo-mineralisation of organic pollutants (eq. 4.9).



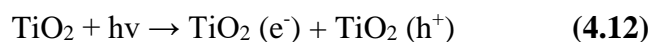
The addition of H₂O₂ along with TiO₂/UV has a synergistic effect, enhancing the efficiency of the treatment system by generating two hydroxyl radicals or producing hydrogen ions for generating perhydroxy radicals (Eqs. 4.6, 4.7, 4.8) (Pipil et al., 2022).



Near complete removal of 2,4-DCP (90%) was observed at a higher concentration of oxidant (15.0mM), although the degradation rate was slower and less efficient in the same reaction time (Figure 4.15). Similar findings were observed in which 2,3-DCP was photocatalytically degraded using 10.0mM of H₂O₂ whereas a higher range reported no significant change in removal efficacy (Kansal et al., 2009). Slow degradation at higher co-oxidant concentrations is attributed to the inhibitory effect of peroxide as (a) H₂O₂ also as a scavenger to ROS, or (b) the active sites for adsorption of water and production of hydroxyl radicals are blocked (Thind et al., 2018; Kansal et al., 2009). Excess H₂O₂ reacts with hydroxyl radicals and forms water molecules decreasing the degradation of 2,4-DCP (eqs. 4.10 and 4.11).



Another reason attributing to the reduced degradation rate of 2,4-DCP is the excess generation of holes causing photo-oxidation of hydroxyl radicals (eqs. 4.12 to 4.15).



Similar observations were also reported in other relevant studies carried out for the treatment of contaminated water using photocatalytic treatment (Thind et al., 2018; Gong et al., 2015). Thus, 10.0mM of H₂O₂ was considered as the optimised oxidant concentration.

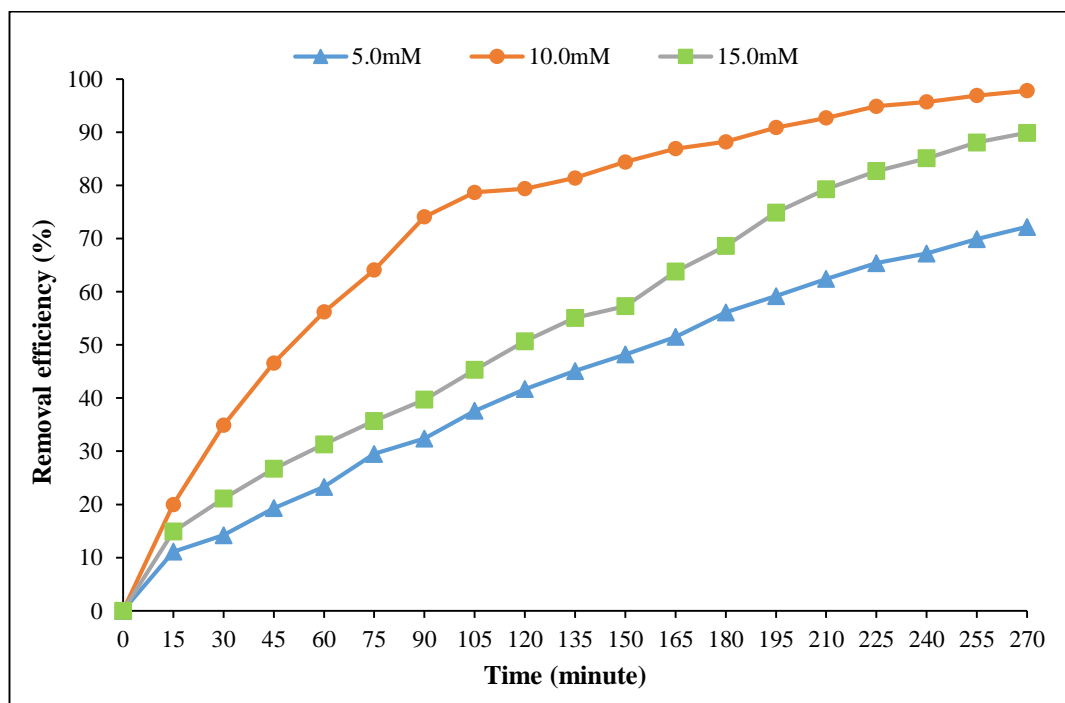


Fig. 4.15 Removal efficiency of 2,4-DCP at different oxidant concentration in Photocatalysis Process

4.8 Photo-Fenton's degradation of 2,4-Dichlorophenol

The effect of different parameters was studied by varying the concentration of regulating factors based on the runs given by MINITAB (version 16.2) software. Factors like pH, Fe^{2+} and H_2O_2 were examined in the range of 1.0 to 5.0, 0.3mM to 0.7mM, and 3.0mM to 7.0mM, respectively, for degradation of 2,4-DCP (strength 100 mg/L) and the results are tabulated in Table 4.7. H_2O_2 imparted a dark brown colour to the reaction mixture and the solution became turbid within a few seconds. As the reaction proceeded, the colour started fading changing from dark brown to light yellow and colourless, indicating completion of the reaction. Under optimum doses of $\text{pH} = 3.0 \pm 0.2$, $\text{Fe}^{2+} = 0.5\text{mM}$ and $\text{H}_2\text{O}_2 = 5.0\text{mM}$, 2,4-DCP was non-detectable within 5 minutes of the reaction time.

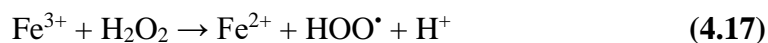
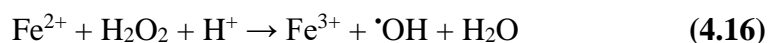
Table 4.7 Box Behnken design (BBD) for three independent variables, predicted and observed responses for Photo-Fenton's degradation of 2,4-DCP

Runs	pH	Fe(II) (mM)	H ₂ O ₂ (mM)	Removal Efficiency (%)	
				Observed	Predicted
1	3	0.5	5	100	100
2	3	0.5	5	100	100
3	3	0.7	7	18	25
4	3	0.7	3	03	06
5	5	0.5	7	20	22
6	5	0.7	5	53	43
7	1	0.5	7	36	29
8	1	0.3	5	23	32
9	3	0.3	3	02	-2.3

10	1	0.7	5	23	23
11	5	0.3	5	03	03
12	5	0.5	3	05	12
13	3	0.5	5	100	100
14	3	0.3	7	05	03
15	1	0.5	3	17	14

Effect of Fe²⁺ dose

Ferrous ions act as the regulating factor in determining the kinetics of the reaction. To elucidate the effect of iron, different concentration of iron was investigated in the range of 0.3mM to 0.7mM towards degradation of 2,4-DCP. Figure 4.16 illustrates the effect of different iron concentrations towards degradation. It can be seen from the figure that the maximum or complete removal of 2,4-DCP was there with an iron concentration of 0.5mM within 5 minutes of the reaction time. The ROS attacks on π bond in the benzene ring of the phenolic compound thus enhancing the oxidation of chlorophenols (Kavitha and Palanivelu, 2016). The redox recycling process of Fe²⁺/Fe³⁺ takes place in the bulk solution producing reactive oxidation species (eq. 4.16), while some ferrous ion species are also formed through reactions (4.17) and (4.18) (Ye et al., 2019).



Further increase in the dose of iron contributed no significant change in the removal efficiency instead, the removal was slower at increased iron concentration. At concentration of 0.7mM, complete degradation was achieved in 11 minutes which is slightly double the time taken to degrade 2,4-DCP at concentration 0.5mM.

This slight reduction in the degradation rate is attributed to the dominating scavenging effect of ferrous ions on hydroxyl radicals. An increasing amount of Fe(III) cannot be complexed and is insoluble and unstable, which stimulates the formation of ferrous hydroxide, $[\text{Fe}(\text{OH})]^{2+}$ and its further hydrolysis and precipitation as $\text{Fe}(\text{OH})_3$ (eq. 4.19 and 4.20)

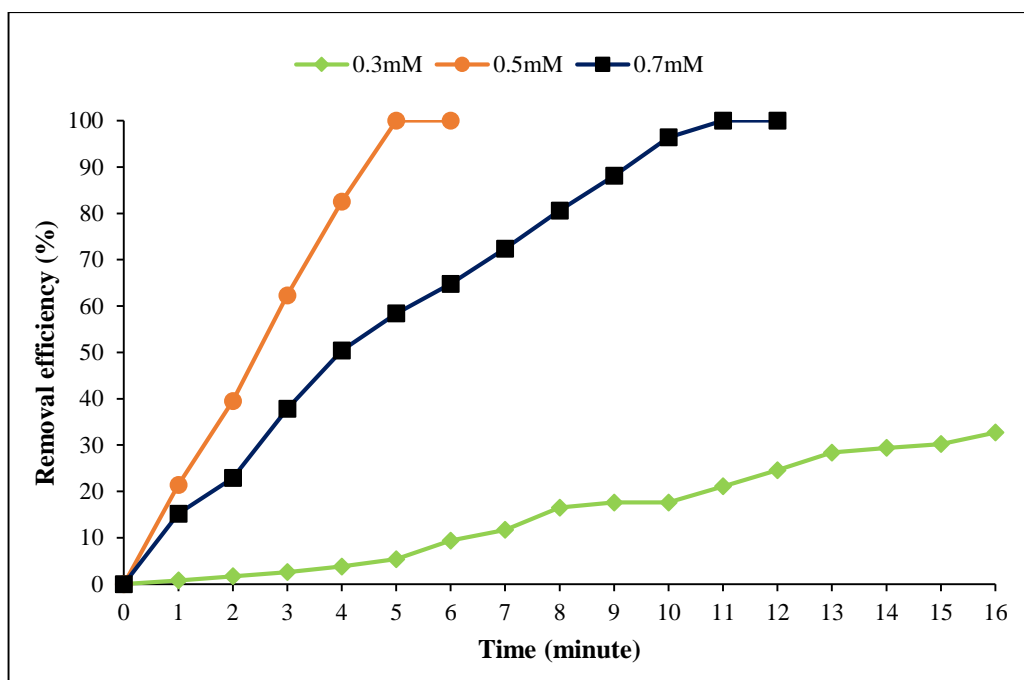
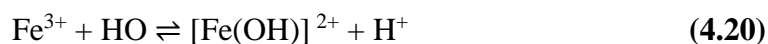


Fig. 4.16 Optimization of Fe^{2+} concentration for 2,4-DCP in Photo-Fenton process

However, at a lower iron dose (0.3mM), mere removal was observed because of the lesser availability of hydroxyl radicals further causing a delay in the oxidation process and efficient removal. The residual concentration of ferrous iron as well as TDI estimated at the end of the experiment revealed complete utilization of ferrous ions while 0.04mM of TDI remained in the solution.

Effect of pH

pH represents an important parameter in Fenton's process, as iron speciation that determines the UV absorption, complexation and dissolution of catalysis is strongly influenced and governed by pH condition. The dissociation constant of chlorophenols lies in the range of 4.7 for PCP to 9.41 for 4-CP, which signifies their ionization to occur under lower pH conditions. The present study aims to optimise the pH conditions keeping the 2,4-DCP concentration constant with a Fe^{2+} dose of 0.5mM and H_2O_2 concentration of 5.0mM. Experiments were conducted at pH= 1.0, 3.0, and 5.0, as suggested by the RSM Model. It can be observed from Figure 4.17 that the complete removal of chlorophenols occurred at pH= 3.0 within 5 minutes of the reaction period.

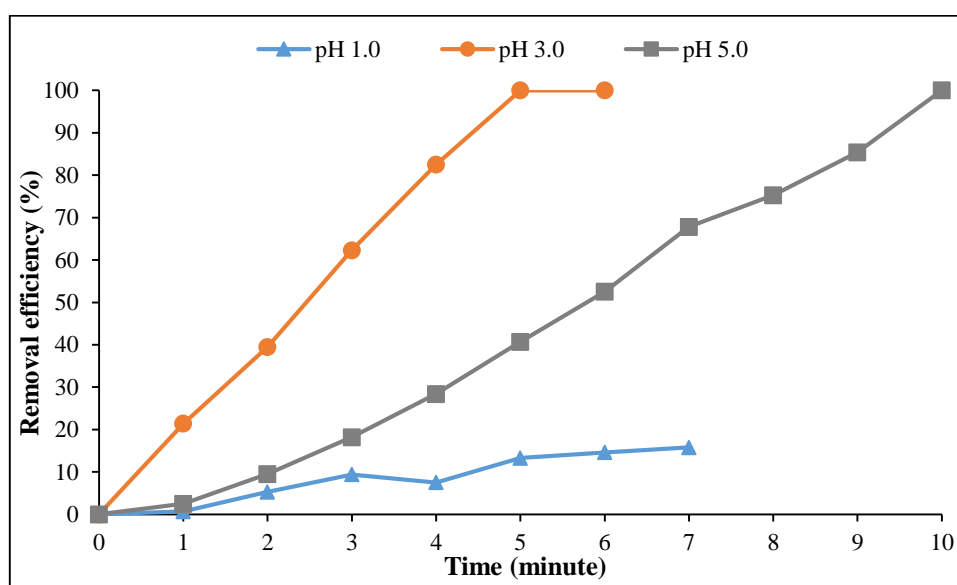


Fig. 4.17 Optimization of pH for 2,4-DCP in Photo-Fenton process

According to literature studies, ferrous ions and peroxide exhibit greater stability at pH = 3.0 (Pipil et al., 2022; Yadav et al., 2023b; 2023a; Verma and Haritash, 2020). The recorded observations have also been established in other relevant literature and are in strong agreement with their findings where at pH = 3.0, an appreciable higher mineralization rate was observed (Ahmadzadeh and Dolatabadi, 2018). Similarly, under at pH = 3.0, compound 2,4,6-TCP was reduced to non-detectable limits within 6 minutes of process duration (Yadav et al., 2023b).

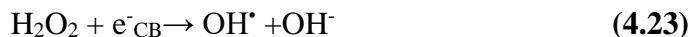
Successful elimination of pharmaceutical compounds like amoxicillin at pH = 3.0 has been reported within a few minutes of the reaction time (Verma and Haritash, 2019). Nonetheless, a very low removal rate i.e. only 25% was observed in 10 minutes under extreme acidic conditions (pH = 1.0). The removal efficiency is lessened due to the scavenging behaviour of the H⁺, consuming hydroxyl radicals (eq.4.21). Furthermore, lesser solubility of ferrous ions results in formation of complex ions species and peroxonium ions, H₃O₂⁺ (eq. 4.21) as well probably because of increased peroxide stability and decreased reactivity of Fe(II) (Ghoneim et al., 2011; Yadav et al., 2023b).



Literature studies have reported pH = 3.0 as the idealistic condition for Fenton's treatment, however, in the present study at higher pH = 5.0, complete removal was achieved (100%), however, the reaction time was approximately twice that of pH = 3.0. The instability of iron above pH 3.0 results in precipitate formation (ferric hydroxide complex), which does not react with peroxide, inhibiting the formation of hydroxyl radicals (Yadav et al., 2023a). Also, the self-decomposition of peroxide leads to the formation of oxygen and water. Furthermore, it has been reported that, with 2.0 < pH > 4.0, the potential for hydroxyl radical decreases (Yadav et al., 2023a). A drop in pH was also observed in the range of 2.3 to 2.5 post-treatment signifying the possibility of the formation of some carboxylic acid species after degradation as reported in other literature as well (Yadav et al., 2023a).

Effect of H₂O₂ concentration

H₂O₂ imparted a dark brown colour to the reaction mixture of iron and 2,4-DCP. As the reaction proceeded, the dark colour started fading from dark brown to colourless at the end indicating completion of the reaction. The presence of H₂O₂ inhibits the recombination of e-h as it acts as e⁻ acceptor and thus facilitates the formation of [•]OH radicals (Verma and Haritash 2019; Yadav et al., 2023a).



The addition of oxidant hydrogen peroxide was done in the concentration range 3.0mM to 10.0mM keeping the iron dose constant at 0.5mM and pH 3.0. Intermediate experimentation was also conducted outside RSM. It can be observed from the graph that complete degradation (100%) was observed in all the varied doses of H₂O₂ except at a higher concentration of 10.0mM. However, rapid removal efficiency was observed with an oxidant dose of 5.0mM within 5 minutes of the reaction period (Figure 4.18).

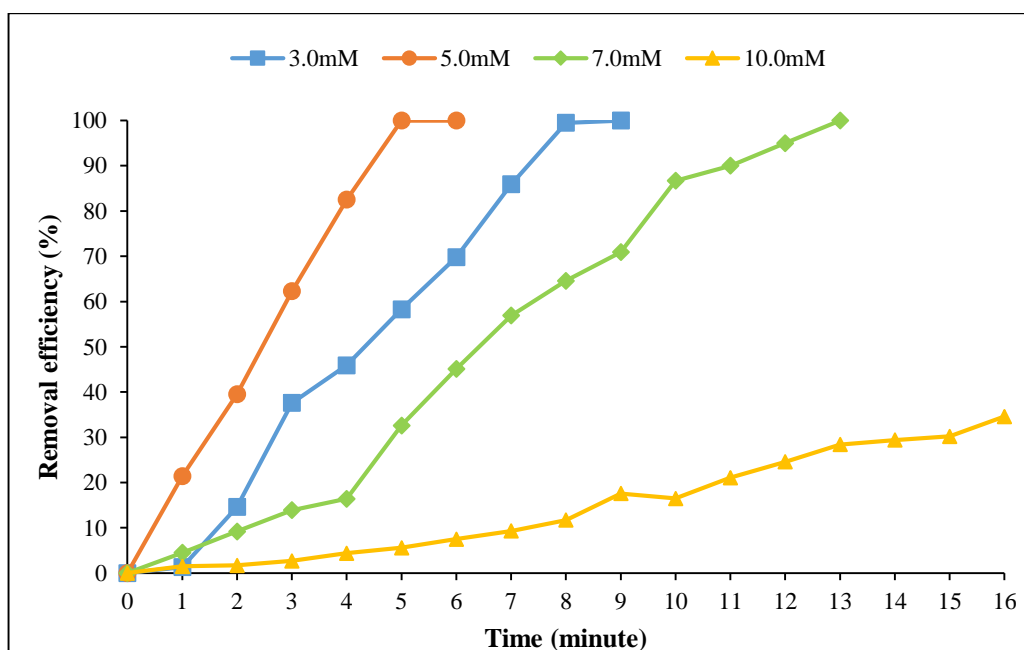
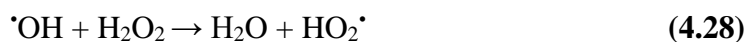


Fig. 4.18 Optimization of oxidant concentration for 2,4-DCP in Photo-Fenton process

At oxidant doses of 3.0mM and 7.0mM, degradation was accomplished in around 10 minutes and 13 minutes, respectively. Correspondingly, very little removal was observed (nearly 30%) at a concentration of 10.0mM. In excess amounts, H₂O₂ has a negative effect as it undergoes self-decomposition and acts as a scavenger.

A similar observation is also reported in other studies as well (Ye et al., 2019; Pipil et al., 2022; Yadav et al 2023b). In such cases, hydroperoxyl radicals are formed whose reduction potential (1.0 V) is less than that of hydroxyl radicals (2.8 V) (Eqs. 4.27-4.29).



Hence, a 5.0mM dose of H_2O_2 was considered optimum for further experimentation, as the current study reports lesser consumption of H_2O_2 and complete degradation in minimum time.

4.9 RSM Modelling and adequacy of model (ANOVA) for degradation of 2,4-DCP

The influence of independent variables of the two treatment processes employed for the degradation of 2,4-DCP was studied. The observed experimental results against the predicted response obtained through RSM towards effective removal are tabulated in Table 4.6 and Table 4.7 for both treatment processes. The two quadratic regression models developed (eq. 3.4) using observed response against predicted is represented using the following equations. Y_1 depicts the photocatalytic response while Y_2 represents the Photo-Fenton's response.

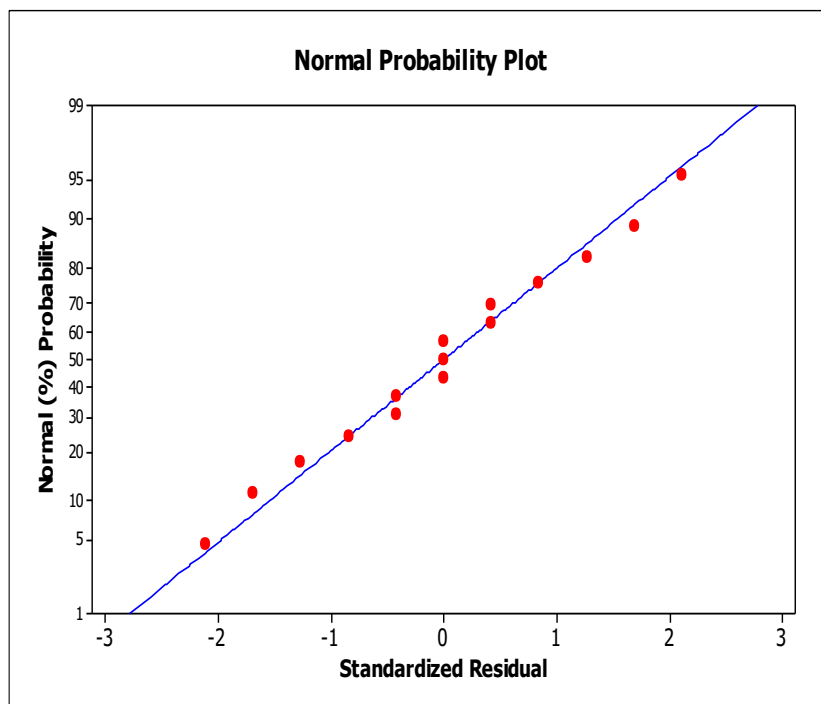
$$Y_1 = -403.375 + 207.5X_1 - 0.321X_2 + 5.575X_3 - 24.625X_1^2 - 0.001X_2^2 - 0.635X_3^2 + 0.125X_1X_2 + 0.500X_1X_3 + 0.027X_2X_3 \quad (4.30)$$

$$Y_2 = -490.25 + 32.25X_1 + 906.25X_2 + 118.75X_3 - 8.50X_1^2 - 1018.75X_2^2 - 12.31X_3^2 + 31.88X_1X_2 + 0.44X_1X_3 + 12.50X_2X_3 \quad (4.31)$$

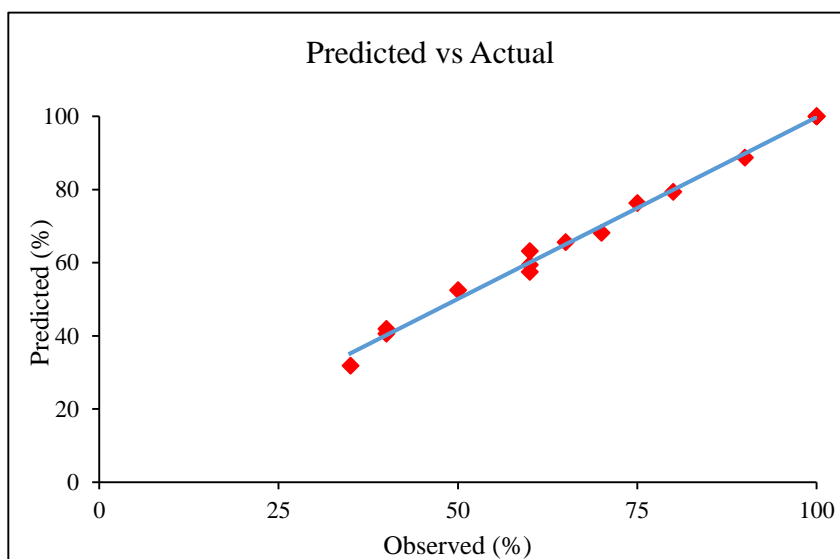
The state of normality of the results is strongly supported by the obtained coefficient of determination, R^2 value for both the processes which is 97.96%

observed R^2 against 94.29% R^2 Adjusted value in the case of Photocatalysis and observed R^2 value of 97.8% against 93.83% R^2 Adjusted value in the case of Photo-Fenton's process. In both the abovementioned cases, it can be noted that the Predicted R^2 value lies in close proximity to actual R^2 values with nominal difference indicating the presence of insignificant factors. Figure 4.19 and Figure 4.20 describe the randomly distributed residuals signifying the reliability of the proposed model; whereas the linear distribution of the normal probability plot supports the reasonability of the model for both the treatment systems respectively. Residuals define the reliability of the models reflecting the difference between predicted and actual responses.

The competency and significance of the proposed regression model were analysed using ANOVA and the results are summarized in Table 4.8. The results reflected an excellent behaviour between experimental and predicted results towards the degradation of 2,4-DCP. It can be seen from the table that the F-value for both the process models (26.67 in the case of photocatalysis and 24.65 in Photo-Fenton's process) are highly significant corresponding to the p -value of regression <0.001 (p -value < 0.05). Complying with the p -values (p -value < 0.05 indicates the model term as significant and vice-versa), the significance of each test variable was evaluated. In the case of photocatalytic treatment, the overall linear, quadratic and interaction coefficients were found significant. However, exceptionally, the linear coefficient of Nano- TiO_2 and H_2O_2 and the interaction coefficient of $\text{pH}*\text{H}_2\text{O}_2$ were found statistically insignificant. Similarly, in the case of Photo-Fenton's process, all the governing parameter's linear, quadratic and interaction coefficients were significant except for the individual interaction coefficient for $\text{pH}*\text{Fe}$, which was exceptionally non-significant.

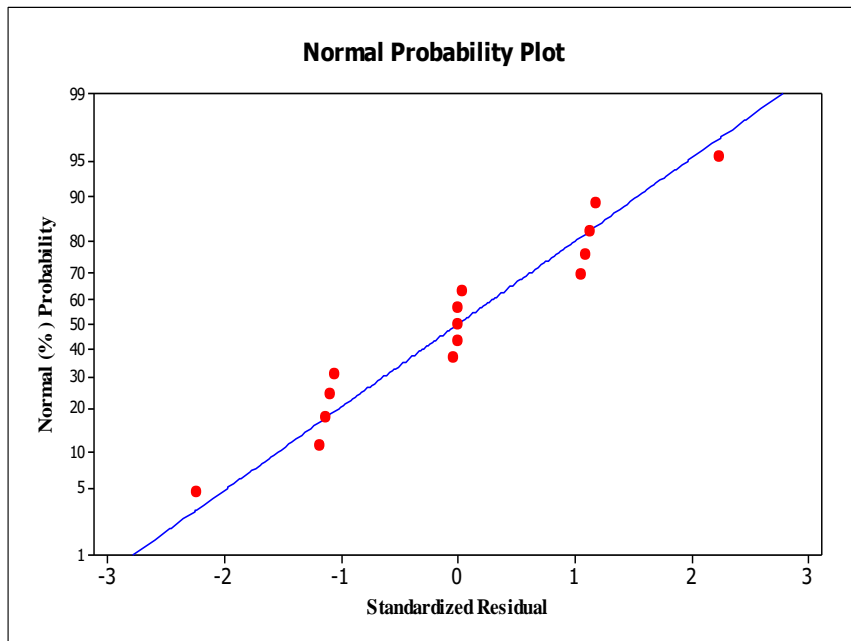


(a)

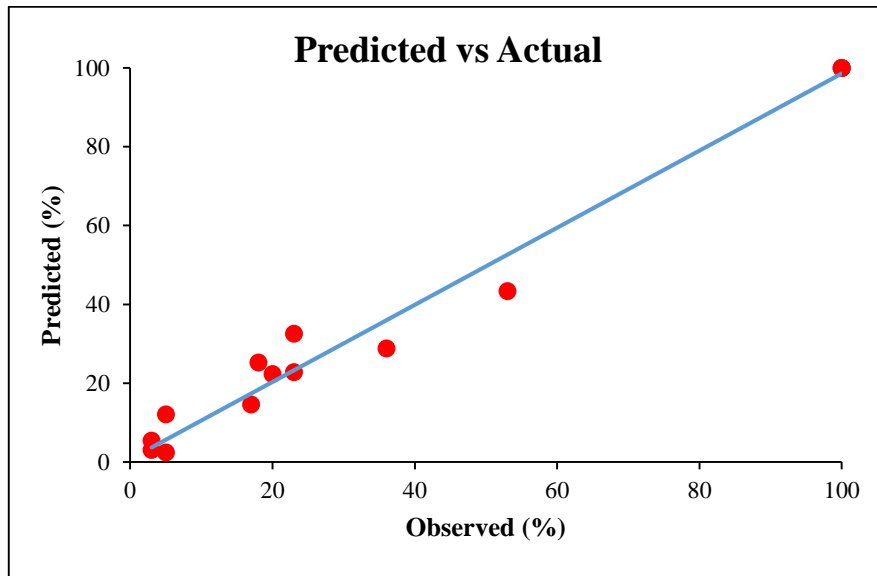


(b)

Fig. 4.19 (a) Normal Plot of residuals, and (b) Predicted vs Observed Photocatalytic response for 2,4-DCP



(a)



(b)

Fig. 4.20 (a) Normal Plot of residuals, and (b) Predicted vs Observed Photo-Fenton's response for 2,4-DCP

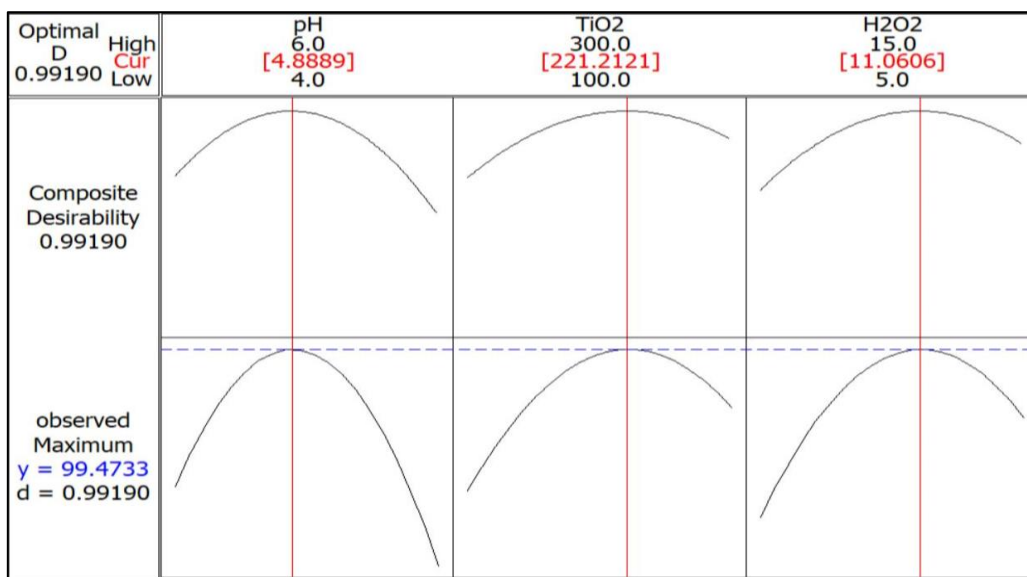
Table 4.8 Analysis of Variance (ANOVA) for percentage degradation of 2,4-DCP by Photocatalysis (UV₃₆₅) and Photo-Fenton's treatment

Photocatalysis (a)							Photo-Fenton (b)						
Source	DF	Seq SS	Adj SS	Adj MS	F	P	Source	DF	Seq SS	Adj SS	Adj MS	F	P
Regression	9	5700.18	5700.18	633.35	26.67	0.001	Regression	9	18445.2	18445.2	2049.46	24.65	0.001
Linear	3	918.75	1756.05	585.35	24.65	0.002	Linear	3	805.8	8883.9	2961.30	35.61	0.001
pH	1	612.5	1474.11	1474.11	62.07	0.001	pH	1	40.5	700.6	700.62	8.43	0.034
TiO₂	1	153.12	88.14	88.14	3.71	0.112	Fe²⁺	1	465.1	4220.6	4220.6	50.76	0.001
H₂O₂	1	153.12	66.36	66.36	2.79	0.155	H₂O₂	1	300.1	6593.1	6593.1	79.29	0.000
Square	3	3375.18	3375.18	1125.06	47.37	0	Square	3	16954.2	16954.2	5651.39	67.97	0.000
pH*pH	1	1896	2238.98	2238.98	94.27	0	pH*pH	1	2293.5	3634.7	3634.7	43.71	0.001
TiO₂*TiO₂	1	548.66	660.52	660.52	27.81	0.003	Fe²⁺*Fe²⁺	1	5750.2	6866.8	6866.8	82.58	0.000
H₂O₂*H₂O₂	1	930.52	930.52	930.52	39.18	0.002	H₂O₂*H₂O₂	1	8910.5	8910.5	8910.5	107.16	0.000

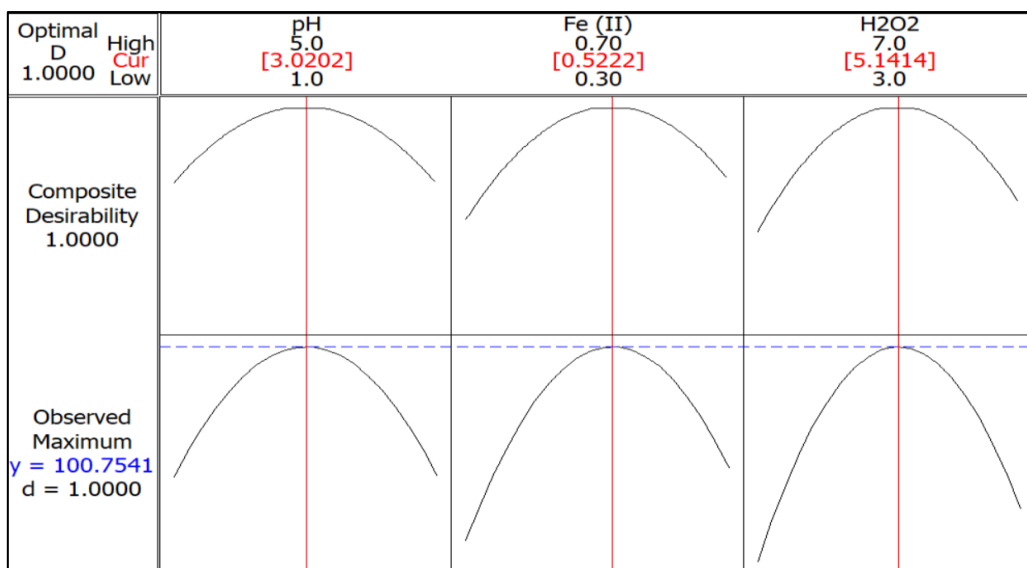
Interaction	3	1406.25	1406.25	1406.25	19.74	0.003	Interaction	3	685	685.3	685.3	2.75	0.152
pH*TiO₂	1	625	625	625	26.32	0.004	pH*Fe²⁺	1	625	625	625	7.52	0.041
pH*H₂O₂	1	25	25	25	1.05	0.352	pH*H₂O₂	1	4	4	4	0.05	0.835
TiO₂*H₂O₂	1	756.25	756.25	756.25	31.84	0.002	Fe²⁺*H₂O₂	1	56.2	56.2	56.2	0.68	0.448
Residual Error	5	118.5	118.5	-	-	-	Residual Error	5	415.7	415.7	83.15	-	-
Lack-of-Fit	3	118.75	118.75	-	-	-	Lack-of-Fit	3	415.7	415.7	138.58	*	*
Pure Error	2	0	0	-	-	-	Pure Error	2	0	0	0	-	-
Total	14	5818.93	-	-	-	-	Total	14	18860.9	-	-	-	-
R.Sq	97.96 %	-	-	-	-	-	R.Sq	97.8%	-	-	-	-	-
R-Sq Adj	94.29 %	-	-	-	-	-	R-Sq Adj	93.83 %	-	-	-	-	-

4.10 Process optimization and effect of variables

An interactive relationship among process variables was established and a desirability function was applied. The desirability number was estimated considering the maximum removal efficiency of 2,4-DCP.



(a)



(b)

Fig. 4.21 Optimisation plot of regulating parameters of 2,4-DCP (a) Photocatalysis (b) Photo-Fenton

The predicted maximal efficiency in the case of photocatalysis was 98% for 2,4-DCP with a desirability of 0.9919 under optimised conditions. Similarly, in the Photo-Fenton process, the software predicted the complete removal of organic pollutant with desirability of 1.00 under optimised conditions. At optimised conditions, the photocatalytic efficiency observed was almost complete (~98%) while 100% degradation was shown in Photo-Fenton's process. The composite desirability for both processes was either unity or closer to unity (Figure 4.21). Furthermore, the observed removal efficiency and the prediction made by RSM closely resembled thus validating the accuracy of the model and proposed RSM-desirability function. Based on the second-order polynomial models (eq 3.3c and 3.3d), 2-D contour plots were generated as shown in Figure 4.22 and Figure 4.23, showcasing the effect of condition operating factors of respective treatment methods towards degradation.

4.10.1 Effect of Photocatalytic variables

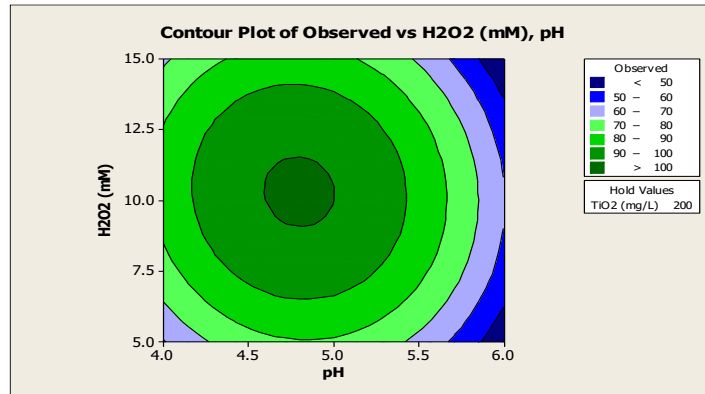
The interactive effect between oxidant concentration and pH can be observed in Figure 4.22(a). Increasing pH doesn't reflect significant degradation at a lower dose of H₂O₂, around 5.0mM. As the concentration increased, degradation efficiency peaked at around 8.0mM to 11.0 mM. It was also observed that pH played a significant role. Around pH 4.0 to 5.0, degradation increased, whereas the removal rate decreased with a further increase in pH (alkaline conditions). At higher pH, the self-decomposition of H₂O₂ reduces the generation of hydroxyl radicals. Lesser presence of H₂O₂ causes more deficient ROS production, thus affecting the degradation rate. It becomes a limiting factor when present in less amount. However, the impact of oxidant concerning catalyst loading was significant (Figure 4.22 (b)). H₂O₂ when present in deficient amounts, reflected a similar degradation rate in the range of 60% to 70% for increasing catalyst load. At the higher dose of H₂O₂ (7.0mM to 12.0mM), the removal efficiency of 2,4-DCP was maximum. An increasing quantity of H₂O₂ and TiO₂ addition had a proportional effect on the removal rate of 2,4-DCP and was risen simultaneously. As the dose of Nano-TiO₂ was in the range of 200-250 mg/L, the rate of 2,4-DCP removal was attained

maximum. However, after a certain amount beyond 200 mg/L, the degradation again declined. This is because of the increased opacity of the solution due to the presence of excess catalyst, which inhibited the effective penetration of UV Light. The photoactivity of Nano-TiO₂ is a function of pH as well (Figure 4.22(c)). Considering the isoelectric point of TiO₂ (discussed in the previous section) and the pK_a value of chlorophenols, the photo-oxidation of chlorophenols was found to be maximum at pH < pH_{pzc} of TiO₂. The removal efficiency was decreased as pH > pH_{pzc}. At optimised loading, electron-hole (e-h) are generated, reacting directly or with surface-bound water, producing hydroxyl radical efficiently.

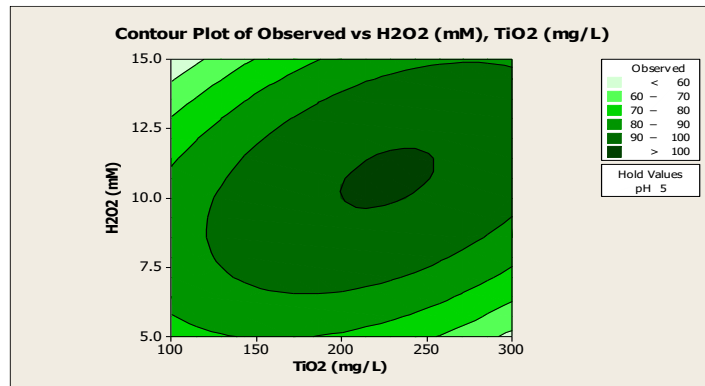
4.10.2 Effect of Photo-Fenton variables

The interactive effect of variables governing the Photo-Fenton process is represented in Figure 4.23. The graph (Figure 4.23(a)) shows that the removal efficiency increased by increasing the concentration of oxidising agent and iron (Fe²⁺). This is attributed to the increased production rate of reactive oxidising species enhancing the removal rate. Around 5.0mM of H₂O₂ and 0.5mM of iron concentration, complete removal of 2,4-DCP was observed. A further increase in the dose of both factors resulted in a reduced removal rate. This is because an excessive amount of iron and H₂O₂ results in the scavenging of hydroxyl radicals. pH plays a significant role in governing the efficacy of the treatment system. It is evident in literature studies that the process contributes to maximum efficiency under acidic conditions. Considering the effect of pH with respect to catalyst concentration (Figure 4.23(b)), increasing pH values and iron dose substantially increased the degradation rate. However, the removal rate declined under alkaline conditions, owing to the relative formation of iron oxo hydroxides and ferric hydroxide precipitate. Lesser availability of ferrous ions results in the mere formation of hydroxyl radicals, hence, lesser degradation. It was observed that the interactive effect of pH and H₂O₂ was insignificant. Degradation suffered drastically at both excessive and deficient dosages of H₂O₂. It can be observed (Figure 4.23(c)) that throughout the range of changing pH conditions, the removal rate at lower H₂O₂ amounts (3mM to 4mM) was 50-70%. As the quantity of H₂O₂

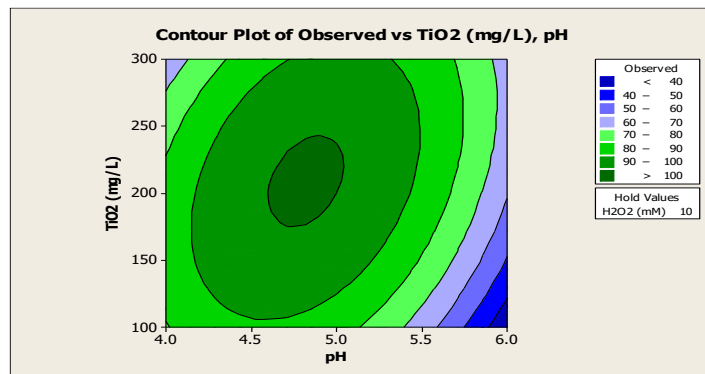
increased, the degradation rate also increased and peaked at around 5.0mM. Further addition resulted in less removal as H₂O₂ curtails the availability of [•]OH radicals. Excess H₂O₂ causes enhanced deactivation of ferrous ions to ferric ions. Also, at higher pH, H₂O₂ is unstablised and undergoes self-decomposition, decreasing the removal efficiency of the system (Ghoneim et al., 2011; Zulfiqar et al., 2019).



(a)

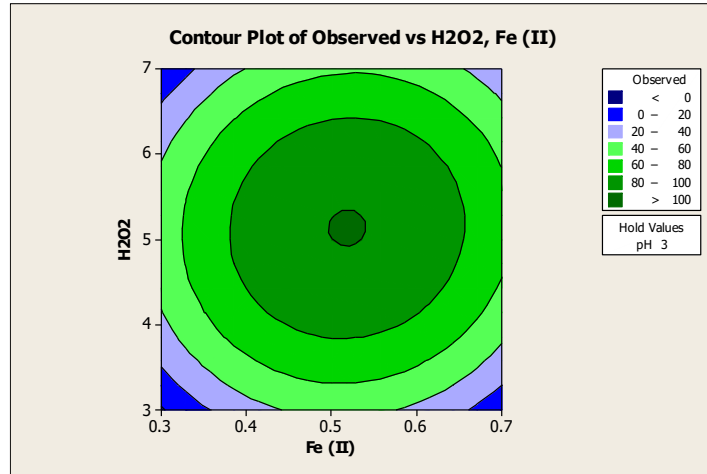


(b)

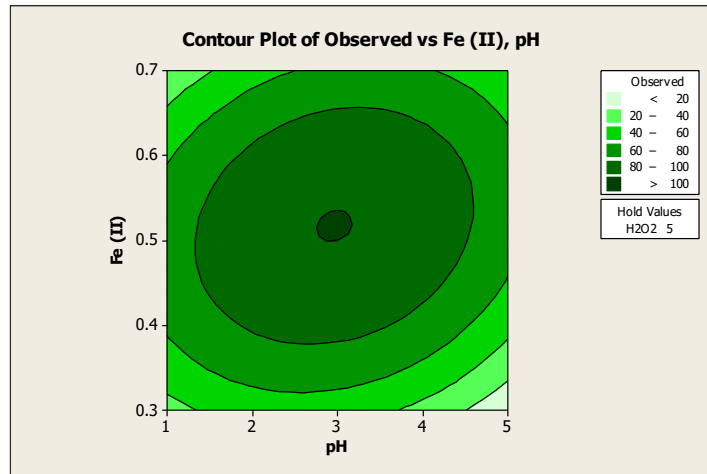


(c)

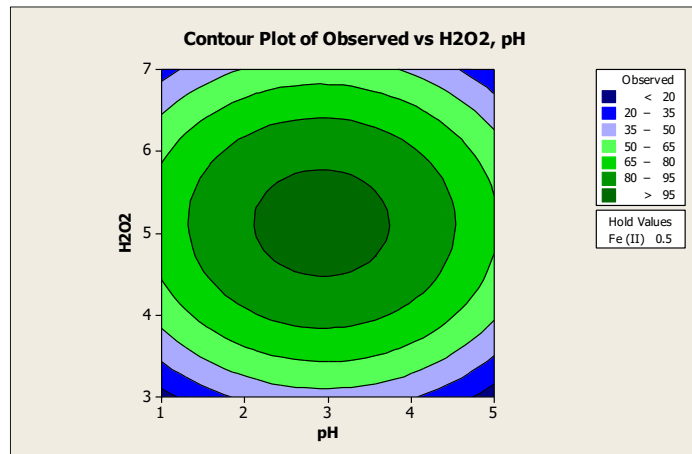
Fig. 4.22 Two-dimensional contour plots showing effect of regulating parameters towards 2,4-DCP degradation in photocatalysis process



(a)



(b)



(c)

Fig. 4.23 Two-dimensional contour plots showing effect of regulating parameters towards 2,4-DCP degradation in Photo-Fenton's process

4.11 Synergistic Effect of Integrated Oxidation Systems

A comparative assessment of different AOPs was studied for degradation of chlorophenolic compound 2,4-DCP (Figure 4.24). The maximum degradation efficiency of respective processes along with their mineralisation percent is illustrated in Table 4.9. Based on optimised conditions obtained for photocatalysis and Photo-Fenton’s treatment processes, different AOPs were coupled to investigate the profound effect on the degradation of refractory organics.

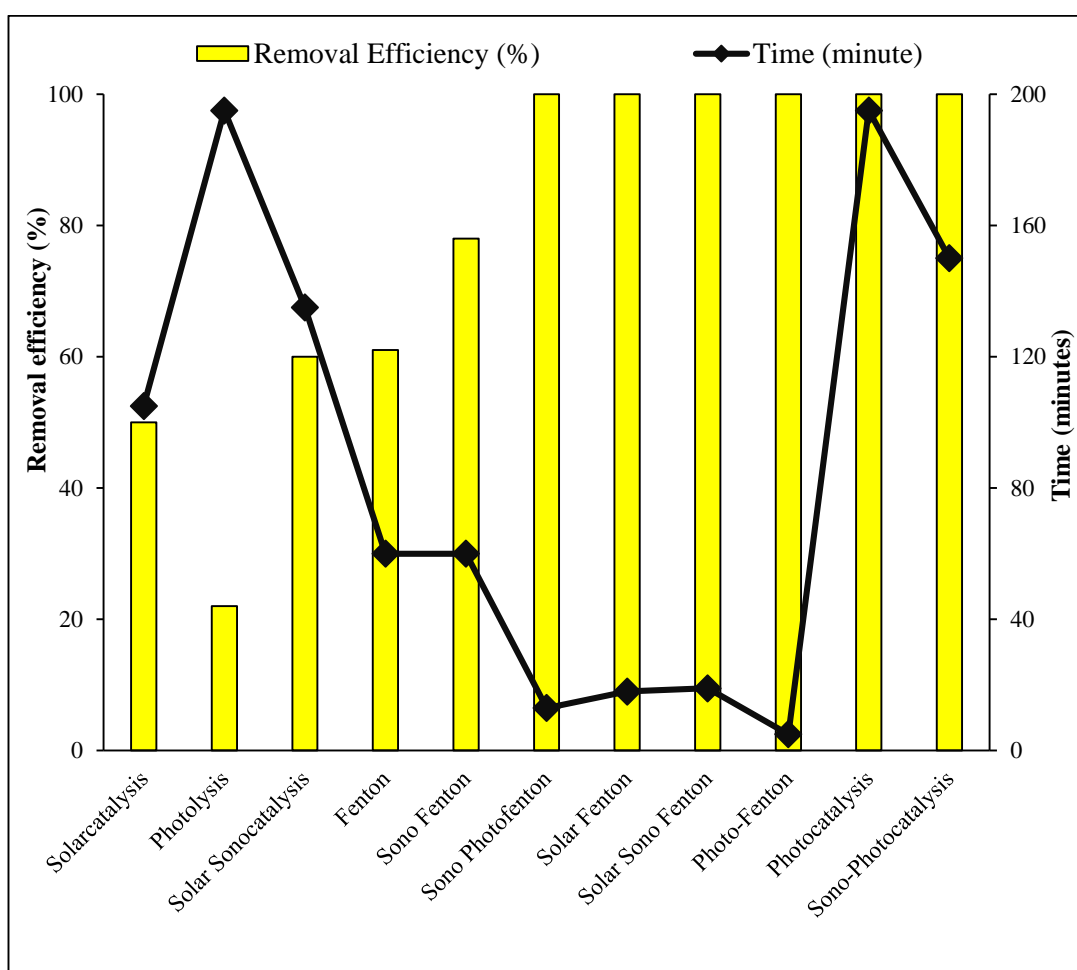


Fig. 4.24 Comparison of different AOPs towards maximum removal of 2,4-DCP

Table 4.9 Comparison of different processes for maximum time taken for degradation of 2,4-DCP

Processes	Conditions	Maximum degradation efficiency (%)	Time for complete/maximum degradation (minutes)	Mineralisation (%)
Solarcatalysis	TiO ₂ : 200 mg/L H ₂ O ₂ : 10.0mM pH: 5.0 Light Source: Solar Intensity: 358.92 W/m ²	50	105	14
Photocatalysis	TiO ₂ : 200 mg/L H ₂ O ₂ : 10.0mM pH: 5.0 Light Source: UV tubes (365nm) Intensity: 672W/m ²	100	210	70
Sono-Photocatalysis	TiO ₂ : 200 mg/L H ₂ O ₂ : 10.0mM pH: 5.0 Light Source: UV tubes (365nm) Intensity: 672W/m ² Ultrasound: 40kHz	100	120	75
Sono-Solarcatalysis	TiO ₂ : 200 mg/L H ₂ O ₂ : 10.0mM pH: 5.0 Light Source: Solar Intensity: 358.92 W/m ² Ultrasound: 40kHz	60	135	36
Fenton	Fe: 0.5mM H ₂ O ₂ : 5.0mM pH: 3.0	61	60	30

Photo-Fenton	Fe: 0.5mM H ₂ O ₂ : 5.0mM pH: 3.0 Light Source: UV tubes (365nm) Intensity: 672W/m ²	100	05	66
Sono-Photo-Fenton	Fe: 0.5mM H ₂ O ₂ : 5.0mM pH: 3.0 Light Source: UV tubes (365nm) Intensity: 672W/m ² Ultrasound Frequency: 40kHz	100	13	72
Sono-Fenton	Fe: 0.5mM H ₂ O ₂ : 5.0mM pH: 3.0 Ultrasound Frequency: 40kHz	78	60	59
Solar-Fenton	Fe: 0.5mM H ₂ O ₂ : 5.0mM pH: 3.0 Light Source: Solar Intensity: 358.92 W/m ²	100	18	88
Solar-Sono-Fenton	Fe: 0.5mM H ₂ O ₂ : 5.0mM pH: 3.0 Light Source: Solar Intensity: 358.92 W/m ² Ultrasound Frequency: 40kHz	100	19	77
Photolysis	Light Source: Solar Intensity: 358.92 W/m ²	20	210	2

4.11.1 Sonication coupled AOPs

The application of ultrasound results in the degradation of organic compounds by generating hydroxyl radicals, and acoustic cavitation bubbles. Ultrasonic power in the sonolytic process generates expansion and compression cycles which form acoustic cavitation (Yadav et al., 2023a). The cavities oscillate in size, following the expansion and compression cycles. Several hundreds of atmosphere pressure and several thousand Kelvin temperatures are achieved with the collapse of the cavitation bubbles (Yadav et al., 2023a). Attributing to the collapse and pressure, organic compounds are degraded either by direct pyrolytic cleavage, or the hydroxyl radicals formed by pyrolysis (Ameta et al., 2018). Coupling of sonication with photocatalytic treatment and Fenton's process resulted in enhanced mineralisation in less time. It was observed that under optimised conditions, Fenton's process was inefficient and only 60% of 2,4-DCP was degraded in an hour with only 30% mineralisation. Coupling of Ultrasound (US) with Fenton, US/ H₂O₂/Fe(II), degradation was around 80% which is 20% more with double mineralisation (60%) as compared to Fenton's process alone. Sonolysis when coupled with Photo-Fenton showed complete degradation in 13 minutes with slightly higher mineralisation (~72%) as compared to Photo-Fenton (66%) alone. Photo-Fenton (UV₃₆₅) alone reported complete degradation within a few minutes (5 minutes) duration because of the direct nucleophilic attack of the [•]OH radicals (Pera-Titus et al., 2004). Although the mineralisation per cent was higher in the case of sonication assisted Photo-Fenton process, the rate was still less than Photo-Fenton (UV) because of the inter-specific competition of Fenton and ultrasound for H₂O₂ for generating [•]OH radicals (Verma and Haritash, 2019).

The drastic change in degradation efficiency rate and mineralisation was observed in the case of the sonication-assisted Photocatalysis treatment system. Ultrasonic power coupled with UV/TiO₂/H₂O₂ system resulted in complete degradation of 2,4-DCP in 120 minutes. Photocatalysis treatment alone took 210 minutes to completely eradicate the phenolic compound. The synergistic effect of US/UV/TiO₂/H₂O₂ reduced the duration of treatment with higher mineralisation

(75%) as compared to 70% mineralisation in the case of photocatalysis alone. The ultrasound irradiation-induced cavitation effect generates heat; facilitates the proper mixing or mass transfer; and promotes the contact between active sites of catalyst with organic impurities (2,4-DCP) and dispersion of contaminated layers of chemicals (Othmer and Overberger, 1982). The physical impact of ultrasound accelerated the reaction by proper mixing of reagents and enhancing the surface area of the catalyst (Anandan et al., 2020). Thus, the synergistic effect of sonication and UV light enhanced the degradation and mineralisation of 2,4-DCP.

4.11.2 Solar driven AOPs

One of the major challenges of AOPs is switching from energy-intensive processes to sustainable and renewable energy sources. Solar-driven AOPs investigated in the present study have reported some promising results. Solar-Fenton reported complete degradation of organic pollutant with 90% TOC reduction. The time taken by Solar-Fenton was 18 minutes which is comparatively four times compared to the Photo-Fenton process. The synergistic effect of Solar-Sono-Fenton was also studied. Although complete removal of 2,4-DCP was observed in 18 minutes, the TOC mineralisation of ~80% was observed. The availability of sufficient high-intensity solar light enhances the degradation rate of 2,4-DCP. Solar coupled Fenton's treatment experiment was conducted in November 2022 on a sunny afternoon between noon to 14:00 hour with an average solar radiation intensity of 358.92 W/m². In photocatalysis, the rate of electron excited from the valence band to the conduction band of the photocatalyst is influenced by the intensity of light affecting the rate of photocatalytic reaction and photocatalyst activation (Ortiz et al., 2019). In Solar driven Nano-TiO₂ induced catalysis, only 50% removal efficiency was attained in 105 minutes whereas solar catalysis when coupled with sonication (Sono-Solar catalysis) reported only a slight increase in removal efficiency (60%) in 135 minutes with TOC reduced by 36% only. In both the above-mentioned oxidation treatment systems, solar light (solar radiation 309.31 W/m²) was found less efficient towards the generation of hydroxyl radicals and degrading 2,4-DCP because of the fractional proportion of

UV in the solar spectrum compared to direct UV light used in photocatalysis effective for photoactivating the photocatalyst (Ortiz et al., 2019). The effect of direct sunlight i.e. photolysis was also studied, however marginal removal (~20%) was observed.

Solar photochemistry plays a vital role in pollution remediation transforming the pollutants into non-toxic compounds. Since no modification in the solar spectrum can take place, solar energy could be channelled to increase the efficiency of treatment systems. The sunlight consists of a wide spectrum of light based on wavelengths ranging from 300 to 2500 nm which includes UV light (<380 nm), visible light (380-780 nm, also referred to as sunlight) and near-infrared (>780 nm), whereas, in the photo process, the exposure of UV light was restricted to a wavelength of 354 nm only. In addition, the solar spectrum is harnessed naturally, thereby offsetting the cost of treatment against UV light. Therefore, the use of solar light is recommended to be a cheaper and more efficient treatment option against UV photocatalysis.

4.12 Economic analysis of different AOPs for degradation of 2,4-DCP

Degussa P25 Nano-TiO₂ was added as a photocatalyst in the photocatalysis experiment and is not consumed in the reaction. Considering the fractional amount of Nano-TiO₂ lost during analysis, sample centrifugation, sample transfer etc, the leftover catalyst was recovered and oven-dried at 105°C. The recovery of Nano-TiO₂ was calculated using the formula given below:

$$TiO_2 \text{ Recovered} = \frac{w_2}{w_1} \times 100 \quad (4.26)$$

Where, w_1 is the initial known weight of Nano-TiO₂ added; w_2 is the residual dried weight of TiO₂ recovered at the end of the experiment. In the present study, under optimized conditions, ~70% of the photocatalyst added was recovered. Thus, the use of optimized TiO₂ reduces the overall cost of the treatment, making the process, both environment and energy-efficient. The economic analysis was

conducted after maximal degradation of 2,4-DCP with respect to photocatalysis, Photo-Fenton, solar-driven oxidation processes and sonication-induced treatment processes and a comparative assessment of treatment cost was done (Table 4.10). In case of photocatalysis treatment, complete removal was achieved in 210 minutes with a 200mg/L dose of catalyst and 10.0mM dose of oxidant. The experiments were conducted in a fabricated UV chamber having 8 UV tubes each with a power rating of 36W making together 288 W; the power rating of the air sparger and magnetic stirrer was 3.5 W and 8.5 W, respectively. Thus, the total power consumption is 300 W or 0.3kWh. The cost of the Degussa P25 Nano-TiO₂ catalyst used is INR 22,680/100g and since only 30% of it was consumed or lost, its cost is INR 13.61/L for treating 100mg/L strength of synthetically prepared wastewater. Considering the consumption of hydrogen peroxide cost INR 1.14/L, the overall operational cost of photocatalysis was INR 17.00 OR USD 0.21. The electricity cost for industrial supply in Delhi, India is INR 8.5 per unit kWh. However, in Photo-Fenton, degradation was attained within a few minutes and since the cost of chemicals especially iron (used as a catalyst) was lesser in comparison, the overall cost of the treatment was much less (INR 0.9) compared to photocatalysis. It was observed that the treatment cost increased in sonication-integrated processes because of the additional power consumed during treatment for sonication with power rating of 100W. Fenton integrated sonication treatment cost was higher because of the increased time of treatment. The operational cost was however, less in the case of sono-photocatalysis because of reduced time compared to UV-Photocatalysis. The cost of treatment was noteworthy in solar energy-driven processes particularly, solar-Fenton and sono-solar-Fenton. Solar energy-assisted sono-photocatalysis was found more energy-efficient compared to photocatalysis. Therefore, considering “sustainability as the need of the hour”, exploiting the solar energy as a renewable and environmentally sustainable sound approach, reducing the dependence on energy-intensive treatment and a pocket-friendly approach.

Table 4.10 Economic analysis of the operating cost of different AOPs used for degradation of 2,4-DCP

Treatment method	Energy (kWh)	Time for treatment (minute)	Rate of energy (per kWh) (INR)	Cost of electricity (INR)	Chemical consumed	Cost of chemical per litre (INR)	Cost of treatment in per litre (INR)	Cost of treatment in per litre (USD)
Photo-Fenton (UV₃₆₅)	0.3	5	8.50	0.21	FeSO ₄ ·7H ₂ O H ₂ O ₂ (30% w/v)	0.08 0.57	0.90	0.01
Photocatalysis (UV₃₆₅)	0.3	210	8.50	2.55	TiO ₂ (P25) H ₂ O ₂ (30% w/v)	13.61* 1.14	17.00	0.21
Fenton	0.01	60	8.50	0.085	FeSO ₄ ·7H ₂ O H ₂ O ₂ (30% w/v)	0.08 0.57	0.70	0.01
Sono-Fenton	0.11	60	8.50	0.935	FeSO ₄ ·7H ₂ O H ₂ O ₂ (30% w/v)	0.08 0.57	1.60	0.02

Sono-Photo-Fenton (UV₃₆₅)	0.4	13	8.50	0.74	FeSO ₄ .7H ₂ O H ₂ O ₂ (30% w/v)	0.08 0.57	1.50	0.02
Sono-Photocatalysis (UV₃₆₅)	0.4	120	8.50	6.8	TiO ₂ (P25) H ₂ O ₂ (30% w/v)	13.61* 1.14	22.00	0.23
Solar –Fenton	0.01	18	8.50	0.03	FeSO ₄ .7H ₂ O H ₂ O ₂ (30% w/v)	0.08 0.57	0.70	0.01
Sono-Solar-Fenton	0.11	19	8.50	0.296	FeSO ₄ .7H ₂ O H ₂ O ₂ (30% w/v)	0.08 0.57	1.00	0.01
Solar-catalysis	0.012	105	8.50	0.179	TiO ₂ (P25) H ₂ O ₂ (30% w/v)	13.61* 1.14	15.00	0.18
Sono-Solar-Catalysis	0.112	60	8.50	0.952	TiO ₂ (P25) H ₂ O ₂ (30% w/v)	13.61* 1.14	16.00	0.19

*30% loss of Nano-TiO₂ is calculated;

4.13 Photocatalytic degradation of 2,4,6-Trichlorophenol

Photocatalytic oxidation of TCP using TiO_2 as a catalyst was found efficient in the removal of the aforementioned pollutant. The study undertook the effect of regulating parameters like catalyst dose, catalyst size, source of light, and presence of oxidizing agent on the removal efficiency of TCP. The pH of the TCP solution was kept neutral since earlier studies have reported optimum degradation of organic impurities using Degussa P-25 TiO_2 at pH 6.8 (Aljuboury et al., 2016).

Effect of Catalyst type

Commercially available analytical grade TiO_2 was analysed and compared against Nano- TiO_2 (Degussa P-25) towards the degradation of 2,4,6-TCP. It was observed that Nano- TiO_2 exhibited greater potential towards the removal of TCP. Nano- TiO_2 reported nearly complete degradation (~97%) of TCP within 210 minutes (3.5 hours) whereas, analytical grade TiO_2 was able to degrade only 75% of model pollutant (TCP) during the same irradiation time (Figure 4.25).

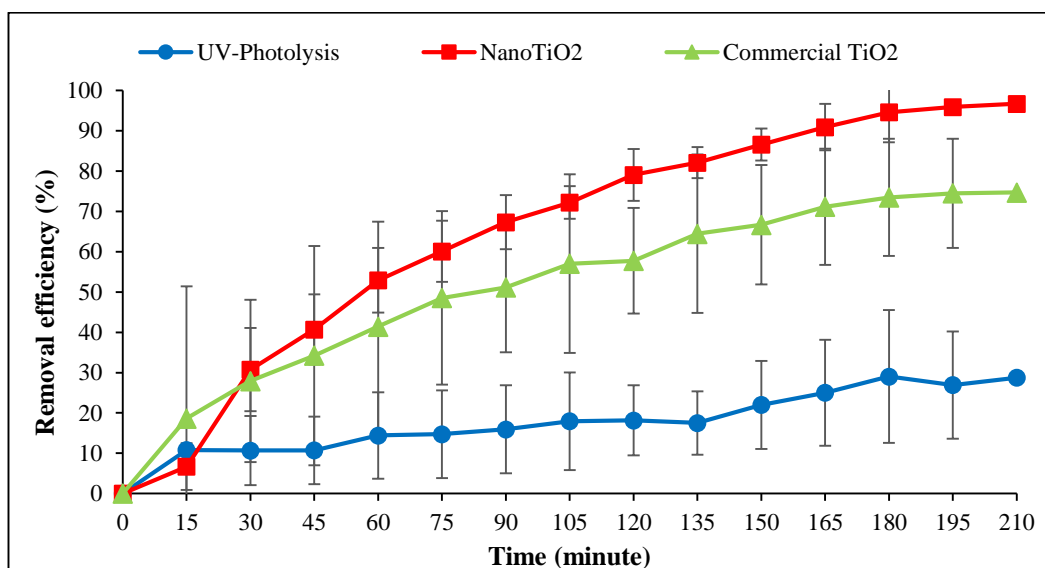


Fig. 4.25 UV₃₆₅ induced degradation of 2,4,6-TCP using Commercial- TiO_2 and Nano- TiO_2

Effectiveness of Nano-TiO₂ is attributed because of increased surface area and absorption of energy as well as increased internal recombination of electrons and holes; and surface-active sites for the removal/ degradation of 2,4,6-TCP (Chen et al., 2020). It was observed that in the absence of photocatalyst, UV₃₆₅ alone removed a significant proportion of TCP (~30%) indicating that photolysis is also playing a role in the removal of TCP. Considering the edge of Nano-TiO₂ over analytical grade TiO₂, further experimentation was conducted using Nano-TiO₂ for degradation of TCP.

Effect of Catalyst Dose and H₂O₂

The photocatalytic oxidation of 2,4,6-TCP (100 mg/L) with different doses of nano-TiO₂ was varied substantially (Figure 4.26). It can be observed from Figure 4.26 that the removal rate increased upon increasing the dose of the photocatalyst. At a dose of 250 mg/L of TiO₂, complete degradation was achieved after 210 minutes of irradiation. However, TiO₂ concentration when increased beyond 250 mg/L, i.e., 275 mg/L, 300 mg/L, 500 mg/L & 750 mg/L, the degradation rate decreased. This can be rationalised concerning the availability of active sites on the surface of TiO₂ and effective penetration of photoactivating light in TCP- TiO₂ suspension. At higher doses of TiO₂, a turbid suspension inhibits the effective penetration of UV₃₆₅ light. Furthermore, a lesser number of photons are absorbed causing fewer generations of hydroxyl radicals to oxidise TCP, thereby affecting the degradation efficiency, as observed in other literature (Pipil , 2022; Verma and Haritash, 2020). The higher degradation efficiency while increasing the dose of TiO₂ is because of the electron-hole pairs generated. The Degussa P-25 Nano-TiO₂ consists of rutile and anatase phases comprising in ratio- 80:20. Anatase TiO₂ exhibits a longer period of electron holes with lower recombination of charge carriers. This causes mass migration of electrons and holes from the interior to the surface of anatase TiO₂. Whereas, the rutile TiO₂ part has a smaller band gap that generates electron-hole pairs when irradiated with low-energy photons making it advantageous for anatase TiO₂ to utilise these electron-hole pairs (Bagbi et al.,

2017). Thus, the synergetic effect of rutile and anatase phases of TiO_2 plays a crucial role in photocatalytic removal/ degradation efficiency of 2,4,6-TCP.

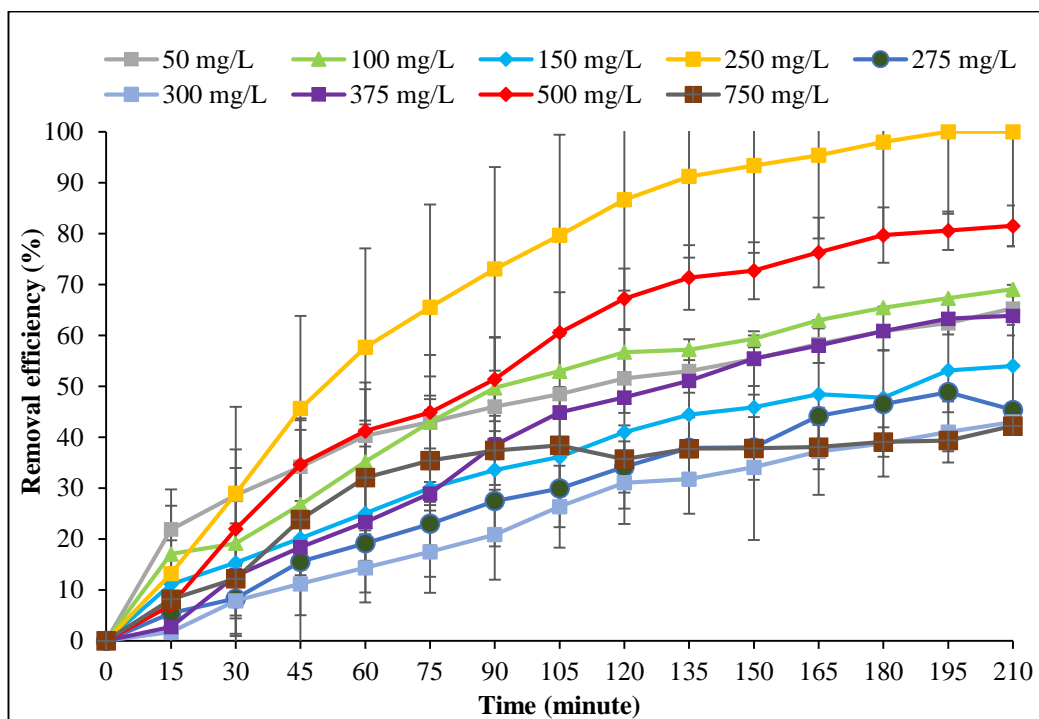


Fig. 4.26 Removal efficiency of 2,4,6-TCP ($C_i=100$ mg/L) at varying catalyst dose

The electron-hole pair generated react either directly with the organic pollutant or with surface-bound water to produce hydroxyl radicals. Increasing the amount of TiO_2 increases the availability of active sites, thus increasing the adsorption process too. Hence, the more the binding of electron-hole pairs with water, the more is the production of the hydroxyl radicals. Earlier studies on photocatalytic degradation of TCP revealed that the time for complete removal of TCP remains extended if optimization for TiO_2 dose is not taken into account. The degradation of TCP ($C_i = 50$ mg/L) at a TiO_2 dose of 500 mg/L reported 100% degradation in 240 minutes (Shoneye and Tang 2020), whereas the present study reports 100% degradation within 210 minutes for an initial concentration of 100 mg/L TCP, but at an optimized TiO_2 dose of 250 mg/L. It may be important to note that optimization resulted in the degradation of two-fold concentrated synthetically prepared wastewater with half the amount of TiO_2 in a relatively short time. This

may favour the treatment of more volume and concentration of effluent efficiently with reduced cost of treatment based on the results of the present study. It is also important to mention that reaction conditions should be optimized to achieve enhanced treatment efficiency. Some studies report lesser reaction time (Rengaraj and Li 2006; Choi et al., 2019) compared to this study but it is because the initial concentration of TCP was significantly less (20-50 mg/L) than the one used (100 mg/L) in the present study. The other reason in few studies is relatively higher doses of TiO₂ being used for photocatalysis (Pandiyani et al., 2002; Choi et al., 2019) which adds to the cost of treatment.

H₂O₂ is a strong oxidizing agent which was added in the experiment to increase the generation of [•]OH radicals and to further enhance the rate of degradation. The effect of the addition of H₂O₂ was studied by varying the concentration at 20mM, 50mM and 100mM at optimised dose of TiO₂ (250 mg/L) for removal of TCP. However, the addition of H₂O₂ did not result in any significant improvement towards the removal of TCP in the present study. The efficacy of photocatalytic degradation in the presence of H₂O₂ was reported less than 80% in 3.5 hours among all the above-mentioned experimental setups.

4.13.1 Mineralisation of TCP

The degradation of TCP was studied using a spectrophotometer in terms of absorbance of residual concentration at regular intervals. To further confirm the mineralization of the organic compound, TOC analysis was done. The degradation profile revealed that approximately 71% of TCP was mineralised based on analysis of TOC. To monitor the feasibility of the formation of any intermediates, HPLC analysis of TCP pre-treatment and post-treated samples was done.

The analysis over HPLC (Retention time (Rt): 6.8 minute) confirmed 99% degradation of TCP but it reported the formation of a few intermediates during the photocatalytic oxidation, thus confirming that there are about 29% TOC leftover in the form of intermediates (Figure 4.27).

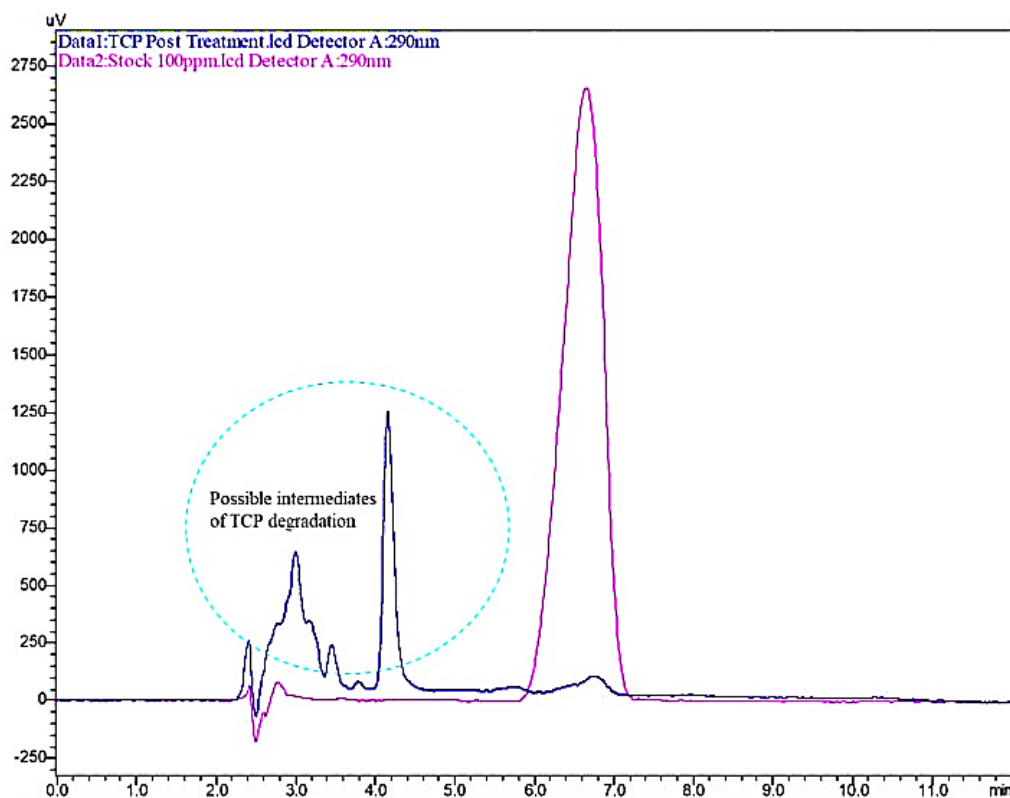


Fig. 4.27 Chromatogram of 2,4,6-TCP before and after degradation depicting intermediate formation

4.14 Photo-Fenton's degradation of 2,4,6-Trichlorophenol

The effect of different parameters was studied by varying the concentration of regulating factors based on the runs given by JMP Design of Experiment (version 16.2) software. Keeping the TCP concentration constant (100 mg/L), the effect of factors like pH, Fe^{2+} and H_2O_2 were examined in the range of 1.0 to 5.0, 0.1mM to 0.5mM, and 10.0mM to 60.0mM, respectively (Table 4.11) for degradation of TCP. Addition of oxidant, H_2O_2 imparted dark brown colour to the reaction mixture having iron and TCP and the solution became turbid within few seconds. As the reaction proceeded, the dark colour starts fading changing to light yellow and colourless at the end indicating completion of the reaction. Under optimum doses of $\text{pH} = 3.0 \pm 0.2$, $\text{Fe}^{2+} = 0.5\text{mM}$ and $\text{H}_2\text{O}_2 = 10.0\text{mM}$, TCP disappeared to non-detectable levels within 6 minutes of the reaction time during Fenton's oxidation process.

Table 4.11 Box Behnken design (BBD) for three independent variables, predicted and observed responses for Photo-Fenton's degradation of 2,4,6-TCP

Run	pH	Fe ²⁺ (mM)	H ₂ O ₂ (mM)	Removal Efficiency (%)	
				Observed	Predicted
1	3	0.3	35	75	75
2	3	0.1	10	25	25
3	3	0.3	35	75	75
4	5	0.5	35	71	78
5	1	0.1	35	18	11
6	3	0.3	35	75	75
7	5	0.3	60	64	57
8	5	0.1	35	11	10
9	3	0.5	60	55	55
10	3	0.5	10	100	92
11	1	0.3	60	20	19
12	1	0.3	10	24	31
13	3	0.1	60	45	53
14	1	0.5	35	12	13
15	5	0.3	10	54	55

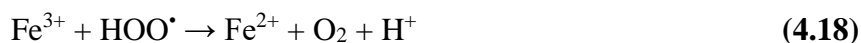
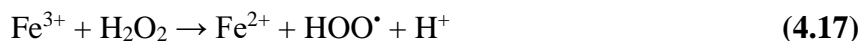
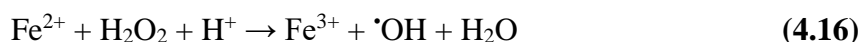
Effect of pH

The pH of solution determines the removal efficiency of organic pollutants in the Photo-Fenton system. It is evident from literature that Fenton's process works efficiently under acidic condition (pH=3) (Verma and Haritash 2019; Sharma et al., 2016). The present study was carried out at pH 1.0, 3.0, and 5.0 in which at pH 3.0, complete (100%) degradation of TCP was observed within 6 to 7 minutes of the reaction time. This is attributed because of the stability of Fe^{2+} and H_2O_2 which is more at pH = 3.0. The results are in strong agreement with observation in the studies carried out by Karci et al., (2012) and Kavitha and Palanivelu (2016). However, at pH 1.0, only 10%-25% of the removal was achieved which took twice the time as taken by the degradation process at pH 3.0. This is due to the formation of complex iron species and oxonium (H_3O_2^+) while H^+ ions scavenge the hydroxyl radicals (Pipil et al., 2022). Additionally, the solubility of Fe (II) is low under acidic pH. Moreover, at pH = 5.0, 60%-70% degradation of TCP was observed and the time taken for degradation was two-fold as compared to degradation at pH 3.0. Under alkaline condition, the solubility of Fe(III)/Fe(II) decreases, and iron precipitate as $\text{Fe}(\text{OH})_3/\text{Fe}(\text{OH})_2$ sludge while H_2O_2 dissociates to form water and oxygen. This results in inactivation and inhibition of further generation of $\cdot\text{OH}$ radicals (Pipil et al., 2022). Also, the electrostatic force of repulsion between 2,4,6-TCP and catalyst surface (Fe acts as catalyst in Fenton's process) dominates under alkaline conditions reducing the dissociation of CPs (Kantar et al., 2019). Furthermore, the dissociation constant (pK_a) for CPs is in the range from 4.7 for PCP to 9.41 for 4-CP and 6.23 for 2,4,6-TCP, suggest the ionization of polychlorophenols to begin at lower pH. Thus, in the present study, complete degradation of TCP was observed at optimum pH of 3.0.

Effect of Fe^{2+} dose

Fe^{2+} is a significant factor determining the removal rate of the recalcitrant pollutants in the Fenton's treatment (Pipil et al., 2022). In the present study, experiments were performed with iron concentrations of 0.1mM, 0.3mM and

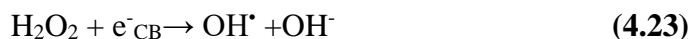
0.5mM. It was observed that at iron concentration 0.5mM and acidic conditions (pH=3.0) with oxidant concentration 10.0mM, rapid and complete degradation (100%) of TCP took place in 6 minutes. However, at lower concentration of Fe²⁺ 0.1mM and 0.3mM, the maximum degradation observed was 45% (oxidant dose=60.0mM) and 75% (oxidant dose=35.0mM), respectively, in 6 minutes. Redox recycling process of Fe²⁺/Fe³⁺ takes place in the bulk solution generating reactive oxidative species (eq. 4.16), while some ferrous ion species are generated through reaction (4.17) and (4.18).



Similar results were observed by Kavitha and Palanivelu (2004; 2016) with iron concentration of 0.4mM and 0.8mM towards degradation of phenol and TCP, respectively. The $\cdot\text{OH}$ radicals generated from the reaction between iron and H₂O₂, attack the π system of the aromatic phenolic ring accelerating the oxidation of TCP (Kavitha and Palanivelu 2004). The residual concentration of total dissolved iron and ferrous ions determined at the end of the experiment reported complete consumption of ferrous ions whereas total dissolved iron concentration measured was 0.03mM.

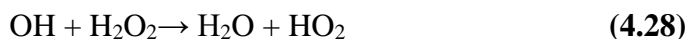
Effect of H₂O₂ Concentration

The effect of H₂O₂ was studied at concentration of 10.0mM, 35.0mM, and 60.0mM. Maximum removal efficiency (100%) of TCP was observed with H₂O₂ dose of 10.0mM (pH=3.0; Fe²⁺=0.5mM) within 6 minutes of treatment time. On increasing the H₂O₂ concentration, no significant improvement towards the degradation of TCP was observed. At maximum concentration of oxidant i.e. 60.0mM, only 55% degradation of TCP was achieved in 7 to 8 minutes of reaction time. Peroxide acts as electron acceptor and inhibits the recombination of electron-hole thus facilitates the generation of $\cdot\text{OH}$ radicals (eq. 4.23)



where e^-_{CB} refers to the presence of electrons in the conduction band

H_2O_2 when present in excess amount acts as scavenger and self-destruction of peroxide occurs (eq. 4.25). The hydroperoxyl radicals are produced from reaction between OH^\cdot radicals and excess peroxide (eq. 4.26). The reduction potential of these hydroperoxyl radicals (1.0V) is less than that of hydroxyl radicals (2.8V) thus is the most probable reason for decrease in the degradation rate with increase in H_2O_2 concentration above the optimised value.



The results of the present study are in agreement with Karci et al., (2012) where under the same optimised dose of H_2O_2 , the degradation of 2,4-DCP took 8 minutes for complete degradation. The residual concentration of H_2O_2 calculated using equation 3.3 at the end of the experiment was 2.5mM indicating that only 7.5mM of H_2O_2 was consumed during the complete oxidation of TCP. Literature has also reported that concentration of $\text{H}_2\text{O}_2 > 15.0\text{mM}$ results in reduction in degradation of chlorophenolic compound in parallel with the scavenging effect of H_2O_2 on OH^\cdot radical (Gan et al., 2018).

4.15 Optimization of TCP-degradation

An interactive relationship between process variables and studied response for degradation of TCP was assessed and response surface plots were drawn (Figure 4.28). The pH had a pronounced effect in governing the degradation of TCP. It played a determining role in controlling the dominant iron species, the activity of oxidant, and its stability. As seen in Figure 4.28(a) and 4.28(b), with increase in pH values, the removal efficiency also improved and was maximum between 3.0 and

4.0 whereas at pH 5.0 the removal efficiency started decreasing. At higher pH levels, iron precipitates as hydroxide and H₂O₂ undergoes self-decomposition (Verma and Haritash 2019). The degradation of TCP was enhanced with increase in the dose of iron and was maximum at 0.5mM with pH= 3.0 and H₂O₂ dose of 10.0mM (Figure 4.28(a)). Positive impact of addition of oxidant on degradation of TCP can be seen in Figure 4.28(b). The effect of variables, Fe and H₂O₂ at pH 3.0 revealed that complete degradation of TCP took place with iron dose of 0.5mM and H₂O₂ concentration of 10.0 mM (Figure 4.28(c)).

On the basis of model prediction and interaction of variable parameters, the optimized values for variable factors were deduced (Figure 4.29). Based on the BBD, the optimized values were found to be 3.8 for pH, 0.53mM for Fe²⁺ and 10.14mM for H₂O₂. The results represent an insight of the effects of parameters towards degradation of 2,4,6-TCP.

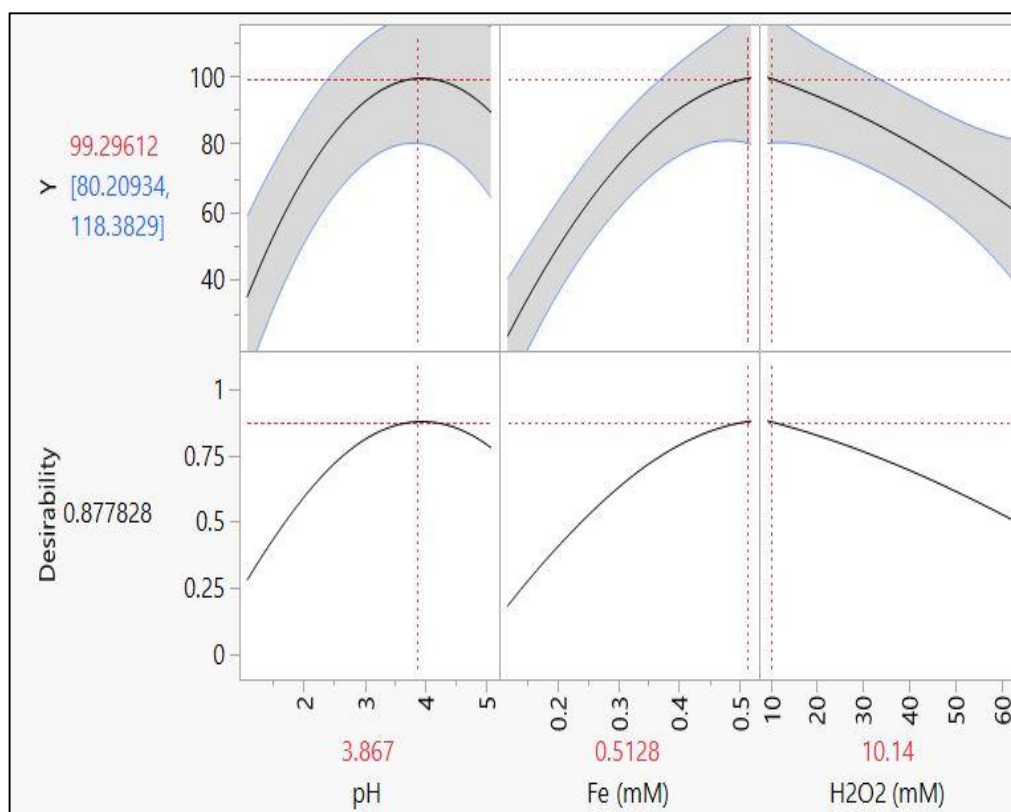
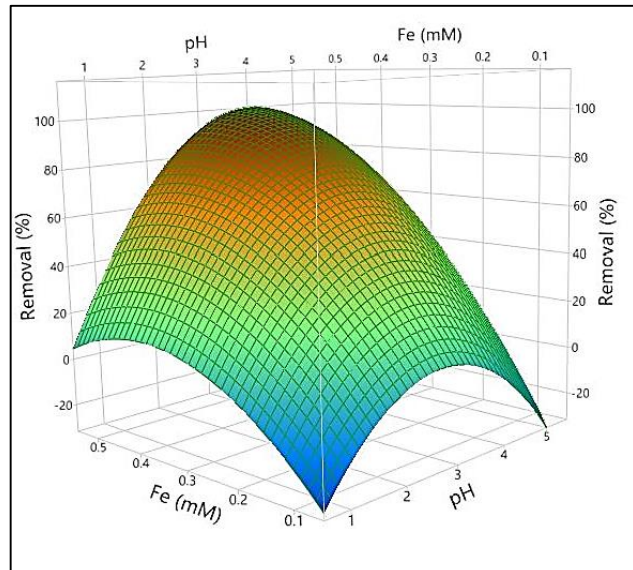
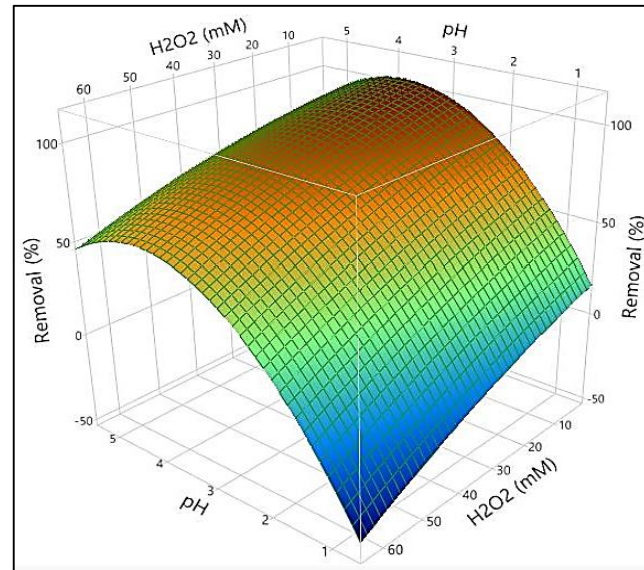


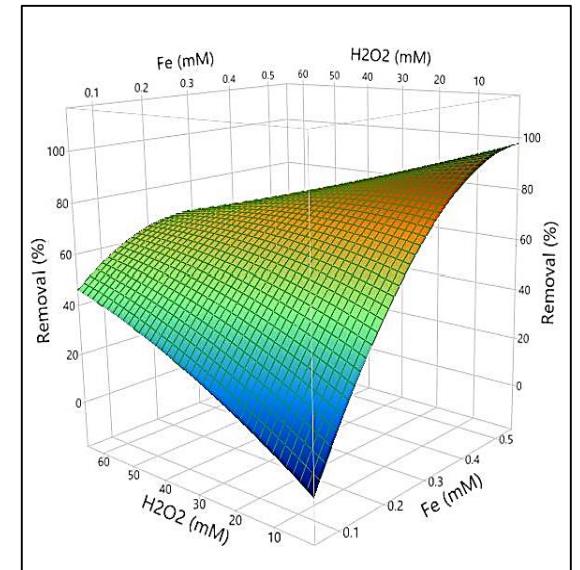
Fig. 4.29 Optimization of regulating parameters for degradation of 2,4,6-TCP by Photo-Fenton (UV₃₆₅) treatment



(a)



(b)



(c)

Fig. 4.28 Response Surface Plot of (a) Fe²⁺ and pH (b) pH and H₂O₂ (c) Fe²⁺ and H₂O₂ as regulating parameters in Photo-Fenton's degradation of 2,4,6-TCP

4.16 Regression model and Analysis of Variance

Analysis of the observed response (degradation of TCP) as given in Table 4.11, is represented by quadratic regression model using eq. 4.32 shown below in the coded factors:

$$Y = 75 + 15.75X_1 + 17.375X_2 - 2.375X_3 - 31.375X_1^2 - 15.625X_2^2 - 3.125X_3^2 + 16.50X_1X_2 - 3.5X_1X_3 + 3.50X_2X_3 \quad (4.32)$$

To determine the goodness of the fit of the above equation, analysis of variance (ANOVA) of the experimental data was done, and the results are summarized in Table 4.12. F-value for the model suggest that it is significant for the value 20.18 with corresponding *p*-value of regression being 0.002. The correlation coefficient (R^2) between Observed response and Predicted response was 0.9732 whereas the corresponding adjusted R^2 value obtained was 0.9250. The values of R^2 and adjusted R^2 ensured the quadratic model a good fit with respect to the experimental response. The comparative plots of the observed value and predicted value for removal of TCP indicated significant agreement between the actual response against the response of model (Figure 4.30).

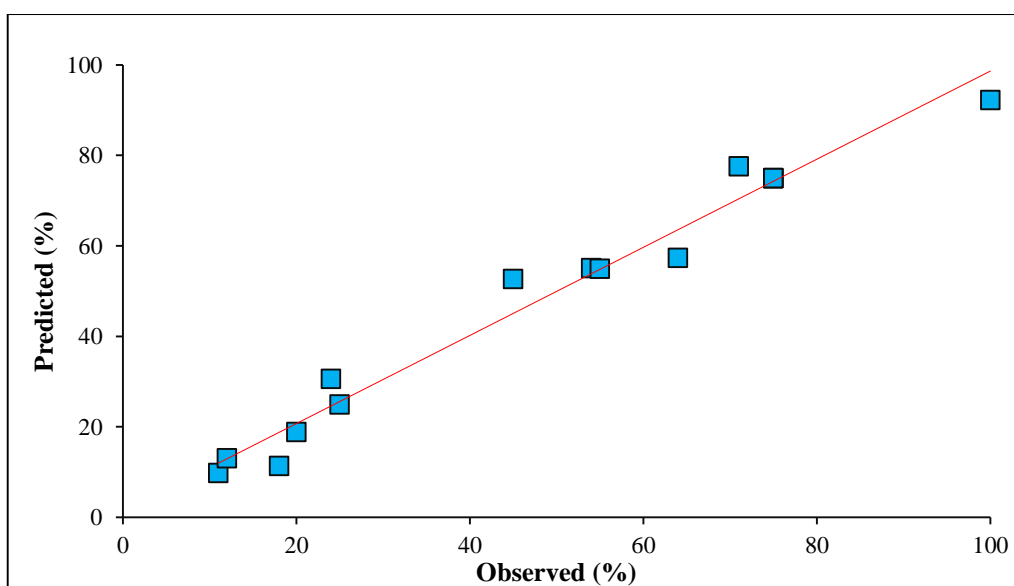


Fig. 4.30 Normal Plot of Observed degradation (%) of 2,4,6-TCP against the Predicted value

The significance of each independent variable was examined as per the p -value (p -value < 0.05 implies the term significant and vice-verse). In the midst of test variables, the pH value (X_1) and Fe(II) (X_2) had significant effect on the degradation of 2,4,6-TCP. The quadratic effect coefficients of pH value (X_1^2) was highly significant whereas coefficient of quadratic effect of Fe^{2+} (X_2^2), and interaction effect of pH and Fe^{2+} (X_1X_2), as well as Fe^{2+} and H_2O_2 (X_2X_3) were slight significant model terms while the rest other factors were statistically insignificant.

Table 4.12 Analysis of Variance (ANOVA) for percentage degradation of 2,4,6-TCP by Photo-Fenton treatment

Source	Degree of freedom	Sum of squares	Mean square	F-ratio	P
Regression	9	10922.2	1213.58	20.18	0.002
pH	1	1984.5	1780.37	29.6	0.002
Fe	1	2415.1	1071.94	17.82	0.001
H_2O_2	1	45.1	192.76	3.2	0.426
pH*pH	1	3634.67	3634.67	60.43	0.0006
Fe*Fe	1	901.44	901.44	14.99	0.012
$H_2O_2^* H_2O_2$	1	36.1	36.1	0.6	0.476
pH*Fe	1	2194.2	2194.2	12.16	0.008
pH* H_2O_2	1	1089	1089	18.1	0.408
Fe* H_2O_2	1	49	49	0.81	0.008
Residual Error	1	1056.3	1056.25	17.56	0.009
Lack-of-Fit	3	300.7	100.25	-	-
Pure Error	2	00	00	*	*
Cor Total	14	11222.9	-	0.002	-

R -squared = 0.9732; Adj. R -squared = 0.925

4.17 Integrated treatment processes for enhanced degradation of 2,4,6-TCP

A comparative study using different AOPs like UV Photocatalysis, solar-catalysis, Fenton's process, solar-Fenton, sonication, sonolysis coupled with Fenton, and Sono-Photo-Fenton was conducted (Figure 4.31).

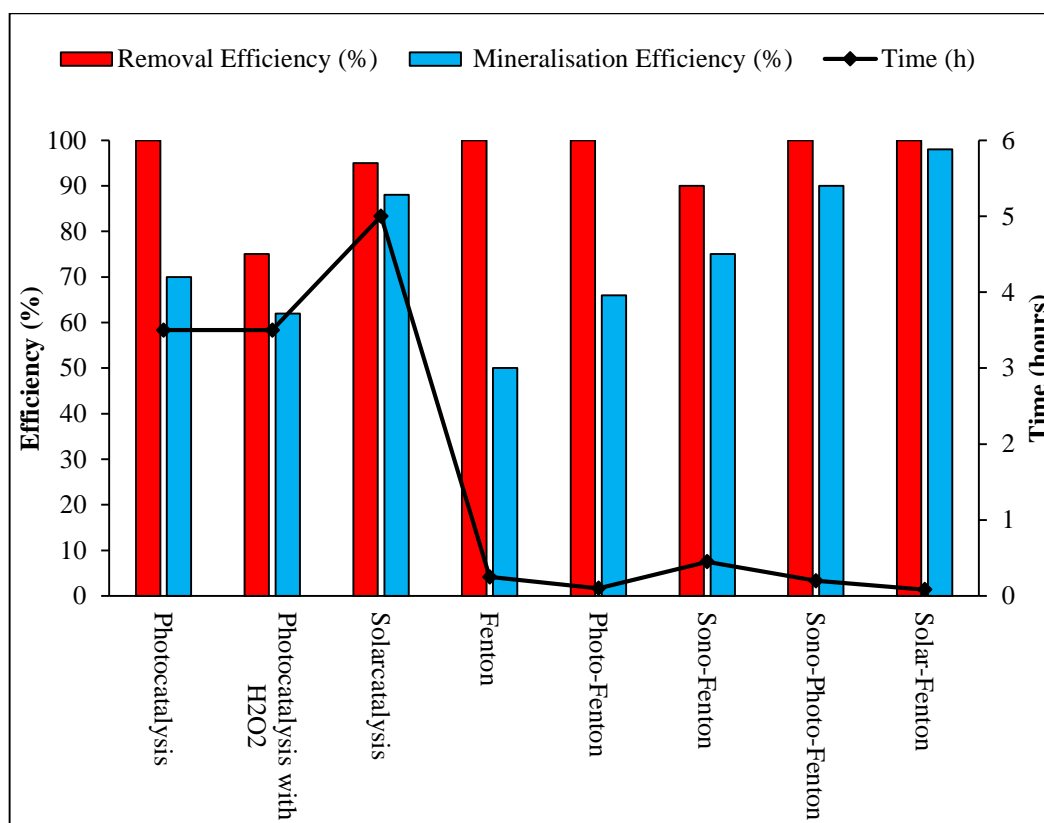


Fig. 4.31 Comparison of different ultrasound and light (UV and solar) integrated AOPs for degradation of 2,4,6-TCP

4.17.1 Solar-induced photocatalysis

The enormity of solar energy consumption is almost four times the total solar energy irradiating the surface of the earth (Balzani et al., 2019). As no alteration can take place in the solar spectrum, the solar energy could be exploited and harnessed to increase the efficiency of treatment system. Although the proportion of UV light is 3% to 5% in natural sunlight, the degradation profile of TCP under natural sunlight (Solar-catalysis) using Nano-TiO₂ at concentration 250

mg/L was also investigated. It was observed that 95% degradation efficiency was attained in 300 minutes (5.0 hours) of sunlight exposure (Figure 4.32).

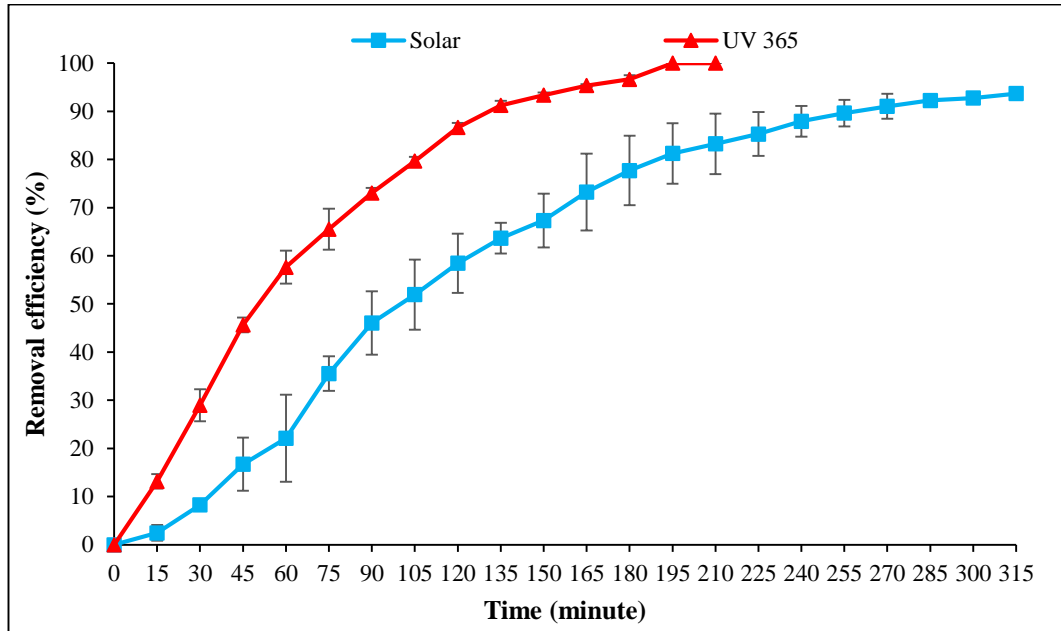


Fig. 4.32 Removal efficiency of 2,4,6-TCP under solar and UV light as a function of time

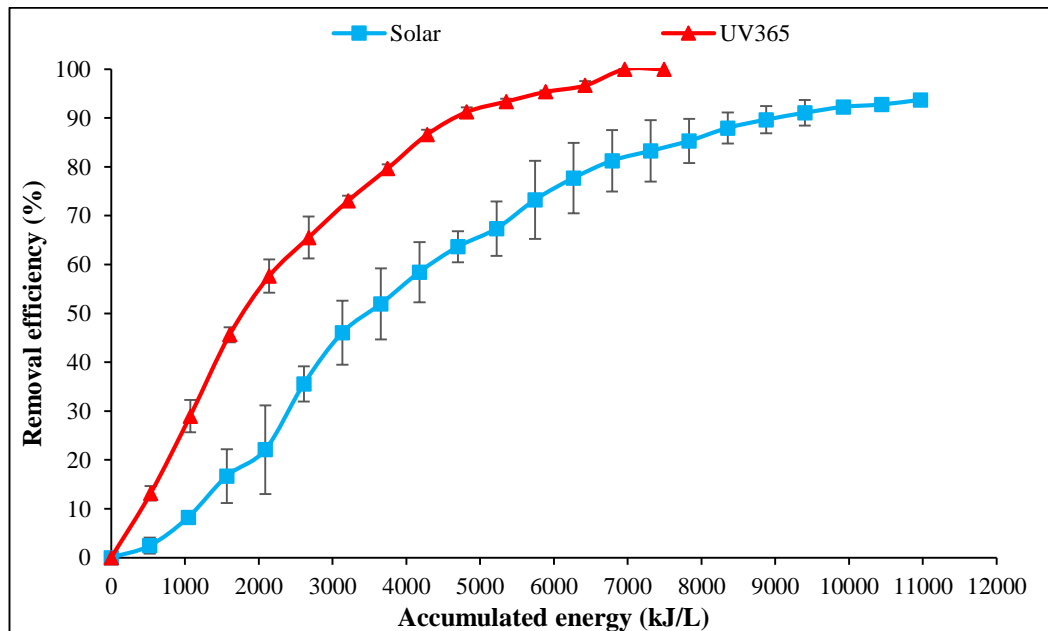


Fig. 4.33 Removal efficiency of 2,4,6-TCP under solar and UV light as a function of accumulated energy

It was also noted that with the increase in the solar intensity, the rate of degradation also increased. The average solar influx radiation intensity was 655.5 W/m^2 with accumulated energy of 522.2 kJ/L . Figure 4.33 represents the degradation profile of 2,4,6-TCP as a function of accumulated energy for every 15 minutes. It has been reported that the rate of electron excited from the valence band to the conduction band is influenced by the intensity of light affecting the rate of photocatalytic reaction and photocatalyst activation. Thus, higher intensity is directly proportional to photocatalytic oxidation (Yadav et al., 2023). However, the rate of photocatalysis is no longer affected by the intensity of light beyond the optimum level because of the limited availability of active sites on the surface of the photocatalyst (Blake et al., 1991). Based on the results of the present study, it is seen that photo exposure and catalyst (based on size) can significantly regulate the removal efficiency of TCP during photocatalysis.

4.17.2 Fenton-integrated process

The experiments were performed at optimised conditions obtained in photo-Fenton process i.e., Fe^{2+} 0.5mM , pH 3.0 and H_2O_2 10.0mM . The experiments involving sonication-integrated processes were conducted at operating frequency of 40kHz . Among all the processes, solar-Fenton was found to be most efficient, resulting in complete degradation of 2,4,6-TCP within 5 minutes of the reaction time. Availability of sufficient high intensity solar light resulted in a faster and complete degradation with 98% mineralisation of the model pollutant. It could also be reasoned from the fact that the average annual sunshine hours of India are 2780 hours with land area receiving 4 to 7KWh/m^2 of the solar energy (Solar Energy, 2022). The solar-Fenton experiments were conducted in presence of sunlight on a hot sunny day with temperature ranged between 43°C to 46°C . Early, quick and complete degradation of 2,4,6-TCP was observed in presence of solar light (Solar-Fenton) in comparison to Photo-Fenton (UV_{365}). In case of Photo-Fenton (UV_{365}), complete removal efficiency was attained within 6 minutes of the reaction duration because of the direct nucleophilic attack of the HO^\bullet radicals.

These reactive oxidation species attack the phenolic ring at the carbon not occupied with chlorine and abstract the π electron cloud over benzene ring causing mineralisation. However, the process resulted in only 50% mineralisation indicating the formation of intermediates. Presence of chlorine atoms at ortho and para position results in steric hindrance and lower mineralisation (Saritha et al., 2009). The HPLC analysis also confirmed the conversion of phenolic compound to intermediates (Figure 4.34).

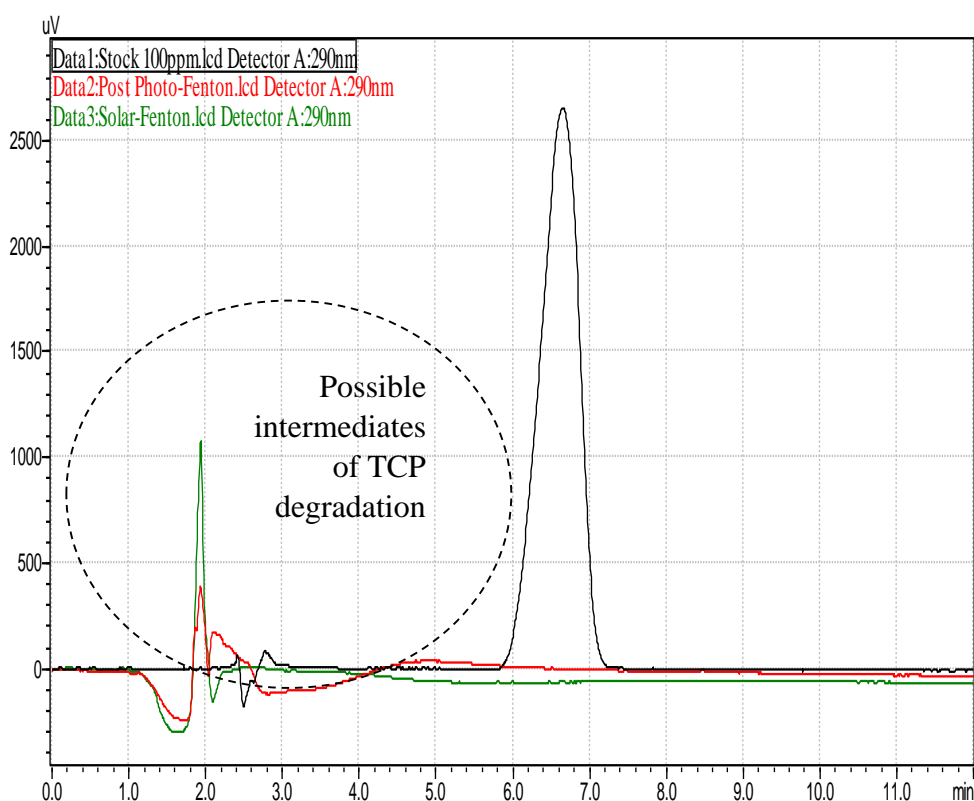


Fig. 4.34 The HPLC spectra of untreated 2,4,6-TCP ($C_i = 100$ mg/L), Photo-Fenton (UV₃₆₅) and Solar-Fenton treated TCP-containing wastewater confirming mineralisation

Table 4.13 Comparison of different processes for maximum time taken for degradation of 2,4,6-TCP

Processes	Conditions	Maximum degradation efficiency (%)	Time for complete/ maximum degradation (minutes)	Mineralisation (%)
Photocatalysis	TiO ₂ : 200 mg/L H ₂ O ₂ : 10.0mM pH: 5.0 Light Source: UV tubes (365nm) Intensity: 672W/m ²	100	210	70
UV-Photocatalysis with H ₂ O ₂	TiO ₂ : 200 mg/L pH: 5.0 Light Source: UV tubes (365nm) Intensity: 672W/m ²	75	210	62
Solarcatalysis	TiO ₂ : 200 mg/L H ₂ O ₂ : 10.0mM pH: 5.0 Light Source: Solar Intensity: 655 W/m ²	95	300	88
Sono-Photo-Fenton	Fe: 0.5mM H ₂ O ₂ : 5.0mM pH: 3.0 Light Source: UV tubes (365nm) Intensity:672W/m ² Ultrasound Frequency: 40kHz	100	12	90

Photo-Fenton	Fe: 0.5mM H ₂ O ₂ : 5.0mM pH: 3.0 Light Source: UV tubes (365nm) Intensity:672W/m ²	100	06	66
Fenton	Fe: 0.5mM H ₂ O ₂ : 5.0mM pH: 3.0	100	15	50
Sono-Fenton	Fe: 0.5mM H ₂ O ₂ : 5.0mM pH: 3.0 Ultrasound Frequency: 40kHz	90	27	75
Solar-Fenton	Fe: 0.5mM H ₂ O ₂ : 5.0mM pH: 3.0 Light Source: Solar Intensity: 655 W/m ²	100	05	98

When Fenton's process was used, though complete degradation was there, the system took 15 minutes, twice the time taken by Photo-Fenton process. The process reported 50% mineralisation while similar observation has also been reported by Saritha et al (2009). Fenton's process when coupled with sonication resulted in 90% of degradation attained in 27 minutes of the reaction time. The slower rate of degradation is because both the processes compete for H₂O₂ for generating HO[•] radicals. Sonolysis coupled with Photo-Fenton demonstrated complete degradation within 15 minutes with higher mineralisation (75%) as compared to Photo-Fenton alone. The transmission of ultrasound waves through the aqueous solution generates acoustic cavitation with production of highly reactive radicals (Anandan et al., 2020). The ultrasound irradiation induced cavitation effect generates heat, facilitates the proper mixing or mass transfer, promotes the contact between materials and dispersion of contaminated layers of chemicals (Othmer et al., 1983). The physical impact of ultrasound accelerated the reaction by proper mixing of reagents and enhancing the surface area of the catalyst (Anandan et al., 2020). Thus, the synergistic effect of sonication and UV light enhanced the degradation and mineralisation of 2,4,6-TCP. Table 4.13 reflects the summary of all the processes employed, conditions and time taken towards maximum degradation.

4.18 Economic analysis of different AOPs for degradation of 2,4,6-TCP

Anticipating the wastewater treatment and economic analysis, it becomes imperative to review not only the efficiency of treatment methods but also their financial status, thus emphasizing the crucial aspects of environmental sustainability, energy-efficiency and cost-effectiveness. Since TiO₂ was added as a catalyst in the experiment and is not consumed in the reaction. However, some fraction of TiO₂ was lost during analysis, sample centrifugation, sample transfer etc. At the end of the reaction process, the leftover TiO₂ was recovered and oven-dried at 105°C. The recovery of TiO₂ was calculated using the formula given below:

$$TiO_2 \text{ Recovered} = \frac{w_2}{w_1} \times 100 \quad (4.26)$$

Where w₁ is the initial known weight of TiO₂ added; w₂ is the residual dried weight of recovered TiO₂. In the present study, ~80% of the TiO₂ added in the experiment was recovered under optimized conditions. Thus, the use of optimized TiO₂ reduces the overall cost of the treatment, making the process environment and energy-efficient.

Table 4.14 Economic analysis of the operating cost of different AOPs used for degradation of 2,4,6-TCP

Treatment method	Energy per hour (kWh)	Time for treatment (h)	Rate of energy (per KWh) (INR)	Cost of electricity (INR)	Chemical consumed	Cost of chemical per litre (INR)	Cost of treatment in per litre (INR)	Cost of treatment in per litre (USD)
Photocatalysis (UV ₃₆₅)	1.05	3.5	8.50	8.93	TiO ₂ (P25)	11.34*	20.27	0.243
UV-Photocatalysis with H ₂ O ₂	1.05	3.5	8.50	8.93	TiO ₂ (P25) H ₂ O ₂ (30% w/v)	13.48*	22.55	0.270
Solar-catalysis	0.06	5	8.50	0.51	TiO ₂ (P25)	11.34*	11.85	0.142
Fenton	0.00225	0.25	8.50	0.02	FeSO ₄ .7H ₂ O H ₂ O ₂ (30% w/v)	0.08 1.14	1.24	0.015
Photo-Fenton (UV ₃₆₅)	0.0297	0.1	8.50	0.25	FeSO ₄ .7H ₂ O H ₂ O ₂ (30% w/v)	0.08 1.14	1.47	0.018
Sono-Fenton	0.04905	0.45	8.50	0.42	FeSO ₄ .7H ₂ O H ₂ O ₂ (30% w/v)	0.08 1.14	1.64	0.020
Sono-Photo-Fenton (UV ₃₆₅)	0.0794	0.2	8.50	0.67	FeSO ₄ .7H ₂ O H ₂ O ₂ (30% w/v)	0.08 1.14	1.89	0.023
Solar –Fenton	0.00075	0.083333	8.50	0.01	FeSO ₄ .7H ₂ O H ₂ O ₂ (30% w/v)	0.08 1.14	1.23	0.015

*20% loss of Nano-TiO₂ is calculated;

The economic analysis was conducted after maximal degradation of TCP with respect to photocatalysis, solar-photocatalysis and photocatalysis with H₂O₂ and a comparative analysis of operational cost was calculated (Table 4.14). Photocatalysis was carried out in a fabricated UV chamber having 8 UV tubes each having a power rating of 36W making together 288 W; also power rating of the magnetic stirrer and air sparger is 8.5 W and 3.5 W, respectively. Therefore, the overall power consumption is 300 W or 0.3KWh. In the case of solar-photocatalysis, only magnetic stirrer and air sparger were used, thus making power consumption of 12 W or 0.012 kWh. The electricity cost for industrial supply in Delhi, India is INR 8.5 per unit KWh. The complete degradation efficiency of TCP under the UV/ TiO₂ system was observed in 210 minutes with a photocatalyst dose of 250 mg/L. The cost of Nano-size TiO₂ (P25) is INR 22,680 per 100g but only 20% of it was consumed while 80% is recovered. Therefore, the cost of the photocatalyst is INR 11.34 per litre for treatment of synthetically prepared wastewater (TiO₂ 250 mg/L) in UV/TiO₂; UV/H₂O₂/TiO₂ and Solar/TiO₂ system. Thus, the overall operational cost of the UV/TiO₂ treatment process was INR 20.27 or US \$ 0.24. In the case of UV/H₂O₂/TiO₂, the additional cost of oxidant chemicals occurred making together the cost of treatment per litre US\$ 0.27. However, a considerable cost of the treatment was saved in the case of solar-photocatalysis (US \$ 0.142 per litre). Nevertheless, in Photo-Fenton, degradation was achieved within minutes, and due to the relatively lower cost of chemicals, the overall operational cost was significantly lower (INR 0.018) compared to photocatalysis. It was observed that in sonication-integrated processes (Sono-Fenton and Sono-Photo-Fenton), the treatment costs increased because of the additional power consumption (100W) during treatment and prolonged reaction time. The operational cost was lower and similarly, in the case of Fenton's process, since no input of energy was required, although reaction time was more as compared to Solar-Fenton and UV-Fenton's process. Since Solar-Fenton took least time with almost complete mineralisation, harnessing the solar energy presents a renewable and environmentally sustainable approach, reducing reliance on energy-intensive treatments and proffering a cost-effective solution.

4.19 Photocatalytic degradation of Mixed-Chlorophenols (Mi-CPs)

Photocatalytic oxidation of Mi-CPs using Nano-TiO₂ Photocatalyst (NPC) was found effective in eliminating the Mi-CPs from synthetically prepared wastewater. The study emphasized the effect of process conditioning parameters like NPC dose, pH, and oxidizing agent H₂O₂ for degradation of Mi-CPs based on the optimised conditions obtained for different chlorophenols. The optimised conditions obtained for Set-A: 4-CP (pH 4.0, TiO₂ 0.15g/L and H₂O₂ 10.0mM); Set-B: 2,4-DCP (pH 5.0, TiO₂ 0.2g/L and H₂O₂ 10.0mM) and for Set-C: 2,4,6-TCP (pH 6.0, TiO₂ 0.25g/L and H₂O₂ 10.0mM) (Figure 4.35).

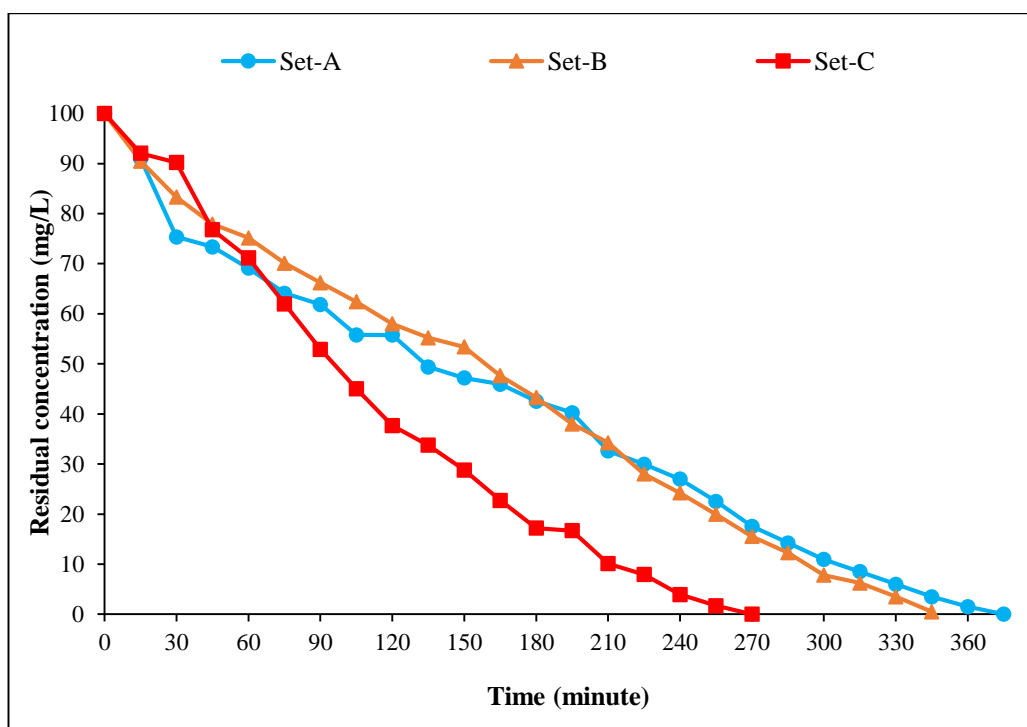


Fig. 4.35 Effect of process conditioning parameters for photocatalytic degradation of Mi-CPs

The sample suspension of 100mg/L Mi-CPs was initially kept in dark for 30 minutes followed by UV irradiation. An initial dark phase was employed to attain adsorption/desorption equilibrium of chlorophenols with the photocatalyst (NPC). It was observed that complete removal occurred in all the experimental runs, however, Set-C was found more efficient and rapid.

4.20 Photo-Fenton's degradation of Mi-CPs

Degradation of mixture of CPs are studied using Photo-Fenton's process. Considering the optimised conditions obtained in the case 4-CP (pH 3.0, Fe^{2+} 0.7mM and H_2O_2 10.0mM); for 2,4-DCP (pH 3.0, Fe^{2+} 0.5mM and H_2O_2 5.0mM) and 2,4,6-TCP (pH 3.0, Fe^{2+} 0.5mM, and H_2O_2 10.0mM), Mi-CPs solution was subjected to degradation at pH 3.0, Fe^{2+} 0.5mM, and H_2O_2 10.0mM (Figure 4.36). Addition of H_2O_2 imparted a dark brown colour to the reaction mixture and the solution became turbid within a few seconds. As the reaction proceeded, the colour started fading changing from dark brown to light yellow and colourless, indicating completion of the reaction and the CPs was non-detectable within 12 minutes of the reaction time.

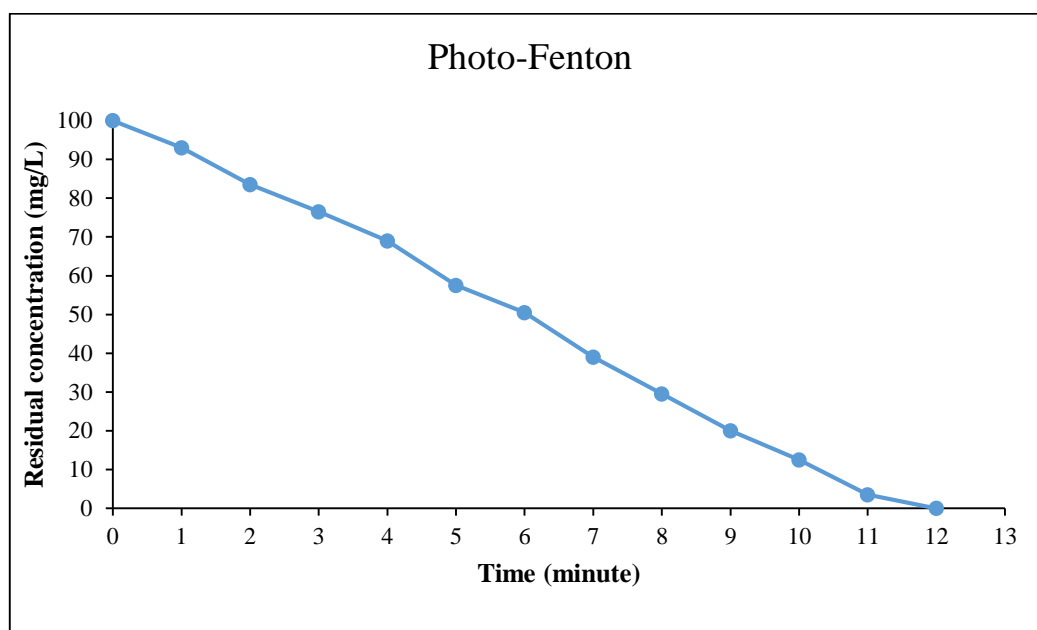


Fig. 4.36 Photo-Fenton degradation of Mi-CPs

In addition, 93% TOC mineralisation was also observed. The residual concentration of total dissolved iron and ferrous ions determined at the end of the experiment reported complete consumption of ferrous ions whereas total dissolved iron concentration measured was 0.03mM. Besides, the residual concentration of H_2O_2 calculated at the end of the experiment was 3.5mM indicating that only 6.5mM of H_2O_2 was consumed during the complete oxidation of CPs.

4.21 Integrated Processes towards degradation of Mi-CPs

Different Photocatalytic and Fenton's Integrated processes were employed at optimised conditions. A comparison of maximum removal efficiency (%) and mineralisation (%) of different processes is illustrated in Table 4.15 and depicted in Figure 4.37

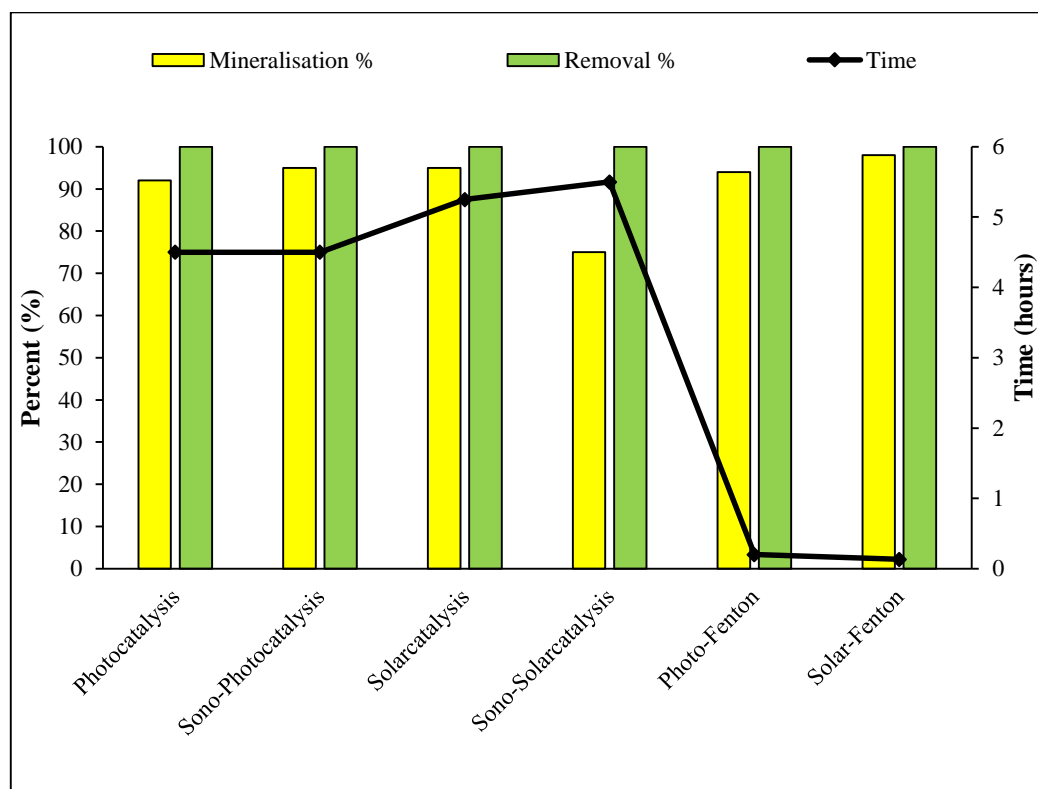


Fig. 4.37 Removal efficiency and mineralisation percent of different AOPs for degradation of Mi-CPs

Table 4.15 Comparison of Different processes for maximum time taken for degradation of Mi-CPs

Processes	Conditions	Maximum degradation efficiency (%)	Time for complete/maximum degradation (minutes)	Mineralisation (%)
Photocatalysis	TiO ₂ : 0.1 g/L H ₂ O ₂ : 10.0mM pH: 5.0 Light Source: UV tubes (365nm) Intensity: 672W/m ²	100	285	92
Sono-Photocatalysis	TiO ₂ : 0.1 g/L H ₂ O ₂ : 10.0mM pH: 5.0 Light Source: UV tubes (365nm) Intensity: 672W/m ² Ultrasound: 40kHz	100	270	95
Solarcatalysis	TiO ₂ : 0.1 g/L H ₂ O ₂ : 10.0mM pH: 5.0 Light Source: Solar Intensity: 760 W/m ²	100	315	95

Processes	Conditions	Maximum degradation efficiency (%)	Time for complete/maximum degradation (minutes)	Mineralisation (%)
Sono-Solarcatalysis	TiO ₂ : 0.1 g/L H ₂ O ₂ : 10.0mM pH: 5.0 Light Source: Solar Intensity: 682 W/m ² Ultrasound: 40kHz	100	330	75
Photo-Fenton	Fe: 0.7mM H ₂ O ₂ : 7.0mM pH: 3.0 Light Source: UV tubes (365nm) Intensity: 672W/m ²	100	12	93
Solar-Fenton	Fe: 0.7mM H ₂ O ₂ : 7.0mM pH: 3.0 Light Source: Solar Intensity: 760 W/m ²	100	08	98

4.21.1 Ultrasound-assisted Photocatalysis process

The sono-photocatalysis pathway involves activation of the surface of photocatalyst, mass transfer of organic contaminants and breaking the aggregation. The sonolysis process was performed in sonication bath with operating frequency of 40kHz (Yadav et al., 2023b). The effect of ultrasound and photocatalysis was reflected in the treatment of Mi-CPs (Figure 4.37). The process reported complete degradation of the CPs-mixture in 270 minutes with 95% mineralisation. The synergistic integration of increased free radical formation and enhanced catalytic activity increased the efficiency of the process. Photocatalyst enhances the bubble cavitation phenomenon causing increased migration of reactive species into the liquid bulk region. Thus, the intensification leads to a higher concentration of free radicals as a result of ultrasound in the peroxide species (Anandan et al., 2020). Cavitation causes cleavage of H_2O_2 produced by the coupling process, increasing the generation of reactive radical species which further carry out the oxidation of the substrate and other intermediates. Higher production of HO^\bullet radicals in the bubble-bulk interface enhances greater interaction with organic pollutant in the bulk-liquid medium (Yadav et al., 2023a). A similar effect was also observed under the influence of solar light.

4.21.2 Solar-induce AOPs

One of the major challenges of AOPs is switching from energy-intensive processes to sustainable and renewable energy sources. Solar photochemistry plays a vital role in pollution remediation transforming the pollutants into non-toxic compounds. Since no solar spectrum modification can occur, solar energy could be harnessed to increase the efficiency of treatment systems. Solar-driven AOPs investigated in the present study have reported some promising results. Solar-assisted degradation processes were conducted in March with an average solar radiation of 760 W/m^2 amid experiment duration. Solar-Fenton reported complete degradation of organic pollutant with 98% TOC reduction within 08 minutes which is comparatively faster compared to the Photo-Fenton process (Figure 4.37). Moreover, Solar-induce sono-

photocatalytic process also reported 100% degradation although nearly 75% mineralisation was there. The lesser mineralisation could be conditional since solar light (average solar radiation 760 W/m² during experiment hours) might be less proficient towards the ample generation of hydroxyl radicals for effectively degrading the intermediary compounds because of the fractional proportion of UV in the solar spectrum compared to direct UV365 light used in photocatalysis effective for photo-activating the photocatalyst (Ortiz et al., 2019). In addition, the solar spectrum is harnessed naturally, thereby offsetting the cost of treatment against UV light.

4.22 Economic analysis of different AOPs for degradation of Mi-CPs

The economic analysis was conducted after maximal degradation of Mi-CPs with respect to photocatalysis, Photo-Fenton, solar-driven oxidation processes and sonication-induced treatment processes and a comparative assessment of treatment cost was done (Table 4.16). In the case of Photocatalysis treatment, complete removal was achieved in 285 minutes with a 0.25mg/L dose of catalyst at pH 6.0 and 10.0mM dose of oxidant. The experiments were conducted in a fabricated UV chamber having 8 UV tubes each with a power rating of 36W making together 288W; the power rating of the air-sparger and magnetic stirrer is 3.5W and 8.5W, respectively. Thus, the total power consumption is 300W or 0.3KWh. The consumption of hydrogen peroxide cost INR 1.14/L. Considering the fractional loss of NPC during analysis, sample centrifugation, sample transfer etc, the residual photo-catalyst was recovered and oven-dried at 105°C. The recovered NPC was analysed using the following formula:

$$TiO_2 \text{ Recovered} = \frac{w_2}{w_1} \times 100 \quad (4.26)$$

Where w_1 is the initial known weight of NPC added; w_2 is the residual dried weight of TiO_2 recovered at the end of the experiment. The cost of the Degussa P25 NPC catalyst used is INR 22,680/100g and since only 20% of it was consumed or lost, it cost INR 11.34/L for treating 100mg/L strength of synthetically prepared wastewater.

Table 4.16 Economic analysis of the operating cost of different AOPs used for degradation of Mi-CPs

Treatment method	Energy per hour (kWh)	Time for treatment (hour)	Rate of energy (per kWh) (INR)	Cost of electricity (INR)	Chemical consumed	Cost of chemical per litre (INR)	Cost of treatment in per litre (INR)	Cost of treatment in per litre (USD)
Photo-Fenton (UV ₃₆₅)	0.06	0.2	8.50	0.5	FeSO ₄ .7H ₂ O H ₂ O ₂ (30% w/v)	0.115 0.8	01	0.02
Photocatalysis (UV ₃₆₅)	1.35	4.5	8.50	11	TiO ₂ (P25) H ₂ O ₂ (30% w/v)	11.34* 1.14	24	0.29
Sono-Photocatalysis (UV ₃₆₅)	1.76	4.5	8.50	15	TiO ₂ (P25) H ₂ O ₂ (30% w/v)	11.34* 1.14	27	0.33
Solar-Fenton	0.001	0.1	8.50	0.010	FeSO ₄ .7H ₂ O H ₂ O ₂ (30% w/v)	0.115 0.8	01	0.01
Solar-catalysis	0.063	5.25	8.50	0.5	TiO ₂ (P25) H ₂ O ₂ (30% w/v)	11.34* 1.14	13	0.016
Sono-Solar-Catalysis	0.57	5.5	8.50	5	TiO ₂ (P25) H ₂ O ₂ (30% w/v)	11.34* 1.14	17	0.21

*15% loss of NPC is calculated

The overall operational cost of photocatalysis was INR 17.00 OR USD 0.21. The electricity cost for industrial supply in Delhi, India is INR 8.5 per unit KWh. However, in Photo-Fenton, degradation was attained within a few minutes and since the cost of chemicals especially iron (used as a catalyst) was lesser in comparison, the overall cost of the treatment was much less (INR 0.9) as compared to photocatalysis. It was observed that the treatment cost increased in sonication-integrated processes because of the additional power (100W) consumption during treatment. The operational cost was however less in the case of sono-photocatalysis because of reduced time compared to UV-Photocatalysis. The cost of treatment was remarkable in solar energy-driven processes particularly, solar-Fenton, solar-catalysis and solar-induce sono-photocatalysis as these were found more energy-efficient compared to photocatalysis. Therefore, the use of solar energy as a renewable and environmentally sustainable sound approach, helps reducing the dependence on energy-intensive treatment and it is a pocket-friendly approach.

4.23 Combination of AOPs with biological treatment for enhanced mineralization of residual chlorophenols and assessment of toxicity of treated effluent

Industrial Ecology seeks to change the once through approach where the materials and energy are retained and used as many times as practicable (Indigo Development, 2004). The ultimate goal of industrial ecology is sustainable development and water hyacinth as an unwanted nuisance on the waterways can be used as a raw material for the sustainable treatment of industrial wastewater. Water hyacinth, a floating aquatic plant is one of the most productive photosynthetic plant in the world (Winkler & Veneman, 1991; Adebayo et al., 2011). This very rapid rate of growth is the reason water hyacinths are a serious nuisance problem in waterways, but this same attribute can become an advantage in a wastewater treatment system. The plant is highly effective in absorbing and accumulating various heavy metals (Von, 1999) and this capability is the reason the effectiveness of water hyacinth is investigated in this study for industrial wastewater treatment.

4.23.1 Toxicity Assessment using *Eichhornia crassipes*

Studies on water hyacinth show that it improves the wastewater effluent from oxidation ponds (Polprasert & Khatiwade, 1998) and integrated treatment systems (Liao & Chang, 2004). Water hyacinth has been reported to reduce biochemical oxygen demand (BOD) and suspended solids (SS) when used in secondary treatment of domestic wastewater (Nesir, 2010) and textile mill effluents (Gamage & Yapa, 2001). The plant was used to assess the toxicity of chlorophenol-contaminated wastewater from treated as well as untreated synthetically prepared industrial effluent. The performance of the water hyacinth was evaluated by assessing the physiological response of the plant (Table 4.17).

Table 4.17 Physiological response of water hyacinth

Particulars	Initial	After 7 days		
		Control	Treated	Untreated
pH	5.5	5.8	6.2	6.3
Chl a (mg/g)	2.048	1.588	1.31	0.934
Chl b (mg/g)	0.649	0.578	0.45	0.312
Carotenoids (mg/g)	0.101	0.07	0.05	0.06
Ascorbic Acid (mg/g)	0.4488	0.421	0.39	0.37
Proline (mg/g)	0.69	0.7699	0.8632	0.8991

The table 4.17 represents the physiological response of water hyacinth over 7 days, assessing the control (presumably conditions without any specific treatment), treated (post AOPs treatment), and untreated (conditions without treatment but not under the controlled, initial conditions) groups. It can be observed from the table the slight shift in pH towards more alkaline conditions. The concentration of photosynthetic pigments was estimated before the experiment and after 7 days at the end of the experiment. It can be observed from the table 4.17 that the chlorophyll content decreased significantly in both treated and untreated sample. Slight difference was observed in case of control. Untreated sample has the

most significant decrease for chlorophyll ‘a’ and chlorophyll ‘b’. Similar trend was observed in carotenoid content as well. The decreased photosynthetic pigments could be attribute to the stressed conditions plants were exposed to. In order to survive under the pollutant/salinity stress condition, plants exhibit defence mechanism or adaptations which might result in reduced pigment content further decelerating the plant metabolism (Lekshmi et al., 2022).

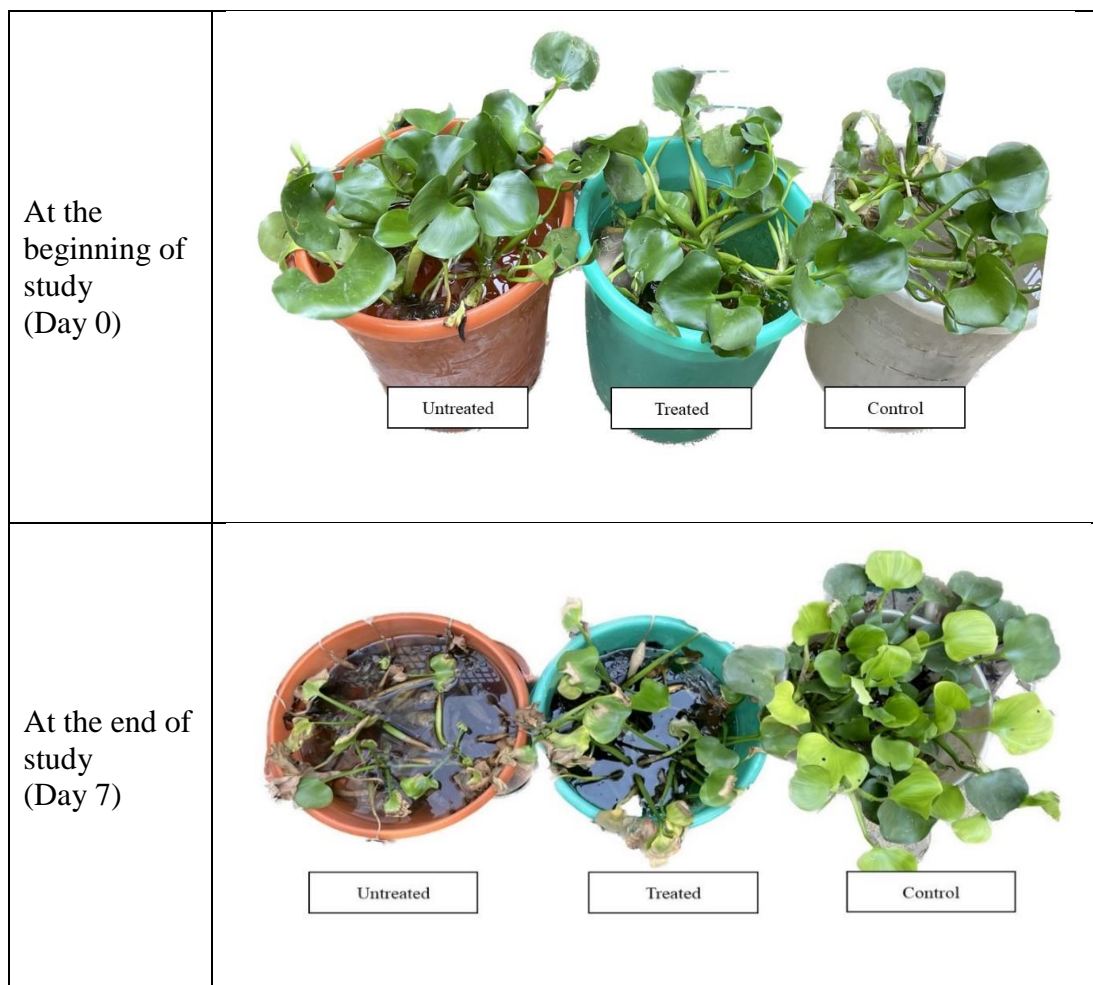


Fig. 4.38 Physical appearance of plant before and after 7 days

Stress conditions induces inactivation of antioxidant enzymes while flavonoid synthesis is up-regulated (Hatier et al., 2008). Ascorbic acid is considered as a powerful water-soluble antioxidant scavenger of reactive oxidative species (ROS) (Smirnoff, 2000). However, in case of *E. crassipes* cultured in treated and

untreated wastewater, the ascorbic acid content was found in decreasing order with not so significant change under controlled conditions. Increased stress conditions and inactivation of antioxidant enzymes could be attributed to the decline in level of ascorbic acid. Another indicator of stress marker estimated in plants is Proline and was found in increased levels. In habitats with stress imparting contaminants, the plants are confronted with high levels of reactive oxygen species (ROS). Proline accumulation corresponds to the defensive mechanism to counteract the oxidative stress damages such as pigment degradation (Khattab, 2007). Studies have reported a similar trend in physiological response of plant under stressed conditions (Lekshmi et al., 2022; Purnamawati et al., 2020). During the current study, at the end of 7 days, the plants cultured in treated and untreated cells could not survive owing to the toxicity of the compound (Figure 4.38). Moreover, in the case of AOPs treated wastewater, there may be a possibility of formation of by-products which are capable enough to inhibit plant growth and disrupting the metabolism leading ultimately to the death of the plant tissues.

4.24 Significance of the study

The treatment of industrial effluent is not restricted to immediate environmental benefits but plays a significant role in safeguarding the public health further aiding in the economic stability and promoting the social equity, thus enhancing the quality of life. The study also aligns with the targets and indicators of the United Nation's Sustainable Development Goals (SDGs) as shown in the figure.

4.24.1 Environmental impact

- i. Industrial effluents are loaded with toxic impurities that disrupt the ecosystem. Treatment of industrial effluent prevents the release of toxicants into the environment, especially the receiving water body, thus protecting the health of aquatic ecosystem and the sensitive species living under water.

- ii. The optimization and application of AOPs play a pivotal role in securing sustainable solutions helping industries towards cost-effective remediation method for hazardous compound removal like chlorophenols. Optimised treatment of effluent prevent the use of excess chemicals used in conventional methods which produces enormous amount of sludge. Thus contributing significantly towards the preservation of diverse environmental matrices.

- iii. Sustainable usage approach, the potential reuse and recycling of AOP treated water in inferior industrial processes, and non-potable uses reduces the burden and dependence upon freshwater extraction, further help in conserving million litres of freshwater, thus preserving the scarce natural water resources.

- iv. The discharge of wastewater containing high levels of toxins like chlorophenols without treatment can leach into the soil, affecting soil and groundwater quality. This not only degrades soil quality but can also harm agricultural productivity and food security. Hence, treatment of wastewater prevents degradation of soil and land.

- v. Implementation of advanced wastewater treatment processes focussing on environment friendly solutions such as solar-driven processes, contributes towards energy efficient and cost effective technologies further reducing the carbon footprint.



Fig. 4.39 United Nation’s Sustainable Development Goals aligning with the current study

4.24.2 Social impact

- i. Complete mineralisation of PCP results in lesser persistence of carcinogens which ultimately leads to lesser cases of cancer patients. The treatment of PCP like carcinogens thus improves the public health, increase longevity of life.
- ii. Adoption of AOPs and generation of treatment facilities based on AOPs requires skilled personnel and results in employment opportunities, thereby improving economic status and social well being.
- iii. The treated effluent/ wastewater can often be recycled and reused in various industrial operations, thus reducing the strain on freshwater resources. The process promotes sustainable resource management, thus ensuring the availability of freshwater for future generations.
- iv. Treatment of effluent ensures that all communities including the marginalized and low-income group irrespective of their socioeconomic status have a safer environment. Having access to clean water is fundamental to human health, thus promoting social equality and justice.
- v. In nation like India, water bodies hold significant culture and spiritual values. Prevention of release of industrial effluent or by treating the effluent, the water bodies can be preserved, allowing the communities to conserve their customs, rituals and cultural practices.

As industries, communities and government continue to ascertain the importance of sustainable use of water and its management, it will contribute to a healthier, more equitable and more sustainable world.

CHAPTER 5

CONCLUSION AND RECOMMENDATION

5.1 Conclusion

On the basis of the present study, the following conclusions can be drawn.

- i. Among all the processes, Fenton's process was found as most effective in degradation of Chlorophenols hence it can be clubbed with other processes such as Solar driven, sonication and Photo in the presence of UV light for the efficient removal of organic contaminants.
- ii. In terms of treatment cost, the Solar-Fenton was found to be most efficient, quick and environmentally friendly among all the AOPs employed in the present study.
- iii. The removal efficiency of different AOPs for the degradation of 4-CP follows the order: Solar-Fenton > Solar-Sono-Fenton > Photo-Fenton > Sono-Photo-Fenton > Sono-Solarcatalysis > Sono-Photocatalysis > Photocatalysis > Solarcatalysis
- iv. The removal efficiency of different AOPs for the degradation of 2,4-DCP follows the order: Solar-Fenton > Solar-sono-Fenton > Sono-photocatalysis > Photocatalysis > Sono-Photo-Fenton > Photo-Fenton > Sono-Fenton > Fenton > Sono-Solarcatalysis > Solarcatalysis > Photolysis
- v. The removal efficiency of different AOPs for the degradation of 2,4,6-TCP follows the order: Solar-Fenton > Photo-Fenton > Sono-Photo-Fenton > Fenton > Sono-Fenton > Photocatalysis > Solarcatalysis > Photocatalysis with H₂O₂.
- vi. At optimised conditions, the removal efficiency of Mi-CPs was found to be 100% for all the processes employed. However, differences were observed in case of their mineralisation percentage which follows the order: Solar-Fenton (98%) > Photo-Fenton (93%) > Solar-catalysis (95%) > Sono-Photocatalysis (95%) > Photocatalysis (92%) > Sono-Solarcatalysis (75%).

- vii. The proposed RSM model showcased a close resemblance between predicted and observed values, thus validating the accuracy of the model for the variables.
- viii. Integration of UV radiation increased the removal efficiencies, but operational costs were also increased due to additional installation of UV light setup. Additionally, the process requires photocatalyst (mainly Nano-TiO₂) which is relatively expensive thus making the overall process costly and energy-intensive.
- ix. Toxicity analysis study suggested the invasive macrophyte water hyacinth is intolerant to oxidative stress conditions even when cultured in treated effluent, thus suggesting the need for further treatment processes of the treated wastewater. The possibility of the formation of intermediates chemical species cannot be ruled out which is evident from death of water hyacinth and the HPLC analysis plot.

5.2 Recommendation

The following recommendations can be provided from the present study.

- i. With the growing emphasis on sustainability, increasing water shortages, and environmental restrictions, industries need to switch to alternative wastewater treatment methods that minimise the water footprint.
- ii. As industries generate large volumes of effluents, several aspects must be considered to increase the feasibility of using AOPs on a large scale, several aspects should be taken into consideration. For instance, cost of treatment, associated toxicity of effluents and by-products, (photo)catalysts technology, and reactors design.
- iii. The overall cost per unit mass of pollutant that is removed from water or unit volume of water, wastewater, or effluent that is treated is lowered, the industrial implementation of these technologies will become much more attractive for industries and/or public administrations.

- iv. The use of solar irradiated AOPs reduces the operational cost and dependence on lamps for light. The application of solar energy could lead to reductions of more than 90% of energy demands, which would help reduce in overall treatment costs. This is particularly important for a developing nation like India, where conventional treatment methods are still being practiced.
- v. Illuminating the imperative need for sustainability, the harnessing of natural light emerges as a judicious approach for treating industrial effluents laden with xenobiotic.

5.3 Future scope

- i. The membranes contactor is another alternative technology, based on solvent extraction using hollow fibre membranes (membrane-based extraction method), to remove aromatic compounds present in low concentration. This process offers a large interfacial area with reduced solvent by-products and lower solvent losses. The process involves extraction of the compound to a second phase stabilizing the aqueous and organic phases within the pores of the polymeric membrane.
- ii. Membrane filtration is an effective treatment option with the limitation of concentration polarization and membrane fouling. Combination of membrane filtration with electrochemical oxidation can simultaneously operate filtration and oxidation of organic impurities thereby extending efficiency of process and life of membrane.
- iii. Synthesis of new photosensitive materials and their application in treatment of organic impurities particularly in a hetero-structured photocatalytic system but with a band structure alignment transition strategy for visible range (400–700 nm) so that naturally available energy can be utilized in the remediation process.
- iv. Electrochemical methods are relatively more effective with rapid treatment rates. Integration of electrochemical process with composite and Nano sized chemical oxidant/reductants can significantly enhance the separation of impurities and their subsequent degradation/mineralization.

REFERENCES

- Abhilash, P. C., Jamil, S., & Singh, N. (2009). Transgenic plants for enhanced biodegradation and phytoremediation of organic xenobiotics. *Biotechnology advances*, 27(4), 474-488. <https://doi.org/10.1016/j.biotechadv.2009.04.002>
- Agarry, S. E., Owabor, C. N., & Ajani, A. O. (2013). Modified plantain peel as cellulose-based low-cost adsorbent for the removal of 2, 6-dichlorophenol from aqueous solution: adsorption isotherms, kinetic modeling, and thermodynamic studies. *Chemical Engineering Communications*, 200(8), 1121-1147. <https://doi.org/10.1080/00986445.2012.740534>
- Agency for Toxic Substances and Disease Registry (ATSDR). Toxicological Profile for Pentachlorophenol (Update) (Draft). Public Health Service, U.S. Department of Health and Human Services, Atlanta, GA. 1999.
- Agostini, E., Coniglio, M. S., Milrad, S. R., Tigier, H. A., Giulietti, A. M. (2003). Phytoremediation of 2, 4-dichlorophenol by *Brassica napus* hairy root cultures. *Biotechnology and applied biochemistry*, 37(2), 139-144. <https://doi.org/10.1042/BA20020079>
- Ahel, M., Hršak, D., Giger, W. (1994). Aerobic transformation of short-chain alkylphenol polyethoxylates by mixed bacterial cultures. *Archives of Environmental Contamination and Toxicology*, 26(4), 540-548. <https://doi.org/10.1007/BF00214159>
- Ahmadzadeh, S., Dolatabadi, M. (2018) In situ generation of hydroxyl radical for efficient degradation of 2, 4-dichlorophenol from aqueous solutions. *Environmental monitoring and assessment*, 190, 1-11. <https://doi.org/10.1007/s10661-018-6697-0>
- Ahmed, S., Rasul, M. G., Martens, W. N., Brown, R., Hashib, M. A. (2011). Advances in heterogeneous photocatalytic degradation of phenols and dyes in wastewater: a review. *Water, Air, & Soil Pollution*, 215(1), 3-29. <https://doi.org/10.1007/s11270-010-0456-3>
- Akhtar, T., Nasir, H., Sitara, E., Bukhari, S. A. B., Ullah, S., & Iqbal, R. M. A. (2022). Efficient photocatalytic degradation of nitrobenzene by copper-doped TiO₂: kinetic study, degradation pathway, and mechanism. *Environmental Science and*

- Pollution Research*, 29(33), 49925-49936. <https://doi.org/10.1007/s11356-022-19422-5>
- Alexander, J. C., Ramírez-Cortina, C. R. (2016). A comparative study: degradation of 2, 5-dichlorophenol in wastewater and distilled water by ozone and ozone-UV. *Ozone: Science & Engineering*, 38(3), 181-193. <https://doi.org/10.1080/01919512.2015.1113853>
- Aljuboury, D. A. D. A., Palaniandy P., Abdul, Aziz, H. B., Feroz S., Abu, Amr, S. S. (2016). Evaluating photo-degradation of COD and TOC in petroleum refinery wastewater by using TiO₂/ZnO photo-catalyst. *Water Sci Technol*, 74(6), 1312-1325. <https://doi.org/10.2166/wst.2016.293>.
- Ameta, S. C., Ameta, R eds. (2018). *Advanced oxidation processes for wastewater treatment: emerging green chemical technology*. Academic press.
- Anandan, S., Ponnusamy, V. K., Ashokkumar, M. (2020). A review on hybrid techniques for the degradation of organic pollutants in aqueous environment. *Ultrasonics Sonochemistry*, 67, 105130. <https://doi.org/10.1016/j.ultsonch.2020.105130>
- Andersson, M. A., Hellman, B. E. (2005). Different roles of Fpg and Endo III on catechol-induced DNA damage in extended-term cultures of human lymphocytes and L5178Y mouse lymphoma cells. *Toxicology in Vitro*, 19(6), 779–786. <https://doi.org/https://doi.org/10.1016/j.tiv.2005.04.011>
- Andini, S., Cioffi, R., Colangelo, F., Montagnaro, F., Santoro, L. (2008). Adsorption of chlorophenol, chloroaniline and methylene blue on fuel oil fly ash. *Journal of Hazardous Materials*, 157(2), 599–604. <https://doi.org/https://doi.org/10.1016/j.jhazmat.2008.01.025>
- Antizar-Ladislao, B., Lopez-Real, J., Beck, A. (2004). Bioremediation of polycyclic aromatic hydrocarbon (PAH)-contaminated waste using composting approaches. *Critical Reviews in Environmental Science and Technology*, 34(3), 249-289. <https://doi.org/10.1080/10643380490434119>
- Arora, P. K., Bae, H. (2014). Bacterial degradation of chlorophenols and their derivatives. *Microbial Cell Factories*, 13(1), 1–17. <https://doi.org/10.1186/1475-2859-13-31>
- Aziz, K. H. H., Miessner, H., Mueller, S., Mahyar, A., Kalass, D., et al., (2018). Comparative study on 2, 4-dichlorophenoxyacetic acid and 2, 4-dichlorophenol

- removal from aqueous solutions via ozonation, photocatalysis and non-thermal plasma using a planar falling film reactor. *Journal of hazardous materials*, 343, 107-115. <https://doi.org/10.1016/j.jhazmat.2017.09.025>
- Bae, H. S., Lee, J. M., & Lee, S. T. (1996). Biodegradation of 4-chlorophenol via a hydroquinone pathway by *Arthrobacter ureafaciens* CPR706. *FEMS Microbiology Letters*. 145(1), 125-129. <https://doi.org/10.1111/j.1574-6968.1996.tb08566.x>
- Bagbi, Y., Sarswat, A., Mohan, D., Pandey, A., Solanki, P. R. (2017). Lead and chromium adsorption from water using L-cysteine functionalized magnetite (Fe₃O₄) nanoparticles. *Sci Rep*, 7(1), 1-15.
- Bahnemann, W., Muneer, M., Haque, M. M. (2007). Titanium dioxide-mediated photocatalysed degradation of few selected organic pollutants in aqueous suspensions. *Catalysis Today*, 124(3-4), 133-148. <https://doi.org/10.1016/j.cattod.2007.03.031>
- Baker, M. D., Mayfield, C. I., Inniss, W. E. (1980). Degradation of chlorophenols in soil, sediment and water at low temperature. *Water Research*, 14(12), 1765–1771. [https://doi.org/10.1016/0043-1354\(80\)90112-8](https://doi.org/10.1016/0043-1354(80)90112-8)
- Balfanz, J., Rehm, H. J. (1991). Biodegradation of 4-chlorophenol by adsorptive immobilized *Alcaligenes* sp. A 7-2 in soil. *Applied Microbiology and Biotechnology*, 35(5), 662–668. <https://doi.org/10.1007/BF00169634>
- Ballivet-Tkatchenko, D., Camy, S., Condoret, J. S. (2005). Carbon dioxide, a solvent and synthon for green chemistry. *Environmental Chemistry: Green Chemistry and Pollutants in Ecosystems*, Vollenbroek, 2002, 541–552. https://doi.org/10.1007/3-540-26531-7_49
- Balzani, V., Pacchioni, G., Prato, M., Zecchina, A. (2019). Solar driven chemistry: towards new catalytic solutions for a sustainable world. *Rend Fis Acc Lincei*, 30(3), 443–452. <https://doi.org/10.1007/s12210-019-00836-2>
- Balzani, V., Ceroni, P. and Juris, A. (2014). *Photochemistry and photophysics: concepts, research, applications*. John Wiley & Sons.
- Barahona, M. V., Sánchez-Fortún, S. (1996). Comparative sensitivity of three age classes of *Artemia salina* larvae to several phenolic compounds. *Bulletin of*

- Environmental Contamination and Toxicology, 56(2), 271–278.
<https://doi.org/10.1007/s001289900041>
- Barbeau, C., Deschênes, L., Karamanev, D., Comeau, Y., Samson, R. (1997). Bioremediation of pentachlorophenol-contaminated soil by bioaugmentation using activated soil. *Applied Microbiology and Biotechnology*, 48(6), 745–752.
<https://doi.org/10.1007/s002530051127>
- Barriuso, E., Houot, S., Serra-Wittling, C. (1997). Influence of compost addition to soil on the behaviour of herbicides. *Pesticide Science*. 49(1), 65-75.
[https://doi.org/10.1002/\(SICI\)1096-9063\(199701\)49:1<65::AID-PS488>3.0.CO;2-Z](https://doi.org/10.1002/(SICI)1096-9063(199701)49:1<65::AID-PS488>3.0.CO;2-Z)
- Batty, L. C., Dolan, C. (2013). The potential use of phytoremediation for sites with mixed organic and inorganic contamination. *Crit Rev Environ Sci Technol*, 43(3), 217–259. <https://doi.org/10.1080/10643389.2011.604254>
- Bayarri, B., Gimenez, J., Curco, D., Esplugas, S. (2005). Photocatalytic degradation of 2, 4-dichlorophenol by TiO₂/UV: kinetics, actinometries and models. *Catalysis Today*, 101(3-4), 227-236.
<https://doi.org/10.1016/j.cattod.2005.03.019>
- Bayramoglu, G., Gursel, I., Tunali, Y., Arica, M. Y. (2009). Biosorption of phenol and 2-chlorophenol by *Funalia trogii* pellets. *Bioresource technology*, 100(10), 2685-2691. <https://doi.org/10.1016/j.biortech.2008.12.042>
- Becker, J. G., Stahl, D. A., Rittmann, B. E. (1999). Reductive dehalogenation and conversion of 2-chlorophenol to 3-chlorobenzoate in a methanogenic sediment community: implications for predicting the environmental fate of chlorinated pollutants. *Applied and environmental microbiology*, 65(11), 5169-5172.
<https://doi.org/10.1128/AEM.65.11.5169-5172.1999>
- Benitez, F. J., Beltran-Heredia, J., Acero, J. L., Rubio, F. J. (2000). Contribution of free radicals to chlorophenols decomposition by several advanced oxidation processes. *Chemosphere*, 41, 1271-1277. [https://doi.org/10.1016/S0045-6535\(99\)00536-6](https://doi.org/10.1016/S0045-6535(99)00536-6)
- Bernhard-Reversat, F. (1998). Changes in relationships between initial litter quality and CO₂ release during early laboratory decomposition of tropical leaf litters.

- European Journal of Soil Biology, 34(3), 117–122.
[https://doi.org/10.1016/S1164-5563\(00\)88648-3](https://doi.org/10.1016/S1164-5563(00)88648-3)
- Bhattacharya, T., Chakraborty, S. (2018). Eco-Restoration Potential of Vegetation for Contaminated Water Bodies. In *Phytomanagement of Polluted Sites: Market Opportunities in Sustainable Phytoremediation*. Elsevier Inc.
<https://doi.org/10.1016/B978-0-12-813912-7.00017-X>
- Bielefeldt, A. R., Cort, T. (2005). Dual substrate biodegradation of a nonionic surfactant and pentachlorophenol by *Sphingomonas chlorophenolica* RA2. *Biotechnology and Bioengineering*, 89(6), 680–689.
<https://doi.org/https://doi.org/10.1002/bit.20365>
- Bilal, M., Iqbal, H., Barceló, D. (2020). Perspectives on the feasibility of using enzymes for pharmaceutical removal in wastewater. *Removal and Degradation of Pharmaceutically Active Compounds in Wastewater Treatment*. 119-143.
https://doi.org/10.1007/698_2020_661
- Blackburn, R., Farrington, D., Lunt, J., Davies, S., Blackburn, R. (2005). Poly(lactic acid) fibers. *Biodegradable and Sustainable Fibres*.
<https://doi.org/10.1201/9781439823781.ch6>
- Blake, D. M., Webb, J., Turchi, C., Magrini, K. (1991). Kinetic and mechanistic overview of TiO₂-photocatalyzed oxidation reactions in aqueous solution. *Sol Energy Mater*, 24(1-4), 584-593. [https://doi.org/10.1016/0165-1633\(91\)90092-Y](https://doi.org/10.1016/0165-1633(91)90092-Y).
- Bolton, J. R., Bircher, K. G., Tumas, W., & Tolman, C. A. (2001). Figures-of-merit for the technical development and application of advanced oxidation technologies for both electric-and solar-driven systems (IUPAC Technical Report). *Pure and Applied Chemistry*, 73(4), 627-637.
<https://doi.org/10.1351/pac200173040627>
- Boparai, H. K., Joseph, M., & O'Carroll, D. M. (2011). Kinetics and thermodynamics of cadmium ion removal by adsorption onto nano zerovalent iron particles. *Journal of hazardous materials*, 186(1), 458-465.
<https://doi.org/10.1016/j.jhazmat.2010.11.029>
- Boule, P., Guyon, C., Lemaire, J. (1982). Photochemistry and environment IV-Photochemical behaviour of monochlorophenols in dilute aqueous solution. *Chemosphere*, 11(12), 1179–1188. [https://doi.org/10.1016/0045-6535\(82\)90031-5](https://doi.org/10.1016/0045-6535(82)90031-5)

- Boyd, S. A. (1982). Adsorption of substituted phenols by soil. *Soil Science*, 134(5), 337-343.
- Boyd, S. A., Shelton, D. R. (1984). Anaerobic biodegradation of chlorophenols in fresh and acclimated sludge. *Appl Environ Microbiol*, 47, 272–277.
- Brown, S. B., Adams, B. A., Cyr, D. G., Eales, J. G. (2004). Contaminant effects on the teleost fish thyroid. *Environmental Toxicology and Chemistry*, 23(7), 1680–1701. <https://doi.org/10.1897/03-242>
- Brusseau, M. L., Rao, P. S. C. (1991). Influence of sorbate structure on nonequilibrium sorption of organic compounds. *Environmental science & technology*, 25(8), 1501-1506. <https://doi.org/10.1021/es00020a022>
- Buffle, M. O., Schumacher, J., Meylan, S., Jekel, M., von Gunten, U. (2006). Ozonation and advanced oxidation of wastewater: effect of O₃ dose, pH, DOM and HO[•]-scavengers on ozone decomposition and HO[•] generation. *Ozone: Sci. Eng.* 28 (4), 247e259. <https://doi.org/10.1080/01919510600718825>
- Bukowska, B, Michałowicz, J., Krokosz, A., & Sicińska, P. (2007). Comparison of the effect of phenol and its derivatives on protein and free radical formation in human erythrocytes (in vitro). *Blood Cells, Molecules, and Diseases*, 39(3), 238–244. <https://doi.org/https://doi.org/10.1016/j.bcmed.2007.06.003>
- Bukowska, B., Rychlik, B., Krokosz, A., Michałowicz, J. (2008). Phenoxyherbicides induce production of free radicals in human erythrocytes: oxidation of dichlorodihydrofluorescein and dihydrorhodamine 123 by 2, 4-D-Na and MCPA-Na. *Food and Chemical Toxicology*, 46(1), 359-367. <https://doi.org/https://doi.org/10.1016/j.fct.2007.08.011>
- Bunce, N. J., Nakai, J. S. (1989). Atmospheric chemistry of chlorinated phenols. *Journal of the Air Pollution Control Association*, 39(6), 820–823. <https://doi.org/10.1080/08940630.1989.10466567>
- Cao, M., Hou, Y., Zhang, E., Tu, S., Xiong, S. (2019). Ascorbic acid induced activation of persulfate for pentachlorophenol degradation. *Chemosphere*, 229, 200–205. <https://doi.org/10.1016/j.chemosphere.2019.04.135>
- Caqueret, V., Bostyn, S., Cagnon, B., Fauduet, H. (2008). Purification of sugar beet vinasse—adsorption of polyphenolic and dark colored compounds on different

- commercial activated carbons. *Bioresource Technology*, 99(13), 5814-5821.
<https://doi.org/10.1016/j.biortech.2007.10.009>
- Carvalho, M. B., Martins, I., Medeiros, J., Tavares, S., Planchon, S., Renaut, J., Núñez, O., Gallart-Ayala, H., Galceran, M. T., Hursthouse, A. Pereira, C. S. (2013). The response of *Mucor plumbeus* to pentachlorophenol: a toxicoproteomics study. *Journal of proteomics*, 78, 159-171.
<https://doi.org/10.1016/j.jprot.2012.11.006>
- Ceylan, Z., Moharramzadeh, M., ATICI, Ö. (2021). Investigating Usage Potential of *Datura stramonium* L. for Phytoremediation of 2, 4-Dichlorophenol. *Hacettepe Journal of Biology and Chemistry*, 49(2), 157-166.
<https://doi.org/10.15671/hjbc.689446>
- Chakma, S., Moholkar, V. S. (2013). Physical mechanism of sono-Fenton process. *AIChE Journal*, 59(11), 4303-4313. <https://doi.org/10.1002/aic.14150>
- Chang, G., Yue, B., Gao, T., Yan, W., Pan, G. (2020). Phytoremediation of phenol by *Hydrilla verticillata* (Lf) Royle and associated effects on physiological parameters. *Journal of hazardous materials*, 388, 121569.
<https://doi.org/10.1016/j.jhazmat.2019.121569>
- Chaudri, A. M., McGrath, S. P., Knight, B. P., Johnson, D. L., Jones, K. C. (1996). Toxicity of organic compounds to the indigenous population of *Rhizobium leguminosarum* biovar *Trifolii* in soil. *Soil Biology and Biochemistry*, 28(10), 1483–1487. [https://doi.org/https://doi.org/10.1016/S0038-0717\(96\)00156-3](https://doi.org/https://doi.org/10.1016/S0038-0717(96)00156-3)
- Chava, R. K., Son, N., Kang, M. (2022). Band structure alignment transitioning strategy for the fabrication of efficient photocatalysts for solar fuel generation and environmental remediation applications. *Journal of Colloid and Interface Science*, 627,247-260. <https://doi.org/10.1016/j.jcis.2022.07.031>
- Chava, R.K., Son, N. and Kang, M., (2022). Bismuth quantum dots anchored one-dimensional CdS as plasmonic photocatalyst for pharmaceutical tetracycline hydrochloride pollutant degradation. *Chemosphere*, 300, 134570.
<https://doi.org/10.1016/j.chemosphere.2022.134570>
- Chen, D., Cheng, Y., Zhou, N., Chen, P., Wang, Y., Li, K., Huo, S., Cheng, P., Peng, P., Zhang, R., Wang, L. (2020). Photocatalytic degradation of organic pollutants using TiO₂-based photocatalysts: A review. *J Clean Prod*, 268, 121725.
<https://doi.org/10.1016/j.jclepro.2020.121725>

- Chen, H., Zhang, L., Zeng, H., Yin, D., Zhai, Q., Zhao, X., Li, J. (2015). Highly active iron-containing silicotungstate catalyst for heterogeneous Fenton oxidation of 4-chlorophenol. *Journal of Molecular Catalysis A: Chemical*. 406, 72-77. <https://doi.org/10.1016/j.molcata.2015.05.017>
- Chen, M., Xu, P., Zeng, G., Yang, C., Huang, D., Zhang, J. (2015). Bioremediation of soils contaminated with polycyclic aromatic hydrocarbons, petroleum, pesticides, chlorophenols and heavy metals by composting: applications, microbes and future research needs. *Biotechnology advances*, 33(6), 745-755. <https://doi.org/10.1016/j.biotechadv.2015.05.003>
- Chen, W. S., Huang, C. P. (2015). Mineralization of aniline in aqueous solution by electro-activated persulfate oxidation enhanced with ultrasound. *Chemical Engineering Journal*, 266, 279-288. <https://doi.org/10.1016/j.cej.2014.12.100>
- Chen, Y., Yu, S., Tang, S., Li, Y., Liu, H., Zhang, X., Su, G., Li, B., Yu, H., Giesy, J.P. (2016). Site-specific water quality criteria for aquatic ecosystems: A case study of pentachlorophenol for Tai Lake, China. *Science of The Total Environment*, 541, 65–73. <https://doi.org/https://doi.org/10.1016/j.scitotenv.2015.09.006>
- Cheng, Y., Ekker, M., Chan, H. M. (2015). Relative developmental toxicities of pentachloroanisole and pentachlorophenol in a zebrafish model (*Danio rerio*). *Ecotoxicology and Environmental Safety*, 112, 7–14. <https://doi.org/https://doi.org/10.1016/j.ecoenv.2014.10.004>
- Chiou, C. T., Schmedding, D. W., & Manes, M. (2005). Improved prediction of octanol-water partition coefficients from liquid-solute water solubilities and molar volumes. *Environmental Science and Technology*. 39(22), 8840–8846. <https://doi.org/10.1021/es050729d>
- Chiou, C. T., Freed, V. H., Peters, L. J., Kohnert, R. L. (1980). Evaporation of solutes from water. *Environment International*, 3(3), 231–236. [https://doi.org/https://doi.org/10.1016/0160-4120\(80\)90123-3](https://doi.org/https://doi.org/10.1016/0160-4120(80)90123-3)
- Choi, K. H., Min, J., Park, S. Y., Park, B. J., Jung, J. S. (2019). Enhanced photocatalytic degradation of tri-chlorophenol by Fe₃O₄@TiO₂@Au photocatalyst under visible-light. *Ceram Int*, 45(7), 9477–9482. <https://doi.org/10.1016/j.ceramint.2018.09.104>.
- Christiansen, N. I. N. A., Ahring, B. K. (1996). *Desulfitobacterium hafniense* sp. nov., an anaerobic, reductively dechlorinating bacterium. *International Journal of*

- Systematic and Evolutionary Microbiology, 46(2), 442-448.
<https://doi.org/10.1099/00207713-46-2-442>
- Chu, W., Choy, W. K., So, T. Y. (2007). The effect of solution pH and peroxide in the TiO₂-induced photocatalysis of chlorinated aniline. *Journal of hazardous materials*, 141(1), 86-91. <https://doi.org/10.1016/j.jhazmat.2006.06.093>
- Chu, M., Hu, K., Wang, J., Liu, Y., Ali, S., Qin, C., Jing, L. (2019). Synthesis of g-C₃N₄-based photocatalysts with recyclable feature for efficient 2, 4-dichlorophenol degradation and mechanisms. *Applied Catalysis B: Environmental*, 243, 57-65. <https://doi.org/10.1016/j.apcatb.2018.10.008>
- Coenye, T., Henry, D., Speert, D. P., Vandamme, P. (2004). *Burkholderia phenoliruptrix* sp. nov., to accommodate the 2, 4, 5-trichlorophenoxyacetic acid and halophenol-degrading strain AC1100. *Systematic and Applied Microbiology*, 27(6), 623-627. <https://doi.org/10.1078/0723202042369992>
- Collins, A. R., Duthie, S. J., Dobson, V. L. (1993). Direct enzymic detection of endogenous oxidative base damage in human lymphocyte DNA. *Carcinogenesis*, 14(9), 1733–1735. <https://doi.org/10.1093/carcin/14.9.1733>
- Coniglio, M. S., Busto, V. D., González, P. S., Medina, M. I., Milrad, S., Agostini, E. (2008). Application of *Brassica napus* hairy root cultures for phenol removal from aqueous solutions. *Chemosphere*, 72(7), 1035-1042. <https://doi.org/10.1016/j.chemosphere.2008.04.003>
- Contreras, S., Rodriguez, M., Al Momani, F., Sans, C., Esplugas, S. (2003). Contribution of the ozonation pre-treatment to the biodegradation of aqueous solutions of 2, 4-dichlorophenol. *Water Research*, 37(13), 3164-3171. [https://doi.org/10.1016/S0043-1354\(03\)00167-2](https://doi.org/10.1016/S0043-1354(03)00167-2)
- Crawford, R. L., Jung, C. M., Strap, J. L. (2007). The recent evolution of pentachlorophenol (PCP)-4-monooxygenase (PcpB) and associated pathways for bacterial degradation of PCP. *Biodegradation*, 18(5), 525–539. <https://doi.org/10.1007/s10532-006-9090-6>
- Crosby, D. G., Wong, A. S. (1978). Photolysis of Pentachlorophenol in Water BT - Pentachlorophenol: Chemistry, Pharmacology, and Environmental Toxicology (K. R. Rao (ed.); pp. 19–25). Springer US. https://doi.org/10.1007/978-1-4615-8948-8_3

- Cunningham, S. D., Berti, W. R., & Huang, J. W. (1995). Phytoremediation of contaminated soils. *Trends in Biotechnology*, 13(9), 393–397. [https://doi.org/10.1016/S0167-7799\(00\)88987-8](https://doi.org/10.1016/S0167-7799(00)88987-8)
- Cunningham, S. D., Ow, D. W. (1996). Promises and prospects of phytoremediation. *Plant physiology*, 110(3), 715. <https://dx.doi.org/10.1104%2Fpp.110.3.715>
- Czaplicka, M. (2004). Sources and transformations of chlorophenols in the natural environment. *Science of the Total Environment*, 322(1–3), 21–39. <https://doi.org/10.1016/j.scitotenv.2003.09.015>
- Dams, R. I., Paton, G. I., Killham, K. (2007). Rhizoremediation of pentachlorophenol by *Sphingobium chlorophenolicum* ATCC 39723. *Chemosphere*, 68(5), 864–870. <https://doi.org/https://doi.org/10.1016/j.chemosphere.2007.02.014>
- Daniel, V., Huber, W., Bauer, K., Suesal, C., Conradt, C., Opelz, G. (2001). Associations of blood levels of PCB, HCHS, and HCB with numbers of lymphocyte subpopulations, in vitro lymphocyte response, plasma cytokine levels, and immunoglobulin autoantibodies. *Environmental Health Perspectives*, 109(2), 173–178. <https://doi.org/10.1289/ehp.01109173>
- Daniel, Volker., Huber, W., Bauer, K., Opelz, G. (1995). Impaired In-Vitro Lymphocyte Responses in Patients with Elevated Pentachlorophenol (PCP) Blood Levels. *Archives of Environmental Health: An International Journal*, 50(4), 287–292. <https://doi.org/10.1080/00039896.1995.9935956>
- De Jong, E., Field, J. A. (1997). Sulfur tuft and turkey tail: Biosynthesis and biodegradation of organohalogenes by Basidiomycetes. *Annual Review of Microbiology*, 51, 375–414. <https://doi.org/10.1146/annurev.micro.51.1.375>
- de la Plata, G. B. O., Alfano, O. M., Cassano, A. E. (2010). Decomposition of 2-chlorophenol employing goethite as Fenton catalyst. I. Proposal of a feasible, combined reaction scheme of heterogeneous and homogeneous reactions. *Applied Catalysis B: Environmental*, 95 (1–2), 1–13. <https://doi.org/10.1016/j.apcatb.2009.12.005>
- de la Plata, G. B. O., Alfano, O. M., Cassano, A. E. (2012). 2-Chlorophenol degradation via photo Fenton reaction employing zero valent iron nanoparticles. *Journal of Photochemistry and Photobiology A: Chemistry*, 233, 53–59. <https://doi.org/10.1016/j.jphotochem.2012.02.023>

- Del Campo, E. M., Romero, R., Roa, G., Peralta-Reyes, E., Espino-Valencia, J., Natividad, R. (2014). Photo-Fenton oxidation of phenolic compounds catalyzed by iron-PILC. *Fuel*, 138, 149-155. <https://doi.org/10.1016/j.fuel.2014.06.014>
- DeLaune, R. D., Gambrell, R. P., Reddy, K. S. (1983). Fate of pentachlorophenol in estuarine sediment. *Environmental Pollution Series B, Chemical and Physical*, 6(4), 297–308. [https://doi.org/10.1016/0143-148X\(83\)90015-0](https://doi.org/10.1016/0143-148X(83)90015-0)
- Dietz, A. C. Schnoor, J. L., (2001b). Phytotoxicity of chlorinated aliphatics to hybrid poplar (*Populus deltoides* × *nigra* DN34). *Environmental Toxicology and Chemistry*, 20, 389-393. <https://doi.org/10.1002/etc.5620200221>.
- Dietz, A. C., Schnoor, J. L. (2001a). Advances in phytoremediation. *Environmental health perspectives*. 109(suppl 1), 163-168. <https://doi.org/10.1289/ehp.01109s1163>
- Ding, N., Sun, Y., Ye, T., Yang, Z., Qi, F. (2018). Control of halophenol formation in seawater during chlorination using pre-ozonation treatment. *Environmental Science and Pollution Research*, 25, 28050-28060. <https://doi.org/10.1007/s11356-018-2828-y>
- Divincenzo, J. P., Sparks, D. L. (1997). Slow sorption kinetics of pentachlorophenol on soil: Concentration effects. *Environmental Science and Technology*, 31(4), 977–983. <https://doi.org/10.1021/es9601494>
- Drever, J. (1997). *The Geochemistry of Natural Waters: Surface and Groundwater Environments*.
- Duchnowicz, P., Koter, M. (2003). Damage to the erythrocyte membrane caused by chlorophenoxyacetic herbicides. *Cellular and Molecular Biology Letters*, 8(1), 25–30.
- Eisenhauer, N., Lanoue, A., Strecker, T., Scheu, S., Steinauer, K., Thakur, M. P., Mommer, L. (2017). Root biomass and exudates link plant diversity with soil bacterial and fungal biomass. *Scientific Reports*, 7(1), 44641. <https://doi.org/10.1038/srep44641>
- El-Sayed, W. S., Ismaeil, M., El-Beih, F., (2009). Cloning and nucleotide sequence analysis of catalytic domain encoding sequence of multicomponent phenolhydroxylase from *Pseudomonas aeruginosa* AT2 and *Alcaligenes* sp. OS2. *Res. J. Cell Molec. Biol*, 3, 20–27.

- Errami, M., Salghi, R., Zarrouk, A., Chakir, A., Al-Deyab, S.S., Hammouti, B., Zarrok, H. (2012). Electrochemical combustion of insecticides endosulfan and deltamethrin in aqueous medium using a boron-doped diamond anode. *International Journal of Electrochemical Science*, 7, 4272-4285. <http://www.electrochemsci.org/papers/vol7/7054272.pdf>
- Eslami, A., Hashemi, M., Ghanbari, F. (2018). Degradation of 4-chlorophenol using catalyzed peroxymonosulfate with nano-MnO₂/UV irradiation: Toxicity assessment and evaluation for industrial wastewater treatment. *Journal of Cleaner Production*, 195, 1389–1397. <https://doi.org/10.1016/j.jclepro.2018.05.137>
- Faizah, U. (1992). Engineering approach to biofeedback. *Japanese Society of Biofeedback Research*, 19(5), 463–466.
- Fang, Q., Shi, X., Zhang, L., Wang, Q., Wang, X., Guo, Y., Zhou, B. (2015). Effect of titanium dioxide nanoparticles on the bioavailability, metabolism, and toxicity of pentachlorophenol in zebrafish larvae. *Journal of Hazardous Materials*, 283, 897–904. <https://doi.org/10.1016/j.jhazmat.2014.10.039>
- Fang, Y., Gao, X., Zha, J., Ning, B., Li, X., Gao, Z., Chao, F. (2010). Identification of differential hepatic proteins in rare minnow (*Gobiocypris rarus*) exposed to pentachlorophenol (PCP) by proteomic analysis. *Toxicology Letters*, 199(1), 69–79. <https://doi.org/10.1016/j.toxlet.2010.08.008>
- Fern, P., Labrador, V., Hazen, M. J. (2005). Cytotoxic effects in mammalian Vero cells exposed to pentachlorophenol. 210, 37–44. <https://doi.org/10.1016/j.tox.2005.01.009>
- Fernández-Luqueño, F., López-Valdez, F., Pérez-Morales, C., García-Mayagoitia, S., Sarabia-Castillo, C. R., Pérez-Ríos, S. R. (2017). Enhancing decontamination of PAHs-polluted soils: role of organic and mineral amendments. In: Anjum N, Gill S, Tuteja N (eds) *Enhancing cleanup of environmental pollutants*, Springer, Cham. 339–368. https://doi.org/10.1007/978-3-319-55423-5_11
- Ferrando, M. D., Andreu-Moliner, E., Fernández-Casalderrey, A. (1992). Relative sensitivity of daphnia magna and brachionus calyciflorus to five pesticides. *Journal of Environmental Science and Health*, 27(5), 511–522. <https://doi.org/10.1080/03601239209372798>

- Field, J. A., Sierra-Alvarez, R. (2008). Microbial degradation of chlorinated phenols. *Reviews in Environmental Science and Biotechnology*, 7(3), 211–241. <https://doi.org/10.1007/s11157-007-9124-5>
- Fletcher, K. (2009). Systems change for sustainability in textiles. *Sustainable Textiles: Life Cycle and Environmental Impact*, 369–380. <https://doi.org/10.1533/9781845696948.2.369>
- Fox, J. E., Gullledge, J., Engelhaupt, E., Burow, M. E., McLachlan, J. A. (2007). Pesticides reduce symbiotic efficiency of nitrogen-fixing rhizobia and host plants. *Proceedings of the National Academy of Sciences*, 104(24), 10282–10287. <https://doi.org/10.1073/pnas.0611710104>
- Fulthorpe, R. R., Allen, D. G. (1995). A comparison of organochlorine removal from bleached kraft pulp and paper-mill effluents by dehalogenating *Pseudomonas*, *Ancylobacter* and *Methylobacterium* strains. *Applied Microbiology and Biotechnology*, 42(5), 782–789. <https://doi.org/10.1007/BF00171962>
- Gałązka, A., Grządziel, J., Gałązka, R., Ukalska-Jaruga, A., Strzelecka, J., Smreczak, B. (2018). Genetic and Functional Diversity of Bacterial Microbiome in Soils With Long Term Impacts of Petroleum Hydrocarbons. *Frontiers in Microbiology*, 9, 1923. <https://doi.org/10.3389/fmicb.2018.01923>
- Gamage, N. S., & Yapa, P. A. J. (2001). Use of water hyacinth [*Eichhornia crassipes* (mart) solms] in treatment systems for textile mill effluents - A case study. *J. Natn. Sci. Foundation, Sri Lanka*, 29(1 & 2), 15-18.
- Gan, L., Li, B., Guo M et al. (2018). Mechanism for removing 2,4-dichlorophenol via adsorption and Fenton-like oxidation using iron-based nanoparticles. *Chemosphere*, 206, 168–174. <https://doi.org/10.1016/j.chemosphere.2018.04.162>
- Garabedian, M. J., Hoppin, J. A., Tolbert, P. E., Herrick, R. F., Brann, E. A. (1999). Occupational Chlorophenol Exposure and Non-Hodgkin's Lymphoma. *Journal of Occupational and Environmental Medicine*, 41(4), 267-272.
- Garba, Z. N., Rahim, A. A. (2016). Evaluation of optimal activated carbon from an agricultural waste for the removal of para-chlorophenol and 2, 4-dichlorophenol. *Process Safety and Environmental Protection*, 102, 54-63. <https://doi.org/10.1016/j.psep.2016.02.006>
- Garba, Z. N., Zhou, W., Lawan, I., Xiao, W., Zhang, M., Wang, L., Chen, L. and Yuan, Z. (2019). An overview of chlorophenols as contaminants and their removal from

- wastewater by adsorption: A review. *Journal of environmental management*, 241, 59-75. <https://doi.org/10.1016/j.jenvman.2019.04.004>
- Ge, T., Han, J., Qi, Y., Gu, X., Ma, L., Zhang, C., Naeem, S., Huang, D. (2017). The toxic effects of chlorophenols and associated mechanisms in fish. *Aquatic Toxicology*, 184, 78–93. <https://doi.org/10.1016/j.aquatox.2017.01.005>
- Gentry, T., Rensing, C., Pepper, I. A. N., Gentry, T. J., Rensing, C., Pepper, I. A. N. L. (2010). New Approaches for Bioaugmentation as a Remediation Technology *New Approaches for Bioaugmentation as a Remediation Technology*, 34(5), 447-494. <https://doi.org/10.1080/10643380490452362>
- Georgieva, S., Godjevargova, T., Portaccio, M., Lepore, M., Mita, D. G. (2008). Advantages in using non-isothermal bioreactors in bioremediation of water polluted by phenol by means of immobilized laccase from *Rhus vernicifera*. *Journal of Molecular Catalysis B: Enzymatic*, 55(3-4), 177-184. <https://doi.org/10.1016/j.molcatb.2008.03.011>
- Gerhardt, K. E., Huang, X. D., Glick, B. R., Greenberg, B. M. (2009). Phytoremediation and rhizoremediation of organic soil contaminants: potential and challenges. *Plant science*. 176(1), 20-30. <https://doi.org/10.1016/j.plantsci.2008.09.014>
- Ghatak, H.R. (2014). Advanced oxidation processes for the treatment of biorecalcitrant organics in wastewater. *Critical Reviews in Environmental Science and Technology*, 44(11), 1167-1219. <https://doi.org/10.1080/10643389.2013.763581>
- Ghoneim, M. M., El-Desoky, H. S., Zidan, N. M. (2011). Electro-Fenton oxidation of Sunset Yellow FCF azo-dye in aqueous solutions. *Desalination*, 274(1-3), 22-30. <https://doi.org/10.1016/j.desal.2011.01.062>
- Gong, X., Wang, H., Yang, C., Li, Q., Chen, X., Hu, J. (2015). Photocatalytic degradation of high ammonia concentration wastewater by TiO₂. *Future Cities Environ*, 1(1), 1–12. <https://doi.org/10.1186/s40984-015-0012-9>
- Govindan, K., Raja, M., Noel, M., James, E.J. (2014). Degradation of pentachlorophenol by hydroxyl radicals and sulfate radicals using electrochemical activation of peroxomonosulfate, peroxydisulfate and hydrogen

- peroxide. *Journal of hazardous materials*, 272, 42-51.
<https://doi.org/10.1016/j.jhazmat.2014.02.036>.
- Graham, N., Chu, W., Lau, C. (2003). Observations of 2, 4, 6-trichlorophenol degradation by ozone. *Chemosphere*, 51(4), 237-243.
[https://doi.org/10.1016/S0045-6535\(02\)00815-9](https://doi.org/10.1016/S0045-6535(02)00815-9)
- Greaves, M.F. (2004). Biological models for leukaemia and lymphoma. IARC Scientific Publications, 157, 351-372.
<http://europepmc.org/abstract/MED/15055306>
- Guo, R., Liang, X., Chen, J., Wu, W., Zhang, Q., Martens, D., & Kettrup, A. (2004). Prediction of soil organic carbon partition coefficients by soil column liquid chromatography. *Journal of Chromatography A*, 1035(1), 31-36.
<https://doi.org/10.1016/j.chroma.2004.02.043>
- Guo, X., Zhang, S., Shan, X.Q. (2008). Adsorption of metal ions on lignin. *Journal of Hazardous Material*, 151(1), 134-142.
<https://doi.org/10.1016/j.jhazmat.2007.05.065>
- Guo, Y., Zhou, B. (2013). Thyroid endocrine system disruption by pentachlorophenol: An in vitro and in vivo assay. *Aquatic Toxicology*, 142-143, 138-145.
<https://doi.org/https://doi.org/10.1016/j.aquatox.2013.08.005>
- Hägglblom, M. M., Young, L. Y. (1995). Anaerobic degradation of halogenated phenols by sulfate-reducing consortia. *Applied and environmental microbiology*, 61(4), 1546-1550. <https://doi.org/10.1002/aic.14150>
- Hamad, B. K., Noor, A. M., Afida, A. R., Mohd Asri, M. N. (2010). High removal of 4-chloroguaiacol by high surface area of oil palm shell-activated carbon activated with NaOH from aqueous solution. *Desalination*, 257(1-3), 1-7.
<https://doi.org/10.1016/j.desal.2010.03.007>
- Hanson, R., Dodoo, D.K., Essumang, D.K., Blay, J., Yankson, K. (2007). The effect of some selected pesticides on the growth and reproduction of fresh water *Oreochromis niloticus*, *Chrysiethys nigrodigitatus* and *Clarias gariepinus*. *Bulletin of Environmental Contamination and Toxicology*, 79(5), 544-547.
<https://doi.org/10.1007/s00128-007-9279-3>

- Hardin, I.R., Wilson, S.S., Dhandapani, R., Dhende, V. (2009). An assessment of the validity of claims for “Bamboo” fibers. American Association of Textile Chemists and Colorists International Conference 2009, October, 250–256.
- Haritash, A.K., Dutta, S., Sharma, A., 2017. Phosphate uptake and translocation in a tropical Canna-based constructed wetland. *Ecological Processes*. 6(1), 1-7. <https://doi.org/10.1186/s13717-017-0079-3>
- Haritash, A.K., Sharma, A., Bahel, K. (2015). The potential of Canna lily for wastewater treatment under Indian conditions. *International journal of phytoremediation*, 17(10), 999-1004. <https://doi.org/10.1080/15226514.2014.1003790>
- Hartmann, J., Bartels, P., Mau, U., Witter, M., Tümping, W.V., Hofmann, J., Nietzsche, E. (2008). Degradation of the drug diclofenac in water by sonolysis in presence of catalysts. *Chemosphere*, 70(3), 453-461. <https://doi.org/10.1016/j.chemosphere.2007.06.063>
- Hatier, J. H., & Gould, K. S. (2008). Foliar anthocyanins as modulators of stress signals. *Journal of Theoretical Biology*, 253(3), 625–627.
- He, Y., Xu, J., Ma, Z., Wang, H., & Wu, Y. (2007). Profiling of PLFA: implications for nonlinear spatial gradient of PCP degradation in the vicinity of *Lolium perenne* L. roots. *Soil Biology and Biochemistry*, 39(5), 1121-1129. <https://doi.org/https://doi.org/10.1016/j.soilbio.2006.11.023>
- He, Y., Xu, J., Tang, C., & Wu, Y. (2005). Facilitation of pentachlorophenol degradation in the rhizosphere of ryegrass (*Lolium perenne* L.). *Soil Biology and Biochemistry*, 37(11), 2017-2024. <https://doi.org/https://doi.org/10.1016/j.soilbio.2005.03.002>
- Hechmi, N., Aissa, N. B., Abdenaceur, H., & Jedidi, N. (2014). Phytoremediation efficiency of a PCP-contaminated soil using four plant species as mono-and mixed cultures. *International journal of phytoremediation*, 16(12), 1241-1256. <https://doi.org/10.1016/j.ultsonch.2006.10.002>
- Hechmi, N., Aissa, N. B., Abdenaceur, H., & Jedidi, N. (2014). Phytoremediation efficiency of a PCP-contaminated soil using four plant species as mono-and mixed cultures. *International journal of phytoremediation*, 16(12), 1241-1256. <https://doi.org/10.1080/15226514.2013.828009>

- Hechmi, N., Aissa, N. B., Abdennaceur, H., & Jedidi, N. (2013). Phytoremediation potential of maize (*Zea mays* L.) in co-contaminated soils with pentachlorophenol and cadmium. *International journal of phytoremediation*, 15(7), 703-713. <https://doi.org/10.1080/15226514.2012.723067>
- Hernández, T., García, E., & García, C. (2015). A strategy for marginal semiarid degraded soil restoration: A sole addition of compost at a high rate. A five-year field experiment. *Soil Biology and Biochemistry*, 89, 61-71. <https://doi.org/10.1016/j.soilbio.2015.06.023>
- Hidalgo, A. M., León, G., Gómez, M., Murcia, M. D., Gómez, E., & Gómez, J. L. (2013). Application of the Spiegler–Kedem–Kachalsky model to the removal of 4-chlorophenol by different nanofiltration membranes. *Desalination*, 315, 70-75. <https://doi.org/10.1016/j.desal.2012.10.008>
- Hirai, H., Nakanishi, S., & Nishida, T. (2004). Oxidative dechlorination of methoxychlor by ligninolytic enzymes from white-rot fungi. *Chemosphere*, 55(4), 641-645. <https://doi.org/https://doi.org/10.1016/j.chemosphere.2003.11.035>
- Hoekstra, E. J., De Weerd, H., De Leer, E. W., & Brinkman, U. A. T. (1999). Natural formation of chlorinated phenols, dibenzo-p-dioxins, and dibenzofurans in soil of a Douglas fir forest. *Environmental science & technology*, 33(15), 2543-2549. <https://doi.org/10.1021/es9900104>
- Hoffmann, M. R., Martin, S. T., Choi, W., & Bahnemann, D. W. (1995). Environmental applications of semiconductor photocatalysis. *Chemical reviews*, 95(1), 69-96. <https://doi.org/10.1021/cr00033a004>
- Holcombe, G. W., Phipps, G. L., & Fiandt, J. T. (1982). Effects of phenol, 2, 4-dimethylphenol, 2, 4-dichlorophenol, and pentachlorophenol on embryo, larval, and early-juvenile fathead minnows (*Pimephales promelas*). *Archives of Environmental Contamination and Toxicology*, 11, 73-78. <https://doi.org/10.1007/BF01055189>
- Hong, P. A., & Zeng, Y. (2002). Degradation of pentachlorophenol by ozonation and biodegradability of intermediates. *Water Research*, 36(17), 4243-4254. [https://doi.org/10.1016/S0043-1354\(02\)00144-6](https://doi.org/10.1016/S0043-1354(02)00144-6)

- Hooived, M., Heederik, D. J., Kogevinas, M., Boffetta, P., Needham, L. L., Patterson Jr, D. G., & Bueno-de-Mesquita, H. B. (1998). Second follow-up of a Dutch cohort occupationally exposed to phenoxy herbicides, chlorophenols, and contaminants. *American journal of epidemiology*, 147(9), 891-899. <https://doi.org/10.1093/oxfordjournals.aje.a009543>
- Hoppin, J. A., Tolbert, P. E., Herrick, R. F., Freedman, D. S., Ragsdale, B. D., Horvat, K. R., & Brann, E. A. (1998). Occupational chlorophenol exposure and soft tissue sarcoma risk among men aged 30-60 years. *American journal of epidemiology*, 148(7), 693-703. <https://doi.org/10.1093/aje/148.7.693>
- Hou, J., Liu, F., Wu, N., Ju, J., & Yu, B. (2016). Efficient biodegradation of chlorophenols in aqueous phase by magnetically immobilized aniline-degrading *Rhodococcus rhodochrous* strain. *Journal of nanobiotechnology*, 14, 1-8. <https://doi.org/10.1186/s12951-016-0158-0>
- Huang, W. J., Fang, G. C., & Wang, C. C. (2005). A nanometer-ZnO catalyst to enhance the ozonation of 2, 4, 6-trichlorophenol in water. *Colloids and Surfaces A: Physicochemical and Engineering Aspects*, 260(1-3), 45-51. <https://doi.org/10.1016/j.colsurfa.2005.01.031>
- Husain, Q., Karim, Z., & Banday, Z. Z. (2010). Decolorization of textile effluent by soluble fenugreek (*Trigonella foenum-graecum* L) seeds peroxidase. *Water, Air, & Soil Pollution*, 212, 319-328. <https://doi.org/10.1007/s11270-010-0345-9>
- IARC (International Agency for Research on Cancer) Overall Evaluations of Carcinogenicity to Humans. 1–82. IARC Monographs; 2004.
- IPCS. (1987). Environmental health criteria 71. Pentachlorophenol . 1–235.
- Ivanciuc, T., Ivanciuc, O., & Klein, D. J. (2006). Prediction of environmental properties for chlorophenols with posetic quantitative super-structure/property relationships (QSSPR). *International Journal of Molecular Sciences*, 7(9), 358-374. <https://doi.org/10.3390/i7090358>
- Janik, F., & Wolf, H. U. (1992). The Ca²⁺-transport-atpase of human erythrocytes as an in vitro toxicity test system—acute effects of some chlorinated compounds. *Journal of applied toxicology*, 12(5), 351-358. <https://doi.org/10.1002/jat.2550120511>

- Jeihanipour, A., Karimi, K., Niklasson, C., & Taherzadeh, M. J. (2010). A novel process for ethanol or biogas production from cellulose in blended-fibers waste textiles. *Waste management*, 30(12), 2504-2509. <https://doi.org/10.1016/j.wasman.2010.06.026>
- Jensen, J. (1996). Chlorophenols in the terrestrial environment. *Reviews of Environmental Contamination and Toxicology: Continuation of Residue Reviews*, 25-51. https://doi.org/10.1007/978-1-4613-8478-6_2.
- Jensen, J. K., Holm, P. E., Nejrup, J., Larsen, M. B., & Borggaard, O. K. (2009). The potential of willow for remediation of heavy metal polluted calcareous urban soils. *Environmental pollution*, 157(3), 931-937. <https://doi.org/https://doi.org/10.1016/j.envpol.2008.10.024>
- Ji, H., Chang, F., Hu, X., Qin, W., & Shen, J. (2013). Photocatalytic degradation of 2, 4, 6-trichlorophenol over g-C₃N₄ under visible light irradiation. *Chemical Engineering Journal*, 218, 183-190. <https://doi.org/10.1016/j.cej.2012.12.033>
- Ji, L. L., Li, F. Y., Luo, Y., Ma, X. P., & Chen, Z. L. (2007). Free radicals in *Carassius auratus* liver: their generation and oxidative stress induced by 2, 4, 6-trichlorophenol. *Ying Yong Sheng tai xue bao= The Journal of Applied Ecology*, 18(1), 129-132.
- Kadhim, H., Graham, C., Barratt, P., Evans, C. S., & Rastall, R. A. (1999). Removal of phenolic compounds in water using *Coriolus versicolor* grown on wheat bran. *Enzyme and Microbial Technology*, 24(5-6), 303-307. [https://doi.org/10.1016/S0141-0229\(98\)00123-9](https://doi.org/10.1016/S0141-0229(98)00123-9)
- Kan, H., Zhao, F., Zhang, X. X., Ren, H., & Gao, S. (2015). Correlations of gut microbial community shift with hepatic damage and growth inhibition of *Carassius auratus* induced by pentachlorophenol exposure. *Environmental Science & Technology*, 49(19), 11894-11902. <https://doi.org/10.1021/acs.est.5b02990>
- Kansal, S. K., & Chopra, M. (2012). Photocatalytic degradation of 2, 6-Dichlorophenol in aqueous phase using titania as a photocatalyst. <https://doi.org/10.4236/eng.2012.48055>
- Kansal, S. K., Kaur, G., & Singh, S. (2009). Studies on the photocatalytic degradation of 2, 3-dichlorophenol using different oxidants in aqueous solutions. *Reaction*

- Kinetics and Catalysis Letters, 98, 177-186. <https://doi.org/10.1007/s11144-009-0058-5>
- Kantar, C., & Oral, O. (2021). Chlorophenolic Compounds and Their Transformation Products by the Heterogeneous Fenton Process: A Review. *Electrokinetic Remediation for Environmental Security and Sustainability*, 541-585. <https://doi.org/10.1002/9781119670186.ch22>
- Kantar, C., Oral, O., Urken, O., Oz, N. A., & Keskin, S. (2019). Oxidative degradation of chlorophenolic compounds with pyrite-Fenton process. *Environmental Pollution*, 247, 349-361. <https://doi.org/10.1016/j.envpol.2019.01.017>
- Karci, A., Arslan-Alaton, I., Olmez-Hanci, T., & Bekbölet, M. (2012). Transformation of 2, 4-dichlorophenol by H₂O₂/UV-C, Fenton and photo-Fenton processes: oxidation products and toxicity evolution. *Journal of Photochemistry and Photobiology A: Chemistry*, 230(1), 65-73. <https://doi.org/10.1016/j.jphotochem.2012.01.003>
- Karim, Z., & Husain, Q. (2010). Application of fly ash adsorbed peroxidase for the removal of bisphenol A in batch process and continuous reactor: Assessment of genotoxicity of its product. *Food and Chemical Toxicology*, 48(12), 3385-3390. <https://doi.org/10.1016/j.fct.2010.09.009>
- Karimi, S., Abdulkhani, A., Karimi, A., Ghazali, A. H. B., & Ahmadun, F. L. R. (2010). The effect of combination enzymatic and advanced oxidation process treatments on the colour of pulp and paper mill effluent. *Environmental technology*, 31(4), 347-356. <https://doi.org/10.1080/09593330903473861>
- Karn, S. K., Chakrabarty, S. K., & Reddy, M. S. (2010a). Pentachlorophenol degradation by *Pseudomonas stutzeri* CL7 in the secondary sludge of pulp and paper mill. *Journal of Environmental Sciences*, 22(10), 1608-1612. [https://doi.org/10.1016/S1001-0742\(09\)60296-5](https://doi.org/10.1016/S1001-0742(09)60296-5)
- Karn, S. K., Chakrabarty, S. K., & Reddy, M. S. (2010b). Pentachlorophenol degradation by *Pseudomonas stutzeri* CL7 in the secondary sludge of pulp and paper mill. *Journal of Environmental Sciences*, 22(10), 1608-1612. [https://doi.org/10.1016/S1001-0742\(09\)60296-5](https://doi.org/10.1016/S1001-0742(09)60296-5)
- Kästner, M., 2000. Degradation of aromatic and polyaromatic compounds. In: Rehm H-J, Reed G, Pühler A, Stadler P (eds) *Biotechnology*, 2nd edition, vol 11b.

- Weinheim, Environmental Processes. Wiley-VCH, pp. 211–239. <https://doi.org/10.1002/9783527620999.ch9m>
- Kavitha, V., & Palanivelu, K. (2004). The role of ferrous ion in Fenton and photo-Fenton processes for the degradation of phenol. *Chemosphere*, 55(9), 1235-1243. <https://doi.org/10.1016/j.chemosphere.2003.12.022>
- Kavitha, V., & Palanivelu, K. (2016). Degradation of phenol and trichlorophenol by heterogeneous photo-Fenton process using Granular Ferric Hydroxide®: comparison with homogeneous system. *International journal of environmental science and technology*, 13, 927-936. <https://doi.org/10.1007/s13762-015-0922-y>
- Kavitha, S. K., & Palanisamy, P. N. (2011). Photocatalytic and sonophotocatalytic degradation of reactive red 120 using dye sensitized TiO₂ under visible light. *International Journal of Materials and Metallurgical Engineering*, 5(1), 1-6.
- Kawaguchi, H. (1992). Photolysis of 2-chlorophenol in natural waters. *Journal of contaminant hydrology*, 9(1-2), 105-114. [https://doi.org/10.1016/0169-7722\(92\)90053-H](https://doi.org/10.1016/0169-7722(92)90053-H)
- Kayan, I., Oz, N. A., & Kantar, C. (2021). Comparison of treatability of four different chlorophenol-containing wastewater by pyrite-Fenton process combined with aerobic biodegradation: Role of sludge acclimation. *Journal of Environmental Management*, 279, 111781. <https://doi.org/10.1016/j.jenvman.2020.11178>
- Khattab, H. (2007). Role of glutathione and polyadenylic acid on the oxidative defense systems of two different cultivars of canola seedlings grown under saline conditions. *Australian Journal of Basic and Applied Sciences*, 1(3), 323-334.
- Kisch, H. (2015). *Semiconductor photocatalysis: principles and applications*. John Wiley & Sons.
- Kishino, T., & Kobayashi, K. (1995). Relation between toxicity and accumulation of chlorophenols at various pH, and their absorption mechanism in fish. *Water Research*, 29(2), 431-442. [https://doi.org/10.1016/0043-1354\(94\)00189-E](https://doi.org/10.1016/0043-1354(94)00189-E)
- Kobayashi, K., Akitake, H., Manabe, K., (1979). Relation between Toxicity and Accumulation of Various Chlorophenols in Goldfish. In *Nippon Suisan Gakkaishi*, 45(2), 173–175. <https://doi.org/10.2331/suisan.45.173>

- Kobkeatthawin, T., Chaveanghong, S., Trakulmututa, J., Amornsakchai, T., Kajitvichyanukul, P., & Smith, S. M. (2022). Photocatalytic activity of TiO₂/g-C₃N₄ nanocomposites for removal of monochlorophenols from water. *Nanomaterials*, 12(16), 2852. <https://doi.org/10.3390/nano12162852>
- Kochany, J., & Bolton, J. R. (1992). Mechanism of photodegradation of aqueous organic pollutants. 2. Measurement of the primary rate constants for reaction of hydroxyl radicals with benzene and some halobenzenes using an EPR spin-trapping method following the photolysis of hydrogen peroxide. *Environmental science & technology*, 26(2), 262-265. <https://doi.org/10.1021/es00026a004>
- Koh, S., McCullar, M. V., & Focht, D. D. (1997). Biodegradation of 2, 4-dichlorophenol through a distal meta-fission pathway. *Applied and environmental microbiology*, 63(5), 2054-2057. <https://doi.org/10.1128/aem.63.5.2054-2057.1997>
- Kondo, T., Yamamoto, H., Tatarazako, N., Kawabe, K., Koshio, M., Hirai, N., & Morita, M. (2005). Bioconcentration factor of relatively low concentrations of chlorophenols in Japanese medaka. *Chemosphere*, 61(9), 1299-1304. <https://doi.org/10.1016/j.chemosphere.2005.03.058>
- Korte, F., Kvesitadze, G., Ugrekhelidze, D., Gordeziani, M., Khatisashvili, G., Buadze, O., Zaalishvili, G., & Coulston, F. (2000). Organic toxicants and plants. *Ecotoxicology and environmental safety*, 47(1), 1-26. <https://doi.org/10.1006/eesa.2000.1929>
- Kringstad, K. P., & Lindström, K. (1984). Spent liquors from pulp bleaching. *Environmental science & technology*, 18(8), 236A-248A. <https://doi.org/10.1021/es00126a714>
- Ku, Y., & Wang, L. K. (2002). Decomposition of 2-chlorophenol in aqueous solutions by ozone and UV/ozone processes in the presence of t-butanol. *Ozone: science & engineering*, 24(2), 133-144. <https://doi.org/10.1080/01919510208901604>
- Kumar, S., Kumari, N., Karmakar, S., Ankit, Singh, R., Behera, M., Rani, A., & Kumar, N. (2020). Advances in plant–microbe-based remediation approaches for environmental cleanup. *Emerging Eco-friendly Green Technologies for Wastewater Treatment*, 103-128. https://doi.org/10.1007/978-981-15-1390-9_5

- Kuo, C. Y., Lo, S. L., & Chan, M. T. (1998). Oxidation of aqueous chlorophenols with photo-Fenton process. *Journal of Environmental Science & Health Part B*, 33(6), 723-747.
- Kuriki, R., Yamamoto, M., Higuchi, K., Yamamoto, Y., Akatsuka, M., Lu, D., Yagi, S., Yoshida, T., Ishitani, O., & Maeda, K. (2017). Robust binding between carbon nitride nanosheets and a binuclear ruthenium (II) complex enabling durable, selective CO₂ reduction under visible light in aqueous solution. *Angewandte Chemie*, 129(17), 4945-4949. <https://doi.org/10.1002/ange.201701627>
- Kurukutla, A. B., Kumar, P. S. S., Anandan, S., & Sivasankar, T. (2015). Sonochemical degradation of rhodamine b using oxidants, hydrogen peroxide/peroxydisulfate/peroxymonosulfate, with Fe²⁺ ion: proposed pathway and kinetics. *Environmental Engineering Science*, 32(2), 129-140. <https://doi.org/10.1089/ees.2014.0328>
- Lachapelle, A., Yavari, S., Pitre, F. E., Courchesne, F., & Brisson, J. (2021). Co-planting of *Salix interior* and *Trifolium pratense* for phytoremediation of trace elements from wood preservative contaminated soil. *International Journal of Phytoremediation*, 23(6), 632-640. <https://doi.org/10.1080/15226514.2020.1847034>
- Laine, M. M., & Jørgensen, K. S. (1997). Effective and safe composting of chlorophenol-contaminated soil in pilot scale. *Environmental science & technology*, 31(2), 371-378. <https://doi.org/10.1021/es960176u>
- Lallai, A., & Mura, G. (2004). Biodegradation of 2-chlorophenol in forest soil: Effect of inoculation with aerobic sewage sludge. *Environmental Toxicology and Chemistry: An International Journal*, 23(2), 325-330. <https://doi.org/10.1897/02-419>
- Lamar, R. T., Larsen, M. J., & Kirk, T. K. (1990). Sensitivity to and degradation of pentachlorophenol by *Phanerochaete* spp. *Applied and Environmental Microbiology*, 56(11), 3519-3526. <https://doi.org/10.1128/aem.56.10.3093-3100.1990>

- Lamb, D. (1998). Large-scale ecological restoration of degraded tropical forest lands: the potential role of timber plantations. *Restoration ecology*, 6(3), 271-279. <https://doi.org/10.1046/j.1526-100X.1998.00632.x>
- Lan, S., Feng, J., Xiong, Y., Tian, S., Liu, S., & Kong, L. (2017). Performance and mechanism of piezo-catalytic degradation of 4-chlorophenol: finding of effective piezo-dechlorination. *Environmental science & technology*, 51(11), 6560-6569. <https://doi.org/10.1021/acs.est.6b06426>
- Lange, C. C., Schneider, B. J., & Orser, C. S. (1996). Verification of the Role of PCP 4-Monooxygenase in Chlorine Elimination from Pentachlorophenol by *Flavobacterium* sp. Strain ATCC 39723. *Biochemical and biophysical research communications*, 219(1), 146-149. <https://doi.org/10.1006/bbrc.1996.0196>
- Laurent, F., Canlet, C., Debrauwer, L., & Pascal-Lorber, S. (2007). Metabolic fate of [¹⁴C]-2, 4-dichlorophenol in tobacco cell suspension cultures. *Environmental Toxicology and Chemistry: An International Journal*, 26(11), 2299-2307. <https://doi.org/10.1897/07-036R.1>
- Laurenti, E., Ghibaudi, E., Ardisson, S., & Ferrari, R. P. (2003). Oxidation of 2, 4-dichlorophenol catalyzed by horseradish peroxidase: characterization of the reaction mechanism by UV-visible spectroscopy and mass spectrometry. *Journal of Inorganic Biochemistry*, 95(2-3), 171-176. [https://doi.org/10.1016/S0162-0134\(03\)00101-6](https://doi.org/10.1016/S0162-0134(03)00101-6)
- Lawrence, A. J., & Poulter, C. (1998). Development of a sub-lethal pollution bioassay using the estuarine amphipod *Gammarus duebeni*. *Water Research*, 32(3), 569-578. [https://doi.org/10.1016/S0043-1354\(97\)00306-0](https://doi.org/10.1016/S0043-1354(97)00306-0)
- Lawrence, S. G. (Ed.). (1981). *Manual for the culture of selected freshwater invertebrates* (Vol. 54). Department of fisheries and oceans.
- Legrini, O., Oliveros, E., & Braun, A. M. (1993). Photochemical processes for water treatment. *Chemical reviews*, 93(2), 671-698. <https://doi.org/10.1021/cr00018a003>
- Lekshmi, P. D., Watson, A. S., & Bai, R. S. (2022). A study on the physiological and biological responses of *Eichhornia crassipes* (Mart.) Solms in relation to

- pollution stress. *Plant Physiology Reports*, 27(2), 308-320.
<https://doi.org/10.1007/s40502-022-00648-x>
- Leontievsky, A., Myasoedova, N., Golovleva, L., Sedarati, M., & Evans, C. (2002). Adaptation of the white-rot basidiomycete *Panus tigrinus* for transformation of high concentrations of chlorophenols. *Applied microbiology and biotechnology*, 59, 599-604. <https://doi.org/10.1007/s00253-002-1037-1>
- Leontievsky, A. A., Myasoedova, N. M., Baskunov, B. P., Evans, C. S., & Golovleva, L. A. (2000). Transformation of 2, 4, 6-trichlorophenol by the white rot fungi *Panus tigrinus* and *Coriolus versicolor*. *Biodegradation*, 11, 331-340. <https://doi.org/10.1023/A:1011154209569>
- Li, J., Ma, M., & Wang, Z. (2010). In vitro profiling of endocrine disrupting effects of phenols. *Toxicology in vitro*, 24(1), 201-207. <https://doi.org/https://doi.org/10.1016/j.tiv.2009.09.008>
- Li, K., Yang, Y., Feng, Y., Ajmal, S., Nabi, I., & Zhang, L. (2019). Efficiently complete degradation of 2, 4-DCP using sustainable photoelectrochemical reduction and sequential oxidation method. *Chemical Engineering Journal*, 378, 122191. <https://doi.org/10.1016/j.cej.2019.122191>
- Li, R., Jin, X., Megharaj, M., Naidu, R., & Chen, Z. (2015). Heterogeneous Fenton oxidation of 2, 4-dichlorophenol using iron-based nanoparticles and persulfate system. *Chemical Engineering Journal*, 264, 587-594. <https://doi.org/10.1016/j.cej.2014.11.128>
- Li, Y., & Loh, K. C. (2005). Cometabolic transformation of high concentrations of 4-chlorophenol in an immobilized cell hollow fiber membrane bioreactor. *Journal of Environmental engineering*, 131(9), 1285-1292. [https://doi.org/10.1061/\(ASCE\)0733-9372\(2005\)131:9\(1285\)](https://doi.org/10.1061/(ASCE)0733-9372(2005)131:9(1285))
- Liao ShaoWei, L. S., & Chang WenLian, C. W. (2004). Heavy metal phytoremediation by water hyacinth at constructed wetlands in Taiwan.
- Liber, K., & Solomon, K. R. (1994). Acute and chronic toxicity of 2, 3, 4, 6-tetrachlorophenol and pentachlorophenol to *Daphnia* and rotifers. *Archives of Environmental Contamination and Toxicology*, 26, 212-221. <https://doi.org/10.1007/BF00224807>

- Lin, Q., Shen, K. L., Zhao, H. M., & Li, W. H. (2008). Growth response of *Zea mays* L. in pyrene–copper co-contaminated soil and the fate of pollutants. *Journal of Hazardous Materials*, 150(3), 515-521. <https://doi.org/10.1016/j.jhazmat.2007.04.132>
- Liu, J., Zhao, Z., Ding, Z., Fang, Z., & Cui, F. (2016). Degradation of 4-chlorophenol in a Fenton-like system using Au–Fe₃O₄ magnetic nanocomposites as the heterogeneous catalyst at near neutral conditions. *RSC advances*, 6(58), 53080-53088. <https://doi.org/10.1039/C6RA10929B>
- Liu, J., Zhao, Z., Shao, P., & Cui, F. (2015). Activation of peroxymonosulfate with magnetic Fe₃O₄–MnO₂ core–shell nanocomposites for 4-chlorophenol degradation. *Chemical Engineering Journal*, 262, 854-861. <https://doi.org/10.1016/j.cej.2014.10.043>
- Liu, M., Zhang, Y., Yang, M., Tian, Z., Ren, L., & Zhang, S. (2012). Abundance and distribution of tetracycline resistance genes and mobile elements in an oxytetracycline production wastewater treatment system. *Environmental science & technology*, 46(14), 7551-7557. <https://doi.org/10.1021/es301145m>
- Loick, N., Hobbs, P. J., Hale, M. D., & Jones, D. L. (2009). Bioremediation of polyaromatic hydrocarbon (PAH)-contaminated soil by composting. *Critical Reviews in Environmental Science and Technology*, 39(4), 271-332. <https://doi.org/10.1080/10643380701413682>
- Lone, M. I., Nabi, A., Dar, N. J., Hussain, A., Nazam, N., Hamid, A., & Ahmad, W. (2017). Toxicogenetic evaluation of dichlorophene in peripheral blood and in the cells of the immune system using molecular and flow cytometric approaches. *Chemosphere*, 167, 520-529. <https://doi.org/10.1016/j.chemosphere.2016.08.131>
- Louie, T. M., Webster, C. M., & Xun, L. (2002). Genetic and biochemical characterization of a 2, 4, 6-trichlorophenol degradation pathway in *Ralstonia eutropha* JMP134. *Journal of bacteriology*, 184(13), 3492-3500. <https://doi.org/10.1128/JB.184.13.3492-3500.2002>
- Lu, M. C., Chen, J. N., & Huang, H. H. (2002). Role of goethite dissolution in the oxidation of 2-chlorophenol with hydrogen peroxide. *Chemosphere*, 46(1), 131-136. [https://doi.org/10.1016/S0045-6535\(01\)00076-5](https://doi.org/10.1016/S0045-6535(01)00076-5)

- Lubzens, E., Minkoff, G., & Marom, S. (1985). Salinity dependence of sexual and asexual reproduction in the rotifer *Brachionus plicatilis*. *Marine Biology*, 85, 123-126. <https://doi.org/10.1007/BF00397430>
- Luo, Y., Su, Y., Lin, R. Z., Shi, H. H., & Wang, X. R. (2006). 2-Chlorophenol induced ROS generation in fish *Carassius auratus* based on the EPR method. *Chemosphere*, 65(6), 1064-1073. <https://doi.org/10.1016/j.chemosphere.2006.02.054>
- Luo, Y., Sui, Y. X., Wang, X. R., & Tian, Y. (2008). 2-chlorophenol induced hydroxyl radical production in mitochondria in *Carassius auratus* and oxidative stress—An electron paramagnetic resonance study. *Chemosphere*, 71(7), 1260-1268. <https://doi.org/10.1016/j.chemosphere.2007.11.066>
- Luo, Y., Wang, X. R., Shi, H. H., Mao, D. Q., Sui, Y. X., & Ji, L. L. (2005). Electron paramagnetic resonance investigation of in vivo free radical formation and oxidative stress induced by 2, 4-dichlorophenol in the freshwater fish *Carassius auratus*. *Environmental Toxicology and Chemistry: An International Journal*, 24(9), 2145-2153. <https://doi.org/10.1897/04-640R.1>
- Lv, Y., Chen, Y., Song, W., & Hu, Y. (2014). Enhanced selection of micro-aerobic pentachlorophenol degrading granular sludge. *Journal of hazardous materials*, 280, 134-142. <https://doi.org/10.1016/j.jhazmat.2014.07.067>
- Ma, Y. S., Sung, C. F., & Lin, J. G. (2010). Degradation of carbofuran in aqueous solution by ultrasound and Fenton processes: effect of system parameters and kinetic study. *Journal of Hazardous Materials*, 178(1-3), 320-325. <https://doi.org/10.1016/j.jhazmat.2010.01.081>
- Madannejad, S., Rashidi, A., Sadeghassani, S., Shemirani, F., & Ghasemy, E. (2018). Removal of 4-chlorophenol from water using different carbon nanostructures: a comparison study. *Journal of Molecular Liquids*, 249, 877-885. <https://doi.org/https://doi.org/10.1016/j.molliq.2017.11.089>
- Madhavan, J., Kumar, P. S. S., Anandan, S., Zhou, M., Grieser, F., & Ashokkumar, M. (2010). Ultrasound assisted photocatalytic degradation of diclofenac in an aqueous environment. *Chemosphere*, 80(7), 747-752. <https://doi.org/10.1016/j.chemosphere.2010.05.018>

- Maleki, A., Mahvi, A. H., & Nabizadeh, F. V. R. (2005). Ultrasonic degradation of phenol and determination of the oxidation by-products toxicity. *Journal of environmental health science & engineering*, 2(3), 201-206.
- Martí, E., Sierra, J., Sánchez, M., Cruañas, R., & Garau, M. A. (2007). Ecotoxicological tests assessment of soils polluted by chromium (VI) or pentachlorophenol. *Science of the Total Environment*, 378(1-2), 53-57. <https://doi.org/10.1016/j.scitotenv.2007.01.012>
- Martin, T. J., Gabure, S., Maise, J., Snipes, S., Peete, M., & Whalen, M. M. (2019). The organochlorine pesticides pentachlorophenol and dichlorodiphenyltrichloroethane increase secretion and production of interleukin 6 by human immune cells. *Environmental toxicology and pharmacology*, 72, 103263. <https://doi.org/10.1016/j.etap.2019.103263>
- Martins, A. D. O., Canalli, V. M., Azevedo, C. M., & Pires, M. (2006). Degradation of pararosaniline (CI Basic Red 9 monohydrochloride) dye by ozonation and sonolysis. *Dyes and Pigments*, 68(2-3), 227-234. <https://doi.org/10.1016/j.dyepig.2005.02.002>
- Massawe, R., Drabo, L., & Whalen, M. (2017). Effects of pentachlorophenol and dichlorodiphenyltrichloroethane on secretion of interferon gamma (IFN γ) and tumor necrosis factor alpha (TNF α) from human immune cells. *Toxicology mechanisms and methods*, 27(3), 223-235. <https://doi.org/10.1080/15376516.2016.1275906>
- Masunaga, S., Susarla, S., Gundersen, J. L., & Yonezawa, Y. (1996). Pathway and rate of chlorophenol transformation in anaerobic estuarine sediment. *Environmental science & technology*, 30(4), 1253-1260. <https://doi.org/10.1021/es950457m>
- Matus, V., Sanchez, M. A., Martínez, M., & González, B. (2003). Efficient degradation of 2, 4, 6-trichlorophenol requires a set of catabolic genes related to tcp genes from *Ralstonia eutropha* JMP134 (pJP4). *Applied and environmental microbiology*, 69(12), 7108-7115. <https://doi.org/10.1128/AEM.69.12.7108-7115.2003>
- Melián, E. P., Díaz, O. G., Rodríguez, J. D., Araña, J., & Peña, J. P. (2013). Adsorption and photocatalytic degradation of 2, 4-dichlorophenol in TiO₂ suspensions. Effect of hydrogen peroxide, sodium peroxodisulphate and ozone. *Applied*

- Catalysis A: General, 455, 227-233.
<https://doi.org/10.1016/j.apcata.2013.02.007>
- Menuet, A., Le Page, Y., Torres, O., Kern, L., Kah, O., & Pakdel, F. (2004). Analysis of the estrogen regulation of the zebrafish estrogen receptor (ER) reveals distinct effects of ERalpha, ERbeta1 and ERbeta2. *Journal of Molecular Endocrinology*, 32(3), 975-986. <https://doi.org/10.1677/jme.0.0320975>
- Michałowicz, J., & Majsterek, I. (2010). Chlorophenols, chlorocatechols and chloroguaiacols induce DNA base oxidation in human lymphocytes (in vitro). *Toxicology*, 268(3), 171-175.
<https://doi.org/https://doi.org/10.1016/j.tox.2009.12.009>
- Mileski, G. J., Bumpus, J. A., Jurek, M. A., & Aust, S. D. (1988). Biodegradation of pentachlorophenol by the white rot fungus *Phanerochaete chrysosporium*. *Applied and Environmental Microbiology*, 54(12), 2885-2889.
<https://doi.org/10.1128/aem.54.12.2885-2889.1988>
- Milliken, C. E., Meier, G. P., Sowers, K. R., & May, H. D. (2004). Chlorophenol production by anaerobic microorganisms: transformation of a biogenic chlorinated hydroquinone metabolite. *Applied and Environmental Microbiology*, 70(4), 2494-2496. <https://doi.org/10.1128/AEM.70.4.2494-2496.2004>
- Min, K., Freeman, C., Kang, H., & Choi, S. U. (2015). The regulation by phenolic compounds of soil organic matter dynamics under a changing environment. *BioMed research international*, 2015(1), 825098.
<https://doi.org/10.1155/2015/825098>
- Minz, S., Gupta, R., & Garg, S. (2019). Degradation of 4-chlorophenol using homogeneous Fenton's oxidation process: kinetic study. In *Sustainable Engineering: Proceedings of EGRWSE 2018* (pp. 213-223). Springer Singapore.
https://doi.org/10.1007/978-981-13-6717-5_21
- Mirabelli, M. C., Hoppin, J. A., Tolbert, P. E., Herrick, R. F., Gnepp, D. R., & Brann, E. A. (2000). Occupational exposure to chlorophenol and the risk of nasal and nasopharyngeal cancers among US men aged 30 to 60. *American journal of industrial medicine*, 37(5), 532-541.

- Mohn, W. W., & Kennedy, K. J. (1992). Reductive dehalogenation of chlorophenols by Desulfomonile tiedjei DCB-1. *Applied and Environmental Microbiology*, 58(4), 1367-1370. <https://doi.org/10.1128/aem.58.4.1367-1370.1992>
- Moozyckine, A. U., & Davies, D. M. (2002). Green S as a prototype for an environmentally-degradable dye: the concept of a 'green dye' in future Green Chemistry. *Green Chemistry*, 4(5), 452-458. <https://doi.org/10.1039/b204556g>
- Muñoz, I., Rieradevall, J., Torrades, F., Peral, J., & Domènech, X. (2006). Environmental assessment of different advanced oxidation processes applied to a bleaching Kraft mill effluent. *Chemosphere*, 62(1), 9-16. <https://doi.org/10.1016/j.chemosphere.2005.04.044>
- Munoz, M., de Pedro, Z. M., Casas, J. A., & Rodriguez, J. J. (2013). Chlorophenols breakdown by a sequential hydrodechlorination-oxidation treatment with a magnetic Pd-Fe/ γ -Al₂O₃ catalyst. *Water research*, 47(9), 3070-3080. <https://doi.org/10.1016/j.watres.2013.03.024>
- Musteret, C. P., & Teodosiu, C. (2017). Experimental assesment of nanofiltration for the removal of chlorophenols from aqueous effluents. *Environmental Engineering and Management Journal*, 16(4), 793-800.
- Nakagawa, S., & Shimokawa, T. (2002). Degradation of halogenated carbons in alkaline alcohol. *Radiation physics and Chemistry*, 63(2), 151-156. [https://doi.org/10.1016/S0969-806X\(01\)00220-1](https://doi.org/10.1016/S0969-806X(01)00220-1)
- Nandakumar, S., Pipil, H., Ray, S., & Haritash, A. K. (2019). Removal of phosphorous and nitrogen from wastewater in Brachiaria-based constructed wetland. *Chemosphere*, 233, 216-222. <https://doi.org/10.1016/j.chemosphere.2019.05.240>
- Neppolian, B., Park, J. S., & Choi, H. (2004). Effect of Fenton-like oxidation on enhanced oxidative degradation of para-chlorobenzoic acid by ultrasonic irradiation. *Ultrasonics Sonochemistry*, 11(5), 273-279. <https://doi.org/10.1016/j.ultsonch.2003.11.001>
- Nesir, N. (2010). Potential Use of Water Hyacinth (*E. Crassipes*) for Wastewater Treatment in Serbia. Retrieved from www.balwois.com/balwois/administration/full-paper/ffp-623.pdf

- Nicholson, D. K., Woods, S. L., Istok, J. D., & Peek, D. C. (1992). Reductive dechlorination of chlorophenols by a pentachlorophenol-acclimated methanogenic consortium. *Applied and Environmental Microbiology*, 58(7), 2280-2286. <https://doi.org/10.1128/aem.58.7.2280-2286.1992>
- Niimi, A. J., & Cho, C. Y. (1983). Laboratory and field analysis of pentachlorophenol (PCP) accumulation by salmonids. *Water research*, 17(12), 1791-1795.
- Niu, H., Zheng, Y., Wang, S., Zhao, L., Yang, S., & Cai, Y. (2018). Continuous generation of hydroxyl radicals for highly efficient elimination of chlorophenols and phenols catalyzed by heterogeneous Fenton-like catalysts yolk/shell Pd@Fe₃O₄@ metal organic frameworks. *Journal of hazardous materials*, 346, 174-183. <https://doi.org/10.1016/j.jhazmat.2017.12.027>
- Njoku, K. L., Oboh, B. O., Akinola, M. O., & Ajasa, A. O. (2012). Comparative effects of *Abelmoschus esculentus* (L) Moench (Okro) and *Corchorus olitorius* L (Jew Mallow) on soil contaminated with mixture of petroleum products. *Research Journal of Environmental and Earth Sciences*, 4(4), 413-418.
- Northup, R. R., Dahlgren, R. A., & McColl, J. G. (1998). Polyphenols as regulators of plant-litter-soil interactions in northern California's pygmy forest: a positive feedback?. *Plant-induced soil changes: Processes and feedbacks*, 189-220. https://doi.org/10.1007/978-94-017-2691-7_10
- Nowak, A., Greń, I., & Mroziak, A. (2016). Changes in fatty acid composition of *Stenotrophomonas maltophilia* KB2 during co-metabolic degradation of monochlorophenols. *World Journal of Microbiology and Biotechnology*, 32, 1-10. <https://doi.org/10.1007/s11274-016-2160-y>
- Ohtsubo, Y., Miyauchi, K., Kanda, K., Hatta, T., Kiyohara, H., Senda, T., Nagata, Y., Mitsui, Y., & Takagi, M. (1999). PcpA, which is involved in the degradation of pentachlorophenol in *Sphingomonas chlorophenolica* ATCC39723, is a novel type of ring-cleavage dioxygenase. *FEBS letters*, 459(3), 395-398. [https://doi.org/https://doi.org/10.1016/S0014-5793\(99\)01305-8](https://doi.org/https://doi.org/10.1016/S0014-5793(99)01305-8)
- Olaniran, A. O., & Igbinsola, E. O. (2011). Chlorophenols and other related derivatives of environmental concern: properties, distribution and microbial degradation processes. *Chemosphere*, 83(10), 1297-1306. <https://doi.org/10.1016/j.chemosphere.2011.04.009>

- Olu-Owolabi, B. I., Alabi, A. H., Diagboya, P. N., Unuabonah, E. I., & Düring, R. A. (2017). Adsorptive removal of 2, 4, 6-trichlorophenol in aqueous solution using calcined kaolinite-biomass composites. *Journal of environmental management*, 192, 94-99. <https://doi.org/10.1016/j.jenvman.2017.01.055>
- Adeola, A. O. (2018). Fate and toxicity of chlorinated phenols of environmental implications: a review. *Medicinal and analytical chemistry international journal*, 2(4), 000126. <https://doi.org/10.23880/macij-16000126>
- Ononye, A. I., McIntosh, A. R., & Bolton, J. R. (1986). Mechanism of the photochemistry of p-benzoquinone in aqueous solutions. 1. Spin trapping and flash photolysis electron paramagnetic resonance studies. *The Journal of Physical Chemistry*, 90(23), 6266-6270. <https://doi.org/10.1021/j100281a039>
- Oputu, O., Chowdhury, M., Nyamayaro, K., Fatoki, O., & Fester, V. (2015). Catalytic activities of ultra-small β -FeOOH nanorods in ozonation of 4-chlorophenol. *Journal of Environmental Sciences*, 35, 83-90. <https://doi.org/10.1016/j.jes.2015.02.013>
- Orser, C. S., & Lange, C. C. (1994). Molecular analysis of pentachlorophenol degradation. *Biodegradation*, 5, 277-288. <https://doi.org/10.1007/BF00696465>
- Ortiz, I., Rivero, M. J., & Margallo, M. (2019). Advanced oxidative and catalytic processes. In *Sustainable Water and Wastewater Processing* (pp. 161-201). Elsevier. <https://doi.org/10.1016/B978-0-12-816170-8.00006-5>
- Othmer, C. G., & Overberger, G. T. (1983) Seaborg Eds. Ultrasonics. In *Kirk-Othmer Encyclopedia of Chemical Technology* 23, 462. <https://doi.org/10.1021/j150469a016>
- Ott, M., Gogvadze, V., Orrenius, S., & Zhivotovsky, B. (2007). Mitochondria, oxidative stress and cell death. *Apoptosis*, 12, 913-922. <https://doi.org/10.1007/s10495-007-0756-2>
- Oturan, N., Panizza, M., & Oturan, M. A. (2009). Cold incineration of chlorophenols in aqueous solution by advanced electrochemical process electro-Fenton. Effect of number and position of chlorine atoms on the degradation kinetics. *The Journal of Physical Chemistry A*, 113(41), 10988-10993. <https://doi.org/10.1021/jp9069674>

- Oyama, T., Otsu, T., Hidano, Y., Koike, T., Serpone, N., & Hidaka, H. (2011). Enhanced remediation of simulated wastewaters contaminated with 2-chlorophenol and other aquatic pollutants by TiO₂-photoassisted ozonation in a sunlight-driven pilot-plant scale photoreactor. *Solar Energy*, 85(5), 938-944. <https://doi.org/10.1016/j.solener.2011.02.008>
- Paaso, N., Peuravuori, J., Lehtonen, T., & Pihlaja, K. (2002). Sediment–dissolved organic matter equilibrium partitioning of pentachlorophenol: The role of humic matter. *Environment international*, 28(3), 173-183. [https://doi.org/10.1016/S0160-4120\(02\)00027-2](https://doi.org/10.1016/S0160-4120(02)00027-2)
- Paisio, C. E., Agostini, E., & González, P. S. (2021). Application of two bioassays as potential indicators of phenol phytoremediation efficiency by tobacco hairy roots. *Environmental Technology*, 42(6), 964-971. <https://doi.org/10.1080/09593330.2019.1649471>
- Paisio, C. E., Fernandez, M., González, P. S., Talano, M. A., Medina, M. I., & Agostini, E. (2018). Simultaneous phytoremediation of chromium and phenol by *Lemma minuta* Kunth: a promising biotechnological tool. *International journal of environmental science and technology*, 15, 37-48. <https://doi.org/10.1007/s13762-017-1368-1>
- Singh, D. P., & Pandey, V. C. (2020). *Phytoremediation potential of perennial grasses*. Elsevier. <https://books.google.co.in/books?id=d33ZDwAAQBAJ>
- Pandiyan, T., Rivas, O. M., Martínez, J. O., Amezcua, G. B., & Martínez-Carrillo, M. A. (2002). Comparison of methods for the photochemical degradation of chlorophenols. *Journal of Photochemistry and Photobiology A: Chemistry*, 146(3), 149-155. [https://doi.org/10.1016/S1010-6030\(01\)00606-2](https://doi.org/10.1016/S1010-6030(01)00606-2)
- Pare, B., Jonnalagadda, S. B., Tomar, H., Singh, P., & Bhagwat, V. W. (2008). ZnO assisted photocatalytic degradation of acridine orange in aqueous solution using visible irradiation. *Desalination*, 232(1-3), 80-90. <https://doi.org/10.1016/j.desal.2008.01.007>
- Pascal-Lorber, S., Despoux, S., Rathahao, E., Canlet, C., Debrauwer, L., & Laurent, F. (2008). Metabolic fate of [14C] chlorophenols in radish (*Raphanus sativus*), lettuce (*Lactuca sativa*), and spinach (*Spinacia oleracea*). *Journal of agricultural and food chemistry*, 56(18), 8461-8469. <https://doi.org/10.1021/jf8016354>

- Patel, B. P., & Kumar, A. (2016). Biodegradation of 2, 4-dichlorophenol by *Bacillus endophyticus* strain: optimization of experimental parameters using response surface methodology and kinetic study. *Desalination and Water Treatment*, 57(34), 15932-15940. <https://doi.org/10.1080/19443994.2015.1076351>
- Pedroza, A. M., Mosqueda, R., Alonso-Vante, N., & Rodríguez-Vázquez, R. (2007). Sequential treatment via *Trametes versicolor* and UV/TiO₂/RuxSey to reduce contaminants in waste water resulting from the bleaching process during paper production. *Chemosphere*, 67(4), 793-801. <https://doi.org/10.1016/j.chemosphere.2006.10.015>
- Peng, S., Tang, Z., Jiang, W., Wu, D., Hong, S., & Xing, B. (2017). Mechanism and performance for adsorption of 2-chlorophenol onto zeolite with surfactant by one-step process from aqueous phase. *Science of the Total Environment*, 581, 550-558. <https://doi.org/https://doi.org/10.1016/j.scitotenv.2016.12.163>
- Pera-Titus, M., García-Molina, V., Baños, M. A., Giménez, J., & Esplugas, S. (2004). Degradation of chlorophenols by means of advanced oxidation processes: a general review. *Applied Catalysis B: Environmental*, 47(4), 219-256. <https://doi.org/10.1016/j.apcatb.2003.09.010>
- Perepelkin, K. E. E. (2007). Lyocell fibres based on direct dissolution of cellulose in N-methylmorpholine N-oxide: development and prospects. *Fibre Chemistry*, 39(2), 163-172. <https://doi.org/10.1007/s10692-007-0032-9>
- Pérez-Moya, M., Graells, M., del Valle, L. J., Centelles, E., & Mansilla, H. D. (2007). Fenton and photo-Fenton degradation of 2-chlorophenol: multivariate analysis and toxicity monitoring. *Catalysis Today*, 124(3-4), 163-171. <https://doi.org/10.1016/j.cattod.2007.03.034>
- Peternel, I., Koprivanac, N., & Grcic, I. (2012). Mineralization of p-chlorophenol in water solution by AOPs based on UV irradiation. *Environmental technology*, 33(1), 27-36. <https://doi.org/10.1080/09593330.2010.504233>
- Peuravuori, J., Paaso, N., & Pihlaja, K. (2002). Sorption behaviour of some chlorophenols in lake aquatic humic matter. *Talanta*, 56(3), 523-538. [https://doi.org/10.1016/S0039-9140\(01\)00579-3](https://doi.org/10.1016/S0039-9140(01)00579-3)
- Pilon-Smits, E. (2005). Phytoremediation. *Annu. Rev. Plant Biol.*, 56(1), 15-39. <https://doi.org/10.1146/annurev.arplant.56.032604.144214>

- Pimentel, M., Oturan, N., Dezotti, M., & Oturan, M. A. (2008). Phenol degradation by advanced electrochemical oxidation process electro-Fenton using a carbon felt cathode. *Applied Catalysis B: Environmental*, 83(1-2), 140-149. <https://doi.org/10.1016/j.apcatb.2008.02.011>
- Guo, P., Wang, J., Kang, C., Chen, W., Chen, T., & Lin, X. (2009, June). The Effects on Solubility of PCP by Sunflower (*Helianthus Annuus*) Root Exudates in Different Environmental Conditions. In 2009 3rd International Conference on Bioinformatics and Biomedical Engineering (pp. 1-4). IEEE. <https://doi.org/10.1109/ICBBE.2009.5163605>
- Pipil, H., Haritash, A. K., & Reddy, K. R. (2021). Seasonal variability and kinetics of phosphate removal in a Phragmites-based engineered wetland. *Rendiconti Lincei. Scienze Fisiche e Naturali*, 32(4), 729-735. <https://doi.org/10.1007/s12210-021-01017-w>
- Pipil, H., Yadav, S., Chawla, H., Taneja, S., Verma, M., Singla, N., & Haritash, A. K. (2022). Comparison of TiO₂ catalysis and Fenton's treatment for rapid degradation of Remazol Red Dye in textile industry effluent. *Rendiconti Lincei. Scienze Fisiche e Naturali*, 33(1), 105-114. <https://doi.org/10.1007/s12210-021-01040-x>
- Pipil, H., Yadav, S., Kumar, S., & Haritash, A. K. (2024a). Synergistic potency of ultrasound and solar energy towards oxidation of 2, 4-dichlorophenol: a chemometrics approach. *Environmental Science and Pollution Research*, 31(5), 8186-8209. <https://doi.org/10.1007/s11356-023-31598-y>
- Pipil, H., Yadav, S., Kumar, S., & Haritash, A. K. (2024b). Evaluating the photocatalytic degradation efficacy of 2, 4, 6-trichlorophenol: performance evaluation and influencing factors. *Journal of Water and Climate Change*, 15(3), 1091-1101. <https://doi.org/10.2166/wcc.2024.483>
- PIWONI, M. D., WILSON, J. T., WALTERS, D. M., WILSON, B. H., & ENFIELD, C. G. (1986). Behavior of organic pollutants during rapid-infiltration of wastewater into soil: I. Processes, definition, and characterization using a microcosm. *Hazardous waste and hazardous materials*, 3(1), 43-55. <https://doi.org/10.1089/hwm.1986.3.43>

- Poirier, D. G., Westlake, G. F., & Abernethy, S. I. (1988). *Daphnia magna* acute lethality toxicity test protocol. http://www.agrienvarchive.ca/download/Daphnia_toxicity_test_protocol_88.pdf
- Pollutants, P.O., 2010. Exploration of management options for Pentachlorophenol (PCP). May, 18–20.
- Polprasert, C., & Khatiwada, N. R. (1998). An integrated kinetic model for water hyacinth ponds used for wastewater treatment. *Water Research*, 32(1), 179-185. [http://dx.doi.org/10.1016/S0043-1354\(97\)00191-7](http://dx.doi.org/10.1016/S0043-1354(97)00191-7)
- Potgieter, J. H., Bada, S. O., & Potgieter-Vermaak, S. S. (2009). Adsorptive removal of various phenols from water by South African coal fly ash. *Water Sa*, 35(1). <https://doi.org/10.4314/wsa.v35i1.76646>
- Poulopoulos, S. G., Nikolaki, M., Karampetsos, D., & Philippopoulos, C. J. (2008). Photochemical treatment of 2-chlorophenol aqueous solutions using ultraviolet radiation, hydrogen peroxide and photo-Fenton reaction. *Journal of Hazardous Materials*, 153(1-2), 582-587. <https://doi.org/10.1016/j.jhazmat.2007.09.002>
- Pulford, I. D., & Watson, C. (2003). Phytoremediation of heavy metal-contaminated land by trees—a review. *Environment international*, 29(4), 529-540. [https://doi.org/https://doi.org/10.1016/S0160-4120\(02\)00152-6](https://doi.org/https://doi.org/10.1016/S0160-4120(02)00152-6)
- Purnamawati, R., Taufikurahman, R. A., Putra, C. R., Dzakamala, D., Rahmatilah, F., & Ashgi, F. (2020). The physiological responses of water hyacinth (*Eichhornia crassipes* (mart). Solms) and water lettuce (*Pistia stratiotes* L.) as trivalent chromium bioaccumulator. *3BIO Journal of Biological Science Technology and Management*, 2(1), 2655-8777. <https://doi.org/10.5614/3bio.2020.2.1.2>
- Qi, C., Liu, X., Zhao, W., Lin, C., Ma, J., Shi, W., ... & Xiao, H. (2015). Degradation and dechlorination of pentachlorophenol by microwave-activated persulfate. *Environmental Science and Pollution Research*, 22, 4670-4679. <https://doi.org/10.1007/s11356-014-3718-6>
- Quan, X., Shi, H., Wang, J., & Qian, Y. (2003). Biodegradation of 2, 4-dichlorophenol in sequencing batch reactors augmented with immobilized mixed culture. *Chemosphere*, 50(8), 1069-1074. [https://doi.org/10.1016/S0045-6535\(02\)00625-2](https://doi.org/10.1016/S0045-6535(02)00625-2)

- Ranjan, J., Joshi, V., Mandal, T., & Mandal, D. D. (2021). Ecotoxicological risk assessment of pentachlorophenol, an emerging DBP to plants: evaluation of oxidative stress and antioxidant responses. *Environmental Science and Pollution Research*, 28, 27954-27965. <https://doi.org/10.1007/s11356-021-12578-6>
- Raza, W., Lee, J., Raza, N., Luo, Y., Kim, K. H., & Yang, J. (2019). Removal of phenolic compounds from industrial waste water based on membrane-based technologies. *Journal of industrial and engineering chemistry*, 71, 1-18. <https://doi.org/10.1016/j.jiec.2018.11.024>
- Reddy, G. V. B., & Gold, M. H. (2000). Degradation of pentachlorophenol by *Phanerochaete chrysosporium*: intermediates and reactions involved. *Microbiology*, 146(2), 405-413. <https://doi.org/https://doi.org/10.1099/00221287-146-2-405>
- Reddy, G. V. B., Sollewijn Gelpke, M. D., & Gold, M. H. (1998). Degradation of 2, 4, 6-trichlorophenol by *Phanerochaete chrysosporium*: involvement of reductive dechlorination. *Journal of Bacteriology*, 180(19), 5159-5164. <https://doi.org/10.1128/JB.180.19.5159-5164.1998>
- Reid, B. J., Jones, K. C., & Semple, K. T. (2000). Bioavailability of persistent organic pollutants in soils and sediments—a perspective on mechanisms, consequences and assessment. *Environmental Pollution*, 108(1), 103-112. [https://doi.org/10.1016/S0269-7491\(99\)00206-7](https://doi.org/10.1016/S0269-7491(99)00206-7)
- Rengaraj, S., & Li, X. Z. (2006). Enhanced photocatalytic activity of TiO₂ by doping with Ag for degradation of 2, 4, 6-trichlorophenol in aqueous suspension. *Journal of Molecular Catalysis A: Chemical*, 243(1), 60-67. <https://doi.org/10.1016/j.molcata.2005.08.010>
- Riser-Roberts E., (1998). *Bioremediation of petroleum contaminated soils*. Lewis Publishers, Boca Raton.
- Sai, K., Kang, K. S., Hirose, A., Hasegawa, R., Trosko, J. E., & Inoue, T. (2001). Inhibition of apoptosis by pentachlorophenol in v-myc-transfected rat liver epithelial cells: relation to down-regulation of gap junctional intercellular communication. *Cancer letters*, 173(2), 163-174. [https://doi.org/https://doi.org/10.1016/S0304-3835\(01\)00616-4](https://doi.org/https://doi.org/10.1016/S0304-3835(01)00616-4)

- Saito, H., Sudo, M., Shigeoka, T., & Yamauchi, F. (1991). In vitro cytotoxicity of chlorophenols to goldfish GF-scale (GFS) cells and quantitative structure-activity relationships. *Environmental Toxicology and Chemistry: An International Journal*, 10(2), 235-241. <https://doi.org/10.1002/etc.5620100212>
- Sakshi, Singh, S. K., & Haritash, A. K. (2019). Polycyclic aromatic hydrocarbons: soil pollution and remediation. *International Journal of Environmental Science and Technology*, 16, 6489-6512. <https://doi.org/10.1007/s13762-019-02414-3>
- Salkinoja-Salonen, M. S., Hakulinen, R., Valo, R., & Apajalahti, J. (1983). Biodegradation of recalcitrant organochlorine compounds in fixed film reactors. *Water Science and Technology*, 15(8-9), 309-319. <https://doi.org/10.2166/wst.1983.0174>
- Samanta, S. K., Singh, O. V., & Jain, R. K. (2002). Polycyclic aromatic hydrocarbons: environmental pollution and bioremediation. *TRENDS in Biotechnology*, 20(6), 243-248. [https://doi.org/10.1016/S0167-7799\(02\)01943-1](https://doi.org/10.1016/S0167-7799(02)01943-1)
- Sandhu, A., Halverson, L. J., & Beattie, G. A. (2007). Bacterial degradation of airborne phenol in the phyllosphere. *Environmental Microbiology*, 9(2), 383-392. <https://doi.org/10.1111/j.1462-2920.2006.01149.x>
- Sanford, R. A., Cole, J. R., Löffler, F. E., & Tiedje, J. M. (1996). Characterization of *Desulfitobacterium chlororespirans* sp. nov., which grows by coupling the oxidation of lactate to the reductive dechlorination of 3-chloro-4-hydroxybenzoate. *Applied and environmental microbiology*, 62(10), 3800-3808. <https://doi.org/10.1128/aem.62.10.3800-3808.1996>
- Santos-Juanes, L., García-Ballesteros, S., Vercher, R. F., Amat, A. M., & Arques, A. (2019). Commercial steel wool used for Zero Valent Iron and as a source of dissolved iron in a combined red-ox process for pentachlorophenol degradation in tap water. *Catalysis Today*, 328, 252-258. <https://doi.org/10.1016/j.cattod.2019.01.007>
- Saritha, P., Raj, D. S. S., Aparna, C., Laxmi, P. N. V., Himabindu, V., & Anjaneyulu, Y. (2009). Degradative oxidation of 2, 4, 6 trichlorophenol using advanced oxidation processes—a comparative study. *Water, air, and soil pollution*, 200, 169-179. <https://doi.org/10.1007/s11270-008-9901-y>

- Schellenberg, K., Leuenberger, C., & Schwarzenbach, R. P. (1984). Sorption of chlorinated phenols by natural sediments and aquifer materials. *Environmental science & technology*, 18(9), 652-657. <https://doi.org/10.1021/es00127a005>
- Sedarati, M. R., Keshavarz, T., Leontievsky, A. A., & Evans, C. S. (2003). Transformation of high concentrations of chlorophenols by the white-rot basidiomycete *Trametes versicolor* immobilized on nylon mesh. *Electronic Journal of Biotechnology*, 6(2), 104-114.
- Sharma, A., Ahmad, J., & Flora, S. J. S. (2018). Application of advanced oxidation processes and toxicity assessment of transformation products. *Environmental research*, 167, 223-233. <https://doi.org/10.1016/j.envres.2018.07.010>
- Sharma, A., Verma, M., & Haritash, A. K. (2016). Degradation of toxic azo dye (AO7) using Fenton's process. *Adv Environ Res*, 5(3), 189-200. <https://doi.org/10.12989/aer.2016.5.3.189>
- Sharma, G., Kumar, A., Naushad, M., Sharma, S., Ghfar, A. A., Ahamad, T., Si, C., & Stadler, F. J. (2019). Graphene oxide supported La/Co/Ni trimetallic nano-scale systems for photocatalytic remediation of 2-chlorophenol. *Journal of Molecular Liquids*, 294, 111605. <https://doi.org/10.1016/j.molliq.2019.111605>
- Shenai, V. A. (2001). Non-ecofriendly textile chemicals and their probable substitutes- An Overview. *Indian Journal of Fibre and Textile Research*. 26(1-2), 50-54. <http://nopr.niscpr.res.in/handle/123456789/24913>
- Sherburne, A. (2009). Achieving sustainable textiles: a designer's perspective. In *Sustainable Textiles* (pp. 3-32). Woodhead Publishing. <https://doi.org/10.1533/9781845696948.1.3>
- Shih, Y. H., Chen, M. Y., Su, Y. F., & Tso, C. P. (2016). Concurrent oxidation and reduction of pentachlorophenol by bimetallic zerovalent Pd/Fe nanoparticles in an oxic water. *Journal of hazardous materials*, 301, 416-423. <https://doi.org/10.1016/j.jhazmat.2015.08.059>
- Shoneye, A., & Tang, J. (2020). Highly dispersed FeOOH to enhance photocatalytic activity of TiO₂ for complete mineralisation of herbicides. *Applied Surface Science*, 511, 145479. <https://doi.org/10.1016/j.apsusc.2020.145479>
- Siczek, A., Frać, M., Gryta, A., Kalembasa, S., & Kalembasa, D. (2020). Variation in soil microbial population and enzyme activities under faba bean as affected by

- pentachlorophenol. *Applied Soil Ecology*, 150, 103466.
<https://doi.org/10.1016/j.apsoil.2019.103466>
- Silveira, G. L., Lima, M. G. F., Dos Reis, G. B., Palmieri, M. J., & Andrade-Vieria, L. F. (2017). Toxic effects of environmental pollutants: Comparative investigation using *Allium cepa* L. and *Lactuca sativa* L. *Chemosphere*, 178, 359-367.
<https://doi.org/10.1016/j.chemosphere.2017.03.048>
- Singh, N., & Balomajumder, C. (2021). Phytoremediation potential of water hyacinth (*Eichhornia crassipes*) for phenol and cyanide elimination from synthetic/simulated wastewater. *Applied Water Science*, 11(8), 144.
<https://doi.org/10.1007/s13201-021-01472-8>
- Singh, S., & Garg, A. (2019). Performance of photo-catalytic oxidation for degradation of chlorophenols: Optimization of reaction parameters and quantification of transformed oxidized products. *Journal of hazardous materials*, 361, 73-84.
<https://doi.org/10.1016/j.jhazmat.2018.08.055>
- Sinkkonen, S., & Paasivirta, J. (2000). Polychlorinated organic compounds in the Arctic cod liver: trends and profiles. *Chemosphere*, 40(6), 619-626.
[https://doi.org/10.1016/S0045-6535\(99\)00309-4](https://doi.org/10.1016/S0045-6535(99)00309-4)
- Smirnoff, N. (2000). Ascorbic acid: metabolism and functions of a multi-faceted molecule. *Current opinion in plant biology*, 3(3), 229-235.
- Smith, J. G., Lee, S. F., & Netzer, A. (1976). Model studies in aqueous chlorination: the chlorination of phenols in dilute aqueous solutions. *Water research*, 10(11), 985-990. [https://doi.org/10.1016/0043-1354\(76\)90077-4](https://doi.org/10.1016/0043-1354(76)90077-4)
- Snell, T. W. (1986). Effect of temperature, salinity and food level on sexual and asexual reproduction in *Brachionus plicatilis* (Rotifera). *Marine Biology*, 92, 157-162. <https://doi.org/10.1007/BF00392832>
- Snell, T. W., & Carmona, M. J. (1995). Comparative toxicant sensitivity of sexual and asexual reproduction in the rotifer *Brachionus calyciflorus*. *Environmental Toxicology and Chemistry: An International Journal*, 14(3), 415-420.
<https://doi.org/10.1002/etc.5620140310>
- Snell, T. W., & Boyer, E. M. (1988). Thresholds for mictic female production in the rotifer *Brachionus plicatilis* (Muller). *Journal of Experimental Marine Biology*

- and Ecology, 124(2), 73-85. [https://doi.org/https://doi.org/10.1016/0022-0981\(88\)90112-8](https://doi.org/https://doi.org/10.1016/0022-0981(88)90112-8)
- Sobana, N., & Swaminathan, M. (2007). The effect of operational parameters on the photocatalytic degradation of acid red 18 by ZnO. Separation and purification technology, 56(1), 101-107. <https://doi.org/10.1016/j.seppur.2007.01.032>
- Solar Energy (2022). Ministry of New and Renewable Energy. <https://mnre.gov.in/solar/current-status/>. Accessed on 28 May 2022
- Steiert, J. G., Thoma, W. J., Ugurbil, K., & Crawford, R. L. (1988). 31P nuclear magnetic resonance studies of effects of some chlorophenols on Escherichia coli and a pentachlorophenol-degrading bacterium. Journal of bacteriology, 170(10), 4954-4957. <https://doi.org/10.1128/jb.170.10.4954-4957.1988>
- Stephenson, G. L., Kaushik, N. K., & Solomon, K. R. (1991). Chronic toxicity of a pure and technical grade pentachlorophenol to Daphnia magna. Archives of environmental contamination and toxicology, 21, 388-394. <https://doi.org/10.1007/BF01060361>
- Suteu, D., Malutan, T., & Bilba, D. (2010). Removal of reactive dye Brilliant Red HE-3B from aqueous solutions by industrial lignin: Equilibrium and kinetics modeling. Desalination, 255(1-3), 84-90. <https://doi.org/10.1016/j.desal.2010.01.010>
- Bauidh, K., Singh, R., & Singh, R. P. (2015). The suitability of Trapa natans for phytoremediation of inorganic contaminants from the aquatic ecosystems. Ecological Engineering, 83, 39-42. <https://doi.org/https://doi.org/10.1016/j.ecoleng.2015.06.003>
- Talano, M. A., Frontera, S., González, P., Medina, M. I., & Agostini, E. (2010). Removal of 2, 4-diclorophenol from aqueous solutions using tobacco hairy root cultures. Journal of hazardous materials, 176(1-3), 784-791. <https://doi.org/10.1016/j.jhazmat.2009.11.103>
- Teodorescu, T. I., Guidi, W., & Labrecque, M. (2011). The use of non-dormant rods as planting material: A new approach to establishing willow for environmental applications. Ecological Engineering, 37(9), 1430-1433. <https://doi.org/https://doi.org/10.1016/j.ecoleng.2011.03.031>

- Thind, P. S., Kumari, D., & John, S. (2018). TiO₂/H₂O₂ mediated UV photocatalysis of Chlorpyrifos: Optimization of process parameters using response surface methodology. *Journal of environmental chemical engineering*, 6(3), 3602-3609. <https://doi.org/10.1016/j.jece.2017.05.031>
- Tiwari, J., Kumar, S., Korstad, J., & Bauddh, K. (2019). Eco restoration of polluted aquatic ecosystems through rhizofiltration. In *Phytomanagement of polluted sites* (pp. 179-201). Elsevier. <https://doi.org/10.1016/B978-0-12-813912-7.00005-3>
- Tobajas, M., Monsalvo, V. M., Mohedano, A. F., & Rodriguez, J. J. (2012). Enhancement of cometabolic biodegradation of 4-chlorophenol induced with phenol and glucose as carbon sources by *Comamonas testosteroni*. *Journal of environmental management*, 95, S116-S121. <https://doi.org/10.1016/j.jenvman.2010.09.030>
- Toprak, T., & Anis, P. (2017). Textile industry's environmental effects and approaching cleaner production and sustainability, an overview. *Journal of Textile Engineering & Fashion Technology*, 2(4), 429-442. <https://doi.org/10.15406/jteft.2017.02.00066>
- Torres, R. A., Nieto, J. I., Combet, E., Pétrier, C., & Pulgarin, C. (2008). Influence of TiO₂ concentration on the synergistic effect between photocatalysis and high-frequency ultrasound for organic pollutant mineralization in water. *Applied Catalysis B: Environmental*, 80(1-2), 168-175. <https://doi.org/10.1016/j.apcatb.2007.11.013>
- Tsai, C. H., Lin, P. H., Waidyanatha, S., & Rappaport, S. M. (2001). Characterization of metabolic activation of pentachlorophenol to quinones and semiquinones in rodent liver. *Chemico-biological interactions*, 134(1), 55-71. [https://doi.org/https://doi.org/10.1016/S0009-2797\(00\)00318-5](https://doi.org/https://doi.org/10.1016/S0009-2797(00)00318-5)
- Udayasoorian, C., Prabu, P. C., & Balasubramanian, G. (2007). Degradation of pentachlorophenol by white rot fungus (*Phanerochaete chrysosporium*-TL 1) grown in ammonium lignosulphonate media.
- Umemura, T., Kai, S., Hasegawa, R., Sai, K., Kurokawa, Y., & Williams, G. M. (1999). Pentachlorophenol (PCP) produces liver oxidative stress and promotes

- but does not initiate hepatocarcinogenesis in B6C3F1 mice. *Carcinogenesis*, 20(6), 1115-1120. <https://doi.org/10.1093/carcin/20.6.1115>
- UNESCO, UN-Water (2020). *United Nations World Water Development Report 2020. Water and Climate Change*, Paris, UNESCO.
- Uotila, J. S., Kitunen, V. H., Saastamoinen, T., Coote, T., Häggblom, M. M., & Salkinoja-Salonen, M. (1992). Characterization of aromatic dehalogenases of *Mycobacterium fortuitum* CG-2. *Journal of bacteriology*, 174(17), 5669-5675. <https://doi.org/10.1128/jb.174.17.5669-5675.1992>
- Uotila, J. S., Salkinoja-Salonen, M. S., & Apajalahti, J. H. A. (1991). Dechlorination of pentachlorophenol by membrane bound enzymes of *Rhodococcus chlorophenolicus* PCP-I. *Biodegradation*, 2, 25-31. <https://doi.org/10.1007/BF00122422>
- Upadhyay, S., Sharma, N., Gupta, K. B., & Dhiman, M. (2018). Role of immune system in tumor progression and carcinogenesis. *Journal of cellular biochemistry*, 119(7), 5028-5042. <https://doi.org/https://doi.org/10.1002/jcb.26663>
- Urrutia, C., Rubilar, O., Parede, C., Benítez, E., Azcón, R., & Diez, M. C. (2013). Removal of pentachlorophenol in a rhizotron system with ryegrass (*Lolium multiflorum*). *Journal of soil science and plant nutrition*, 13(2), 499-510. <https://doi.org/10.4067/S0718-95162013005000039>
- Utkin, I., Woese, C., & Wiegel, J. (1994). Isolation and characterization of *Desulfitobacterium dehalogenans* gen. nov., sp. nov., an anaerobic bacterium which reductively dechlorinates chlorophenolic compounds. *International Journal of Systematic and Evolutionary Microbiology*, 44(4), 612-619. <https://doi.org/10.1099/00207713-44-4-612>
- Valli, K., & Gold, M. H. (1991). Degradation of 2, 4-dichlorophenol by the lignin-degrading fungus *Phanerochaete chrysosporium*. *Journal of bacteriology*, 173(1), 345-352. <https://doi.org/10.1128/jb.173.1.345-352.1991>
- Valo, R., Apajalahti, J., & Salkinoja-Salonen, M. (1985). Studies on the physiology of microbial degradation of pentachlorophenol. *Applied microbiology and biotechnology*, 21, 313-319. <https://doi.org/10.1007/BF00252710>

- Valo, R., Kitunen, V., Salkinoja-Salonen, M., & Räsänen, S. (1984). Chlorinated phenols as contaminants of soil and water in the vicinity of two Finnish sawmills. *Chemosphere*, 13(8), 835-844. [https://doi.org/10.1016/0045-6535\(84\)90156-5](https://doi.org/10.1016/0045-6535(84)90156-5)
- Valo, R., & Salkinoja-Salonen, M. (1986). Bioreclamation of chlorophenol-contaminated soil by composting. *Applied Microbiology and Biotechnology*, 25, 68-75. <https://doi.org/10.1007/BF00252515>
- Van Aken, P., Lambert, N., Van den Broeck, R., Degève, J., & Dewil, R. (2019). Advances in ozonation and biodegradation processes to enhance chlorophenol abatement in multisubstrate wastewaters: a review. *Environmental Science: Water Research & Technology*, 5(3), 444-481. <https://doi.org/10.1039/C8EW00562A>
- Van Maele-Fabry, G., Duhayon, S., & Lison, D. (2007). A systematic review of myeloid leukemias and occupational pesticide exposure. *Cancer Causes & Control*, 18, 457-478. <https://doi.org/10.1007/s10552-007-0122-2>
- Verma M, Haritash AK (2020) Photocatalytic degradation of Amoxicillin in pharmaceutical wastewater: A potential tool to manage residual antibiotics. *Environ Technol Innov* 20:101072. <https://doi.org/10.1016/j.eti.2020.101072>
- Verma, M., & Haritash, A. K. (2019). Degradation of amoxicillin by Fenton and Fenton-integrated hybrid oxidation processes. *Journal of Environmental Chemical Engineering*, 7(1), 102886. <https://doi.org/10.1016/j.jece.2019.102886>
- Verma, M., & Haritash, A. K. (2020). Photocatalytic degradation of Amoxicillin in pharmaceutical wastewater: A potential tool to manage residual antibiotics. *Environmental Technology & Innovation*, 20, 101072. <https://doi.org/10.1016/j.eti.2020.101072>
- Villemur, R. (2013). The pentachlorophenol-dehalogenating *Desulfitobacterium hafniense* strain PCP-1. *Philosophical Transactions of the Royal Society B: Biological Sciences*, 368(1616), 20120319. <https://doi.org/10.1098/rstb.2012.0319>
- Vinita, M., Dorathi, R. P. J., & Palanivelu, K. (2010). Degradation of 2, 4, 6-trichlorophenol by photo Fenton's like method using nano heterogeneous

- catalytic ferric ion. *Solar Energy*, 84(9), 1613-1618.
<https://doi.org/10.1016/j.solener.2010.06.008>
- Von, W. N., Klair, S., Bansal, S., Briat, J. F., Khodr, H., Shiori, T., Leigh, R. A. & Hider, R. C. (1999). Nicotianamine Chelates both Fe (III) and Fe (II). Implications for Metal Transport in Plants. *Plant Physiol*, 119, 1109-1111.
<http://dx.doi.org/10.1104/pp.119.3.1107>
- Wagner, M., & Nicell, J. A. (2002). Detoxification of phenolic solutions with horseradish peroxidase and hydrogen peroxide. *Water research*, 36(16), 4041-4052. [https://doi.org/10.1016/S0043-1354\(02\)00133-1](https://doi.org/10.1016/S0043-1354(02)00133-1)
- Wang, C. C., Lee, C. M., & Kuan, C. H. (2000). Removal of 2, 4-dichlorophenol by suspended and immobilized *Bacillus insolitus*. *Chemosphere*, 41(3), 447-452.
[https://doi.org/10.1016/S0045-6535\(99\)00263-5](https://doi.org/10.1016/S0045-6535(99)00263-5)
- Wang, P (2017) Aggregation of TiO₂ nanoparticles in aqueous media: effects of pH, ferric ion and humic acid. *International Journal of Environmental Sciences & Natural Resources*, 1(5): 157-162.
<https://doi.org/10.19080/IJESNR.2017.01.555575>
- Wang, Q., Li, Y., Li, J., Wang, Y., Wang, C., Wang, P., 2015. Experimental and kinetic study on the cometabolic biodegradation of phenol and 4-chlorophenol by psychrotrophic *Pseudomonas putida* LY1. *Environmental Science and Pollution Research*. 22, 565-573. <https://doi.org/10.1007/s11356-014-3374-x>
- Wang, S., Zhou, N., 2016. Removal of carbamazepine from aqueous solution using sono-activated persulfate process. *Ultrasonics Sonochemistry*. 29, 156-162.
<https://doi.org/10.1016/j.ultsonch.2015.09.008>
- Wang, S., Zhou, N., Wu, S., Zhang, Q., Yang, Z., 2015. Modeling the oxidation kinetics of sono-activated persulfate's process on the degradation of humic acid. *Ultrasonics Sonochemistry*. 23, 128-134.
<https://doi.org/10.1016/j.ultsonch.2014.10.026>
- Wang, Y.J, Ho, Y.S., Jeng, J.H., Su, H.J., Lee, C.C., 2000b. Different cell death mechanisms and gene expression in human cells induced by pentachlorophenol and its major metabolite, tetrachlorohydroquinone. *Chemico-Biological Interactions*. 128(3), 173–188. [https://doi.org/https://doi.org/10.1016/S0009-2797\(00\)00194-0](https://doi.org/https://doi.org/10.1016/S0009-2797(00)00194-0)

- Wang, Y.J., Lin, J.K., 1995. Estimation of selected phenols in drinking water with In situ acetylation and study on the DNA damaging properties of polychlorinated phenols. *Archives of Environmental Contamination and Toxicology*. 28(4), 537–542. <https://doi.org/10.1007/BF00211639>
- Wang, Y. J., Ho, Y. S., Chu, S. W., Lien, H. J., Liu, T. H., & Lin, J. K. (1997). Induction of glutathione depletion, p53 protein accumulation and cellular transformation by tetrachlorohydroquinone, a toxic metabolite of pentachlorophenol. *Chemico-biological interactions*, 105(1), 1-16. [https://doi.org/https://doi.org/10.1016/S0009-2797\(97\)00023-9](https://doi.org/https://doi.org/10.1016/S0009-2797(97)00023-9)
- Wang, Y. J., Lee, C. C., Chang, W. C., Liou, H. B., & Ho, Y. S. (2001). Oxidative stress and liver toxicity in rats and human hepatoma cell line induced by pentachlorophenol and its major metabolite tetrachlorohydroquinone. *Toxicology letters*, 122(2), 157-169. [https://doi.org/https://doi.org/10.1016/S0378-4274\(01\)00361-7](https://doi.org/https://doi.org/10.1016/S0378-4274(01)00361-7)
- Webb, B. N., Ballinger, J. W., Kim, E., Belchik, S. M., Lam, K. S., Youn, B., Nissen, M. S., Xun, L. & Kang, C. (2010). Characterization of chlorophenol 4-monooxygenase (TftD) and NADH: FAD oxidoreductase (TftC) of *Burkholderia cepacia* AC1100. *Journal of Biological Chemistry*, 285(3), 2014-2027. <https://doi.org/10.1074/jbc.M109.056135>
- Wenzel, W. W. (2009). Rhizosphere processes and management in plant-assisted bioremediation (phytoremediation) of soils. <https://doi.org/10.1007/s11104-008-9686-1>
- Werheni Ammeri, R., Di Rauso Simeone, G., Hassen, W., Smiri, M., Sadfi, N., Hidri, Y., & Hassen, A. (2022). *Aspergillus sydowii* and *Typha angustifolia* as useful tools for combined bio-processes of PCP removal in wastewater. *International Journal of Environmental Science and Technology*, 19(11), 11487-11500. <https://doi.org/10.1007/s13762-021-03853-7>
- Werheni Ammeri, R., Kraiem, K., Riahi, K., Eturki, S., Hassen, W., Mehri, I., & Hassen, A. (2021). Removal of pentachlorophenol from contaminated wastewater using phytoremediation and bioaugmentation processes. *Water Science and Technology*, 84(10-11), 3091-3103. <https://doi.org/10.2166/wst.2021.328>

- Weyens, N., van der Lelie, D., Taghavi, S., & Vangronsveld, J. (2009). Phytoremediation: plant–endophyte partnerships take the challenge. *Current opinion in biotechnology*, 20(2), 248-254. <https://doi.org/10.1016/j.copbio.2009.02.012>
- Willis, K. J., Ling, N., & Chapman, M. A. (1995). Effects of temperature and chemical formulation on the acute toxicity of pentachlorophenol to *Simocephalus vetulus* (Schoedler, 1858) (Crustacea: Cladocera). <https://doi.org/10.1080/00288330.1995.9516662>
- Xie, T. M., Abrahamsson, K., Fogelqvist, E., & Josefsson, B. (1986). Distribution of chlorophenolics in a marine environment. *Environmental science & technology*, 20(5), 457-463. <https://doi.org/10.1021/es00147a003>
- Xu, C., Liu, R., Chen, L., & Tang, J. (2016). Enhanced dechlorination of 2, 4-dichlorophenol by recoverable Ni/Fe–Fe₃O₄ nanocomposites. *Journal of Environmental Sciences*, 48, 92-101. <https://doi.org/10.1016/j.jes.2015.10.033>
- Xu, L., & Wang, J. (2012). Fenton-like degradation of 2, 4-dichlorophenol using Fe₃O₄ magnetic nanoparticles. *Applied Catalysis B: Environmental*, 123, 117-126. <https://doi.org/10.1016/j.apcatb.2012.04.028>
- Xu, L., & Wang, J. (2015). Degradation of 2, 4, 6-trichlorophenol using magnetic nanoscaled Fe₃O₄/CeO₂ composite as a heterogeneous Fenton-like catalyst. *Separation and Purification Technology*, 149, 255-264. <https://doi.org/10.1016/j.seppur.2015.05.011>
- Xu, L. J., & Wang, J. L. (2013). Degradation of chlorophenols using a novel Fe₀/CeO₂ composite. *Applied Catalysis B: Environmental*, 142, 396-405. <https://doi.org/10.1016/j.apcatb.2013.05.065>
- Xu, Q., Zhang, L., Cheng, B., Fan, J., & Yu, J. (2020). S-scheme heterojunction photocatalyst. *Chem*, 6(7), 1543-1559. <https://doi.org/10.1016/j.chempr.2020.06.010>
- Xu, T., Zhao, J., Hu, P., Dong, Z., Li, J., Zhang, H., ... & Zhao, Q. (2014). Pentachlorophenol exposure causes Warburg-like effects in zebrafish embryos at gastrulation stage. *Toxicology and applied pharmacology*, 277(2), 183-191. <https://doi.org/10.1016/j.taap.2014.03.004>

- Xue, X., Hanna, K., Despas, C., Wu, F., & Deng, N. (2009). Effect of chelating agent on the oxidation rate of PCP in the magnetite/H₂O₂ system at neutral pH. *Journal of molecular catalysis A: chemical*, 311(1-2), 29-35. <https://doi.org/10.1016/j.molcata.2009.06.016>
- Yadav, S., Kumar, S., & Haritash, A. K. (2023). A comprehensive review of chlorophenols: Fate, toxicology and its treatment. *Journal of Environmental Management*, 342, 118254. <https://doi.org/10.1016/j.jenvman.2023.118254>
- Yadav, S., Kumar, S., & Haritash, A. K. (2023b). Solar light and ultrasound-assisted rapid Fenton's oxidation of 2, 4, 6-trichlorophenol: comparison, optimisation, and mineralisation. *Rendiconti Lincei. Scienze Fisiche e Naturali*, 34(4), 1197-1207. <https://doi.org/10.1007/s12210-023-01192-y>
- Yadav, S., Pipil, H., Chawla, H., Taneja, S., Kumar, S., & Haritash, A. K. (2022). Textile Industry Wastewater Treatment Using Eco-Friendly Techniques. In *Proceedings of International Conference on Innovative Technologies for Clean and Sustainable Development (ICITCSD-2021)* (pp. 63-74). Cham: Springer International Publishing. https://doi.org/10.1007/978-3-030-93936-6_6
- Yagub, M. T., Sen, T. K., Afroze, S., & Ang, H. M. (2014). Dye and its removal from aqueous solution by adsorption: a review. *Advances in colloid and interface science*, 209, 172-184. <https://doi.org/10.1016/j.cis.2014.04.002>
- Yamaguchi, A., Ishibashi, H., Kohra, S., Arizono, K., & Tominaga, N. (2005). Short-term effects of endocrine-disrupting chemicals on the expression of estrogen-responsive genes in male medaka (*Oryzias latipes*). *Aquatic toxicology*, 72(3), 239-249. <https://doi.org/https://doi.org/10.1016/j.aquatox.2004.12.011>
- Yang, C. F., & Lee, C. M. (2008). Pentachlorophenol contaminated groundwater bioremediation using immobilized *Sphingomonas* cells inoculation in the bioreactor system. *Journal of hazardous materials*, 152(1), 159-165. <https://doi.org/10.1016/j.jhazmat.2007.06.102>
- Yang, J., Dai, J., Chen, C., & Zhao, J. (2009b). Effects of hydroxyl radicals and oxygen species on the 4-chlorophenol degradation by photoelectrocatalytic reactions with TiO₂-film electrodes. *Journal of Photochemistry and Photobiology A: Chemistry*, 208(1), 66-77. <https://doi.org/10.1016/j.jphotochem.2009.08.007>

- Yang SuYin, Y. S., Shibata, A., Yoshida, N., & Katayama, A. (2009a). Anaerobic mineralization of pentachlorophenol (PCP) by combining PCP-dechlorinating and phenol-degrading cultures. <https://doi.org/10.1002/bit.22032>
- Yang, W. J., Wu, H. B., Zhang, C., Zhong, Q., Hu, M. J., He, J. L., Li, G. A., Zhu, Z. Y., Zhu, J. L., Zhao, H. H., Zhang, H. S. & Huang, F. (2021). Exposure to 2, 4-dichlorophenol, 2, 4, 6-trichlorophenol, pentachlorophenol and risk of thyroid cancer: a case-control study in China. *Environmental Science and Pollution Research*, 28(43), 61329-61343. <https://doi.org/10.1007/s11356-021-14898-z>
- Yang, Y., Wang, N., Guo, X., Zhang, Y., & Ye, B. (2017). Comparative analysis of bacterial community structure in the rhizosphere of maize by high-throughput pyrosequencing. *PLoS One*, 12(5), e0178425. <https://doi.org/10.1371/journal.pone.0178425>
- Yang, Z., Zhang, X., Pu, S., Ni, R., Lin, Y., & Liu, Y. (2019). Novel Fenton-like system (Mg/Fe-O₂) for degradation of 4-chlorophenol. *Environmental Pollution*, 250, 906-913. <https://doi.org/10.1016/j.envpol.2019.04.096>
- Yanitch, A., Kadri, H., Frenette-Dussault, C., Joly, S., Pitre, F. E., & Labrecque, M. (2020). A four-year phytoremediation trial to decontaminate soil polluted by wood preservatives: phytoextraction of arsenic, chromium, copper, dioxins and furans. *International Journal of Phytoremediation*, 22(14), 1505-1514. <https://doi.org/10.1080/15226514.2020.1785387>
- Ye, Z., Sirés, I., Zhang, H., & Huang, Y. H. (2019). Mineralization of pentachlorophenol by ferrioxalate-assisted solar photo-Fenton process at mild pH. *Chemosphere*, 217, 475-482. <https://doi.org/10.1016/j.chemosphere.2018.10.221>
- Yen, J. H., Lin, K. H., & Wang, Y. S. (2002). Acute lethal toxicity of environmental pollutants to aquatic organisms. *Ecotoxicology and Environmental Safety*, 52(2), 113-116. <https://doi.org/10.1006/eesa.2002.2167>
- Yıldız, S., Şentürk, İ., & Canbaz, G. T. (2023). Degradation of phenol and 4-chlorophenol from aqueous solution by Fenton, photo-Fenton, sono-Fenton, and sono-photo-Fenton methods. *Journal of the Iranian Chemical Society*, 20(1), 231-237. <https://doi.org/10.1007/s13738-022-02663-z>

- Yin, D., Zhang, L., Zhao, X., Chen, H., & Zhai, Q. (2015). Iron-glutamate-silicotungstate ternary complex as highly active heterogeneous Fenton-like catalyst for 4-chlorophenol degradation. *Chinese Journal of Catalysis*, 36(12), 2203-2210. [https://doi.org/10.1016/S1872-2067\(15\)61011-7](https://doi.org/10.1016/S1872-2067(15)61011-7)
- Yu, L. Q., Zhao, G. F., Feng, M., Wen, W., Li, K., Zhang, P. W., Peng, X., Huo, W. J. & Zhou, H. D. (2014). Chronic exposure to pentachlorophenol alters thyroid hormones and thyroid hormone pathway mRNAs in zebrafish. *Environmental toxicology and chemistry*, 33(1), 170-176. <https://doi.org/10.1002/etc.2408>
- Zada, A., Qu, Y., Ali, S., Sun, N., Lu, H., Yan, R., ... & Jing, L. (2018). Improved visible-light activities for degrading pollutants on TiO₂/g-C₃N₄ nanocomposites by decorating SPR Au nanoparticles and 2, 4-dichlorophenol decomposition path. *Journal of hazardous materials*, 342, 715-723. <https://doi.org/10.1016/j.jhazmat.2017.09.005>
- Zhang, C., & Bennett, G. N. (2005). Biodegradation of xenobiotics by anaerobic bacteria. *Applied microbiology and biotechnology*, 67, 600-618. <https://doi.org/10.1007/s00253-004-1864-3>
- Zhang, G., Chen, L., Fu, X., & Wang, H. (2018). Cellulose microfiber-supported TiO₂@ Ag nanocomposites: a dual-functional platform for photocatalysis and in situ reaction monitoring. *Industrial & Engineering Chemistry Research*, 57(12), 4277-4286. <https://doi.org/10.1021/acs.iecr.8b00006>
- Zhang, J., Xu, Z., Chen, H., & Zong, Y. (2009). Removal of 2, 4-dichlorophenol by chitosan-immobilized laccase from *Coriolus versicolor*. *Biochemical engineering journal*, 45(1), 54-59. <https://doi.org/10.1016/j.bej.2009.02.005>
- Zhang, M. H., Dong, H., Zhao, L., Wang, D. X., & Meng, D. (2019). A review on Fenton process for organic wastewater treatment based on optimization perspective. *Science of the Total Environment*, 670, 110-121. <https://doi.org/10.1016/j.scitotenv.2019.03.180>
- Zhang, X., Zha, J., Li, W., Yang, L., & Wang, Z. (2008). Effects of 2, 4-dichlorophenol on the expression of vitellogenin and estrogen receptor genes and physiology impairments in Chinese rare minnow (*Gobiocypris rarus*). *Environmental Toxicology: An International Journal*, 23(6), 694-701. <https://doi.org/https://doi.org/10.1002/tox.20375>

- Zhang, Y., Ou, H., Liu, H., Ke, Y., Zhang, W., Liao, G., & Wang, D. (2018). Polyimide-based carbon nanofibers: A versatile adsorbent for highly efficient removals of chlorophenols, dyes and antibiotics. *Colloids and surfaces A: Physicochemical and engineering aspects*, 537, 92-101. <https://doi.org/10.1016/j.colsurfa.2017.10.014>
- Zhao, B., Yang, J., Liu, Z., Xu, Z., Qiu, Y., & Sheng, G. (2006). Joint anti-estrogenic effects of PCP and TCDD in primary cultures of juvenile goldfish hepatocytes using vitellogenin as a biomarker. *Chemosphere*, 65(3), 359-364. <https://doi.org/10.1016/j.chemosphere.2006.02.019>
- Zhao, L., Zhu, C., Gao, C., Jiang, J., Yang, J., & Yang, S. (2011). Phytoremediation of pentachlorophenol-contaminated sediments by aquatic macrophytes. *Environmental Earth Sciences*, 64, 581-588. <https://doi.org/10.1007/s12665-011-1164-z>
- Zheng Xiong, Z. X., Su YingLong, S. Y., Chen YinGuang, C. Y., Wan Rui, W. R., Liu Kun, L. K., Li Mu, L. M., & Yin DaQiang, Y. D. (2014). Zinc oxide nanoparticles cause inhibition of microbial denitrification by affecting transcriptional regulation and enzyme activity. <https://doi.org/10.1021/es504251v>
- Zhou, T., Li, Y., & Lim, T. T. (2010). Catalytic hydrodechlorination of chlorophenols by Pd/Fe nanoparticles: comparisons with other bimetallic systems, kinetics and mechanism. *Separation and Purification Technology*, 76(2), 206-214. <https://doi.org/10.1016/j.seppur.2010.10.010>
- Zulfiqar, M., Samsudin, M. F. R., & Sufian, S. (2019). Modelling and optimization of photocatalytic degradation of phenol via TiO₂ nanoparticles: An insight into response surface methodology and artificial neural network. *Journal of Photochemistry and Photobiology A: Chemistry*, 384, 112039. <https://doi.org/10.1016/j.jphotochem.2019.112039>

LIST OF PUBLICATIONS

S. No.	Title of Paper	Name of the Authors	Name of the Journal	Indexation	Publisher	DOI
1.	Solar light and ultrasound-assisted rapid Fenton's oxidation of 2,4,6-trichlorophenol: comparison, optimisation, and mineralisation	Shivani Yadav, Sunil Kumar, Anil Kumar Haritash	Rendiconti Lincei. Scienze Fisiche e Naturali	Science Citation Index Expanded (SCIE)	Springer	https://doi.org/10.1007/s12210-023-01192-y
2.	A comprehensive review of chlorophenols: Fate, toxicology and its treatment	Shivani Yadav, Sunil Kumar, Anil Kumar Haritash	Journal of Environmental Management	Science Citation Index Expanded (SCIE)	Elsevier	https://doi.org/10.1016/j.jenvman.2023.118254
3.	Synergistic potency of ultrasound and solar energy towards oxidation of 2,4-dichlorophenol: a chemometrics approach	Harsh Pipil, Shivani Yadav, Sunil Kumar, Anil Kumar Haritash	Environmental Science and Pollution Research	Science Citation Index Expanded (SCIE)	Springer	https://doi.org/10.1007/s11356-023-31598-y

To be continued...

S. No.	Title of Paper	Name of the Authors	Name of the Journal	Indexation	Publisher	DOI
4.	Evaluating the Photocatalytic degradation efficacy of 2,4,6-Trichlorophenol: Performance evaluation and influencing factors	Harsh Pipil, Shivani Yadav, Sunil Kumar, Anil Kumar Haritash	Journal of Water and Climate Change	Science Citation Index Expanded (SCIE)	IWA Publisher	https://doi.org/10.2166/wcc.2024.483
5.	Integrating oxidation system for degradation of 4-Chlorphenol: Exergy Analysis and Optimization	Harsh Pipil, Akansh Gupta, Shivani Yadav, Sunil Kumar, Anil Kumar Haritash	Journal of the Indian Chemical Society	Science Citation Index Expanded (SCIE)	Elsevier	https://doi.org/10.1016/j.jics.2024.101481
6.	Integrated advanced oxidation processes for chlorophenol degradation: parameter influence, efficacy evaluation, and Toxicity assessment with <i>Eichhornia crassipes</i>	Harsh Pipil, Shivani Yadav, Sunil Kumar, Anil Kumar Haritash	Journal of Water Chemistry and Technology	Science Citation Index Expanded (SCIE)	Springer	-

CIRCULAR VITAE

Name: Shivani Yadav

Email: shivaniyadav0711@gmail.com

Education Qualification

Period	Board/University	Degree	Subject	Percentage/ CGPA
2019	Delhi Technological University	Ph.D.	Environmental Engineering	NA
2017-2019	YMCA University of Science and Technology, Faridabad, Haryana	Masters of Science (M.Sc.)	Environmental Sciences	8.96
2014-2017	Gargi College, University of Delhi	Bachelor of Science (B.Sc.)	Zoology (Honors)	72%
2012-2013	CBSE	Senior Secondary	English, Physics, Chemistry, Biology, Hindi, Physical Education	85%
2010-2011	CBSE	Matriculation	English, Hindi, Maths, Science, Social Science	9.6

Publication

SCI/SCIE Indexed Publications:

1. Harsh Pipil, Akansh Gupta, **Shivani Yadav**, Sunil Kumar, Anil Kumar Haritash (2024). Integrating oxidation system for degradation of 4-Chlorophenol: Exergy Analysis and Optimization. Journal of the Indian Chemical Society, 101481. <https://doi.org/10.1016/j.jics.2024.101481>

2. **Shivani Yadav**, Harsh Pipil, Sunil Kumar, Anil Kumar Haritash (2024). Integrated advanced oxidation processes for chlorophenol degradation: parameter influence, efficacy evaluation, and Toxicity assessment with *Eichhornia crassipes*. J. Water Chem. Technol.
3. **Shivani Yadav**, Harsh Pipil, Krishna R. Reddy, Anil Kumar Haritash (2024). Fe(III)-modified bamboo biochar for the removal of phosphate from synthetic and field stormwater runoff. Sustain. Water Resour. Manag. 10, 140. <https://doi.org/10.1007/s40899-024-01123-1>
4. Naman Jain, **Shivani Yadav**, Sonam Taneja, Sanak Ray, Anil Kumar Haritash, Harsh Pipil (2024). Phosphate removal from urban stormwater runoff using *Canna lily* and *Cyperus alternifolius*-based bioretention system. Sustainable Water Resources Management, 10(2), 1-10. <https://doi.org/10.1007/s40899-024-01076-5>
5. Harsh Pipil, **Shivani Yadav**, Sunil Kumar, Anil Kumar Haritash (2024). "Evaluating the photocatalytic degradation efficacy of 2, 4, 6-trichlorophenol: performance evaluation and influencing factors". Journal of Water and Climate Change, jwc2024483. <https://doi.org/10.2166/wcc.2024.483>
6. Harsh Pipil, **Shivani Yadav**, Sunil Kumar, Anil Kumar Haritash (2024). "Synergistic potency of ultrasound and solar energy towards oxidation of 2, 4-dichlorophenol: a chemometrics approach". Environmental Science and Pollution Research, 1-24. <https://doi.org/10.1007/s11356-023-31598-y>
7. **Shivani Yadav**, Sunil Kumar, A. K. Haritash (2023). "Solar light and ultrasound-assisted rapid Fenton's oxidation of 2, 4, 6-trichlorophenol: comparison, optimisation, and mineralization". Rendiconti Lincei. Scienze Fisiche e Naturali, 34(4), 1197-1207. <https://doi.org/10.1007/s12210-023-01192-y>
8. **Shivani Yadav**, Sunil Kumar, A. K. Haritash (2023). "A comprehensive review of chlorophenols: Fate, toxicology and its treatment". Journal of Environmental Management, 2023, 342, 118254. <https://doi.org/10.1016/j.jenvman.2023.118254>
9. Harsh Pipil, **Shivani Yadav**, Harshit Chawla, Sonam Taneja, Manisha Verma, Nimisha Singla, and A. K. Haritash (2022). "Comparison of TiO₂ catalysis and Fenton's treatment for rapid degradation of Remazol Red Dye in textile industry effluent." Rendiconti Lincei. Scienze Fisiche e Naturali 33, no. 1 (2022): 105-114. <https://doi.org/10.1007/s12210-021-01040-x>

Book Chapters:

1. Harsh Pipil, **Shivani Yadav**, Sonam Taneja, Harshit Chawla, Anil Kumar Haritash, Krishna R Reddy. "Removal of Phosphate from Stormwater Runoff Using Bench Scale Constructed Wetland". In: Yukselen-Aksoy, Y., Reddy, K.R., Agnihotri, A.K. (eds) Sustainable Earth and Beyond. EGRWSE 2022. Lecture Notes in Civil Engineering, vol 370. Springer, Singapore. https://doi.org/10.1007/978-981-99-4041-7_39
2. Sonam Taneja, **Shivani Yadav**, Harsh Pipil, Oznur Karaca, AK Haritash. "Soil–Water Interactions and Arsenic Enrichment in Groundwater". Hydrogeochemistry of Aquatic Ecosystems, 97-120. <https://doi.org/10.1002/9781119870562.ch5>
3. **Shivani Yadav**, Harsh Pipil, Harshit Chawla, Sonam Taneja, Sunil Kumar, and A. K. Haritash. "Textile Industry Wastewater Treatment Using Eco-Friendly Techniques." In Proceedings of International Conference on Innovative Technologies for Clean and Sustainable Development (ICITCSD–2021), pp. 63-74. Springer, Cham, 2022. DOI: https://doi.org/10.1007/978-3-030-93936-6_6
4. Harsh Pipil, **Shivani Yadav**, Sonam Taneja, Harshit Chawla, A. K. Haritash, and Krishna R. Reddy. "Water Sensitive Urban Design (WSUD) for Treatment of Storm Water Runoff." In Proceedings of International Conference on Innovative Technologies for Clean and Sustainable Development (ICITCSD–2021), pp. 49-61. Springer, Cham, 2022. DOI: https://doi.org/10.1007/978-3-030-93936-6_5
5. Harshit Chawla, Sonam Taneja, **Shivani Yadav**, Harsh Pipil, Nimisha Singla, and A. K. Haritash. "Eco-Restoration of Lakes and Water Sustainability in Urban Areas." In Proceedings of International Conference on Innovative Technologies for Clean and Sustainable Development (ICITCSD–2021), pp. 85-94. Springer, Cham, 2022. DOI: https://doi.org/10.1007/978-3-030-93936-6_8
6. Sonam Taneja, Harshit Chawla, Harsh Pipil, **Shivani Yadav**, Oznur Karaca, and A. K. Haritash. "Sustainable Treatment of Metal-Contaminated Soil by Electrokinetic Remediation." In Proceedings of International Conference on Innovative Technologies for Clean and Sustainable Development (ICITCSD–2021), pp. 75-84. Springer, Cham, 2022. DOI: https://doi.org/10.1007/978-3-030-93936-6_7

Other Responsibilities:

- Member of Monitoring/Inspection Team of Gross Polluting Industries (GPI) conducted by Central Pollution Control Board (CPCB), 2023

Academic Achievements

UGC-NET-JRF Qualified: Decemebr 2018

UGC-NET Qualified: June 2018

Strength:

- Good hands-on analytical instruments including Atomic Absorption Spectrophotometer (AAS), High Performance Liquid Chromatography (HPLC), Elemental Analyser, Proximate Analyser, UV-Vis Spectrophotometer, water quality monitoring Hand-held instruments.
- Good verbal and written communication skills.
- Hard working, sincere, leadership quality and dedicated towards my work.

Personal Information:

Father's Name : Mr. Ved Prakash
Mother's Name : Mrs. Aman Yadav
Date of Birth : November 07, 1996
Communication Address : P-88, Sector 48, Gurgaon, Haryana